

The Role of Histone Modification in DNA Double-Strand Break Repair in *Schizosaccharomyces pombe*

Rachel Deegan

A thesis presented for the degree of Doctor of Philosophy

Chromosome Integrity Group
Gray Institute for Radiation Oncology and Biology
Department of Oncology
University of Oxford

Trinity Term 2012





Acknowledgements

Firstly, I would like to thank my supervisor, Dr Tim Humphrey, for giving me the opportunity to work in his lab over the past four years; it has been a great experience and this project would not have progressed as it has without his guidance, support and encouragement. I would also like to thank Eric Bernhard for giving me the opportunity to work at ROB. In addition, I would like to thank the Medical Research Council for funding this work. I would also like to thank all past and present members of the Humphrey lab who have helped me along the way, especially Chen Chun for constant technical advice and assistance. In particular, I would like to thank Jenny, who made the first three years of my PhD so much fun, and has been at the end of the phone whenever I needed her to listen to my moaning, answer my stupid questions and cheer me up!

This project has been made possible by help from various collaborators. Thank you to Sandra Codlin and Jürg Bähler for the microarray, Brian Strahl for help with nuclear extraction and Robin Allshire for strains and advice. I would especially like to thank the Kearsey group, especially Stephen and Marianne, for letting me hijack the microscope and flow cytometer on so many occasions and for guidance regarding the DNA replication section of this work.

A special thanks goes to my family, especially Dad and Tom for their love, support and constant belief in me. I wouldn't be here without the 26 years of help and encouragement Dad. Tom, you have always been there whenever I needed you for questions about 'real' biochemistry, and have provided much needed love and encouragement. I would also like to thank Gran for housing and feeding me on my numerous trips back to the lab.

A huge thank you goes to Joe, for his endless love and support over the past 6 years; there have been some really tough times, and you have always stood by me, inspired me to do better and made me smile. I am truly grateful for everything you do for me Joe and I can't wait to begin this new, exciting chapter of our life together.

I wish to dedicate this thesis to my Mum, who inspired my love of science, and always offered unwavering support and belief in everything I did. I wouldn't have got here without you and I wish you could be here to share this with me.

DECLARATION

I declare:

The work presented in this thesis is my own, with the exception of the microarray analysis, which was performed by Sandra Codlin, from the lab of Jürg Bähler, and the irradiations for the survival curves which were performed by Carol Walker.

No portion of this work has been previously submitted for another qualification at this, or any other university.

Signed ……..……

Rachel Deegan

The Role of Histone Modification in DNA Double-Strand Break Repair in *Schizosaccharomyces pombe*

Rachel Deegan
Christ Church
Medical Sciences Division

Doctor of Philosophy
University of Oxford
Trinity 2012

DNA double-strand breaks (DSBs) are highly genotoxic lesions, which when incorrectly repaired can lead to gross chromosomal rearrangements and tumourigenesis through oncogene activation or loss of heterozygosity at tumour suppressor loci. Chromatin structure and therefore histone modification can play a key role in the repair of these lesions through affecting the access of repair machinery to the break. To identify novel histone-modifying enzymes involved in DSB repair, nineteen histone-modifying mutants from an *S. pombe* deletion library were screened for altered DSB repair. Eleven genes were identified as required for normal DSB repair: *set1*$^+$, *set2*$^+$, *mst2*$^+$, *sir2*$^+$, *set3*$^+$, *set11*$^+$, *hat1*$^+$, *set13*$^+$, *clr4*$^+$, *gcn5*$^+$ and *elp3*$^+$. Two genes, *hat1*$^+$ and *set13*$^+$ are required for efficient homologous recombination (HR). In addition, four genes *set1*$^+$, *set2*$^+$, *set3*$^+$and *mst2*$^+$ are required for non-homologous end-joining (NHEJ). Analysis of *set1*Δ, *set2*Δ, *set3*Δ and *mst2*Δ deletion mutants showed impaired NHEJ was associated with significantly increased levels of repair by HR, supporting the existence of a competitive relationship between these mechanisms of repair.

Further work focused on Set2, a H3K36 methyltransferase. In addition to a role for Set2 in NHEJ, a role for Set2 in promoting efficient DNA replication was identified. This is likely through regulation of MBF-dependent genes. However, this altered progression of DNA replication was not responsible for the repair phenotype seen. The methyltransferase activity of Set2 was required for its role in NHEJ and DNA replication. Further analysis of a *H3K36R* mutant identified an additional role for H3K36 in DSB repair. Results indicate that H3K36 is also acetylated by Gcn5; quantitative analysis of DSB repair in a *gcn5*Δ mutant, identified a role for Gcn5 in promoting HR repair. Modification of H3K36 by methylation and acetylation is mutually exclusive, and preliminary analysis of the levels of these modifications suggests that they are cell cycle controlled. The findings presented here support a model whereby differential modification of H3K36 by Gcn5 and Set2 defines the DNA repair mechanism utilised. Methylation of H3K36 by Set2, which peaks in G1, promotes NHEJ whereas acetylation of H3K36 by Gcn5, which peaks in S phase, promotes HR.

Nomenclature

S. pombe

Genes are denoted by lower-case letters in italics. Genes in the wild-type locus given the $^{+}$ suffix e.g. *set2*$^{+}$, deletion/null mutants are denoted by Δ e.g. *set2*Δ. A double colon (::) indicates an insertion into the genome disrupting the gene in question e.g. *set2::ura4* signifies the *set2* gene disrupted by *ura4*. Letters and numbers following the gene name identify mutant alleles e.g. *ade6-M210*. Protein names are given an initial capital letter followed by lower-case letters in non-italics e.g. Set2.

S. cerevisiae

Genes are denoted by capital letters in italics e.g. *MEC1*. Deletion/null mutants are indicated by lower-case italics e.g. *mec1* with a suffix designating the allele where necessary e.g. *mre11-D65N*. Protein names are given an initial capital letter followed by lower-case letters in non-italics e.g. Mec1.

Mammalian

Genes are denoted by capital letters in italics e.g. *ATM*. Homozygous/heterozygous knockouts are shown as $^{-/-}$ or $^{+/-}$ respectively e.g. *ATM* $^{-/-}$ and *ATM* $^{+/-}$. Protein names are denoted by capital letters in non-italics e.g. ATM.

Designated prefixes are used where necessary to avoid confusion:

Sp = Schizosaccharomyces pombe

Sc = Saccharomyces cerevisiae

Hs = Homo sapien

Abbreviations

Δ	gene disruption
°C	degree Celsius
Ac	acetyl
Amp	ampicillin
APS	ammonium persulphate
BIR	break-induced replication
bp	base pair
BSA	bovine serum albumin
CDK	cyclin-dependent kinase
CFP	cyan fluorescent protein
Ch	chromosome
Ch^{16}	minichromsome 16
DAPI	6'-diamidino-2-phenylindole
DDK	Dbf4-dependent kinase
DDR	DNA damage response
D-loop	displacement-loop
DMSO	dimethyl sulphoxide
DNA	deoxyribonucleic acid
dNTP	deoxyribonucleotide triphosphate (A, C, G or T)
DSB	double-strand break
E. coli	*Escherichia coli*
EDTA	ethylenediamine tetra-acetic acid, disodium salt
EMM	Edinburgh minimal medium
EtBr	ethidium bromide
g	relative centrifugal force
G418	geneticin
GC	gene conversion
GCR	gross chromosomal rearrangement
GFP	green fluorescent protein
Gy	Gray
H	histone
H3K36	histone 3 lysine 36
HAT	histone acetyltransferase
HCl	hydrochloric acid
HDAC	histone deacetylase
HJ	Holliday junction
HMT	histone methyltransferase
HO	Homothallic endonuclease
HR	homologous recombination
HU	hydroxyurea
Hyg	hygromycin
IR	ionising radiation
Kb	kilobase

LB	Luria-Bertani medium
LOH	loss of heterozygosity
M	molar
Mb	megabase
MBF	MCB binding factor
MCB	*MluI* cell cycle box
Me	methyl
MMEJ	microhomology-mediated end-joining
MMS	methylmethane sulphonate
MQ	milli Q water
MRN complex	Mre11/Rad32-Rad50-Nbs1 complex
NaCl	sodium chloride
NaOH	sodium hydroxide
NHEJ	non-homologous end-joining
nmt	no message in thiamine
O/N	overnight
PAGE	polyacrylamide gel electrophoresis
PBS	phosphate-buffered saline
PCR	polymerase chain reaction
PEG	polyethylene glycol
PFGE	pulsed field gel electrophoresis
pre-RC	pre-replicative complex
RNA	ribonucleic acid
RNaseA	ribonuclease A
rpm	revolutions per minute
S. cerevisiae	*Saccharomyces cerevisiae*
S. pombe	*Schizosaccharomyces pombe*
SCC	sister chromatid conversion
SDS	sodium dodecyl sulphate
SSA	single strand annealing
SSB	single strand break
ssDNA	single-stranded DNA
TAE	tris acetate EDTA
TCA	trichloroacetic acid
TE	tris EDTA
TEMED	N,N,N',N'-tetramethylethylenediamine
TES	Tris/EDTA/SDS
Tris	tris (hydroxymethyl) methylamine
V	volts
w/v	weight per volume
YE6S	yeast extract 6 supplements

Contents

Acknowledgements……i
Declaration……ii

Abstract……iii

Nomenclature……iv

Abbreviations……v

CHAPTER 1: Introduction……1

1.1 MAINTAINING GENOME STABILITY: THE DNA DAMAGE RESPONSE (DDR)....1

1.2 DNA DOUBLE-STRAND BREAK (DSB) FORMATION 2
1.2.1 DNA Damaging Agents....2
1.2.2 Enzyme-Induced DSBs....4

1.3 MECHANISMS OF DSB REPAIR 4
1.3.1 Homologous recombination (HR)....5
1.3.2 Break-Induced Replication (BIR) and Single-Stand Annealing (SSA)....9
1.3.3 Non-Homologous End-Joining (NHEJ)....9

1.4 A SYSTEM FOR ANALYSING DSB REPAIR IN *S. POMBE*....12

1.5 ORGANISATION OF CHROMATIN....13
1.5.1 Regulation of Chromatin....15

1.6 HISTONE MODIFICATION....19
1.6.1 Lysine acetylation and bromodomains 20
1.6.2 Lysine methylation and the Royals....21
1.6.3 Histone modification crosstalk 22
1.6.4 H3K36 modification 24

1.7 HISTONE MODIFICATION AND DSB REPAIR 26
1.7.1 Histone modification and the initial response to a DSB 26
1.7.2 Histone modification and HR repair 29
1.7.3 Histone modification and NHEJ repair....30

1.8 DNA REPLICATION 31
1.8.1 Preventing re-replication....34
1.8.2 Histone modification and DNA replication 35

1.9 AIMS OF THIS WORK....38

CHAPTER 2: Materials and Methods……39

2.1 GENERAL LABORATORY SUPPLIES 39

2.2 BUFFERS AND SOLUTIONS....39

2.3 MEDIA 41
2.3.1 Growth of *Escherichia coli* (*E. coli*) 41
2.3.2 Growth of *Schizosaccharomyces pombe* (*S. pombe*) 41
2.4 STRAINS 42
2.4.1 *E. coli* 42
2.4.2 *S. pombe* 43
2.5 PLASMIDS 49
2.6 STORAGE AND GROWTH CONDITIONS 49
2.6.1 Growth and storage of *E. coli* strains 49
2.6.2 Growth and storage of *S. pombe* strains 49
2.6.3 Genetic crosses, tetrad analysis and random spore analysis 50
2.6.4 Analysis of cell growth and viability 50
2.6.4.1 Serial dilution assay 50
2.6.4.2 Survival curve 51
2.7 DNA TRANSFORMATION 51
2.7.1 Transformation of *E. coli* 51
2.7.1.1 Preparation of competent bacteria 51
2.7.1.2 Transformation 51
2.7.2 Transformation of *S. pombe* 52
2.7.2.1 Transormation by electroporation 52
2.7.2.2 Transformation by LiAc method 52
2.7.2.3 Transformation by PLATE method 52
2.8 DNA ISOLATION 53
2.8.1 Plasmid isolation from *E. coli* (mini-prep and maxi-prep) 53
2.8.2 Isolation of *S. pombe* genomic DNA 53
2.8.3 Isolation of DNA from agarose gels 53
2.8.4 PCR purification 53
2.9 DNA MANIPULATION AND ANALYSIS 53
2.9.1 Restriction digestion of DNA 53
2.9.2 DNA dephosphorylation and ligation 53
2.9.3 Polymerase Chain Reaction (PCR) 54
2.9.4 Quantification of DNA samples 54
2.9.5 DNA sequencing 54
2.9.6 Analysis of DNA by gel electrophoresis 55
2.9.6.1 Agarose gel electrophoresis 55
2.9.6.2 Contour-clamped homogeneous electric field (CHEF) pulsed field gel electrophoresis (PFGE) 55
2.10 DNA DOUBLE-STRAND BREAK (DSB) REPAIR ASSAYS 56
2.10.1 The DSB assay 56
2.10.2 The NHEJ assay 57
2.11 RNA EXTRACTION, MANIPULATION AND ANALYSIS 57
2.11.1 RNA extraction 57
2.11.2 Quantification of RNA samples 58

2.11.3 Microarray analysis....58
2.12 PROTEIN EXTRACTION, MANIPULATION AND ANALYSIS....59
2.12.1 TCA protein extraction....59
2.12.2 Nuclear protein extraction....59
2.12.3 SDS-polyacrylamide gel electrophoresis (SDS-PAGE)....60
2.12.4 Western blotting....60
2.13 MICROSCOPY....61
2.13.1 Light microscopy....61
2.13.2 Fluorescence microscopy....61
2.14 FLOW CYTOMETRY....62

CHAPTER 3: A screen for histone-modifying enzymes involved in DNA double-strand break repair……63

3.1 INTRODUCTION....63
3.2 RESULTS....63
3.2.1 Identification of bleomycin resistant histone-modifying mutants....63
3.2.2 Analysis of DSB repair in histone-modifying mutants....67
3.2.3 Analysis of NHEJ repair in histone-modifying mutants....73
3.2.4 Hat1 and Set13 are required for efficient HR repair....80
3.2.4.1 *hat1*Δ displays a genetic interaction with *rad3*Δ....80
3.2.4.2 *hat1*Δ and *set13*Δ cells are checkpoint proficient....82
3.2.4.3 *hat1*Δ and *set13*Δ cells display aberrant Rhp51 foci kinetics....82
3.3 DISCUSSION....86
3.3.1 The relationship between DNA damage sensitivity and DSB repair outcome in histone-modifying mutants....86
3.3.1.1 Fifteen mutants are associated with increased resistance to bleomycin....86
3.3.1.2 *elp3*Δ cells show sensitivity to bleomycin and IR....89
3.3.2 *gcn5*Δ and *elp3*Δ mutants show increased levels of NHEJ/SCC....90
3.3.3 Hat1, Set13 and Clr4 are required for efficient HR....90
3.3.4 Increased DSB repair by GC is frequently associated with inefficient NHEJ in histone-modifying mutants....92
3.3.4.1 A role for Set11 and Sir2 in DSB repair....92
3.3.4.2 A role for Set1, Set2, Set3 and Mst2 in promoting efficient NHEJ....93
3.3.4.3 A relationship between inefficient NHEJ and increased HR....96
3.4 SUMMARY....97

CHAPTER 4: A role for Set2 in DSB repair by non-homologous end-joining ……98

4.1 INTRODUCTION....98
4.2 RESULTS....98
4.2.1 Set1, Set2 and Mst2 are required for normal DNA double-strand break repair....98
4.2.2 *set2*$^{+}$ deletion does not result in resistance to all DNA damaging agents....99

4.2.3 *set2*$^{+}$ deletion is epistatic with NHEJ mutants 101
4.2.4 *set2*$^{+}$ deletion exhibits negative genetic interactions with early-acting HR mutants..104
4.2.5 *lig4*$^{+}$ and *ku70*$^{+}$ are not equivalent to *set2*$^{+}$ in their interaction with *exo1*Δ..... 109
4.2.6 Altering phosphorylation of RNAP II CTD does not result in the same repair phenotype as a *set2*$^{+}$ deletion mutant..... 111
4.2.7 The Clr6 HDAC complex is not required for the role of Set2 in NHEJ..... 114

4.3 DISCUSSION..... 118
4.3.1 An essential role for resection in a *set2*$^{+}$ deletion mutant 118
4.3.2 A Cdk9-independent role for Set2 119
4.3.3 A Clr6-independent role for Set2..... 121

4.4 SUMMARY..... 123

CHAPTER 5: Microarray analysis of a *set2*$^{+}$ deletion mutant……124

5.1 INTRODUCTION..... 124

5.2 RESULTS..... 124
5.2.1 Microarray analysis of wildtype and *set2*Δ cells 124
5.2.2 The expression of fifty-nine transcripts is altered following bleomycin treatment in wildtype cells 125
5.2.2.1 Seventeen transcripts are at least 1.5-fold up-regulated in wildtype cells following treatment with bleomycin..... 125
5.2.2.2 Forty-two transcripts are at least 1.5-fold down-regulated in wildtype cells following treatment with bleomycin 126
5.2.3 The expression of 186 transcripts is altered in untreated *set2*Δ cells compared to wildtype..... 127
5.2.3.1 140 transcripts are over 2-fold higher in untreated *set2*Δ cells compared to wildtype..... 127
5.2.3.2 Forty-six transcripts are at least two-fold lower in untreated *set2*Δ cells compared to wildtype..... 127
5.2.4 Transcription levels of genes involved in NHEJ and HR repair are not significantly changed in untreated s*et2*Δ cells 129
5.2.5 The level of 250 transcripts is altered in *set2*Δ cells compared to wildtype following treatment with bleomycin 129
5.2.5.1 Thirty transcripts are increased in wildtype cells following bleomycin treatment, and increased less in *set2*Δ cells..... 133
5.2.5.2 Fifty-six transcripts are increased in wildtype cells following bleomycin treatment, and decreased following treatment in *set2*Δ cells 136
5.2.5.3 Six transcripts are decreased in wildtype cells following bleomycin treatment, and further decreased following treatment in *set2*Δ cells 136
5.2.5.4 Ninety-one transcripts are increased in *set2*Δ cells following bleomycin treatment, and increased less in wildtype..... 136
5.2.5.5 Sixty-two transcripts are decreased in wildtype cells following bleomycin treatment, but increased following treatment in *set2*Δ cells..... 140

5.2.5.6 Five transcripts are decreased after treatment in wildtype, but decreased less in *set2*Δ cells 140
5.3 DISCUSSION 140
5.3.1 Fifty-nine transcripts show altered expression following DNA damage in wildtype cells 142
5.3.2 Two transcripts that are significantly altered in *set2*Δ cells compared to wildtype following treatment with bleomycin are involved in DNA repair 143
5.3.3 A role for Set2 in the efficient transcription of MBF-regulated genes 144
5.4 SUMMARY 146

CHAPTER 6: A role for Set2 in efficient DNA replication……...147

6.1 INTRODUCTION 147
6.2 RESULTS 147
6.2.1 *cdc18*$^{+}$, *cdt1*$^{+}$, *cdc22*$^{+}$ and *tos4*$^{+}$ are down-regulated following DNA damage in *set2*Δ cells 147
6.2.2 *set2*Δ cells show perturbed progression through S phase 148
6.2.3 *tos4*Δ cells exhibit normal cell cycle progression 153
6.2.4 Cdt1 and Cdc18 are misregulated in *set2*Δ cells 153
6.2.5 Cdc22 levels are lower, but do not show cell cycle changes in *set2*Δ cells 157
6.2.6 Ectopic expression of *cdt1* and *cdc18* does not rescue the cell cycle defect of *set2*Δ cells 157
6.2.7 *cdt1-19* shows some phenotypic similarity to *set2*Δ cells 160
6.2.8 Increasing the G1 population of *set2*Δ cells does not rescue the NHEJ defect 163
6.3 DISCUSSION 167
6.3.1 Set2 is required for efficient DNA replication 167
6.3.2 An interaction between replication initiation factors and Exo1 170
6.3.3 Slower DNA replication in *set2*Δ cells does not result in NHEJ deficiency 172
6.4 SUMMARY 174

CHAPTER 7: A role for H3K36 modification in controlling DSB repair pathway choice ……175

7.1 INTRODUCTION 175
7.2 RESULTS 175
7.2.1 Set2 methyltransferase activity is required for its role in DSB repair and replication 175
7.2.2 Lysine 36 of histone H3 is essential for survival following a DSB 179
7.2.3 Gcn5 is required for repair of a DSB by HR 182
7.2.4 *gcn5*Δ cells display aberrant Rhp51 foci kinetics 182
7.2.5 NHEJ is increased in *gcn5*Δ cells 184
7.2.6 *set2*Δ*gcn5*Δ cells exhibit wildtype DSB repair 186
7.2.7 Overexpression of *gcn5* results in increased repair by GC 188

7.2.8 Methylation and acetylation of H3K36 are mutually inhibitory....192
7.2.9 Methylation and acetylation of H3K36 occur in a cell cycle dependent manner....192
7.2.10 *gcn5*Δ cells exhibit a slight cell cycle delay....195
7.2.11 Global methylation and acetylation of H3K36 are unchanged following DNA damage....195
7.2.12 Gcn5 levels increase following treatment with bleomycin....198
7.3 DISCUSSION....198
7.3.1 Methylation of H3K36 by Set2 is required for efficient NHEJ and DNA replication....202
7.3.2 A role for Gcn5 in efficient HR repair....206
7.3.3 A model for the role of differential modification of H3K36 in directing DSB repair pathway choice....209
7.4 SUMMARY....213

CHAPTER 8: General Discussion……...214

8.1 The importance of histone modification in control of DNA-templated processes....214
8.2 A conserved role for histone methylation in NHEJ....215
8.3 A role for 'chromatin switches' in directing distinct biological events....216

REFERENCES…….....219

APPENDICES……...244

CHAPTER 1
Introduction

This thesis describes the identification and characterisation of histone-modifying enzymes required for efficient DNA double-strand break (DSB) repair in *Schizosaccharomyces pombe* (*S. pombe*). Focus on the role of Set2 in DSB repair led to identification of an additional role for this histone modifier in efficient DNA replication. Therefore, this introduction will focus on the mechanisms of DSB repair in addition to histone modification and DNA replication.

1.1 MAINTAINING GENOME STABILITY: THE DNA DAMAGE RESPONSE (DDR)

Genome stability is crucial for cell survival and is maintained through the coordination of a number of pathways, including DNA repair, checkpoint and cell cycle control. These mechanisms enable the cell to respond appropriately to DNA damage, thus preventing elevated mutation rates, gross chromosomal rearrangements (GCRs) and changes in chromosome number. Cancer cells exhibit numerous GCRs including translocations, deletions, inversions and duplications (Lengauer *et al*, 1998). These events can promote tumourigenesis through oncogene activation and tumour suppressor inactivation. Consequently, disruption of the pathways that control genome stability has been linked to various types of cancer and other diseases associated with genomic instability (Aguilera & Gomez-Gonzalez, 2008). Developing an understanding of how genomic instability arises and how it is suppressed in normal cells is a central goal of cancer research.

The term "DNA damage response" (DDR) is used to describe the intricate network of pathways that are mobilised in response to DNA damage, to prevent the accumulation of mutations and their subsequent propagation to the next generation (reviewed in Ciccia & Elledge, 2010; Ljungman, 2010). In addition to utilising various DNA repair pathways to

maintain genome stability, the DDR utilises checkpoint pathways to sense the damage, transduce the signal and modulate an appropriate cellular response. Following DNA damage, the checkpoints function to delay the cell cycle, promote repair, induce transcriptional changes, modulate chromatin structure and if necessary trigger apoptosis (Kastan & Bartek, 2004; Su, 2006). Disruption of the DNA damage checkpoint results in inefficient repair and subsequent genome instability. In *S. pombe*, the DNA damage and DNA replication checkpoints, collectively known as the DNA integrity checkpoint, share many components and are essential for maintaining genome stability (Figure 1.1).

1.2 DNA DOUBLE-STRAND BREAK (DSB) FORMATION

DSBs are highly genotoxic lesions, which if left undetected or incorrectly repaired can lead to mutations and genome instability. These lesions are caused by both endogenous sources, such as collapsed replication forks and oxidative damage and exogenous sources, such as ionising radiation (IR) and chemicals. Further, programmed DSBs are produced during normal cell processes such as mating type switching in yeast and V(D)J recombination (Pfeiffer *et al*, 2000).

1.2.1 DNA Damaging Agents

DNA damage can be induced through the use of various DNA damaging agents and throughout this study IR and bleomycin are used to characterise the response of mutants to DSBs. IR damages DNA both directly, through the deposition of energy, and indirectly, through the ionisation of water molecules to hydroxyl radicals that further damage the DNA. IR induces a range of lesions including DNA base damage, interstrand crosslinks and single-strand breaks (SSBs). If these SSBs occur within 10-20 bp of each other, on opposite DNA strands, then DSBs are formed. Further, lesions induced by IR can occur in clusters, which also results in DSB formation (Dianov *et al*, 2001).

Figure 1.1

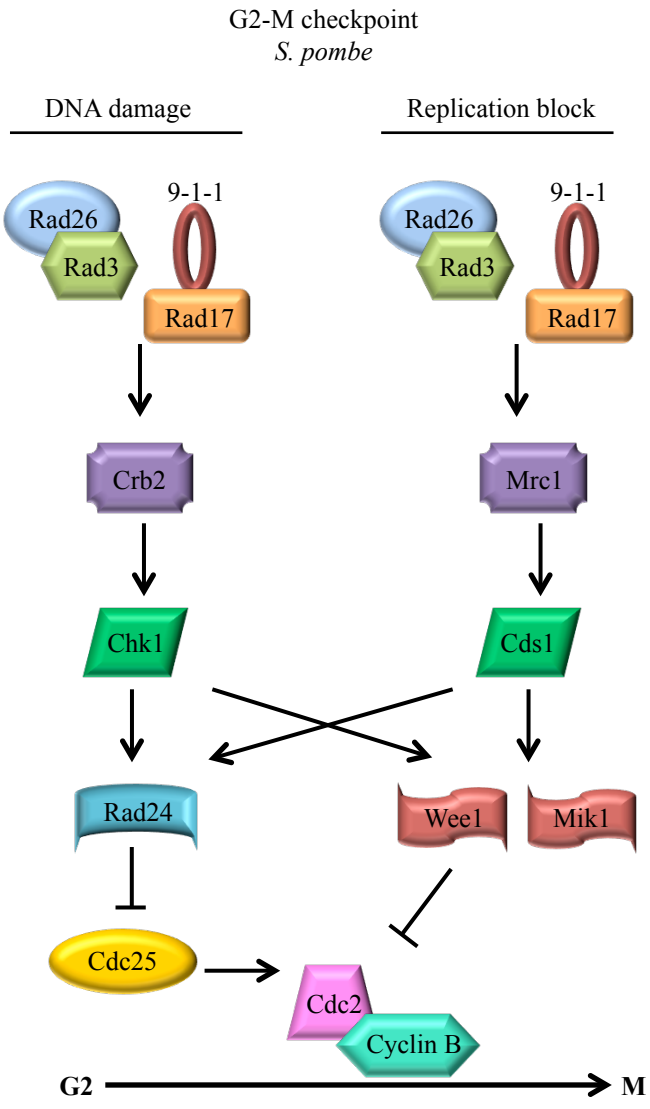


Figure 1.1 The G2-M checkpoint in *S. pombe* In *S. pombe,* in response to DNA damage or a replication block, the sensor proteins Rad9, Rad1, Hus1 (9-1-1 complex), Rad17, Rad3 and Rad26 are recruited to the sites of DNA damage. These in turn activate Crb2 and Mrc1 which transduce the signal downstream to Chk1 and Cds1. Chk1 and Cds1 act to promote the inhibitory phosphorylation of Cdc2 by up-regulation of Wee1 and Mik1 kinase activity in addition to down-regulation of Cdc25 phosphatase activity both directly and through the action of the 14-3-3 protein Rad24. Consequently Cdc2 is inactivated and G2-M transition inhibited.

Bleomycin is a radiomimetic produced by the bacterium *Streptomyces verticillus*. Treatment with this drug results in the production of SSBs and DSBs through a free radical mechanism, similar to that observed through treatment with IR (Povirk, 1996).

1.2.2 Enzyme-Induced DSBs

When cells are treated with bleomycin, or exposed to IR, DSBs occur throughout the genome. Restriction enzymes can be utilised to induce site-specific DSBs; in this work, the *S. cerevisiae* homothallic (HO) endonuclease was used to introduce a single site-specific break in a non-essential minichromosome (Ch^{16}). The HO endonuclease recognises a 22 bp target present in the budding yeast mating-type (*MAT*) locus that it cuts to produce a 4 bp staggered cut with 3'-OH overhangs (Nickoloff *et al*, 1990; Paques & Haber, 1999). The HO endonuclease is usually expressed in haploid cells in G1. However, in the system used here it is expressed on a plasmid under control of a weak REP81X no-message in thiamine (*nmt*) promoter, allowing DSB induction on the minichromosome 20-24 hours following removal of thiamine from the media (Cullen *et al*, 2007; Prudden *et al*, 2003; Tinline-Purvis *et al*, 2009).

1.3 MECHANISMS OF DSB REPAIR

There are two highly conserved pathways by which a DSB can be repaired: non-homologous end-joining (NHEJ) and homologous recombination (HR). HR utilises a homologous DNA sequence as a repair template, and therefore this mechanism of repair occurs predominantly in S and G2 phases of the cell cycle, when a sister chromatid is available (Ferreira & Cooper, 2004). HR is the major pathway used in fission yeast, as the majority of the cell cycle is spent in G2. NHEJ involves simply re-ligating the broken ends, irrespective of their sequence and this is the major pathway utilised in higher eukaryotes (Rothkamm *et al*, 2003). As HR repair requires a DNA template, the two mechanisms of repair are reciprocally regulated through the cell cycle, so that when damage is encountered in G1, NHEJ is used to repair the break (Ferreira & Cooper, 2004).

1.3.1 Homologous recombination (HR)

HR utilises several hundred base pairs of perfect, or near perfect homology from a homologous donor for efficient repair, preferably the sister chromatid, but often a homologous chromosome or ectopic site on a non-homologous chromosome (Kadyk & Hartwell, 1992). The core HR machinery is highly conserved throughout eukaryotes reflecting the essential nature of these genes in maintaining genome stability (Table 1.1).

A key step in the decision between HR and NHEJ is the initiation of 5'-3' resection of the broken DNA ends to form a 3' ssDNA overhang. Resection is required for HR but not NHEJ and therefore takes place most efficiently in S and G2 phases of the cell cycle (Aylon *et al*, 2004; Ira *et al*, 2004). Resection is initiated by the MRN/MRX complex, which constitutes Mre11-Rad50-Nbs1 in *S. pombe* (*Sp*) and *Homo sapiens* (*Hs*) and Mre11-Rad50-Xrs2 in *S. cerevisiae* (*Sc*; Llorente & Symington, 2004; Paques & Haber, 1999). In addition, the action of Ctp1^{Sp}/Sae2^{Sc}/CtIP^{Hs} is utilised for initiation of resection (Clerici *et al*, 2006; Huertas *et al*, 2008; Limbo *et al*, 2007; Sartori *et al*, 2007). Further, long tract resection requires the action of Exo1, the RecQ helicase Sgs1^{Sc}/BLM^{Hs} and Dna2^{Sc} (Llorente & Symington, 2004; Mimitou & Symington, 2008; Mimitou & Symington, 2009; Tomita *et al*, 2003; Tsubouchi & Ogawa, 2000; Zhu *et al*, 2008). The ssDNA created through resection is then bound by Replication Protein A (RPA), which eliminates any secondary structures. This creates an appropriate ssDNA structure for binding of Rhp51^{Sp}/Rad51$^{Sc\text{-}Hs}$ and subsequent nucleofilament formation, an essential step for invasion of the homologous DNA template. Formation of the Rhp51 nucleofilament requires Rad22^{Sp}/Rad52^{Sc} and the heterodimer Rhp55-Rhp57^{Sp}/Rad55-Rad57^{Sc} (Sugawara *et al*, 2003; Sung, 1997). These mediator complexes overcome the inhibitory effects of RPA and the helicases Fbh1$^{Sp/Hs}$ and Srs2^{Sc}, which act to displace Rhp51 from the ssDNA (Fugger *et al*, 2009; Krejci *et al*, 2003; Liu *et al*, 2011; Osman *et al*, 2005; Veaute *et al*, 2003). Although the RAD52 mediator function has

not been demonstrated in mammalian cells, this is likely due to the presence of additional mediators including the RAD51 paralogues (RAD51B, RAD51C, RAD51D, XRCC2, XRCC3) and BRCA2.

Table 1.1 HR proteins in *S. pombe*, *S. cerevisiae* and humans

Function in HR	*S. pombe*	*S. cerevisiae*	Humans
Resection	Mre11-Rad50-Nbs1 (MRN complex)	Mre11-Rad51-Xrs2 (MRX complex)	MRE11-RAD50-NBS1 (MRN complex)
	Ctp1	Sae2	CtIP
	Exo1	Exo1	EXO1
	Rqh1	Sgs1	BLM1
	Dna2	Dna2	DNA2
ssDNA binding	RPA (large subunit: Rad11)	RPA (large subunit: Rfa1)	RPA (large subunit: RPA70)
Homologous pairing and strand exchange	Rhp51	Rad51	RAD51
	Rad22	Rad52	RAD52
	Rhp54	Rad54	RAD54
	Rti1	Rad59	?
	Rhp55-Rhp57 (Rlp1, Rdl1, Sws1)	Rad55-Rad57	RAD51B-RAD51C RAD51D-XRCC2 RAD51C-XRCC3
	?	?	BRCA2
	Mnd1-Hop2	Mnd1-Hop2	MND1-HOP2
	Swi5-Sfr1	Sea3-Mei5	SWI5-MEI5
Inhibition of Rad51 filament formation	Fbh1	?	FBH1
	Srs2	Srs2	RTEL
DNA synthesis	PCNA, Pol δ, Pol ε	PCNA, Pol δ, Pol ε	PCNA, Pol δ, Pol ε
HJ dissolution	Rqh1-Top3	Sgs1-Top3	BLM-TOPIIIα
HJ resolution	Mus81-Eme1	Mus81-Mms4	MUS81-EME1
	?	YEN1	GEN1
	Slx1-4	Slx1-4	SLX1-4

Formation of the Rad51 nucleofilament is sufficient for the subsequent location of homology, which is achieved through random collisions in which duplex DNA is bound and tested, until significant homology is found (Bianco *et al*, 1998; Sinha & Peterson, 2008). Once homology has been found, strand invasion into the homologous DNA generates a displacement loop (D-loop), which is stabilised through interaction between Rhp51 and Rhp54^{Sp}/Rad54$^{Sc/Hs}$ (Mazin

et al, 2003). In addition to the presynaptic role for RPA, a postsynaptic role exists in promoting DNA pairing, through stabilisation of the displaced strand (Eggler *et al*, 2002; Wang & Haber, 2004). Mnd1-Hop2 can also function here in stabilisation of the Rad51 nucleofilament and promoting capture of the duplex DNA (Chi *et al*, 2007). In addition, another mediator complex Swi5-Sfr1^{Sp}/Sea3-Mei5^{Sc}/SWI5-MEI5^{Hs} has been shown to play a role in the stabilisation of Rhp51 binding to ssDNA and strand exchange, although in budding yeast this is meiosis specific (Akamatsu *et al*, 2003; Haruta *et al*, 2006; Yuan & Chen, 2011).

Following invasion and D-loop formation, DNA synthesis occurs, using the homologous DNA as a template. At this stage, HR proceeds through a number of sub-pathways; the DSB repair (DSBR) pathway requires capture of a second end, whereas the synthesis-dependent strand-annealing (SDSA) pathway relies on displacement of the newly synthesised strand (reviewed in Paques & Haber, 1999; Figure 1.2). The DSBR model, proposed by Szostak *et al* (1983) results in double Holliday junction (HJ) formation, which can be resolved with or without crossovers, whereby flanking markers are exchanged. HJ resolution requires the activity of resolvases GEN1^{Hs}/Yen1^{Sc}, Mus81-Eme1^{Sp}/Mus81-Mms4^{Sc} and SLX1-SLX4$^{Hs/Sc}$ (Boddy *et al*, 2001; Chen *et al*, 2001; Fekairi *et al*, 2009; Ip *et al*, 2008; Munoz *et al*, 2009; Svendsen & Harper, 2010; Svendsen *et al*, 2009). Alternatively, to avoid potentially mutagenic crossovers, HJs can be dissolved through the action of Sgs1-Top3^{Sc} (Ira *et al*, 2003; Karow *et al*, 2000; Mankouri & Hickson, 2006; Seki *et al*, 2006; Wu & Hickson, 2003). Repair by SDSA prevents crossovers, and thus avoids accumulation of potentially dangerous chromosomal rearrangements.

Figure 1.2

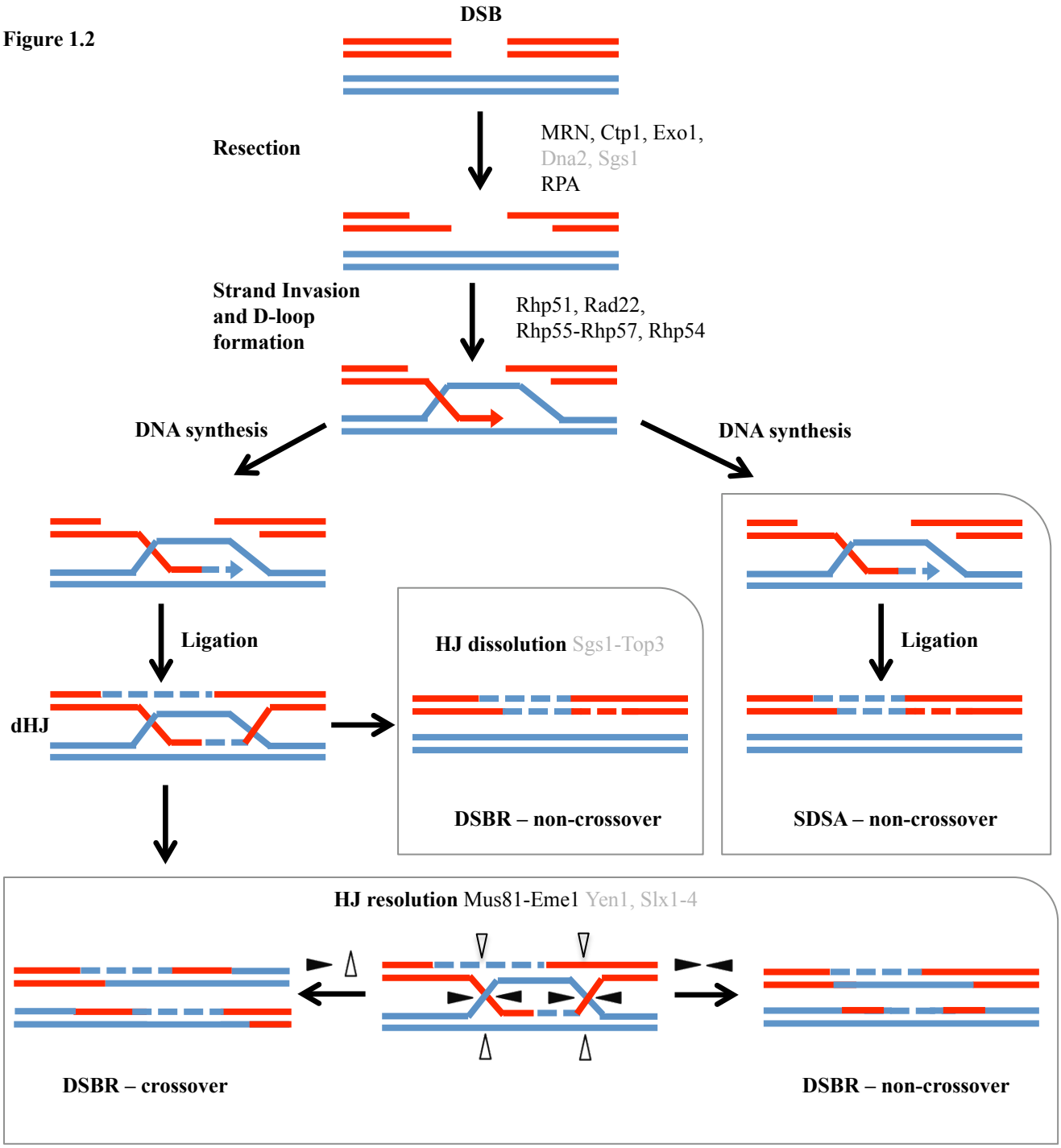


Figure 1.2 Schematic of HR repair Following formation of a DSB, the DNA ends are resected to form 3' ssDNA overhangs. This ssDNA is bound by RPA, followed by replacement with Rhp51 to form a nucleofilament, assisted by mediator complexes. The nucleofilament invades the homologous DNA template and forms a D-loop. DNA synthesis is primed within the D-loop, by the invading strand. If repair proceeds by SDSA, the invading strand in expelled from the homologous duplex DNA and re-anneals to the second end of the break, resulting in a non-crossover product. If repair proceeds by DSBR, the second end of the break anneals to the D-loop forming a double Holliday junction (dHJ). This can either be dissolved through the action of helicases resulting in non-crossover product formation, or resolved by resolvases resulting in the formation of either crossovers or non-crossover products. Proteins utilised in *S. pombe* are shown in black and those shown to be involved in HR in other organisms are shown in grey. Adapted from Heyer e*t al*., 2010.

1.3.2 Break-Induced Replication (BIR) and Single-Stand Annealing (SSA)

In addition to the major HR pathways described, there are other sub-pathways: break-induced replication (BIR) and single-strand annealing (SSA). BIR occurs when only one end is available for repair, such as when a replication fork collapses. These breaks are incompatible with SDSA and DSBR, as second end capture cannot occur. Therefore, following invasion of the template, DNA synthesis continues to the end of the chromosome; this can lead to loss of heterozygosity of all genetic information distal to the break site (Llorente *et al*, 2008). SSA occurs when a DSB is created between direct repeats (Fishman-Lobell *et al*, 1992). Following resection, homologous ssDNA sequences are exposed which can anneal, leaving the non-homologous ssDNA as flaps, which are then cleaved by nucleases (Paques & Haber, 1999). SSA results in loss of all genetic information between the repeats in addition to one of the repeats, and so this pathway is highly mutagenic (Krogh & Symington, 2004). However, its contribution to DSB repair *in vivo* remains unclear.

1.3.3 Non-Homologous End-Joining (NHEJ)

NHEJ is the major pathway of DSB repair in mammalian cells, and is active throughout the cell cycle, whereas in yeast it appears to be restricted to G1 (Guirouilh-Barbat *et al*, 2004; Moore & Haber, 1996). Unlike HR, NHEJ does not require a homologous sequence and instead involves re-ligation of the broken DNA ends (Figure 1.3A). In vertebrates, the core NHEJ factors comprise Ku70, Ku80, DNA-dependent protein kinase catalytic subunit (DNA-PKcs), Artemis, DNA ligase IV, XRCC4 and XLF (reviewed in Lieber, 2010). Although the majority of these core factors are conserved in *S. pombe* (Ku70, Ku80, Lig4, Xlf1), many other factors have not been identified.

NHEJ is initiated by binding of the Ku70-Ku80 heterodimer to the DNA ends, which acts as a docking station for the recruitment of other factors. Binding of Ku to DNA ends results in the recruitment of DNA-PKcs through interaction with the C-terminal domain of Ku80 (Falck *et*

al, 2005; Gell & Jackson, 1999; Singleton *et al*, 1999); this results in formation of the active DNA-PK holoenzyme. Formation of the active kinase results in phosphorylation of other proteins involved in NHEJ in addition to auto-phosphorylation of DNA-PKcs. This auto-phosphorylation causes a conformational change, allowing access of the processing and ligation machinery to the DNA (Block *et al*, 2004; Reddy *et al*, 2004; Weterings *et al*, 2003).

IR-induced damage is often associated with damage to the sugar backbone or bases, and so DNA ends often need to be processed prior to ligation. In this respect, NHEJ can be associated with limited or extensive additions or deletions of nucleotides (reviewed in Lieber, 2010). Processing through either deletion or addition is achieved by the exonuclease Artemis (Ma *et al*, 2002), polymerases such as Polλ and Polμ (Mahajan *et al*, 2002), terminal deoxynucleotidyltransferase (TdT; Mahajan *et al*, 1999; Mickelsen *et al*, 1999) and polynucleotide kinase (PNK; Chappell *et al*, 2002). Following processing, the DNA ends are ligated by DNA ligase IV and XRCC4 which are recruited by Ku and DNA-PKcs (Costantini *et al*, 2007; Hsu *et al*, 2002; Lee *et al*, 2000; Mari *et al*, 2006; Nick McElhinny *et al*, 2000). Ligation is further stimulated by XLF and Ku (Ahnesorg *et al*, 2006; Gu *et al*, 2007; Tsai *et al*, 2007).

The pathway known as alternative NHEJ (A-NHEJ), or microhomology-mediated end-joining (MMEJ) functions when repair by the classical mechanism is impaired (Figure 1.3B). A-NHEJ was first discovered in mammalian cells and is conserved in yeast (McVey & Lee, 2008; Roth & Wilson, 1986). This pathway exhibits slower kinetics than the classical pathway, is always error prone and can result in significant deletions (Han & Yu, 2008; McVey & Lee, 2008; Virsik-Kopp *et al*, 2003). This is due to a bias towards microhomology-mediated joins whereby joinings occur preferentially between sequences near the DNA ends

Figure 1.3

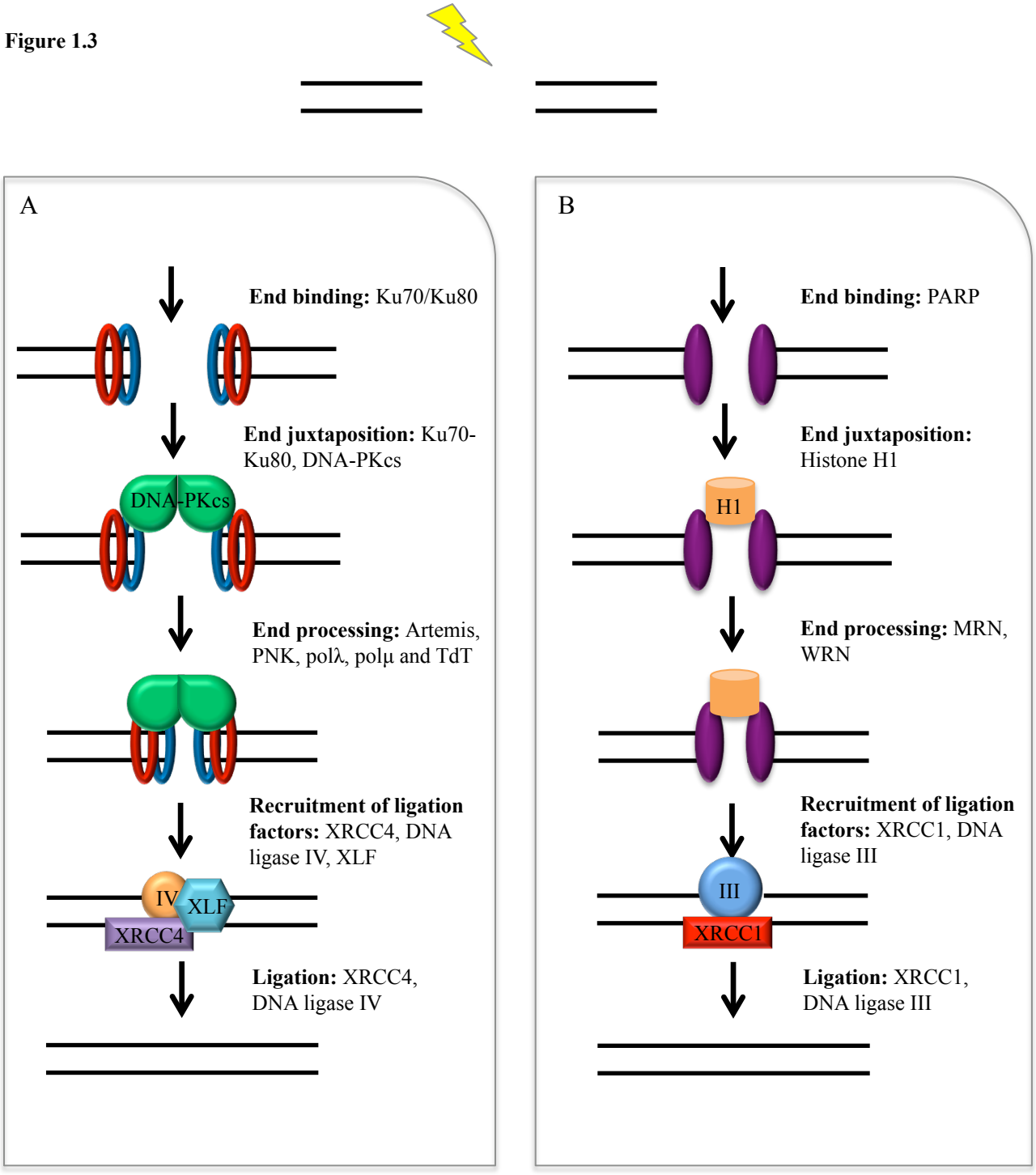


Figure 1.3 Non-homologous end-joining (NHEJ) in mammalian cells Following DSB formation, end joining can occur through one of two pathways. In classical NHEJ (A) Ku70-Ku80 binds to the break, which leads to the recruitment of DNA-PKcs. DNA-PKcs holds the two DNA ends together. End processing factors such as Artemis, pol λ, pol μ, TdT and PNK are recruited if processing is required. Finally DNA ligase IV and XRCC4 ligate the broken ends, promoted by XLF1, restoring the molecular integrity of the DNA. If classical NHEJ is impaired, repair can occur by alternate NHEJ (A-NHEJ; B). Although this mechanism is not well understood, it is thought that PARP1 binds the DNA ends, which are held together by histone H1. End processing by MRN and WRN is suggested, followed by DNA ligase III and XRCC1 dependent re-ligation of the DNA ends. A-NHEJ often results in deletions due to the preferential utilisation of microhomology.

that share up to seven nucleotides of homology (Kabotyanski *et al*, 1998). Thus, significant resection must occur to expose regions sharing some homology, resulting in deletion of the intervening DNA. Although the mechanisms of A-NHEJ are not fully understood, repair using this pathway is Ku, LigIV and DNA-PK independent. Instead, Ligase III (LigIII) is utilised in a complex with XRCC1, and regulated by PARP1 (McKinnon & Caldecott, 2007; Wang *et al*, 2001). It is suggested that Ku and PARP1 compete for DNA ends, but Ku binds predominantly, explaining the prevalence of classical NHEJ compared to A-NHEJ (Wang *et al*, 2006). Other factors involved in A-NHEJ are histone H1 which is thought to align the DNA ends via an unknown mechanism (Rosidi *et al*, 2008), the helicase WRN (Sallmyr *et al*, 2008) and the MRN complex (Davis & Chen, 2010; Deriano *et al*, 2009; Rahal *et al*, 2010; Xie *et al*, 2009).

1.4 A SYSTEM FOR ANALYSING DSB REPAIR IN *S. POMBE*

Throughout this work, a non-essential minichromosome, Ch^{16}, derived from chromosome III (ChIII; Niwa *et al*, 1986) has been utilised to address the outcome of DSB repair. Ch^{16} has been modified in this laboratory to carry a *MATa* site, which allows introduction of a single DSB through expression of the HO endonuclease (Prudden *et al*, 2003). Various genetic markers have also been introduced onto the minichromosome; a kanamycin or hygromycin resistance cassette lies adjacent to the *MAT*a site, and additional auxotrophic markers are present on either arm of the minichromosome. Using this minichromosome it is possible to analyse the response to a DSB in various genetic backgrounds by analysing marker loss or retention (Cullen *et al*, 2007; Tinline-Purvis *et al*, 2009). Following break induction, repair can occur by NHEJ (Figure 1.4A); however, this is difficult to discern from sister chromatid conversion (SCC; Figure 1.4B), as both outcomes result in retention of all the genetic markers. Wildtype cells predominantly repair the break by HR, resulting in GC, and loss of the marker adjacent to the break, through use of ChIII as a repair template (Figure 1.4C). The non-essential nature of the minichromosome also allows chromosomal rearrangements to

occur without loss of cell viability, and previous studies in the laboratory have shown that extensive end processing can give rise to loss of heterozygosity (LOH; Figure 1.4E-G) and chromosome loss (Ch^{16} loss; Figure 1.4D). In our system, LOH has been shown to occur through non-reciprocal translocation (Figure 1.4E), isochromosome formation (Figure 1.4F) and *de novo* telomere addition (Figure 1.4G; Cullen *et al*, 2007; Tinline-Purvis *et al*, 2009); all three outcomes result in loss of genetic markers distal to the break site.

1.5 ORGANISATION OF CHROMATIN

In eukaryotes, DNA is packaged into a highly condensed state, termed chromatin, via its association with histone proteins. The basic unit of chromatin is the nucleosome which consists of approximately 147 bp of DNA wrapped twice around a histone octamer, which comprises two copies each of the four core histone proteins, H2A, H2B, H3 and H4 (Luger *et al*, 1997). The core histones consist of a structured globular domain, containing the conserved histone fold motif, and an N-terminal highly charged flexible tail. These tails play key roles in the compaction of chromatin as they allow interactions to form within and between nucleosomes. Linker DNA is present between the core nucleosome particles, although the length of this DNA varies between species and cell type (Van Holde, 1988). Nucleosomes containing linker DNA can form the 10 nm 'beads on a string' chromatin fibre. This can further compact to form higher order chromatin structures including the '30 nm fibre'. The arrangement of the nucleosomes and linker DNA within these higher order structures is poorly understood, although there has been some success in structural studies including X-ray diffraction of a tetranucleosome, showing a zigzig organisation (Schalch *et al*, 2005). However, whether these findings can be extrapolated to longer chromatin fibres is unclear. In addition to the four core histones, an additional histone H1 (or linker histone) is generally conserved, although it is not present in *S. pombe*. H1 binds linker DNA, protecting it from nucleases and plays a key role in the formation of higher order chromatin structures. In the presence of H1 the linker DNA entering and exiting the nucleosome is brought together and

Figure 1.4

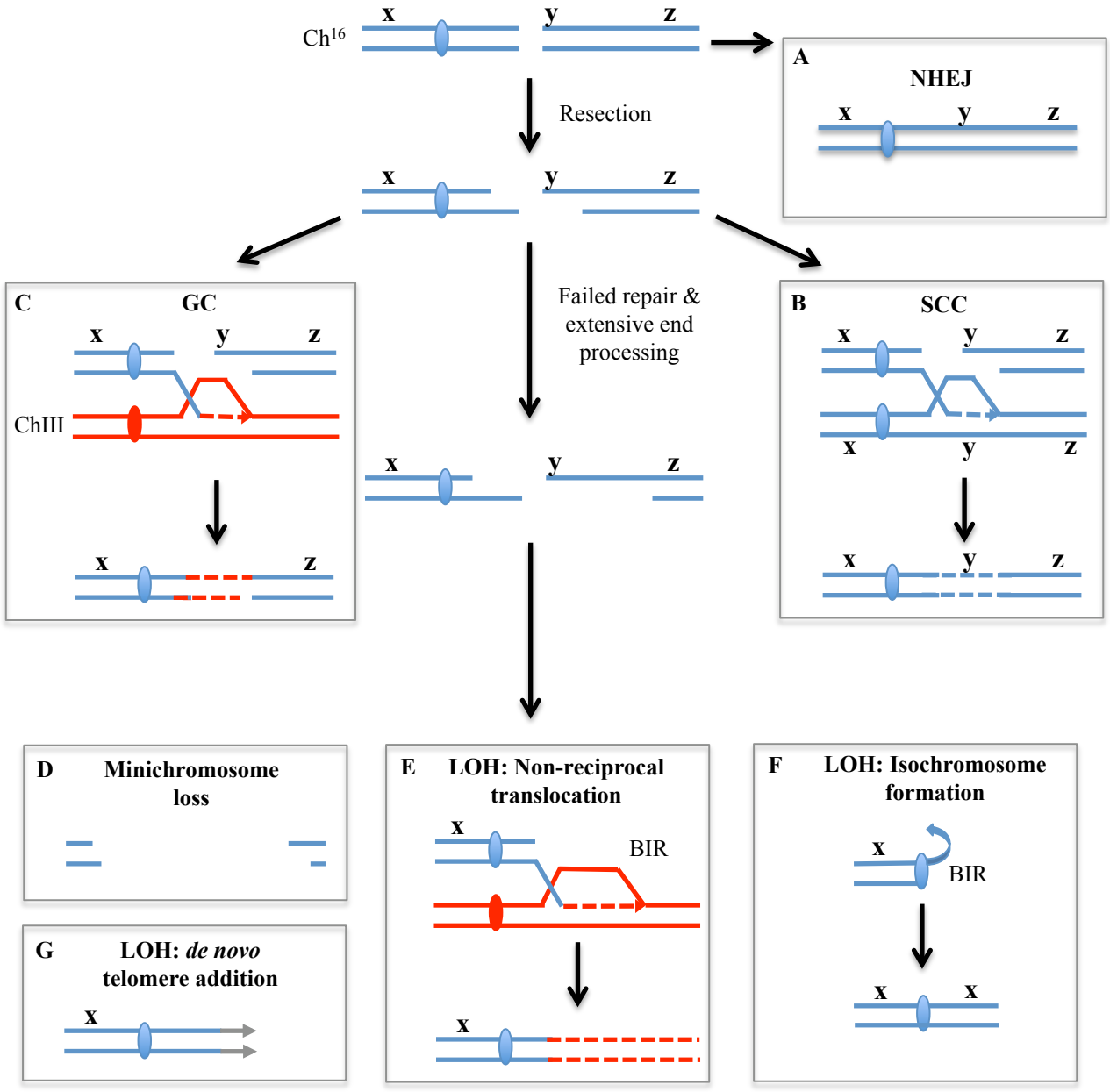


Figure 1.4 Schematic of DSB repair outcomes using the Ch[16] minichromosome Expression of the HO endonuclease results in formation of a single DSB at the *MATa* site on Ch[16] (blue). Repair by NHEJ (A), which does not require resection, cannot be discerned from SCC (B), as both outcomes result in retention of all markers on the minichromosome. In wildtype cells, the majority of repair is performed by HR, utilising ChIII (red) as a repair template, which results in loss of the marker adjacent to the break site (y; C). Failed repair results in extensive end processing which can lead to minichromosome loss (D) or LOH, through a non-reciprocal translocation (E), isochromosome formation (F) or *de novo* telomere addition at the break site (G). LOH results in loss of markers distal to the break (y and z), whereas minichromosome loss results in loss of all markers (x, y and z).

thus compacted (Bednar *et al*, 1998). Further, the absence of H1 prevents the proper condensation of chromosomes during mitosis in *Xenopus laevis* egg extracts (Maresca & Heald, 2006). The compaction of chromatin into these higher order structures helps distinguish two regions of chromosomes: euchromatin and heterochromatin. Whereas euchromatin is less condensed, gene-rich and highly transcribed, heterochromatin is considered more condensed, gene-poor and transcriptionally silent (Huisinga *et al*, 2006). Heterochromatin is generally associated with telomeric regions, centromeric regions and mating type loci in fission yeast, although in higher eukaryotes, there are often larger, more distinct heterochromatic regions.

The proper formation and regulation of chromatin is essential in preserving chromosome integrity, as in the absence of nucleosome assembly, spontaneous DNA damage occurs (Gunjan *et al*, 2005); thus, the factors that regulate this highly complex structure are of considerable interest.

1.5.1 Regulation of Chromatin

The regulation of chromatin structure is essential, as many processes taking place in the cell such as DNA repair, DNA replication and transcription, require the access of large protein complexes to DNA. Chromatin is highly restrictive in nature, and so for these processes to take place successfully, the chromatin structure must be modified. Among these mechanisms of regulation are chromatin remodelling, the incorporation of histone variants and histone modification.

Chromatin remodelling utilises energy produced during the hydrolysis of ATP by Snf2-like ATPases to alter the compaction of DNA. Chromatin remodellers have various functions in altering chromatin structure. They can function during chromatin organisation ensuring even

nucleosome spacing, in the restructuring of chromatin through incorporation of histone variants and in altering chromatin access through shifting or ejection of nucleosomes, which allows biological processes such as DNA repair and transcription to occur (reviewed in Clapier & Cairns, 2009).

Snf2 proteins are DNA translocases that apply ATP-dependent torsional strain on DNA, which disrupts histone-DNA contacts allowing nucleosome remodelling to occur (Bowman, 2010). There are four families of remodellers (SWI/SNF, ISWI, CHD and INO80) that all share a core ATPase domain, but also contain unique domains specialised for their particular functions (reviewed in Clapier & Cairns, 2009). The SWI/SNF family are characterised by the presence of a bromodomain and can slide and eject nucleosomes but are not involved in chromatin assembly (Mohrmann & Verrijzer, 2005). Alternatively, the ISWI group of remodellers contain SANT and SLIDE domains which cooperate to achieve nucleosome recognition. This group of remodellers are involved in optimising nucleosome spacing to promote chromatin assembly and some members of this group (e.g. NURF) are involved in randomly spacing nucleosomes to promote RNA polymerase II (RNAP II) activation (Corona & Tamkun, 2004). The CHD group of remodellers have ATPase domains that contain a chromodomain and PHD fingers, and this group slides and ejects nucleosomes and has various roles in the regulation of transcription and nucleosome spacing (Marfella & Imbalzano, 2007). Finally the INO80 group of remodellers contain split ATPase domains and are involved in various processes such as transcription and DNA repair. Furthermore, the SWR1 member of this group is involved in the incorporation of H2AZ-H2B dimers whereas another member INO80 replaces H2AZ-H2B with H2A-H2B (Bao & Shen, 2007b; Papamichos-Chronakis *et al*, 2011).

The activity of chromatin remodellers is controlled in a number of ways. Non-catalytic subunits of remodelling complexes are often involved in stabilising the interactions between the core nucleosome and the remodelling complex. Further, flanking linker DNA is required for the activity of various chromatin remodellers including Chd1, INO80 and the ISWI group (Clapier & Cairns, 2009). Remodeller ATPase activity is also regulated by histone determinants. For example, the ATPase activity of ISW2 and Chd1 is lowered by H4 acetylation whereas H4 acetylation stimulates RSC-dependent remodelling (Ferreira *et al*, 2007). This control of chromatin remodelling activity ensures the recruitment of factors required for biological processes that require a DNA template, such as DNA repair, DNA replication and transcription, occurs only at the appropriate time and location.

A second mechanism of regulating chromatin structure is through the incorporation of histone variants. In addition to the core histones that are synthesised in S phase, several histone variants exist which are synthesised constitutively at low levels and can be incorporated into the nucleosome during a range of distinct biological processes (Santenard & Torres-Padilla, 2009). There are universal histone variants found in the majority of eukaryotes in addition to lineage-specific variants specialised for their host organism. There are two highly conserved H2A variants, H2AX and H2AZ; in fission yeast two H2A genes share homology to H2AX and the third is a H2AZ orthologue. H2AX has well documented roles in DSB repair, where it is rapidly phosphorylated by the phosphoinositide 3-kinase-like kinases, ATM, ATR and DNA-PKcs resulting in recruitment and retention of repair factors (see section 1.7.1; Rogakou *et al*, 1999; Stiff *et al*, 2004; Ward & Chen, 2001). H2AZ-containing nucleosomes are usually found either side of nucleosome free regions at transcription start sites where they promote efficient RNAP II recruitment (Adam *et al*, 2001). Furthermore, there are additional roles for H2AZ in DNA repair, heterochromatin formation, gene activation and repression and nucleosome turnover (Altaf *et al*, 2009; Zlatanova & Thakar, 2008). Highly conserved histone

variants of H3 include CenH3 and H3.3. CenH3 is a centromere specific H3 variant that is essential for assembly of the kinetochore (Santaguida & Musacchio, 2009) and H3.3 can be deposited in both a replication-dependent and independent manner, is found in promoters and activated genes and is involved in transcription elongation (Henikoff, 2008; Schwartz & Ahmad, 2005; Sutcliffe *et al*, 2009). Additional lineage-specific histone variants exist including macroH2A, H2ABbd, TH2B and a number of H1 variants (reviewed in Talbert & Henikoff, 2010).

The final layer of regulation is through histone modification. Histone proteins can be post-translationally modified in a number of ways, including phosphorylation, acetylation, methylation, ubiquitylation and sumoylation (reviewed in Kouzarides, 2007). These modifications occur predominately on the histone tails, and thus affect interactions within and between nucleosomes and consequently chromatin compaction. The modification of histones has been implicated in a range of biological functions, including DNA repair, DNA replication and transcription. A more detailed introduction to histone modification will be undertaken in the subsequent section, with a particular focus on modification of lysine residues by acetylation and methylation.

These multiple layers of regulation of chromatin structure indicate the importance of altering compaction of DNA to allow distinct biological effects to take place. However, these regulatory mechanisms do not always act independently and interplay is common. For example, nucleosome remodelling at a promoter may be required before histone modification can occur and chromatin remodellers are often recruited and stimulated by specific histone modifications. In addition, the incorporation of histone variants requires the action of

chromatin remodellers. These complex interactions allow the chromatin to be rapidly altered to respond to changing situations in the cell.

1.6 HISTONE MODIFICATION

Post-translational histone modifications constitute a major mechanism by which cells regulate the structure and function of chromatin. At least eight types of histone modification have been documented: phosphorylation, methylation, acetylation, ubiquitylation, sumoylation, ADP ribosylation, deamination and proline isomerisation (reviewed in Kouzarides, 2007). These modifications occur mainly on the N-terminal histone tails, although some have been found on the globular domain, such as H3K56 which is acetylated by CBP/p300 in mammalian cells and Rtt109 in yeast (Das *et al*, 2009; Schneider *et al*, 2006; Xhemalce *et al*, 2007). Histone modifications bring about changes in two ways: either through disrupting DNA-histone contacts and altering chromatin compaction, or through affecting the recruitment of enzyme complexes for specific biological functions. This second function led to the proposal of the "histone code" whereby specific histone modifications lead to recruitment of enzyme complexes that stimulate distinct biological effects (Jenuwein & Allis, 2001; Strahl & Allis, 2000). This histone code relies on histone modifications being dynamic; indeed in addition to the identification of enzymes that modify histone residues, enzymes have been found that remove them. Further, for enzyme complexes to be recruited to specific modifications, domains that bind specific modifications are often present in the recruited complexes. Thus for each modification, there are 'writers' that catalyse addition of the modification, 'readers' that recognise and bind the modification, and 'erasers' that remove the modification.

The two most well characterised histone modifications are lysine methylation and acetylation, which have documented roles in transcription, DNA repair, DNA replication and chromosome compaction (reviewed in Kouzarides, 2007). The work in this thesis focuses on histone-

modifying enzymes that catalyse methylation or acetylation of lysine residues. Thus, the next section of this introduction will focus on these modifications, and the 'writers', 'readers' and 'erasers' associated with them.

1.6.1 Lysine acetylation and bromodomains

Acetylation of lysine residues has the most potential to 'unfold' chromatin, as addition of an acetyl group neutralises the basic charge of lysine, thus reducing the interaction between histones and DNA, allowing access of protein complexes to the DNA (Sterner & Berger, 2000). This is supported by the finding that acetylation of H4K16 has a negative impact on formation of the 30 nm chromatin fibre (Shogren-Knaak *et al*, 2006). Lysine acetylation and deacetylation is catalysed by histone acetyltransferases (HATs) and histone deacetylases (HDACs) respectively (Figure 1.5). HATs utilise Acetyl-CoA as a cofactor, and catalyse the transfer of an acetyl group to the ε-amino group of lysine side chains. There are several families of HATs including the GCN5 family, the p300/CBP family and the MYST family of which the core features of the catalytic domain are conserved. However, the N- and C-terminal flanking regions vary, allowing HATs to discriminate between targets (Marmorstein, 2001). There is however, some functional redundancy between HATs; a HAT can often acetylate various histone residues. For example in *S. pombe* both Gcn5 and Mst2 acetylate H3K14 and have additional histone targets (Howe *et al*, 2001; Nugent *et al*, 2010; Wang *et al*, 2012). Acetylation of lysine residues is a highly dynamic modification, and can be reversed within minutes through the action of HDACs (Sun *et al*, 2003; Waterborg, 2001). In general HDACs have fairly low substrate specificity and can target several residues for deacetylation (Robyr *et al*, 2002). The interaction of protein complexes with acetyl-lysines is mediated through protein interaction domains termed bromodomains (Dhalluin *et al*, 1999; Zeng & Zhou, 2002). Bromodomains are highly conserved through evolution, share a conserved fold and are often present in HATs and chromatin remodellers (Mujtaba *et al*, 2007; Owen *et al*, 2000). For example, the HAT Gcn5 contains a bromodomain which helps coordinate

nucleosome remodelling (Syntichaki *et al*, 2000) and the chromatin remodeller RSC is recruited to H3K14ac through tandem bromodomains in the Rsc4 subunit (Kasten *et al*, 2004).

1.6.2 Lysine methylation and the Royals

Unlike acetylation, methylation is considered a more stable modification. Is does not significantly alter the charge of the lysine residue and therefore acts mainly through the recruitment of protein complexes. Methylation occurs on both lysine and arginine residues, but here the focus is on the modification of lysine residues. Unlike acetylation, there is added complexity, in that lysine residues can be mono-, di- and tri- methylated by histone methyltransferases (HMTs; Figure 1.5), giving increased opportunity for functional output. The first HMT to be identified was the mammalian SUV39H1 which targets H3K9 for methylation (Rea *et al*, 2000). Since then many HMTs have been identified, the majority containing a SET (*Su(var)3-9, Ez, Trithorax*) domain, a 130 amino acid catalytic methyltransferase domain initially identified in *Drosophila melanogaster* (Jenuwein *et al*, 1998). However, some HMTs including members of the Suv-39 family require additional domains including pre- and post-SET domains for catalytic activity (Rea *et al*, 2000). In mammalian cells there are at least seventy gene sequences containing SET domains (Rea *et al*, 2000), but in fission and budding yeasts this number is much lower. Lysine HMTs function through the transfer of a methyl group from S-adenosylmethionine to lysine's ε-amino group. Demethylases (DMs) were first identified in 2004; LSD1 was shown to demethylate dimethylated H3K4 using FAD as a cofactor (Shi *et al*, 2004). LSD1 homologues exist in fission yeast; they demethylate H3K9 and are involved in heterochromatin propagation (Lan *et al*, 2007). Subsequent studies have shown the presence of another group of DMs which contain a Jumonji-C domain (reviewed in Mosammaparast & Shi, 2010). Indeed, many key histone methylations have now been shown to have a corresponding DM. Both HMTs and DMs have high specificity for their substrates compared

to HATs and HDACs. Further, some may only target the lysine residue to a specific degree, for example monomethylation; X-ray crystallography studies have shown this is often due to the presence of a specific residue in the catalytic domain. For example, SET7/9 can only monomethylate H3K4 and this is dependent on the presence of tyrosine 305 in the active site (Xiao *et al*, 2003).

There are many distinct domains that recognise methyl-lysine residues and lead to the recruitment of proteins. These include the 'royal' family of proteins, comprising chromo-, Tudor-, PWWP- and MBT-domains in addition to the PHD fingers (Kim *et al*, 2006; Maurer-Stroh *et al*, 2003; Shi *et al*, 2006). For example, the heterochromatin HP1 protein is recruited to H3K9me3, through its N-terminal chromodomain to regulate the formation of heterochromatin (Bannister *et al*, 2001).

1.6.3 Histone modification crosstalk

The large number of histone modifications that occur, mean that chromatin structure can be carefully regulated. However, additional complexity results from crosstalk between different modifications, further increasing the potential for control. There are several levels at which this crosstalk functions (reviewed in Bannister & Kouzarides, 2011). Multiple modifications can occur on a single residue; lysine residues can be methylated, acetylated and ubiquitylated, although these modifications are mutually exclusive at an individual lysine residue. For example, H3K36 can be both methylated and acetylated (Figure 1.5); in this way alternative modification may result in distinct biological effects. Further, an enzyme may recognise its substrate preferably when a second modification is present; an example of this is the recognition of H3 by GCN5, which is improved when it is phosphorylated at H3S10 (Clements *et al*, 2003). Alternatively, binding of an enzyme may be disrupted by an adjacent modification; H3S10p, the same modification that promotes GCN5 binding, inhibits HP1 binding and subsequent heterochromatin formation (Fischle *et al*, 2005). Furthermore, the

Figure 1.5

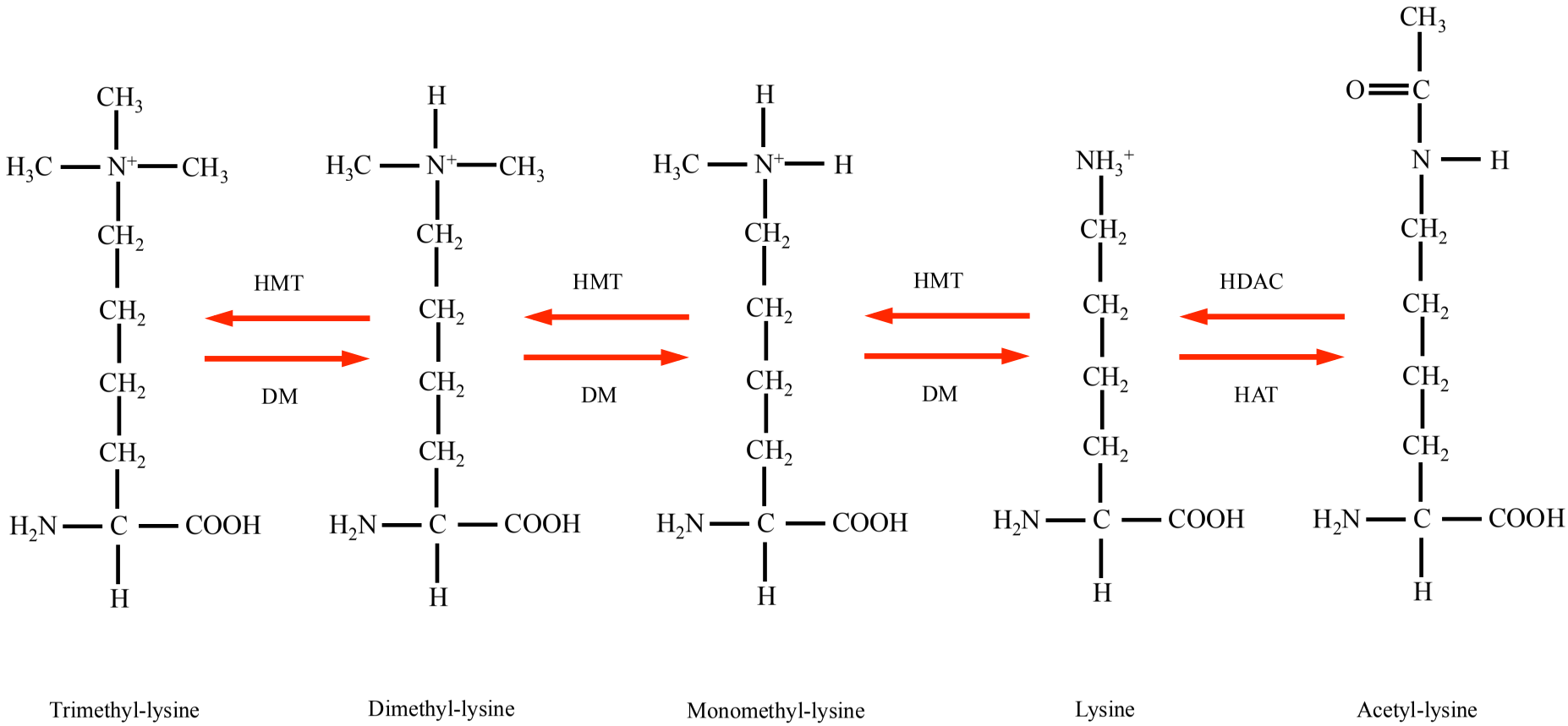


Figure 1.5 Acetylation and methylation of lysine residues Lysine residues can be acetylated and methylated. Histone acetyltransferases (HATs) acetylate lysine residues and this can be reversed by the action of histone deacetylases (HDACs). Lysine residues can also be mono-, di-or tri-methylated through the action of histone methyltransferases (HMTs); these methyl groups can be removed through the action of demethylases (DMs).

activity of a histone-modifying enzyme can be altered by substrate changes. For example, H3P38 isomerisation can affect H3K36 methylation by Set2 (Nelson *et al*, 2006). Finally, there may be cooperation between modifications on different histone tails, for example monoubiquitylation of H2BK123 is required for H3K4me3 (Lee *et al*, 2007). These various mechanisms of crosstalk, allow 'fine-tuning' of the biological consequences of histone modification.

1.6.4 H3K36 modification

This thesis focuses on the post-translational modification of H3K36. Methylation of H3K36 is highly conserved, and in mammalian cells there are at least eight enzymes that control methylation of this residue, to different degrees (reviewed in Wagner & Carpenter, 2012). On the other hand, in budding and fission yeast, a single enzyme, Set2 is responsible for all methylation of this residue (Morris *et al*, 2005; Strahl *et al*, 2002). Interestingly, whereas Set2 in yeast has only been shown to methylate H3K36, in mammalian cells, several of the H3K36 HMTs also methylate other histone residues, in addition to non-histone proteins, making it more difficult to assign loss of function phenotypes to these enzymes (reviewed in Wagner & Carpenter, 2012). In all species, methylation of H3K36 is associated with transcription, and SET2 proteins from multiple species interact with RNAP II via its C-terminal domain (Kizer *et al*, 2005). The function of H3K36me in transcription has been extensively characterised; in yeast Set2 is required for efficient transcription elongation and in budding yeast is required for the inhibition of spurious transcription through the recruitment of the Rpd3(S) HDAC complex (Carrozza *et al*, 2005; Li *et al*, 2007; Lickwar *et al*, 2009). This is conserved in mammalian cells where NSD3 is involved in transcriptional elongation and in creating a repressive chromatin environment during elongation, although not through deacetylation (Fang *et al*, 2010). Further, in mammalian cells NSD1 and NSD3 are also implicated in transcription initiation (Lucio-Eterovic *et al*, 2010; Rahman *et al*, 2011) and roles in transcriptional repression have also been documented in yeast and mammalian cells (Huang *et*

al, 1998; Landry *et al*, 2003; Strahl *et al*, 2002). In addition to well-characterised roles in transcription, methylation of H3K36 is also implicated in DNA replication and repair. A study in budding yeast showed reduced recruitment of Cdc45 to replication origins in *set2* cells (Pryde *et al*, 2009), and dimethylation by the mammalian METNASE is required for efficient DSB repair by NHEJ (Fnu *et al*, 2011). H3K36 DMs have also been identified; in mammalian cells KDM2A and JMJD2 (Klose *et al*, 2006; Whetstine *et al*, 2006), and in budding yeast Rph1, Jhd1 and Gis1 (Klose *et al*, 2007; Tu *et al*, 2007). However, despite the presence of orthologues in fission yeast, no H3K36 DM has been identified. It is worth noting that mutations in genes that code for H3K36 HMTs are associated with various diseases, including cancer (Table 1.2); further knowledge regarding the biological consequences of this modification may provide insights into how loss of this function results in the development of disease.

Table 1.2 H3K36 methyltransferases and their role in disease

Mutated Gene	Disease	Associated genetic changes
SETD2	Clear cell renal cell carcinoma, breast cancer	Deletions and missense mutations
NSD1	Cancers: breast, prostate, neuroblastoma, acute myeloid leukaemia	Translocations, silencing, overexpression
NSD1	Sotos syndrome	Point mutations, deletions, translocations, haploinsufficiency
NSD1	Myelodysplastic syndrome	Translocations
NSD2	Multiple myeloma	Translocations
NSD2	Wolf–Hirschhorn syndrome	Deletions
NSD3	Cancers: acute myeloid leukaemia, breast cancer	Translocations and gene amplifications
NSD3	Myelodysplastic syndrome	Translocations

Table adapted from Wagner and Carpenter 2012

In addition to methylation, H3K36 is acetylated in budding yeast, and this modification is conserved in human cells (Morris *et al*, 2007). Little is known about acetylation of H3K36, although the study by Morris *et al*, (2007) shows that this modification is located in the promoters of genes transcribed by RNAP II, an inverse pattern to methylation.

1.7 HISTONE MODIFICATION AND DSB REPAIR

Given the importance of chromatin in regulating and orchestrating the recruitment of enzyme complexes to DNA, it is not surprising that many histone modifications have roles in promoting efficient DSB repair. The work in this thesis focuses on the role of histone modification in DSB repair; therefore this section of the introduction will focus on previously characterised roles of histone modifications in promoting the efficient repair of DSBs. This is split into the role of histone modification in the early response to a DSB, in HR repair and in NHEJ repair (Figure 1.6). It is worth noting that chromatin remodelling is equally important in DSB repair (reviewed in Bao & Shen, 2007a); however, here the focus is on histone modification. The roles of histone modifications in DSB repair are highly complex, and often appear contradictory, with enzymes of opposing actions involved in the same mechanism of repair. Further characterisation will be required to determine how these modifications are orchestrated to promote a timely response to a DSB.

1.7.1 Histone modification and the initial response to a DSB

Several histone modifications have key roles in recruiting checkpoint and repair factors to a DSB. In DSB repair, the most well characterised histone modification is phosphorylation of H2AXS139 (H2A in yeast), an evolutionary conserved response to a DSB. This is one of the earliest events to occur at a DSB and is catalysed by the phosphoinositide 3-kinase-like kinases ATM, ATR and DNA-PKcs (Rogakou *et al*, 1999; Stiff *et al*, 2004; Ward & Chen, 2001). This modification can spread megabases from the break, and is required for the recruitment and retention of DDR proteins (e.g. NBS1, 53BP1 and BRCA1; Celeste *et al*, 2003) other histone modifiers (e.g. E3 ubiquitin ligases RNF8 and RNF168; reviewed in Greenberg, 2011) and chromatin remodellers (e.g. INO80; van Attikum *et al*, 2004). Acetylated H3K56 is also present early in the response to a DSB and this modification colocalises with γH2AX in addition to ATM and Chk2 (Vempati *et al*, 2010); however, whether this modification is required for recruitment of additional factors is not known.

Figure 1.6

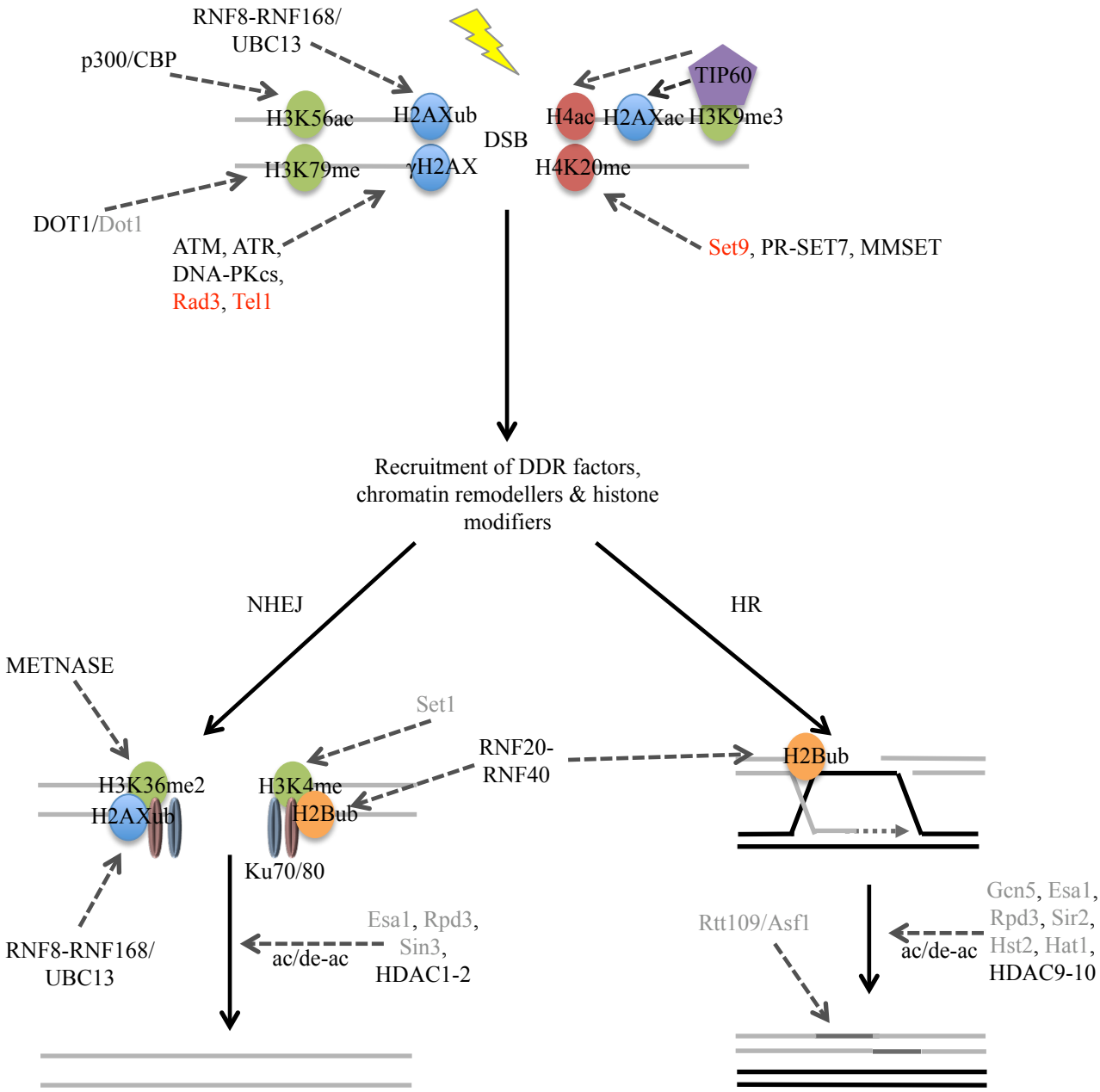


Figure 1.6 Schematic overview of histone modifications and histone-modifying enzymes involved in DSB repair Following DSB induction, H2AX is rapidly phosphorylated by kinases. This plays a key role in the recruitment of other factors to the break. H4K20 is methylated, which acts with H3K79me, H2AX ubiquitylation and H2AX phosphorylation to recruit further factors. TIP60 is activated by H3K9me3, which results in it acetylating H4, H2AX in addition to acetylating and further activating the ATM kinase. H3K56ac is also present on γH2AX nucleosomes. Histone modifications are also directly implicated in specific pathways of DSB repair. H3K4 and H3K36 methylation are required for efficient NHEJ through Ku70-80 recruitment. Acetylation, ubiquitylation and phosphorylation are also implicated in NHEJ repair. In both yeast and mammalian cells, acetylation has been shown to be important for HR repair. Local increases in acetylation are observed at DSBs, and acetylation of H4 is linked to repair factor recruitment. Ubiquitylation of H2B by Bre1 is also involved in HR repair, and maintaining genome stability. In addition, chromatin reassembly promoted by Rtt109 and Asf1 is required for signalling the completion of HR repair. Mammalian proteins are shown in black, *S. pombe* proteins in red and *S. cerevisiae* proteins in grey.

Another key histone modification in the early stages of DSB repair is H4K20 methylation. In fission yeast, methylation of this residue by Set9 is required for the recruitment of Crb2 (Sanders *et al*, 2004). However, there is no increase in H4K20 methylation following DNA damage; rather Sanders *et al* suggest increased exposure of this residue occurs following break induction. 53BP1 is recruited in a similar way in mammalian cells (Botuyan *et al*, 2006; Oda *et al*, 2010). However, there are additional layers of control: H3K79 methylation in budding yeast and mammalian cells (Huyen *et al*, 2004), RNF8 and RNF168 mediated H2AX-, and JMJ2A-ubiquitylation (Huen *et al*, 2007; Mallette *et al*, 2012) and H2A phosphorylation (Nakamura *et al*, 2004) are also required for the recruitment of these factors; this redundancy may reflect the importance of recruitment of these factors to ensure an appropriate DSB response.

TIP60 is a mammalian HAT, which is involved in DSB repair. It is recruited to a DSB via an interaction with ATM; however, the activation of TIP60 requires the release of HP1 from H3K9me3 (Sun *et al*, 2009). H3K9me3 is recognised by the TIP60 chromodomain, which leads to the activation of its HAT activity. TIP60 acetylates H4 at DSBs and this acetylation may lead to a more open chromatin structure, facilitating DSB factor recruitment (Murr *et al*, 2006). In addition, acetylation of H2AX by TIP60 results in its subsequent ubiquitylation (Ikura *et al*, 2007). Further TIP60 also acetylates ATM, which further activates this kinase (Sun *et al*, 2005).

These examples highlight the importance of crosstalk between histone modifications in fine tuning biological output. However, the presence of this crosstalk further complicates the elucidation of the precise mechanisms by which histone modifications affect DSB repair.

1.7.2 Histone modification and HR repair

There is evidence suggesting that some histone modifications are required specifically for HR repair. A study in budding yeast showed the HATs Gcn5 and Esa1 and the HDACs Rpd3, Sir2, and Hst2 are recruited to a HO-induced break 2-3 hours following induction. This recruitment is associated with an increase in acetylation of H3 and H4 residues. Following repair, this acetylation is removed in a HR-dependent manner (Tamburini & Tyler, 2005). Further studies in budding yeast have shown that Hat1 is required for HR repair, and is recruited directly to the site of the break (Qin & Parthun, 2002; Qin & Parthun, 2006). In mammalian cells the regulation of acetylation is also important for HR repair; HDAC9 and HDAC10 have been shown to be required for HR repair (Kotian *et al*, 2011). In addition, TRAAP (a HAT cofactor) and TIP60 localise to DSBs, and are associated with increased acetylation of H4 at a break; deletion of TRAPP results in reduced repair factor recruitment and reduced HR efficiency (Murr *et al*, 2006). Further work has also shown that TIP60 is required for homology-directed repair and RAD50 foci formation (Chailleux *et al*, 2010). A role for histone ubiquitylation in HR repair has also been reported. Ubiquitylation of H2B by the E3 ligase RNF20-RNF40 is required for HR repair in mammalian cells and defects in RNF20-RNF40 result in replication stress and chromosome instability (Chernikova *et al*, 2010; Chernikova *et al*, 2012; Moyal *et al*, 2011).

There are also important roles for histone modification in the restoration of chromatin structure following HR repair. In budding yeast, Rtt109 acetylates H3K56, which along with the histone chaperone Asf1 is required for the restoration of chromatin at the break site following successful repair (Chen *et al*, 2008). This acts as a signal of complete repair and results in checkpoint inactivation.

1.7.3 Histone modification and NHEJ repair

Specific histone modifications are also involved in NHEJ. Methylation of a number of residues has been shown to be important for efficient NHEJ repair, through recruitment of proteins to a DSB. In budding yeast, Set1, a H3K4 HMT, is recruited to a DSB in an RSC complex dependent manner, where it methylates H3K4 (Faucher & Wellinger, 2010). This methylation is required for the subsequent recruitment of Ku80 and efficient NHEJ. H3K36 methylation in mammalian cells has also been shown to be required for efficient NHEJ (Fnu *et al*, 2011). H3K36 dimethylation by METNASE occurs following IR treatment and is present at a DSB site; this methylation is required for the recruitment of Ku70 and NBS1. These data indicate that methylation of histone residues play an important role in recruiting Ku to a DSB; however, a role for histone methylation in NHEJ has not been documented in fission yeast.

Acetylation has also been implicated in NHEJ repair; in budding yeast acetylation of H4 lysine residues by Esa1 is required for efficient NHEJ, although the mechanism by which it functions is unknown (Bird *et al*, 2002). Confusingly, Rpd3 and Sin3 HDACs are also required for efficient NHEJ in budding yeast (Jazayeri *et al*, 2004) and HDAC1 and HDAC2, which deacetylate H3K56, stimulate NHEJ in mammalian cells, perhaps through preventing spreading of Ku70 from the break site (Miller *et al*, 2010). Furthermore, in mammalian cells the HAT GCN5 interacts with the Ku70-Ku80 heterodimer, which leads to its phosphorylation by DNA-PKcs and subsequent inhibition of its HAT activity (Barlev *et al*, 1998).

Ubiquitylation and phosphorylation of histones is also required for effective NHEJ repair. The E3 ubiquitin ligase RNF8 which ubiquitylates H2AX following induction of a DSB regulates

the abundance of KU80 at sites of DNA damage, and is required for efficient NHEJ repair (Feng & Chen, 2012). In addition, depletion of the mammalian Bre1 homologue, RNF20-RNF40, which ubiquitylates H2B, results in reduced KU80 and XRCC4 recruitment (Moyal *et al*, 2011). Phosphorylation of H2A in budding yeast is also required for efficient NHEJ (Downs *et al*, 2000). Clearly, the regulation of NHEJ by histone modification is highly complex, and further work will be required to discern the exact mechanisms by which these modifications function.

It is surprising that both HATs and HDACs are required for efficient NHEJ and HR repair; however, if opening of the chromatin structure by acetylation is required for the efficient recruitment of factors, chromatin structure must be restored following repair. In addition, it is possible that compaction of chromatin further from the break may allow the repair machinery to be focused at the DSB. Further, acetylation of some histone residues but not others may facilitate repair, which could explain the requirement of both enzyme classes.

1.8 DNA REPLICATION

DNA replication is a highly coordinated process that must occur only once per cell cycle to ensure the viability of the cell is maintained. DNA replication initiates from regions of the genome called replication origins and proceeds bidirectionally. DNA replication can be split into three stages: initiation, elongation and termination. Initiation is a highly regulated process, which leads to the formation of the repliosome. For initiation to occur the origins must first be licensed, by formation of the pre-replicative complex (pre-RC; Figure 1.7).

Pre-RC formation occurs in G1 phase, when the activity of cyclin-dependent kinase (CDK) is low (Baldinger & Gossen, 2009; Detweiler & Li, 1998; Piatti *et al*, 1996; Remus *et al*, 2005).

Figure 1.7

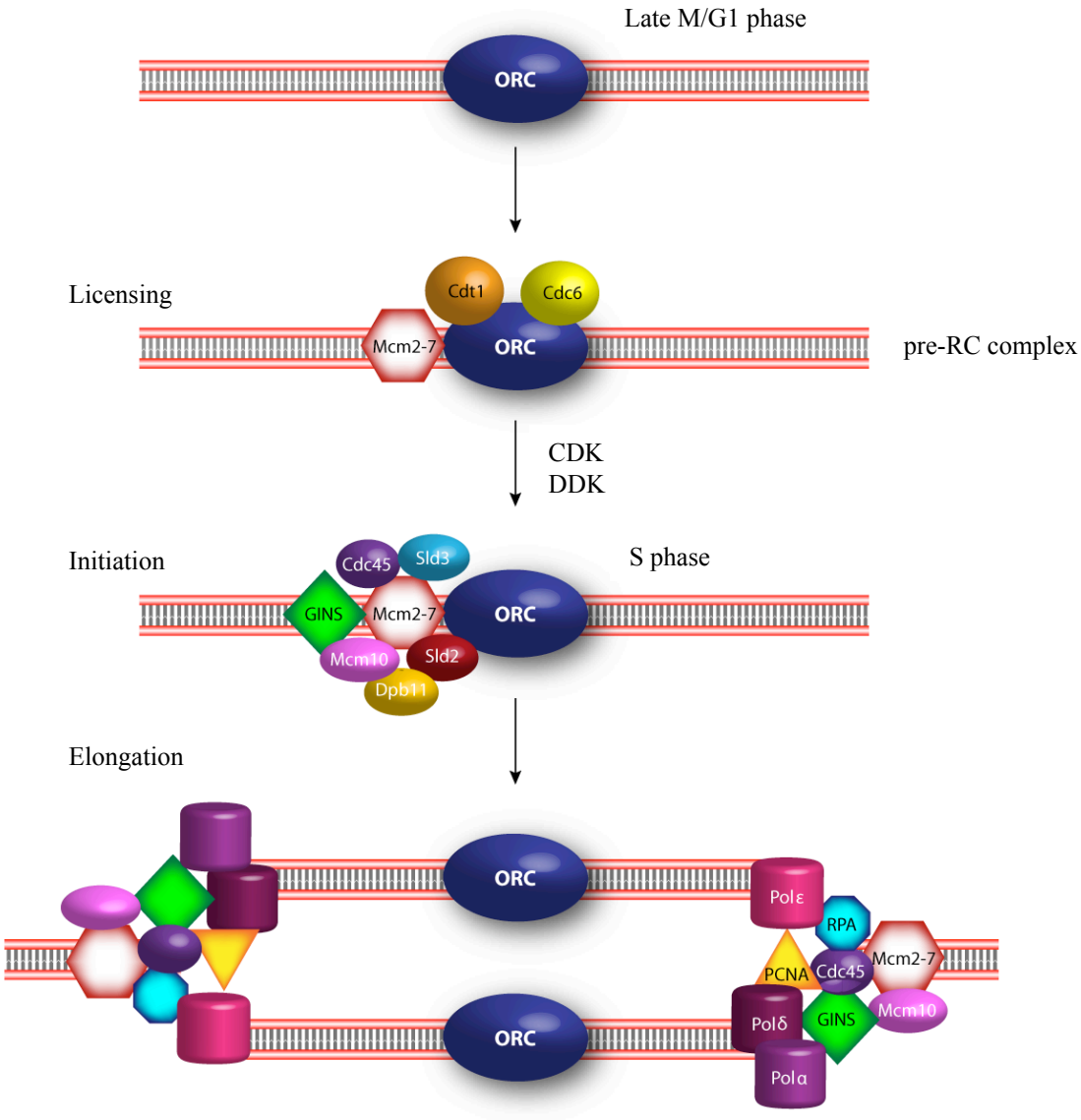


Figure 1.7 Schematic representation of DNA replication in eukaryotes Replication begins with the formation of the pre-replicative complex (pre-RC) by binding of Mcm2-7 proteins to the ORC, facilitated by Cdc6 and Cdt1. This occurs in late M and G1 phases, when CDK is inactive. Initiation of replication begins in S phase, when CDK is activated, resulting in recruitment of further replication factors. Recruitment of PCNA and DNA polymerases allows elongation to proceed. Adapted from Kearsey and Cotterill, 2003.

This begins with the binding of the origin recognition complex (ORC) to the origin; in fission yeast this is bound to the origin throughout the cell cycle, although this is not the case in higher eukaryotes (reviewed in Kearsey & Cotterill, 2003). Subsequent binding of $Cdc6^{Sc/Hs}$/$Cdc18^{Sp}$ and Cdc10-dependent transcript 1 (Cdt1) is dependent on the presence of ORC at the origin. Licensing is complete following the recruitment of the minichromosome maintenance 2-7 protein complex (Mcm2-7), facilitated by $Cdc6^{Sc/Hs}$/$Cdc18^{Sp}$ and Cdt1 (Donovan *et al*, 1997; Tanaka *et al*, 1997). The Mcm2-7 complex is the replicative helicase, and exhibits ATPase activity presumed to be required for unwinding of the DNA, to allow replicative polymerases to access ssDNA (Bochman & Schwacha, 2008; Pacek & Walter, 2004; Shechter *et al*, 2004).

Subsequent initiation takes place at the G1/S transition and requires the activity of CDK ($Cdc2^{Sp}$) and Dbf4-dependent kinase (DDK). The activation of CDK and DDK is required for the recruitment of numerous other replication factors including Cdc45 and GINS to the pre-RC (Figure 1.7). The Cdc45-Mcm2-7-GINS complex functions as an activated replicative helicase and is essential for DNA unwinding during the elongation phase of replication (Labib *et al*, 2000; Moyer *et al*, 2006; Pacek *et al*, 2006; Pacek & Walter, 2004; Shechter *et al*, 2004; Tercero *et al*, 2000). Next RPA binds the ssDNA at the replication origin, protecting it from nucleases and the formation of secondary structure that would prevent replication (Heyer *et al*, 1990; Szuts *et al*, 2003). DNA polymerases α, ε and δ are then recruited to the origin; Pol α functions in the synthesis of short primers for Okazaki fragments on the lagging strand and in priming the leading strand, Pol ε is the leading strand polymerase and Pol δ is the lagging strand polymerase (reviewed in Burgers, 2009; Hubscher *et al*, 2002; Pursell *et al*, 2007). Replication factor C (RFC) then loads the processivity factor proliferating cell nuclear antigen (PCNA) onto DNA; PCNA interacts with many proteins involved in DNA replication and is

involved in tethering Pol ε and δ to the leading and lagging strands respectively (Maga & Hubscher, 2003).

1.8.1 Preventing re-replication

To ensure that the genome is only replicated once per cell cycle, the formation of the pre-RC is tightly regulated and restricted to late M/G1 phases. In eukaryotes this regulation occurs in several ways: geminin-dependent inhibition of Cdt1 in metazoa; Cul4-Ddb1^{Cdt2} (CRL4^{Cdt2}) and PCNA dependent degradation of Cdt1 in S phase; and CDK-dependent inhibition of licensing. In addition, in *S. pombe* many replication genes are regulated by the MCB binding factor (MBF). MBF is a transcription factor comprising Cdc10, Res1, Res2, Rep1 and Rep2 that regulates genes containing MCB (*MluI* cell cycle box) motifs in their promoter (Lowndes *et al*, 1992; McInerny *et al*, 1995; White *et al*, 2001). The *cdt1*$^{+}$ and *cdc18*$^{+}$ genes are targets of MBF and so only transcribed in late M and G1 phases when licensing takes place (Hofmann & Beach, 1994; Jackson & Martin, 2006; Kelly *et al*, 1993).

Geminin is an inhibitor of Cdt1 present only in metazoa, and is proposed to prevent Cdt1 interaction with Mcm2-7 through steric hindrance (Lee *et al*, 2004). It also blocks Cdt1 DNA-binding as the geminin-binding and DNA-binding regions overlap (Yanagi *et al*, 2002) Geminin is recruited to chromatin following pre-RC formation, where it binds Cdt1 (Maiorano *et al*, 2004). Cdt1 is then exported from the nucleus in G2 and inhibited until the anaphase-promoting complex (APC) is activated in M phase, resulting in geminin destruction (McGarry & Kirschner, 1998).

During S phase, Cdt1 is targeted for proteolysis by ubiquitylation; the Cul4-Ddb1^{Cdt2} E3 ubiquitin ligase is responsible for this. In this system, Cdt1 is recruited to chromatin in S phase via an interaction with PCNA, through a PCNA-interaction protein motif (PIP box) in

the N-terminal of Cdt1; this targets Cdt1 for ubiquitylation and destruction (Arias & Walter, 2006; Guarino *et al*, 2011; Hu & Xiong, 2006; Jin *et al*, 2006; Senga *et al*, 2006).

A further level of control exists through CDK inhibition of licensing, a mechanism that is conserved throughout eukaryotes. This involves the direct inhibition of pre-RC components by CDK (reviewed in Diffley, 2004). In fission yeast targets include Cdc18 which is phosphorylated in S phase and targeted for degradation by the $SCF^{pop1/pop2}$ E3 ligase (Jallepalli *et al*, 1997; Kominami & Toda, 1997), and ORC, which is directly bound by Cdc2-Cdc13 in G2 and M phase, preventing pre-RC formation (Wuarin *et al*, 2002).

Although in fission yeast overexpression of $cdt1^{+}$ alone or inhibition of Cdc2 binding to ORC does not result in re-replication (Wuarin *et al*, 2002; Yanow *et al*, 2001), having three mechanisms for preventing re-replication ensures that genome integrity is maintained.

1.8.2 Histone modification and DNA replication

The structure of chromatin represents a significant barrier to DNA replication. Consistent with this is the observation that late firing origins are associated with heterochromatic DNA (Lima-de-Faria & Jaworska, 1968). In order for DNA replication to proceed, chromatin must be 'de-compacted' so that the replication machinery can access the origin and pre-RC formation can occur (reviewed in Falbo & Shen, 2006). In addition, during replication fork formation and progression, nucleosomes ahead of the replication fork must be disrupted and transferred behind the fork to reform chromatin structure. The histones are deposited on both the leading and lagging strand, and new histones incorporated to restore nucleosome density (reviewed in Groth *et al*, 2007). Re-establishment of histone modifications behind the replication fork is also essential to ensure the correct chromatin structure is maintained. In addition, some histone modifications are transient, and are involved in successful completion of DNA

replication; the current knowledge regarding the involvement of histone modification in DNA replication will briefly be considered here.

There is mounting evidence that the recruitment of replication factors can be influenced by the presence of histone modifications; either through the creation of specific binding sites for replication factors, or through creating a more permissive chromatin structure. H4K20 methylation is linked to DNA replication, and in mammalian cells monomethylation of this residue is performed by PR-SET7 (SET8; Fang *et al*, 2002). PR-SET7 is required for efficient S phase progression (Huen *et al*, 2008; Jorgensen *et al*, 2007; Tardat *et al*, 2007). In addition, PR-SET7 interacts with PCNA, and this interaction is required for the recruitment of PR-SET7 to replication forks and its subsequent degradation via the $CRL4^{Cdt2}$ E3 ubiquitin ligase (Abbas *et al*, 2010; Centore *et al*, 2010). Failure to degrade PR-SET7 in S phase results in accumulation of H4K20me1, premature chromatin compaction and G2/M arrest (Abbas *et al*, 2010; Centore *et al*, 2010). Although it is suggested that the role of PR-SET7 and H4K20me1 is primarily due to its role in chromatin condensation, other studies show that tethering PR-SET7 to a random locus promotes ORC1 recruitment and subsequent binding of MCM2 and MCM5 (Tardat *et al*, 2010). Thus degradation of PR-SET7 may constitute a mechanism to prevent re-replication by preventing ORC binding.

A number of other histone modifiers have been linked to MCM recruitment. H4K16ac is suggested to be required for proper recruitment of MCM, possibly through its function in inhibiting the formation of higher order chromatin structure, resulting in a more open chromatin state (Chiani *et al*, 2006; Shogren-Knaak *et al*, 2006; Shogren-Knaak & Peterson, 2006). HATs Gcn5 and Hbo1 have also been implicated in the recruitment of MCM; CDT1 recruits HBO1 to replication origins and this enhances Mcm2-7 loading, perhaps through

increasing DNA accessibility (Iizuka *et al*, 2006; Miotto & Struhl, 2008; Miotto & Struhl, 2010) and a study in budding yeast showed *gcn5* cells displayed reduced binding of MCM proteins to a replication origin (Espinosa *et al*, 2010).

There is also evidence of an involvement for histone modification in replication factor recruitment following successful pre-RC formation. In budding yeast, deletion mutants of the H3K36 HMT *SET2* show delayed DNA replication associated with a delay in Cdc45 binding to the origin (Pryde *et al*, 2009). Furthermore, a recent study in mammalian cells has identified a DNA replication associated modification, H3K56me1 (Yu *et al*, 2012). The authors suggest that H3K56 monomethylation by G9a acts as a docking site for PCNA; consequently when this modification is impaired there is reduced chromatin bound PCNA. Interestingly H3K56 acetylation by Rtt109 and Gcn5 is required for proper replication coupled nucleosome assembly (Burgess *et al*, 2010), and so differential modification of this residue at different stages of replication may control distinct biological effects.

The mechanisms underlying the involvement of histone modification in DNA replication are not well understood; in addition there are likely other histone-modifying activities involved that are as yet, unidentified. However, it is clear that chromatin structure plays a key role in the control of many processes that require access of large protein complexes to the DNA, including DNA replication.

1.9 AIMS OF THIS WORK

The efficient detection and repair of DSBs is essential to maintain genome stability, thereby preventing tumourigenesis. Given the necessity of appropriate chromatin structure in permitting effective DNA repair, the aim of this study was to utilise histone-modifying mutants from an *S. pombe* deletion library to identify novel histone-modifying enzymes required for DSB repair. The homologues of these genes may act as tumour suppressors in higher eukaryotes and thus their identification is of significant interest. Further, characterisation of any identified genes may help clarify the complex network of histone modifications that contribute to DSB repair.

CHAPTER 2
Materials and Methods

2.1 GENERAL LABORATORY SUPPLIES

General laboratory chemicals were of analytical grade purchased from Sigma-Aldrich, Fisher Scientific, BDH Laboratory Supplies and Invitrogen. Bacto-agar and Bacto-tryptone were purchased from Scientific Laboratory Supplies. EZmix™ yeast extract was purchased from Sigma-Aldrich. Gensieve LE agarose was obtained from Flowgen. All DNA ladders, restriction endonucleases, ligases, phosphatases, *Taq* DNA polymerase and Phusion High Fidelity DNA polymerase were obtained from New England Biolabs. dNTPs were purchased from Abgene and oligonucleotides from Sigma-Aldrich.

During this research, the following kits were used: Maxi-prep, Mini-prep, Gel extraction and PCR purification kits (Qiagen), MasterPure™ Yeast DNA Purification kit (Epicentre) and CHEF™ Yeast Genomic Plug Kit (Biorad).

During the course of this research the following centrifuges were used: Jouan CR4.12, Beckman Coulter Avanti J-26 XP, Beckman Coulter Optima L-100 XP Ultracentrifuge and Eppendorf microcentrifuge 5415D.

2.2 BUFFERS AND SOLUTIONS

Where appropriate, buffers provided with commercially obtained enzymes were used at concentrations specified by the manufacturer.

Non-commercial buffers and solutions used are listed below. All were made using purified water (MQ; Millipore system) and autoclaved or filter sterilised.

- **Phosphate buffered saline (PBS)**

  1 PBS tablet (Oxoid) per 100 ml MQ water.

- **PLATE solution**

  50% polyethylene glycol, 100 mM lithium acetate, 10 mM Tris-HCl (pH 4.2), 1 mM EDTA.

- **Lithium acetate/TE buffer (LiAc/TE)**

  100 mM lithium acetate, 10 mM Tris-HCl (pH 8.0), 1 mM EDTA (pH 8.0).

- **Polyethylene glycol/lithium acetate/TE buffer (PEG/LiAc/TE)**

  40% polyethylene glycol (PEG), 100 mM lithium acetate (pH 8.0), 10 mM Tris-HCl (pH 8.0), 1 mM EDTA (pH 8.0).

- **Tris-EDTA (TE) buffer**

  10 mM Tris-HCl (pH 8.0), 1 mM EDTA (pH 8.0).

- **10x loading dye**

  0.25% (w/v) bromophenol blue, 0.25% (w/v) xylene cyanol, 15% (w/v) ficoll.

- **50x Tris-Acetate EDTA (TAE) buffer**

  2 M Tris-HCl, 0.1 M EDTA (pH 8.0), 1 M acetic acid. Adjusted to pH 8.0 with acetic acid.

- **Laemmli buffer**

  125 mM Tris-Cl (pH 6.8), 100 mM dithiothreitol (DTT), 2% (w/v) sodium dodecyl sulphate (SDS), 0.1% (w/v) bromophenol blue, 10% (w/v) glycerol.

- **1x Running buffer**

  10 g/l SDS, 30 g/l Tris-Cl, 144 g/l glycine.

- **1x Transfer buffer**

  48 mM Tris-Cl, 39 mM glycine, 0.04% SDS, 10% methanol.

- **Spheroplasting buffer (SP buffer)**

  1 M sorbitol, 50 mM potassium phosphate (pH 6.5), 14 mM β-mercaptoethanol.

- **Lysis buffer**

  18% ficoll 400, 20 mM potassium phosphate (pH 6.5), 1 mM $MgCl_2$, 0.5 M EDTA (pH 8.0), 1 mM PMSF, 1 µg/ml leupeptin, 1 µg/ml pepstatin, 1x phosphate inhibitor cocktail, 2 µg/ml aprotinin.

- **NP buffer**

  0.34 M sucrose, 20 mM Tris-HCl (pH 7.4), 50 mM KCl, 5 mM $MgCl_2$, 1 mM PMSF, 1 µg/ml leupeptin, 1 µg/ml pepstatin, 1x phosphate inhibitor cocktail, 2 µg/ml aprotinin.

- **Cushion buffer**

  1.7 M sucrose in NP buffer.

- **Buffer A (for nuclear extraction)**

  10 mM Tris-HCl (pH 8.0), 0.5% NP-40, 75 mM NaCl, 1x protease inhibitor cocktail.

- **Buffer B (for nuclear extraction)**

  10 mM Tris-HCl (pH 8.0), 0.4 M NaCl, 1x protease inhibitor cocktail.

2.3 MEDIA

2.3.1 Growth of *Escherichia coli* (*E. coli*)

Luria-Bertani (LB) medium: 10 g/l Bacto-tryptone, 5 g/l Bacto-yeast extract, 10 g/l NaCl. 2% Bacto-agar added for solid media. When required, ampicillin was added to a final concentration of 50-100 µg/ml.

2.3.2 Growth of *Schizosaccharomyces pombe* (*S. pombe*)

Edinburgh Minimal Medium (EMM): 14.7 mM potassium hydrogen phthalate, 15.5 mM disodium hydrogen orthophosphate, 93.5 mM ammonium chloride, 2% glucose, 1x salt stock, 1x vitamin stock, 1x mineral stock. Supplements of adenine (A), leucine (L), uracil (U), histidine (H) and arginine (R) were added to a final concentration of 150 mg/l. When required thiamine was added to a final concentration of 2 µM. 2% Bacto-agar added for solid media.

Salts (x50): 260 mM magnesium chloride, 5 mM calcium chloride, 670 mM potassium chloride, 14.1 mM disodium phosphate.

Vitamins (x1000): 4.2 mM pantothenic acid, 81.2 mM nicotinic acid, 55.5 mM inositol, 40.8 μM biotin.

Minerals (x10000): 80.9 mM boric acid, 23.7 mM manganese sulphate, 13.9 mM zinc sulphate, 7.4 mM iron chloride, 2.47 mM molybdic acid, 6.02 mM potassium iodide, 1.6 mM copper sulphate, 47.6 mM citric acid.

SPAS6S: 10 g/l glucose, 1 g/l KH_2PO_4, 1 ml/l vitamins, 45 mg/l supplements. 2% Bacto-agar added for solid media.

YE6S (Yeast Extract + 6 supplements): 3% glucose, 0.5% EZmix™ yeast extract, 1.31 mM adenine, 1.45 mM L-histidine, 1.71 mM L-leucine, 2.01 mM uracil, 1.29 mM arginine, 1.23 mM L-lycine, 2% Bacto-agar added for solid media.

- YE6S and G418: 500 μg/ml Geneticin (G418) added post sterilisation.
- YE6S and Hyg: 180-240 μg/ml Hygromycin B (Hyg) added post sterilisation.

Yeast freezing mix (YFM)

1:1 mix of YE6S and glycerol.

***S. pombe* minimal glutamate (PMG)**

2% glucose, 14.7 mM potassium hydrogen phthalate, 15.5 mM Na_2HPO_4, 22 mM L-glutamic acid, 1x salt stock, 1x vitamin stock, 1x mineral stock. 2% Bacto-agar added for solid media. Required supplements were then added, as with EMM. PMG is compatible for selection with G418. G418 was added to agar media at 500 μg/ml post sterilisation.

2.4 STRAINS

2.4.1 *E. coli*

DH5α (*supE44, Δlac*U169, (*φ80lac*ZDM15), *hsdR*17, *rec*A1, *end*A1, *gyr*A96, *thi-1, rel*A1)

2.4.2 *S. pombe*

Non-minichromosome *S. pombe* strains used during this study are listed in Table 2.1. Minichromosome containing *S. pombe* strains used during this study are listed in Table 2.2.

Table 2.1 Non-minichromosome strains used in this study

Strain	Genotype	Source
TH2093/2094	*leu1-32 arg3-D4 ade6-M210 ura4-D18 his3-D1 h⁻/ h⁺*	Lab stock
TH4024	*leu1-32 arg3-D4 ade6-M210 ura4-D18 his3-D1 mat1_m-cyhS, smt0; rpl42::cyhR* (sP56Q) *h⁻*	Lab stock
TH3270/4500	***set1::ura4*** *ade6-M210 arg3-D4 his3-D1 leu1-32 ura4-D18 h⁻/ h⁺*	Robin Allshire
TH3271	***set2::ura4*** *ade6-M210 arg3-D4 his3-D1 leu1-32 ura4-D18 h⁻*	Robin Allshire
TH3771	***mst2::ura4*** *ade6-M210 arg3-D4 his3-D1 leu1-32 ura4-D18 h⁺*	Robin Allshire
TH3518	***sir2::ura4*** *leu1-32 his3-D1 ade6-M210 arg3-D4 ura4-D18 h?*	Lab stock
TH4827	***set5::kanMX*** *ade6-M210 leu1-32 ura4-D18 arg3-D4 his3-D1 rpl42::cycR* (sP56Q) *h⁺*	This study
TH3278	***hst2:: kanMX*** *h⁻*	Robin Allshire
TH4904	***set6:: kanMX*** *ade6-M210 leu1-32 ura4-D18 arg3-D4 his3-D1 rpl42::cycR* (sP56Q) *h⁺*	This study
TH3272	***set9::kanMX*** *leu1-32 uraDS/E arg3-D4 his3-D1 ade6-210 h⁺*	Robin Allshire
TH4826	***set8::kanMX*** *ade6-M210 leu1-32 ura4-D18 arg3-D4 his3-D1 rpl42::cycR* (sP56Q) *h⁺*	This study
TH5469	***set3::kanMX*** *ade6-M210 leu1-32 ura4-D18 arg3-D4 his3-D1 rpl42::cycR* (sP56Q) *h⁺*	This study
TH5468	***set13::kanMX*** *ade6-M210 leu1-32 ura4-D18 arg3-D4 his3-D1 rpl42::cycR* (sP56Q) *h⁺*	This study
TH3276	***clr3::kanMX*** *ade6-M210 ura4-D18 leu1-32 h⁺*	Robin Allshire
TH3718	***gcn5::kanMX*** *ade6-M210 leu1-32 ura4-D18 his-D1 arg3-D4 h⁺*	Lab stock
TH5467	***set10::kanMX*** *ade6-M210 leu1-32 ura4-D18 arg3-D4 his3-D1 rpl42::cycR* (sP56Q) *h⁺*	This study
TH5466	***SPBC16C6.01c::kanMX*** *ade6-M210 leu1-32 ura4-D18 arg3-D4 his3-D1 rpl42::cycR* (sP56Q) *h⁺*	This study
TH5464	***set11::kanMX*** *ade6-M210 leu1-32 ura4-D18 arg3-D4 his3-D1 rpl42::cycR* (sP56Q) *h⁺*	This study
TH5465	***hat1::kanMX*** *ade6-M210 leu1-32 ura4-D18 arg3-D4 his3-D1 rpl42::cycR* (sP56Q) *h⁺*	This study
TH6509	***elp3::kanMX*** *ade6-M210 leu1-32 ura4-D18 arg3-D4 his3-D1 rpl42::cycR* (sP56Q) *h⁺*	This study
TH3720	***clr4::kanMX*** *ade6-M210 leu1-32 ura4-D18 arg3-D4 his3-D1 h⁻*	Lab stock
TH2799	***rad3::ura4*** *ade6-M210 leu1-32 ura4-D18 arg3-D4 his3-D1 h⁺*	Lab stock
TH6316	***rad3::ura4 hat1::kanMX*** *ade6-M210 leu1-32 ura4-D18 arg3-D4 his3-D1 h?*	This study
TH6315	***rad3::ura4 set13::kanMX*** *ade6-M210 leu1-32 ura4-D18 arg3-D4 his3-D1 h?*	This study
TH3608	***rhp51::rhp51-eCFP-ura4*** *ade6-M210 leu1-32 ura4-D18 his3-D1 smt0 h⁻*	Lab stock
TH6313	***set13::kanMX rhp51::rhp51-eCFP-ura4*** *ade6-M210 leu1-32 ura4-D18 his3-D1 h?*	This study
TH6314	***hat1::kanMX rhp51::rhp51-eCFP-ura4*** *ade6-M210 leu1-32 ura4-D18 his3-D1 h?*	This study
TH3992-3	***rhp51::kanMX*** *ade6-210 arg3-D4 his3-D1 leu1-32 ura4-D18 h⁻/ h⁺*	Lab stock
TH1069	***lig4::ura4*** *ade6-704 leu1-32 ura4-D18 h⁻*	Tony Carr
TH5376-7	***set2::ura4 lig4::ura4*** *ade6-210 arg3-D4 his3-D1 leu1-32 ura4-D18 h⁻/ h⁺*	This study
TH5593	***ku70::kanMX*** *ade6-210 arg3-D4 his3-D1 leu1-32 ura4-D18 h?*	This study
TH5654-5	***set2::ura4 ku70::kanMX*** *ade6-210 arg3-D4 his3-D1 leu1-32 ura4-D18 h?*	This study
TH5153	***set2::ura4 rhp51::kanMX*** *ade6-210 arg3-D4 his3-D1 leu1-32 ura4-D18 h?*	This study
TH5310	***exo1::kanMX*** *ade6-210 arg3-D4 his3-D1 leu1-32 ura4-D18 h⁻*	This study
TH4999, 6199	***set2::ura4 exo1::kanMX*** *ade6-210 arg3-D4 his3-D1 leu1-32 ura4-D18 h?*	This study
DL1.6A9	***rqh1::kanMX*** *ade6-210 arg3-D4 his3-D1 leu1-32 ura4-D18 h⁺*	Lab stock
TH6197-8	***set2::ura4 rqh1::kanMX*** *ade6-210 arg3-D4 his3-D1 leu1-32 ura4-D18 h?*	This study

Strain	Genotype	Source
TH3423	***ctp1::kanMX*** *ade6-210 arg3-D4 his3-D1 leu1-32 ura4-D18 h*$^-$	Lab stock
TH6844	***set2::ura4 ctp1::kanMX*** *ade6-210 arg3-D4 his3-D1 leu1-32 ura4-D18 h?*	This study
TH6360	***lig4::ura4 exo1::kanMX*** *ade6-210 arg3-D4 his3-D1 leu1-32 ura4-D18 h?*	This study
TH6657-8	***exo1::ura4 ku70::kanMX*** *ade6-210 arg3-D4 his3-D1 leu1-32 ura4-D18 h?*	This study
TH5231	***nbs1::kanMX*** *ade6-210 arg3-D4 his3-D1 leu1-32 ura4-D18 h*$^+$	This study
TH5282	***set2::ura4 nbs1::kanMX*** *ade6-210 arg3-D4 his3-D1 leu1-32 ura4-D18 h?*	This study
TH5347	***rad50::kanMX*** *ade6-210 arg3-D4 his3-D1 leu1-32 ura4-D18 h*$^+$	This study
TH5390	***set2::ura4 rad50::kanMX*** *ade6-210 arg3-D4 his3-D1 leu1-32 ura4-D18 h?*	This study
TH5346	***rad32::kanMX*** *ade6-210 arg3-D4 his3-D1 leu1-32 ura4-D18 h?*	This study
TH5145	***set2::ura4 rad32::kanMX*** *ade6-210 arg3-D4 his3-D1 leu1-32 ura4-D18 h?*	This study
TH1542-3	***cdc25-22*** *leu1-32 ade6-D1 ura4-D18 his3-D1 h*$^+$*/h*$^-$	Lab stock
TH6707	***set2::ura4 cdc25-22*** *leu1-32 ade6-D1 ura4-D18 his3-D1 h?*	This study
TH6877	*h*$^-$	Lab stock
TH6236	***set2::kanMX*** *ade6-M210 leu1-32 ura4-D18 h*$^+$	Robin Allshire
TH6919-21	***set2::kanMX h?***	This study
TH6916	***set1::kanMX h?***	This study
TH6932	***tos4::kanMX cdc25-22*** *leu1-32 ade6-D1 ura4-D18 his3-D1 h?*	This study
TH6895	**Cdt1-TAP:kanMX** *cdc25-22 h*$^-$	Stephen Kearsey
TH6935	**Cdt1-TAP:kanMX** ***set2::kanMX*** *cdc25-22 h?*	This study
TH6959	**Cdc18-TAP:kanMX** *cdc25-22 h*$^-$	Stephen Kearsey
TH7011	**Cdc18-TAP:kanMX** ***set2::ura4*** *cdc25-22 h?*	This study
TH7018	**Cdc22-CFP:kanMX** *cdc25-22 ade6-704 leu1-32 ura4-D18 h?*	This study
TH6986	**Cdc22-CFP:kanMX** ***set2::ura4*** *cdc25-22 h?*	This study
TH6960	***cdc18-K46*** *h*$^-$	Paul Nurse
TH6961	***cdt1-19-ura4*** *leu1-32 ade6-D1 ura4-D18 his3-D1 h*$^+$	Paul Nurse
TH7014	***cdt1-19-ura4 exo1::ura4*** *leu1-32 ade6-D1 ura4-D18 his3-D1 h?*	This study
TH7039	***cdc18-K46 exo1::ura4*** *h?*	This study
TH7118	***cdt1-19-ura4*** *h?*	This study
TH6999	***set2::ura4 cdc25-22*** + p268 + p269 *h?*	This study
TH7002	***cdc25-22*** *leu1-32 ade6-D1 ura4-D18 his3-D1* + p268 + p269 *h?*	This study
TH7024	***wee1-50*** *ura4-D18 leu1-32 h?*	This study
TH7121	***set2::kanMX wee1-50*** *leu1-32 h?*	This study
TH244	*leu1-32 ade6-216 h*$^+$	Lab stock
TH7152-3	***set2::kanMX*** *leu1-32 ade6-216 h?*	This study
TH6366-7	***set2::set2-R255G-ura4*** *ade6-210 arg3-D4 his3-D1 leu1-32 ura4-D18 h*$^-$	This study
TH6835	***set2::set2-R255G-ura4 exo1::kanMX*** *h?*	This study
TH6842	***set2::set2-R255G-ura4 rad32::kanMX*** *h?*	This study
TH6843	***set2::set2-R255G-ura4 nbs1::kanMX*** *h?*	This study
TH6841	***set2::set2-R255G-ura4 rad50::kanMX*** *h?*	This study

Strain	Genotype	Source
TH7131	***set2::set2-R255G-ura4*** *h?*	This study
TH6238	***H3.1/H4.1::his3 H3.3/H4.3::arg3*** *ura4-DS/E ade6-M210 leu1-32 his3-D1 arg3-D4 h*$^{-}$	Robin Allshire
TH6241	***H3.2K36R H3.1/H4.1::his3 H3.3/H4.3::arg3*** *ura4-DS/E ade6-M210 leu1-32 his3-D1 arg3-D4 h*$^{-}$	Robin Allshire
TH6318	***set2:ura4 gcn5::kanMX*** *ade6-210 arg3-D4 his3-D1 leu1-32 ura4-D18 h?*	This study
TH7042	***gcn5::kanMX*** *h?*	This study
TH2148	***rad22::rad22-GFP-kanMX*** *h*$^{-}$	Miguel Ferreira
TH4823	***set2::set2-GFP-HA-kanMX*** *ade6-M216 leu1-32 lys1-131 ura4-D18 h*^{90}	YGRC*
TH7140	***gcn5::gcn5-GFP-HA-kanMX*** *ade6-M216 leu1-32 lys1-131 ura4-D18 h*^{90}	YGRC*
TH7289-90	***gcn5::kanMX rhp51::rhp51-eCFP-ura4*** *ade6-M210 leu1-32 ura4-D18 his3-D1 h?*	This study
TH5591	***alp13::kanMX*** *ade6-210 arg3-D4 his3-D1 leu1-32 ura4-D18 h?*	Shiv Grewal
TH6525	***set2::ura4 alp13::kanMX*** *ade6-210 arg3-D4 his3-D1 leu1-32 ura4-D18 h?*	This study
TH3274	***clr6-1*** *ade6-210 eu1-32 ura4-DS/E h*$^{-}$	Robin Allshire
TH6108	***cdk9::cdk9-T212A:kanMX*** *leu1-32 ura4-D18 his3-D1 ade6-M210 h*$^{+}$	Robert Fisher
TH6109	***cdk9::cdk9-T212E:kanMX*** *leu1-32 ura4-D18 his3-D1 ade6-M210 h*$^{+}$	Robert Fisher
TH1228	***csk1::ura4*** *ade6-210 his3-D1 leu1-32 ura4-D18 h*$^{-}$	Robert Fisher
TH6199	***set2::ura4 ku70::kanMX exo1::kanMX*** *leu1-32 ura4-D18 his3-D1 ade6-M210 h?*	This study

Table 2.2 Minichromosome strains used in this study

Strain	Genotype	Parent strain	pREP81X-HO	pREP81X
TH2125/6	*leu1-32 arg3-D4 ade6-M210 ura4-D18 his3-D1* **Ch^{16}-RMGAH**	-	TH2130-2	TH2357
TH2654/3165	*leu1-32 arg3-D4 ade6-M210 ura4-D18 his3-D1* **Ch^{16}-RMYAH**	-	TH4104, 4121-2 (6815 pREP82X-HO)	TH4125
TH3764-6	***set1::ura4*** *ade6-210 arg3-D4 his3-D1 leu1-32 ura4-D18* **Ch^{16}-RMGAH**	TH3270	TH3837-40	TH4247
TH3779-81	***set2::ura4*** *ade6-210 arg3-D4 his3-D1 leu1-32 ura4-D18* **Ch^{16}-RMGAH**	TH3271	TH3841-3	TH4249
TH3851-2	***mst2::ura4*** *ade6-210 arg3-D4 his3-D1 leu1-32 ura4-D18* **Ch^{16}-RMGAH**	TH3771	TH4292-4	TH4295
TH3602	***sir2::ura4*** *ade6-210 arg3-D4 his3-D1 leu1-32 ura4-D18* **Ch^{16}-RMGAH**	TH3519	TH3628-30	TH3657
TH5556-7	***set3::kanMX*** *ade6-210 arg3-D4 his3-D1 leu1-32 ura4-D18* **Ch^{16}-RMYAH**	TH5469	TH5635-7	TH5638
TH5592	***set11::kanMX*** *ade6-210 arg3-D4 his3-D1 leu1-32 ura4-D18* **Ch^{16}-RMYAH**	TH5464	TH5704-6	TH5766
TH5544-6	***hat1::kanMX*** *ade6-210 arg3-D4 his3-D1 leu1-32 ura4-D18* **Ch^{16}-RMYAH**	TH5465	TH5623-5	TH5626
TH5553-5	***set13::kanMX*** *ade6-210 arg3-D4 his3-D1 leu1-32 ura4-D18* **Ch^{16}-RMYAH**	TH5468	TH5631-3	TH5634
TH3782	***clr4::kanMX*** *ade6-210 arg3-D4 his3-D1 leu1-32 ura4-D18* **Ch^{16}-RMYAH**	TH3273	TH4296, 4383-4	TH3850
TH3785	***gcn5::kanMX*** *ade6-210 arg3-D4 his3-D1 leu1-32 ura4-D18* **Ch^{16}-RMYAH**	TH3280	TH3864, 6338-9	TH3844
TH5288-90	***set5::kanMX*** *ade6-210 arg3-D4 his3-D1 leu1-32 ura4-D18* **Ch^{16}-RMYAH**	TH4827	TH5342-4	TH5345
TH5053-5	***set6::kanMX*** *ade6-210 arg3-D4 his3-D1 leu1-32 ura4-D18* **Ch^{16}-RMYAH**	TH4904	TH5311-3	TH5314
TH5205	***set8::kanMX*** *ade6-210 arg3-D4 his3-D1 leu1-32 ura4-D18* **Ch^{16}-RMYAH**	TH4826	TH5319, 5478-9	TH5320
TH3786-8	***clr3::kanMX*** *ade6-210 arg3-D4 his3-D1 leu1-32 ura4-D18* **Ch^{16}-RMYAH**	TH3276	TH3865-7	TH3846
TH5550-2	***set10::kanMX*** *ade6-210 arg3-D4 his3-D1 leu1-32 ura4-D18* **Ch^{16}-RMYAH**	TH5467	TH5627-9	TH5630
TH5547-9	***SPBC16C6.01c::kanMX*** *ade6-210 arg3-D4 his3-D1 leu1-32 ura4-D18* **Ch^{16}-RMYAH**	TH5466	TH5619-21	TH5622
TH5943-5	***set2::ura4 lig4::ura4*** *ade6-210 arg3-D4 his3-D1 leu1-32 ura4-D18* **Ch^{16}-RMGAH**	TH3780 & 3516	TH5988-90	TH5987
TH3514-6	***lig4::ura4*** *ade6-210 arg3-D4 his3-D1 leu1-32 ura4-D18* **Ch^{16}-RMGAH**	TH3444	TH3568-70	TH3575
TH4741-3	***ku70::ura4*** *ade6-210 arg3-D4 his3-D1 leu1-32 ura4-D18* **Ch^{16}-RMGAH**	TH4454	TH4766-7, 4762	TH4763
TH5707-8, 6213	***set2::ura4 ku70::kanMX*** *ade6-210 arg3-D4 his3-D1 leu1-32 ura4-D18* **Ch^{16}-RMYAH**	TH5655	TH5770, 5772, 6853	TH5769
TH3353-5	***exo1::ura4*** *ade6-210 arg3-D4 his3-D1 leu1-32 ura4-D18* **Ch^{16}-RMGAH**	TH3326	TH3378-80	TH3392
TH3680-2	***set2::set2-R255G-ura4*** *ade6-210 arg3-D4 his3-D1 leu1-32 ura4-D18* **Ch^{16}-RMGAH**	TH6366/7	TH6397, 6415-7	TH6398
TH6512-3	***set2::ura4 gcn5::kanMX*** *ade6-210 arg3-D4 his3-D1 leu1-32 ura4-D18* **Ch^{16}-RMYAH**	TH6318	TH6545-7	TH6548
TH6506-8	***set2::kanMX*** *ade6-210 arg3-D4 his3-D1 leu1-32 ura4-D18* **Ch^{16}-RMYAH**	TH6236	TH6549-51	TH6552
TH6566-7	***elp3::kanMX*** *ade6-210 arg3-D4 his3-D1 leu1-32 ura4-D18* **Ch^{16}-RMYAH**	TH6509	TH6521-2, 6656	TH6520
TH7035-7	***set2::ura4 exo1::ura4*** *ade6-210 arg3-D4 his3-D1 leu1-32 ura4-D18* **Ch^{16}-RMGAH**	TH3779, 3354	TH7091-4	TH7095
TH6947-9	***gcn5::kanMX lig4::ura4*** *ade6-210 arg3-D4 his3-D1 leu1-32 ura4-D18* **Ch^{16}-RMYAH**	TH3785, 3444	TH6973-6	TH6978
TH6806-8	***cdk9::cdk9-T212E-kanMX*** *ade6-210 arg3-D4 his3-D1 leu1-32 ura4-D18* **Ch^{16}-RMYAH**	TH6751	TH6846-8	TH6845
TH6799, 6802, 6817-8, 6780	***gcn5::kanMX*** **pREP3X-Gcn5(p255)** *ade6-210 arg3-D4 his3-D1 leu1-32 ura4-D18* **Ch^{16}-RMYAH**	TH3280	TH6799, 6802, 6817-8	TH6780

*Yeast Genetic Resource Center

DL1 = strain from deletion library version 1.

Mating types are shown where possible; mating type is not shown where multiple isolates were constructed and consequently $h^+$and h^- strains exist.

The parental strain given is the auxotrophic deletion strain into which the minichromosome was added, achieved through mating with the corresponding parental minichromosome strains shown in lines 1 and 2 of the table.

Minichromosome genotypes:

Ch^{16}-RMGAH (Ch^{16} *yps1::arg3$^+$ert1::MAT*a-*kanMX ade6-M216 cid2::his3$^+$*)

Ch^{16}-RMYAH (Ch^{16} *yps1::arg3$^+$ert1::MAT*a-*hph ade6-M216 cid2::his3$^+$*)

2.5 PLASMIDS

Plasmids used and created during this study are described in Appendix I.

2.6 STORAGE AND GROWTH CONDITIONS

2.6.1 Growth and storage of *E. coli* strains

E. coli transformed with plasmid DNA were plated onto LB+Amp, and incubated O/N at 37°C to obtain single bacterial colonies. For small-scale plasmid DNA preparation (mini-prep) single *E. coli* colonies were picked from an LB+Amp plate, inoculated into 5 ml LB+Amp media and cultured O/N at 37°C with shaking. For large-scale plasmid DNA preparations (maxi-prep), a 3 ml culture from a single colony was grown for 6-8 hours and used to prepare a 500 ml LB+Amp culture. This was subsequently cultured O/N at 37°C with shaking. Permanent stocks of *E. coli* strains were stored in Nunc cryo-tubes containing 0.5 ml of prepared culture and 0.5 ml of glycerol at -80°C.

2.6.2 Growth and storage of *S. pombe* strains

Strains were cultured and stored as described in Moreno *et al*, 1991. Cells were cultured in either non-selective, nutrient rich media (YE6S) or Edinburgh minimal media (EMM) with 15 mg/l required supplements. Strains were grown at 32°C for 2-3 days and then stored at room temperature.

Liquid cultures were prepared by inoculating a single colony or a loop of cells, taken from a fresh agar plate, into medium. Cultures were grown O/N with shaking at the appropriate temperature. The absorbance at 595 nm (optical density OD_{595}) in a Pharmacia Biotech Ultraspec 2000 was used as a measure of cell density; an OD_{595} of 0.1 being ~2 x 10^6 cells/ml. Unless stated, cultures were maintained in mid-exponential growth between 2 x 10^6 and 1 x 10^7 cells/ml (OD_{595} between 0.1 to 0.5). Permanent stocks of yeast strains were stored in Nunc cryo-tubes in 0.5 ml YE6S and 0.5 ml YFM at -80°C.

2.6.3 Genetic crosses, tetrad analysis and random spore analysis

Genetic crosses were carried out on SPAS6S agar and incubated at 25°C for 48 hours. Light microscopy was used to check for spores and the correct genotype identified using tetrad or random spore analysis.

Tetrad analysis was performed by micromanipulation of the asci onto YE6S agar plates using a Singer MSM micro-manipulator. Asci walls were allowed to break down at 18°C O/N, after which the spores were separated onto a virtual grid. The spores were incubated until colonies were visible, these could then be replica plated onto selective plates to determine the phenotype and identify desired progeny.

For free spore analysis, a 1 µl loop of cells from the desired mating was mixed with 1 ml MQ water and 5 µl β-glucuronidase, and incubated at 37°C for 6 hours. A 1:100 dilution was plated onto selective media and grown for 4-5 days at 32°C. The desired progeny were selected by replica plating onto selective plates and the phenotype determined.

2.6.4 Analysis of cell growth and viability

2.6.4.1 Serial dilution assay

Cells were grown in liquid culture at 32°C with shaking until the culture reached an OD_{595} of approximately 0.2. Cell concentration was adjusted to OD_{595} 0.2 in 200 µl, and 5-fold serial dilutions made using MQ water. 8 µl of each dilution was spotted onto appropriate plates. To test for sensitivity to DNA damaging agents, the dilution series was spotted onto YE6S plates containing 1 or 0.3 µg/ml bleomycin, 5 mM hydroxyurea (HU), 0.005% methylmethane sulphonate (MMS) or 5 µM camptothecin (CPT). To test for sensitivity to ionising radiation (IR), spotted YE6S plates were exposed to the desired Gy of gamma radiation (^{60}Co). The resultant plates were incubated at 32°C for 2 days and then photographed.

2.6.4.2 Survival curve

Logarithmically growing cells were either irradiated using a ^{60}Co source at a dose rate of 31 Gy/minute or treated with bleomycin for 1 hour. Following treatment cells were plated onto 3x YE6S plates and incubated at 32°C for 3 days before colonies were counted. Percentage survival for each damage dose was calculated by (number of colonies following damage/number of colonies before damage) x 100. Experiments were performed in triplicate.

2.7 DNA TRANSFORMATION

2.7.1 Transformation of *E. coli*

2.7.1.1 Preparation of competent bacteria

A single DH5α colony was inoculated in 5 ml LB medium and cells were grown overnight at 37°C. A 1:100 dilution of the overnight culture was made in LB, and this was grown for 1-2 hours at 37°C until OD_{595} was 0.6. Cells were chilled on ice for 15 minutes and then centrifuged at 1730 *g* for 15 minutes at 4°C. The pellet was resuspended in 20 ml cold 50 mM $CaCl_2$ and left on ice for 15 minutes. The cells were centrifuged at 1730 *g* for 10 minutes at 4°C, the pellet resuspended in 1 ml cold 50 mM $CaCl_2$ and then left on ice for 15 minutes. Cells were stored at −80°C until required.

2.7.1.2 Transformation

0.2 ml of competent cells were added to 0.1 ml 0.1 M Tris-Cl (pH 7.2) and incubated with the DNA on ice for 30 minutes, heat shocked for 90 seconds at 42°C and left on ice for 2 minutes. 1 ml LB medium was added and cells were incubated at 37°C for 1 hour with shaking. Cells were plated onto LB + Amp and incubated at 37°C overnight.

2.7.2 Transformation of *S. pombe*

2.7.2.1 Transformation by electroporation

50 ml culture was incubated at 32°C until OD_{595} reached 0.3-0.5, and cells were chilled on ice for 10 minutes. Cells were centrifuged at 931 *g* for 2 minutes, washed once with MQ water, once with 1 M sorbitol and then resuspended in 1 ml 1 M sorbitol. The cell suspension was centrifuged at 15700 *g* for 10 seconds and resuspended in 1 M sorbitol at a 1:1 ratio. 45 µl of cells were mixed with 1 µg DNA in a chilled electroporation cuvette (0.1 cm gap), and electroporation was performed at: Field strength, 0.66 kV/cm; Resistance 200 Ω; Capacitance, 25 µF. 600 µl 1 M sorbitol was immediately added to the cells and 150 µl was plated onto selective media and grown at 32°C for 4 days.

2.7.2.2 Transformation by LiAc method

20 ml of culture was grown at 32°C until OD_{595} reached 0.5. Cells were washed once in MQ water, resuspended in 1 ml MQ water and transferred to an eppendorf tube. Cells were centrifuged at 1500 *g* for 1 minute, resuspended in 1 ml 1 M LiAc/TE, centrifuged at 1500 *g* for 1 minute and then resuspended in 100 µl 1 M LiAc/TE. The cell suspension was mixed with 1 µg DNA and 2 µl sheared carrier DNA (10 mg/ml) and left at room temperature for up to 1 hour. 260 µl 40% PEG/LiAc/TE was added and the cell suspension incubated at 30°C for 1 hour. 43 µl DMSO was added and cells heated at 42°C for 5 minutes. Cells were plated onto selective media and grown at 32°C for 4 days.

2.7.2.3 Transformation by PLATE method

A 1 µl loop of cells was added to 500 µl PLATE solution, 10 µl sheared carrier DNA (10 mg/ml) and 1 µg transforming DNA. The cell suspension was left at room temperature for 4 days and then heat shocked at 42°C for 15 minutes. Cells were plated onto selective media and grown at 32°C for 4 days.

2.8 DNA ISOLATION

2.8.1 Plasmid isolation from *E. coli* (mini-prep and maxi-prep)

An LB culture with ampicillin was inoculated with a single colony and grown at 37°C overnight. Qiagen Mini-prep or Maxi-prep was performed according to manufacturer's instructions, based on rapid alkaline lysis.

2.8.2 Isolation of *S. pombe* genomic DNA

Genomic DNA was isolated and purified using the MasterPure^{TM} Yeast DNA Purification Kit (Epicentre), as per manufacturer's instructions.

2.8.3 Isolation of DNA from agarose gels

DNA was first separated by agarose gel electrophoresis. The desired band was excised and the DNA isolated using a Qiagen Gel Extraction Kit, as per manufacturer's instructions.

2.8.4 PCR purification

DNA from PCR was purified using Qiagen PCR Purification Kit, as per manufacturer's instructions.

2.9 DNA MANIPULATION AND ANALYSIS

2.9.1 Restriction digestion of DNA

1 µg of DNA was added to 1x enzyme specific buffer, 1x BSA if required and 1 µl restriction enzyme. This was incubated at 37°C for 2 hours, and the enzyme inactivated where possible. Digested DNA was visualised by agarose gel electrophoresis.

2.9.2 DNA dephosphorylation and ligation

Plasmid DNA was dephosphorylated where appropriate using 1 U Antarctic Phosphatase (NEB) in 1x Antarctic Phosphatase buffer for up to 1 hour. For DNA ligation, 50 ng vector and a 3x molar excess of insert was added to 1x T4 DNA ligase buffer and 1 U T4 ligase (NEB), and incubated at room temperature for 4 hours.

2.9.3 Polymerase Chain Reaction (PCR)

The polymerases used to amplify DNA were Phusion™ or *Taq* (both from NEB). For Phusion PCR, a typical reaction consisted of 1x Phusion GC buffer, 800 µM dNTP mix, 0.5 µM forward and reverse primers, 50 ng template DNA, 3% DMSO and 1 U Phusion polymerase. For *Taq* PCR, a typical reaction consisted of 1 x *Taq* buffer, 800 µM dNTP mix, 0.5 µM forward and reverse primers, 50 ng template DNA, and 1 U *Taq* polymerase. For colony PCR, Megamix Blue was used; in this case, template DNA was added to 20 µl Megamix Blue, and primers added to 0.5 µM. Oligonucleotides used in this study are shown in Appendix II.

Standard PCR conditions used:

94°C for 5 minutes, 30 cycles (94°C for 20 seconds, X°C for 30 seconds, 68°C for Y minutes), 68°C for 7 minutes.

Y, the extension time was determined by size of PCR product and processivity of polymerase. For Phusion™ processivity is 15-30 seconds/kb and for *Taq* is 1 minute/kb.

X, the annealing temperature was generally set at 4°C below the lowest melting temperature of the forward and reverse primers.

The PCR product was examined using agarose gel electrophoresis.

2.9.4 Quantification of DNA samples

DNA concentration was determined using a Nanodrop 1000 spectrophotometer (Thermo Scientific). Samples were diluted in MQ to a suitable concentration and read at an absorbance at 260 nm and 280 nm. An A_{260}/A_{280} ratio of 1.8 signifies a pure, protein-less DNA solution. Concentration was calculated in µg/µl.

2.9.5 DNA sequencing

Purified plasmid or PCR DNA was sequenced by Source BioScience LifeSciences (Oxford).

2.9.6 Analysis of DNA by gel electrophoresis

2.9.6.1 Agarose gel electrophoresis

Generally DNA was separated on 1% agarose TAE gels, unless DNA was <500 bp in which case 1.8% agarose gels were used. DNA was stained using 500 ng/ml EtBr. NEB 1 kb ladder and low molecular weight ladders were used, and gels were run at 80 V for 1 hour. The DNA was then observed using a UV transilluminator and an image captured using Quantity-One (BioRad).

2.9.6.2 Contour-clamped homogeneous electric field (CHEF) pulsed field gel electrophoresis (PFGE)

Chromosomal DNA was prepared using the CHEF^{TM} Yeast Genomic Plug Kit. 10 ml culture was grown O/N in selective medium and a volume corresponding to 5 x 10^8 cells was harvested (931 *g* for 2 minutes). The pellet was subsequently washed 3x in ~2 ml chilled 0.05 M EDTA. 122 µl Cell Suspension Buffer and 6 µl Lyticase was added to the pellet, this was suspended in 70 µl 2% Clean Cut agarose and transferred into 3x plug moulds. After the plugs had solidified (4°C for 1 hour), 463 µl Lyticase Buffer and 16 µl Lyticase was added and incubated O/N at 37°C. The lyticase solution was removed, washed 3 times with MQ water and replaced with 470 µl Proteinase K buffer and 19 µl Proteinase K, which was incubated at 50°C O/N. Following the removal of the proteinase solution the plugs were washed 3x in 1x Wash Buffer with agitation and an hour between each wash. Plugs were stored at 4°C before being loaded.

Samples were run on a 0.8 % (w/v) chromosomal grade agarose gel in 1xTAE. Chromosomes were separated using the CHEF Mapper^{TM} system, at 2 V/cm and 106° angle for 72 hours at 14°C. Switch times increased in a linear fashion from 20 minutes initially to a final time of 60 minutes. Gels were post stained in 1 µg/ml EtBr for an hour, and subsequently visualised using a UV transilluminator and imaged using Quantity-One.

2.10 DNA DOUBLE-STRAND BREAK (DSB) REPAIR ASSAYS

2.10.1 The DSB assay

Three independently isolated Ch^{16}-RMGAH or Ch^{16}-RMYAH strains for each mutant background were analysed, each transformed with pREP81X-HO plasmid (p28). Break-independent events were assessed by analysis of strains transformed with a blank plasmid, pREP81X (p40). A wildtype strain was analysed alongside all mutant strains to monitor experimental variation. The assay was carried out at 32°C unless otherwise stated.

The strains were grown on selective media (+ thiamine; DSB off), and then streaked onto YE6S + G418 or hygromycin and incubated O/N at 32°C, to ensure the *MATa* site is present. 20 ml selective cultures were grown O/N and diluted the following morning to OD_{595} 0.1. Following a further 3 hours growth cells were harvested (931 *g* for 2 minutes) and washed twice with 20 ml PBS. Pellets were resuspended in EMM+RAHU (-T; DSB on) and the cultures incubated with agitation for 48 hours at 32°C, maintained in logarithmic phase. Following 48 hours growth the cells were plated onto 3x YE6S plates such that ~500 colonies were present per plate and incubated at 32°C for 3 days. The plates were replica plated onto selective plates, which allowed the percentage of non-homologous end-joining or sister chromatid conversion (NHEJ/SCC), interchromosomal gene conversion (GC), minichromosome loss (Ch^{16} loss) and loss of heterozygosity (LOH) to be calculated (Table 2.3). Spontaneous levels of Ch^{16} loss, GC or LOH, calculated from the blank plasmid controls, were subtracted from the levels observed following break induction to give final levels of break-dependent outcomes. Statistical significance was calculated using the student T-test. Certain colony endpoints from the DSB assay were isolated and analysed via PFGE.

Table 2.3 Outcomes of the DSB assay and the marker loss associated with each event

Ch^{16}	Replica plated onto:	Outcome			
		NHEJ/SCC	GC	Ch^{16} loss	LOH
RMYAH	EMM+ AHULT (arg-)	arg^+	arg^+	arg^-	arg^+
	EMM+ RHULT (ade-)	ade^+	ade^+	ade^-	ade^-
	EMM+ RAULT (his-)	his^+	his^+	his^-	his-
	YE6S + hyg	hyg^R	hyg^S	hyg^S	hyg^S
RMGAH	EMM+ AHULT (arg-)	arg^+	arg^+	arg^-	arg^+
	EMM+ RHULT (ade-)	ade^+	ade^+	ade^-	ade^-
	EMM+ RAULT (ura-)	his^+	his^+	his^-	his-
	YE6S + G418	$G418^R$	$G418^S$	$G418^S$	$G418^S$

2.10.2 The NHEJ assay

The cohesive-ended substrates for the NHEJ assay were prepared by excision of a ~500 bp PstI fragment from PS (p100) or a ~540 bp EcoRI fragment from PI (p101) followed by gel purification of the remaining linear vector. Logarithmically growing cells (20 ml of OD_{595} 0.5) were transformed with 1 µg of undigested control plasmid pAL19 (p102) or linear DNA using the lithium acetate method (2.7.2.2). The plasmids contain a LEU2 marker, so NHEJ frequency was calculated as the percentage of *leu*+ colonies arising from cells transformed with linear plasmid over those transformed with undigested DNA (See Appendix I for plasmid details). At least three experiments were performed for each strain, and the average percentage rejoining calculated.

2.11 RNA EXTRACTION, MANIPULATION AND ANALYSIS

2.11.1 RNA extraction

1 x 10^8 cells were centrifuged at 931 *g* for 2 minutes, the supernatant discarded and the pellet snap frozen and stored at -80°C until processing. Cells were thawed on ice, resuspended in 1 ml pre-chilled diethyl pyrocarbonate (DEPC) water and transferred to a 2 ml tube. Cells were centrifuged at 2300 *g* for 10 seconds and the pellet resuspended in 750 µl TES (10 mM Tris

(pH 7.5), 10 mM EDTA (pH 8.0), 0.5% SDS). 750 µl acidic phenol-chloroform was added, samples vortexed and incubated at 65°C for 1 hour, with vortexing for 10 seconds every 10 minutes. Samples were placed on ice for 1 minute, vortexed for 20 seconds and centrifuged for 15 minutes at 16100 *g* at 4°C. 700 µl of the water phase was mixed with 700 µl acidic phenol-chloroform in a pre-spun 2 ml phase-lock (heavy) tube, and centrifuged for 5 minutes at 16100 *g* at 4°C. 700 µl of the water phase was mixed with 700 µl chloroform-isoamyl alcohol (24:1) in a pre-spun 2 ml phase-lock (heavy) tube, and centrifuged for 5 minutes at 16100 *g* at 4°C. 500 µl of the water phase was added to 1.5 ml 100% ethanol (-20°C) and 50 µl 3 M NaAc (pH 5.2), and RNA precipitated at -80°C for 30 minutes. Samples were centrifuged at 16100 *g* for 10 minutes at room temperature and the supernatant discarded. The pellet was washed with 500 µl cold 70% ethanol, air dried for 10 minutes and then resuspended in 100 µl DEPC water.

2.11.2 Quantification of RNA samples

RNA concentration was determined using a Nanodrop 1000 spectrophotometer (Thermo Scientific). Samples were diluted in DEPC water to a suitable concentration and read at an absorbance at 260 nm and 280 nm. Concentration was calculated in µg/µl.

2.11.3 Microarray analysis

Microarray analysis was performed by Sandra Codlin from the group of Jürg Bähler, UCL. In brief, Alexa 555- or 647-labeled cDNA was produced from the RNA, using a Superscript direct cDNA labeling system (Invitrogen) and Alexa 555 and 647 dUTP label mix. The cDNA was then purified using an Invitrogen PureLink PCR Purification system. The cDNA was hybridized to the array using a Gene Expression Hybridization kit (Agilent). The array was an Agilent custom-designed array containing 60-mer oligonucleotides synthesized *in situ* on the array and contained 4x44,000 probes. Following hybridization for at least 17 hours, the array was washed using a Gene Expression Wash Buffer kit (Agilent) and scanned in an Agilent Array Scanner. The microarray signal was extracted using GenePix.

2.12 PROTEIN EXTRACTION, MANIPULATION AND ANALYSIS

2.12.1 TCA protein extraction

Approximately 1 x 10^8 cells were taken per sample, centrifuged at 931 *g* for 2 minutes and the pellet resuspended in 1 ml 1.2 M sorbitol. The cells were centrifuged at 16100 *g* for 30 seconds, the pellet resuspended in 100 µl 20% TCA and vortexed. Glass beads were added to 0.5 ml volume and the tubes vortexed for 5 minutes at 4°C. 900 µl 5% TCA was added and the extract vortexed briefly. 800 µl was centrifuged at 800 *g* for 10 minutes. The protein pellet was then resuspended in 250 µl 1 x Laemmli buffer, vortexed, then boiled for 3 minutes. The extract was centrifuged at 800 *g* for 10 minutes and the supernatant stored at -20°C.

2.12.2 Nuclear protein extraction

1 litre of cells at $O.D_{595}$ 0.8 was taken per sample. Cells were centrifuged at 1673 *g* for 5 minutes at 4°C, washed once in ice cold water and the pellet stored at -80°C. To process, pellets were defrosted, and washed once in spheroplasting (SP) buffer. Cells were resuspended in 10 ml SP buffer containing 0.4 mg/ml zymolyase 20T and incubated at 30°C with slow shaking for 30 minutes. Spheroplasted cells were centrifuged at 1730 *g* for 5 minutes at 4°C, washed with 10 ml SP buffer and resuspended in 10 ml lysis buffer. Cells were lysed for 10 minutes with a Dounce homogeniser. After homogenisation, cells were diluted into 30 ml/litre cells, and centrifuged at 2120 *g* for 20 minutes at 4°C. The supernatant was then ultracentrifuged at 20000 rpm (SW32-Ti rotor) for 30 minutes at 4°C. The pellet was resuspended in 8 ml NP buffer and overlayed onto 2 ml cushion buffer before further ultracentrifugation at 20000 rpm (SW32-Ti rotor) for 30 minutes at 4°C. The pellet was resuspended in 1 ml NP buffer and stored at -80°C. For protein extraction, the nuclei were washed 3x with 500 µl buffer A, and resuspended in 100 µl buffer B. 10 µl 4N H_2SO_4 was added and the samples rotated for 30 minutes at 4°C. Nuclei were centrifuged at 16100 *g* for 5 minutes, the supernatant kept on ice, and H_2SO_4 treatment repeated on the pellet. TCA precipitation of the supernatant was performed by adding 50 µl 100 % TCA and incubating

for 1 hour at 4°C on a rotator. Samples were centrifuged at 16100 *g* for 10 minutes at 4°C, and the pellet washed once with 0.1% HCl in acetone, followed by one wash in 100% acetone. The pellet was resuspended in 100 µl water and stored at -20°C.

2.12.3 SDS-polyacrylamide gel electrophoresis (SDS-PAGE)

Protein samples were separated on SDS-PAGE mini-gels of an appropriate concentration (15% for histone modification, 10% for all others). The 10% running gel was made with 2.5 ml 40% acrylamide-bis (37.5:1) (Promega), 2.5 ml 1.5 M Tris-HCl (pH 8.7), 4.8 ml MQ, 0.1 ml 10% SDS, 0.1 ml 10% ammonium persulphate (APS) and 0.02 ml N,N,N,N-tetramethylethylenediamine (TEMED). The 15% running gel was made with 4.6 ml 40% acrylamide-bis, 2.5 ml 1.5 M Tris-HCl (pH 8.7), 2.7 ml MQ, 0.1 ml 10% SDS, 0.1 ml 10% APS and 0.02 ml TEMED. The stacking gel (5%) was made with 0.6 ml acrylamide-bis, 0.6 ml 1 M Tris-Cl (pH 6.8), 3.5 ml MQ, 0.1 ml 10% SDS, 0.05 ml 10% APS and 0.03 ml TEMED. The gel was placed in an electrophoresis chamber containing 1x running buffer. Protein samples were boiled for 3 minutes before loading, and 10-25 µg protein was added to each lane. The gels were run at 200 V for 2 hours.

2.12.4 Western blotting

The proteins were transferred to a nitrocellulose Immobilon-P membrane by the semi-dry western blotting procedure. Six 9 cm x 6 cm pieces of 3M chromatography paper were soaked in transfer buffer. The Immobilon-P (Millipore) membrane was soaked in methanol to activate its positive charge, then rinsed in transfer buffer. The blotting stack was assembled in the semi-dry western blotting apparatus, with the gel placed on top of the membrane, sandwiched between two triple layers of 3M paper. The proteins were transferred to the membrane by blotting at 16 V and 250 mA for 1 hour. The membrane was blocked in Marvel buffer (5% in 1x PBS) for 30 minutes with shaking. The antibodies used in this study are shown in Table 2.4. The secondary antibodies were HRP-labelled; Supersignal West Dura (Pierce) was used for chemiluminescence detection as per manufacturer's instructions.

Table 2.4 Antibodies used in this study

Antibody	Source	Dilution	Conditions
Peroxidase anti-peroxidase (PAP)	Sigma, P1291	1:1000	4°C overnight/ 2 hours, room temperature
α-tubulin	Sigma, T5168	1:10000	1 hour, room temperature
α-GFP	Roche, 11814460001	1:500	4°C overnight/ 3 hours, room temperature
α-H3K36me3	Abcam, ab9050	1:500	4°C overnight/ 3 hours, room temperature
α-H3K36ac	Active Motif, 39379	1:500	4°C overnight/ 3 hours, room temperature
α-H3	Abcam, ab1791	1:500	4°C overnight/ 3 hours, room temperature
α-cdc2	Dr Chris Norbury	1:800	4°C overnight/ 3 hours, room temperature
Peroxidase labelled anti-mouse IgG	Vector Laboratories, PI-2000	1:10000	1 hour, room temperature
Peroxidase labelled anti-rabbit IgG	GE Healthcare, RPN2108	1:8000-1:10000	1 hour, room temperature

2.13 MICROSCOPY

2.13.1 Light microscopy

Cells were visualised using a Nikon microscope-Eclipse E-E400 with a 50x objective lens. Cells growing on agar plates were visualised by streaking out using a sterile toothpick. Cells growing in culture were visualised by adding 8 µl culture to a microscope slide with coverslip.

2.13.2 Fluorescence microscopy

Asynchronous cultures were treated as required; 50 Gy IR using a ^{137}Cs source with a dose rate of 2.8 Gy per minute, 5 µg/ml bleomycin (1hr, 26°C) or left untreated before being fixed in 100% methanol and stored in 100% acetone at -20°C. Synchronous cultures were fixed in 70% ethanol and stored at -20°C. Samples were rehydrated and stained with 6'-diamidino-2-phenylindole (DAPI) and mounted (ProLong® Gold antifade rearent with DAPI; Invitrogen), and examined with a Zeiss Axioplan 2ei microscope, Hamamatsu Orca ER camera and micromanager software. For visualisation of septum a 1:20 dilution of methyl blue was added to DAPI mountant.

2.14 FLOW CYTOMETRY

To measure cellular DNA content, $1x10^7$ cells were collected and centrifuged (931 *g*, 5 minutes). The cell pellet was resuspended in cold 70% ethanol and stored at -20°C. For analysis, $3x10^6$ cells were added to 4.5 ml 10 mM EDTA (pH 8.0), vortexed and centrifuged (931 *g*, 5 minutes). The cell pellet was resuspended in 0.5 ml 10 mM EDTA (pH 8.0) containing 0.1 mg/ml RNaseA and incubated overnight at 37°C. 0.5 ml 10 mM EDTA (pH 8.0) containing 2 μM sytox green nucleic acid stain was added to the sample. Samples were sonicated (W-375 sonicator, Heat Systems Ultrasonics Inc) for 10 seconds before DNA measurement using an EPICS XL-MCL flow cyometer (Beckman-Coulter), and analysis using WinMDI software.

CHAPTER 3

A screen for histone-modifying enzymes involved in DNA double-strand break repair

3.1 INTRODUCTION

The maintenance of genome integrity and prevention of gross chromosomal rearrangements (GCRs) is essential for tumour suppression and the faithful transfer of genetic material to subsequent generations. Such genome stability relies on appropriate cellular responses to DNA damage. DNA DSBs are one of the most dangerous types of DNA lesion, and if incorrectly repaired, they can lead to GCRs. Although much research has been done to address the complex pathways that control DSB repair, it is likely that novel factors remain to be identified. One important consideration is the compaction of the DNA in chromatin as this may influence the accessibility of the DNA to repair factors. Modification of the histone proteins around which DNA is wrapped alters this compaction. Consequently, the aim of this study was to identify and characterise novel genes that affect DSB repair through histone modification in *S. pombe*. To achieve this, histone-modifying mutants present in an *S. pombe* deletion library were analysed for an altered DSB response. It was predicted that this may lead to the identification of genes required to maintain genome integrity, which may act as tumour suppressors in higher eukaryotes, and are thus of substantial interest.

3.2 RESULTS

3.2.1 Identification of bleomycin resistant histone-modifying mutants

For this project, a genome-wide haploid deletion library provided by the Bioneer Corporation and the Korea Research Institute of Biotechnology and Bioscience was utilised. The library consists of 3,308 deletion strains, covering 92.8% of the non-essential *S. pombe* genome. Each deletion strain was created by replacement of the gene of interest with a deletion

cassette comprising a *KanMX4* marker gene flanked by a pair of unique molecular barcodes, used to identify the mutant (Kim *et al*, 2010).

The library contains nineteen histone-modifying mutants; these were isolated and assayed for a potential role in DNA double-strand break (DSB) repair. Of the nineteen mutants, twelve were potential histone methyltransferases (HMTs; *set1*Δ, *set2*Δ, *set3*Δ, *set5*Δ, *set6*Δ, *set8*Δ, *set9*Δ, *set10*Δ, *set11*Δ, *set13*Δ, *SPBC16C6.01c*Δ and *clr4*Δ), four were histone acetyltransferases (HATs; *mst2*Δ, *gcn5*Δ, *hat1*Δ and *elp3*Δ) and three were histone deacetylases (HDACs; *sir2*Δ, *hst2*Δ and *clr3*Δ).

Mutations in genes that are required for the repair of DSBs often confer a change in sensitivity to DNA damaging agents, such as IR and the radiomimetic bleomycin. For example, HR mutants such as *rhp51*Δ show a striking sensitivity to these agents (Figure 3.1 and 3.2). Therefore, an initial analysis of the histone-modifying mutants present in the deletion library was performed to identify mutants that exhibited a differential response to these agents, compared to wildtype.

The nineteen histone-modifying mutants were analysed for their sensitivity to bleomycin using a serial dilution assay (Figure 3.1). Surprisingly, fifteen of the mutants showed an increased resistance to bleomycin, compared to wildtype, which included all but two of the HMTs and all of the HDACs (Figure 3.1, * indicates resistance). Only *elp3*Δ cells showed any sensitivity compared to wildtype.

IR is a powerful inducer of DSBs and so the mutants were also analysed for their response to IR using the serial dilution assay. *rhp51*Δ cells are exquisitely sensitive to a dose of 500 Gy (Figure 3.2); however, only one of the histone-modifying mutants showed any obvious

Figure 3.1

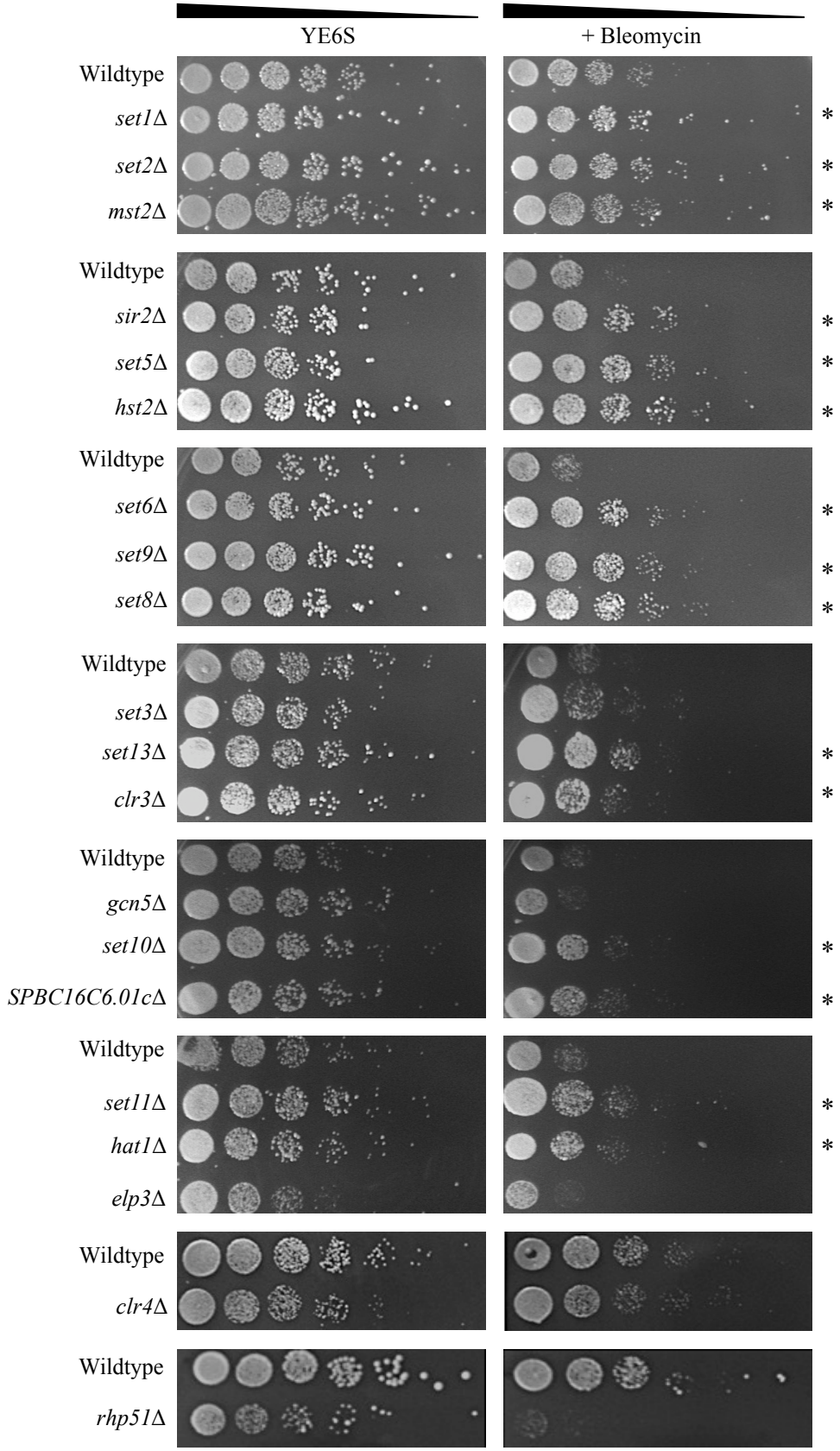


Figure 3.1 Response of histone-modifying mutants to the IR-mimetic bleomycin 5-fold serial dilutions of wildtype (2094), *set1*Δ (3270), *set2*Δ (3271), *mst2*Δ (3771), *sir2*Δ (3518), *set5*Δ (4827), *hst2*Δ (3278), *set6*Δ (4904), *set9*Δ (3272), *set8*Δ (4826), *set3*Δ (5469), *set13*Δ (5468), *clr3*Δ (3276), *gcn5*Δ (3718), *set10*Δ (5467), *SPBC16C6.01c*Δ (5466), *set11*Δ (5464), *hat1*Δ (5465), *elp3*Δ (6509), *clr4*Δ (3720) and *rhp51*Δ (3992) were spotted onto YE6S and YE6S + 1 μg/ml bleomycin. * indicates resistance to bleomycin compared to wildtype.

Figure 3.2

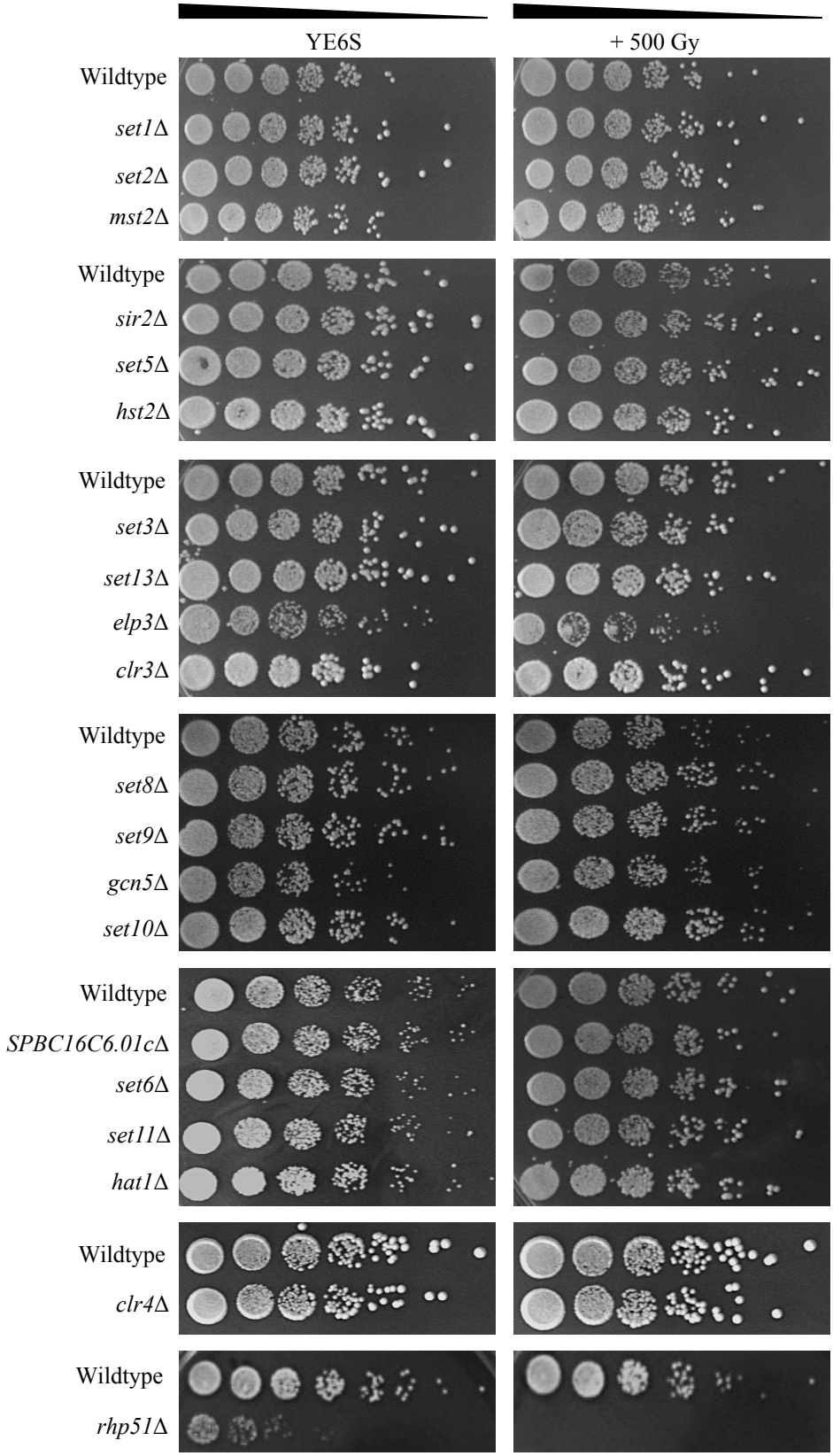


Figure 3.2 Response of histone-modifying mutants to ionising radiation (IR) 5-fold serial dilutions of wildtype (2094), *set1*Δ (3270), *set2*Δ (3271), *mst2*Δ (3771), *sir2*Δ (3518), *set5*Δ (4827), *hst2*Δ (3278), *set6*Δ (4904), *set9*Δ (3272), *set8*Δ (4826), *set3*Δ (5469), *set13*Δ (5468), *clr3*Δ (3276), *gcn5*Δ (3718), *set10*Δ (5467), *SPBC16C6.01c*Δ (5466), *set11*Δ (5464), *hat1*Δ (5465), *elp3*Δ (6509), *clr4*Δ (3720) and *rhp51*Δ (3992) were spotted onto YE6S and irradiated with 500 Gy.

change in its viability, compared to wildtype. The mutant that was sensitive to bleomycin, *elp3*Δ, was also sensitive to IR, suggesting that this gene is required for an appropriate DNA damage response. The resistance to bleomycin observed in the majority of the HMTs was not as striking in response to IR. The inconsistency between IR and bleomycin resistance may be a reflection of the damaging capability of the relative concentration of bleomycin or dose of IR used. A more quantitative analysis was therefore used to determine whether any role in DSB repair exists in these mutants.

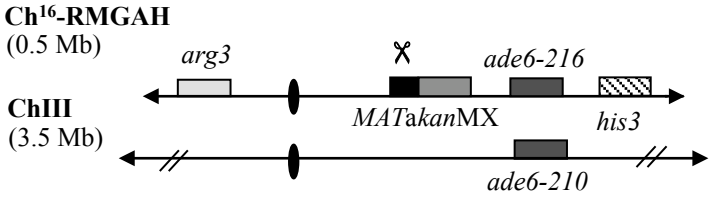
3.2.2 Analysis of DSB repair in histone-modifying mutants

Analysis of viability using the serial dilution assay requires a 5-fold difference in growth between the treated and untreated cells in order for a phenotype to be seen. Given the resistance to bleomycin shown in many of the mutants it was of interest to further quantify their ability to repair a DSB. A more quantitative analysis of these mutants was performed by introducing Ch^{16}-RMGAH or Ch^{16}-RMYAH (Figure 3.3) into the strains and assessing DSB-induced marker loss using the DSB assay (described in section 2.10.1). Unfortunately, DSB repair in two of the mutants, *set9*Δ and *hst2*Δ could not be analysed, as these genes are present on the minichromosome, negating the deletion made on chromosome 3. These genes could have been deleted from the minichromosome but this was not pursued due to time constraints. Further, a role for Set9 in methylation of H4K20, which leads to recruitment of the checkpoint protein Crb2 to sites of DNA damage, has previously been identified (Sanders *et al*, 2004). Given this prior characterisation, the *set9*Δ mutant was excluded from further analysis, as was the *hst2*Δ mutant.

Six out of the seventeen mutants analysed (*set1*Δ, *set2*Δ, *mst2*Δ, *sir2*Δ, *set3*Δ and *set11*Δ) exhibited significantly increased levels of gene conversion (GC), compared to wildtype (Figure 3.4A and C). This was associated with lower levels of *ade6-M216* loss following a DSB, resulting from decreased levels of loss of heterozygosity (LOH) and/or chromosome

Figure 3.3

A



B

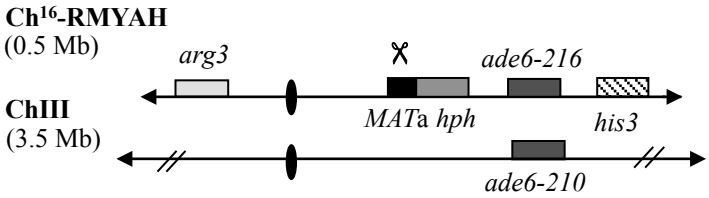


Figure 3.3 Schematic of minichromosomes (A) Schematic of Ch^{16}-RMGAH. Ch^{16}-RMGAH, a 530 Kb fragment of ChIII contains a *MATa* site with an adjacent kanamycin resistance marker gene (*kanMX*), an *ade6* heteroallelle (*ade6-M216*; complemented by *ade6-M210* present on ChIII), in addition to a *his3* marker ~50 Kb centromere-distal to *ade6-M216* at the *cid2* locus, and *arg3* marker located on the left arm at the *yps1* locus. **(B)** Schematic of Ch^{16}-RMYAH. Ch^{16}-RMYAH has the same backbone structure as to Ch^{16}-RMGAH (A) however a hygromycin resistance marker (*hph*) is adjacent to the *MATa* site rather than a kanamycin marker. Derepression of HO endonuclease (by removal of thiamine) generates a DSB at the *MATa* target site (indicated by scissors).

loss (Ch^{16} loss; Figure 3.4B and D). Of these six mutants, *mst2*Δ and *sir2*Δ also exhibited a significant decrease in non-homologous end-joining/sister chromatid conversion (NHEJ/SCC; p=0.02). Interestingly, five of these mutants exhibited resistance to bleomycin in the serial dilution assay (Figure 3.1). This may reflect the fact that HR is an error free mechanism of repair, which may result in a greater proportion of surviving cells following DSB induction.

Three mutants, *hat1*Δ, *set13*Δ and *clr4*Δ exhibited a repair profile in which GC was decreased compared to wildtype (39%, p<0.01; 54%, p=0.02 and 39%, p=0.08 respectively; Figure 3.5A). In keeping with the finding that efficient HR repair suppresses LOH and Ch^{16} loss (Tinline-Purvis *et al*, 2009; J. Moss, unpublished data) both *hat1*Δ and *set13*Δ mutants showed significantly increased levels of LOH (13%, p=0.05 and 11%, p<0.01 respectively) and *hat1*Δ cells also exhibited significantly increased levels of Ch^{16} loss (42%, p<0.01; Figure 3.5B). This indicates that Hat1 and Set13 are required for efficient DSB repair by HR. *clr4*Δ cells exhibited a significantly decreased level of LOH (0%, p=0.03), which is unusual given its decreased level of GC. However, this may be explained by an exquisitely high level of spontaneous Ch^{16} loss in this mutant (42%). Given Clr4 is required for methylation of H3K9, which recruits Swi6 (a HP1 family protein) leading to heterochromatin formation (Rea *et al*, 2000; Shankaranarayana *et al*, 2003), it is possible that in the absence of Clr4, heterochromatin formation is ineffective which may destabilise chromosomes leading to the high level of spontaneous chromosome loss observed.

A further two mutants, *gcn5*Δ and *elp3*Δ showed significantly increased levels of NHEJ/SCC (33%, p<0.01 and 18%, p<0.01 respectively; Figure 3.6). In the case of *gcn5*Δ this was associated with significantly decreased levels of GC (45%, p<0.01) and LOH (6%, p=0.04). However, *elp3*Δ showed wildtype levels of GC, but significantly decreased levels of Ch^{16} loss (6%, p<0.01) and LOH (3%, p=0.03). This is somewhat surprising given that *elp3*Δ was the

Figure 3.4

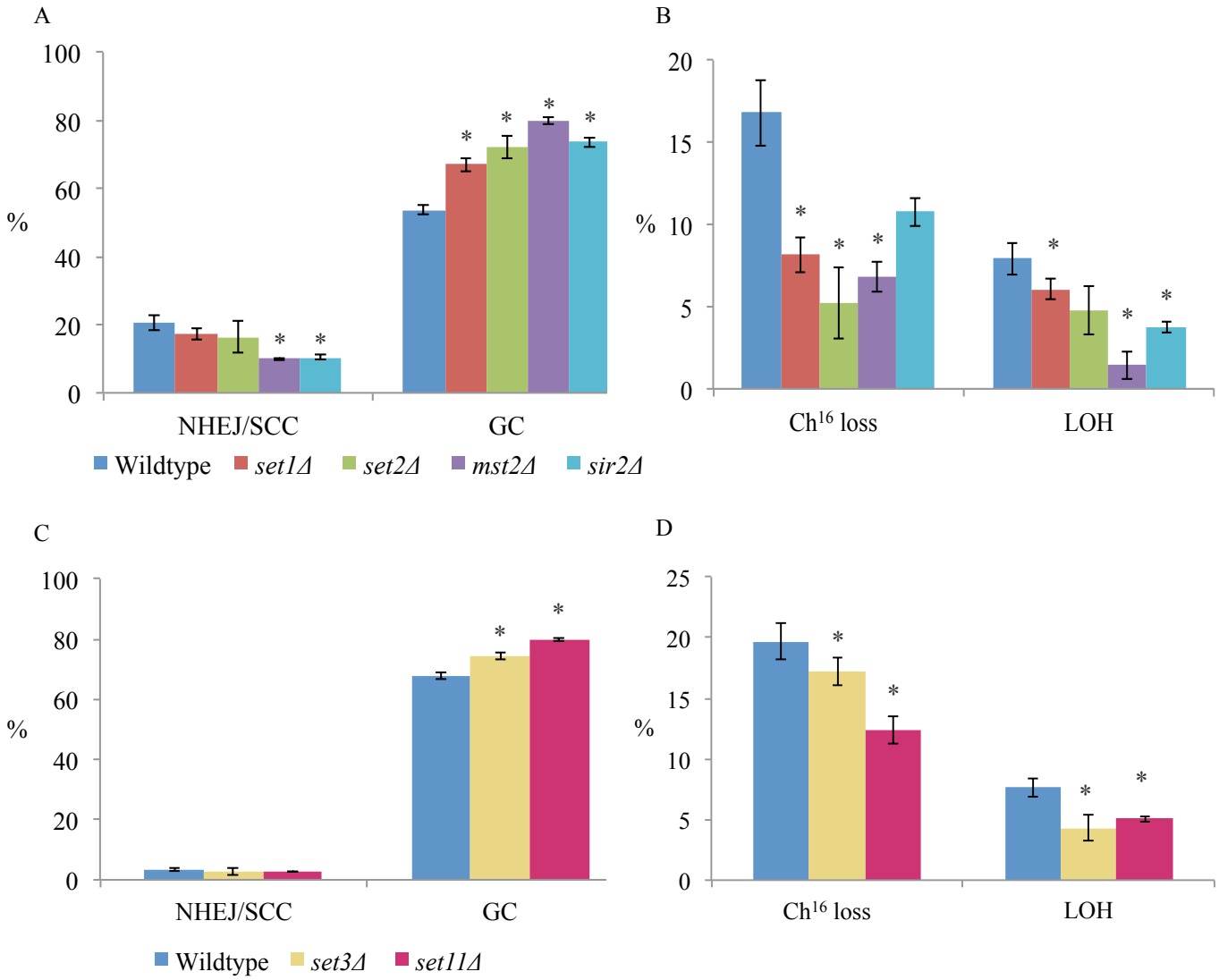


Figure 3.4 A subset of histone-modifying mutants show increased DSB repair by gene conversion associated with decreased Ch[16] loss and/or LOH (A) Percentage DSB-induced marker loss in wildtype (2131), *set1*Δ (3837-40), *set2*Δ (3841-3), *mst2*Δ (4292-4) and *sir2*Δ (3628-30) containing Ch[16]-RMGAH. The levels of non-homologous end-joining/sister chromatid conversion (NHEJ/SCC) and gene conversion (GC) are shown. **(B)** Percentage DSB-induced marker loss in wildtype, *set1*Δ, *set2*Δ, *mst2*Δ and *sir2*Δ containing Ch[16]-RMGAH. The levels of chromosome loss (Ch[16] loss) and loss of heterozygosity (LOH) are shown. **(C)** Percentage DSB-induced marker loss in wildtype (4104), *set3*Δ (5635-7) and *set11*Δ (5704-6) containing Ch[16]-RMYAH. The levels of NHEJ/SCC and GC are shown. **(D)** Percentage DSB-induced marker loss in wildtype, *set3*Δ and *set11*Δ containing Ch[16]-RMYAH. The levels of Ch[16] loss and LOH are shown. Data are the mean of three experiments and error bars (± SE) are shown. * indicates statistical significance.

Figure 3.5

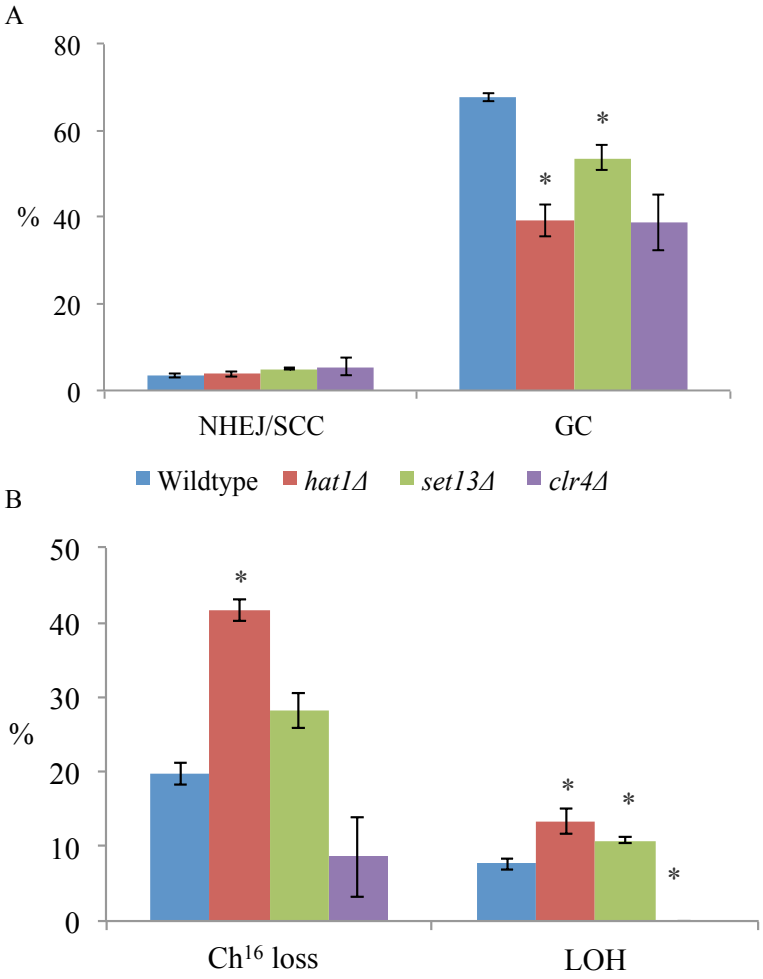


Figure 3.5 *hat1*Δ, *set13*Δ and *clr4*Δ show decreased DSB repair by gene conversion associated with increased Ch[16] loss and/or LOH (A) Percentage DSB-induced marker loss in wildtype (4104), *hat1*Δ (5623-5), *set13*Δ (5631-3) and *clr4*Δ (4296, 4383-4) containing Ch[16]-RMYAH. The levels of NHEJ/SCC and GC are shown. **(B)** Percentage DSB-induced marker loss in wildtype, *hat1*Δ, *set13*Δ and *clr4*Δ containing Ch[16]-RMYAH. The levels of Ch[16] loss and LOH are shown. Data are the mean of three experiments and error bars (± SE) are shown. * indicates statistical significance.

Figure 3.6

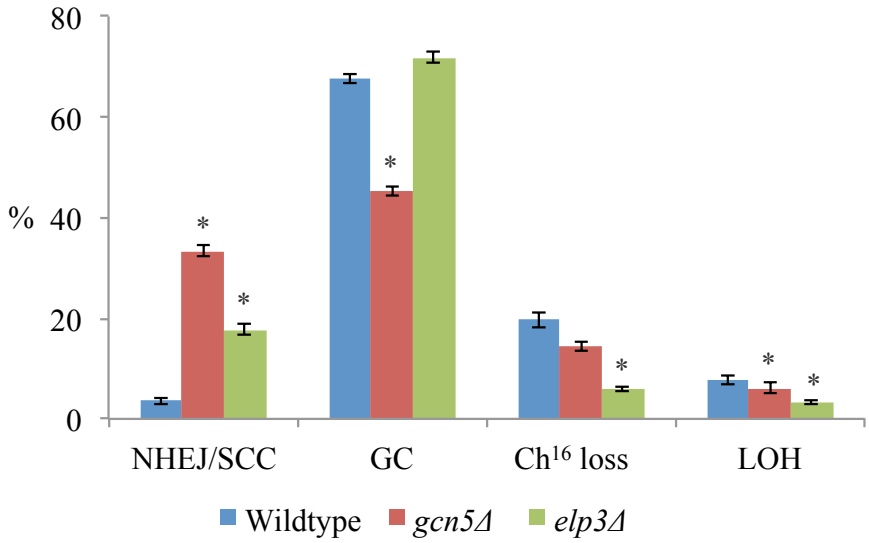


Figure 3.6 *gcn5*Δ and *elp3*Δ show increased NHEJ/SCC Percentage DSB-induced marker loss in wildtype (4104), *gcn5*Δ (3864, 6338-9) and *elp3*Δ (6521-2, 6656) containing Ch^{16}-RMYAH. The levels of NHEJ/SCC, GC, Ch^{16} loss and LOH are shown. Data are the mean of three experiments and error bars (± SE) are shown. * indicates statistical significance.

only mutant to show increased sensitivity to both IR and bleomycin in the serial dilution assay. Excluding *clr3*Δ, which exhibits a significant decrease in LOH (4%, $p<0.01$) the remaining five mutants (*set5*Δ, *set6*Δ, *set8*Δ, *set10*Δ and *SPBC16C6.01c*Δ) showed no significant difference in their DSB repair profile compared to wildtype (Figure 3.7).

3.2.3 Analysis of NHEJ repair in histone-modifying mutants

A number of the histone-modifying mutants exhibited a significantly altered NHEJ/SCC level when analysed by the DSB assay. However, it is not possible to discern between NHEJ and SCC using the DSB assay as all the genetic markers are retained (see Figure 1.4). Thus, further analysis of the mutants was performed using a plasmid-rejoining NHEJ assay (described in section 2.10.2). In this assay, a plasmid containing a *LEU2* marker is linearised by restriction digestion. Cells are then transformed with uncut plasmid or linearised plasmid, and the NHEJ frequency determined by calculating the percentage of *leu*+ colonies arising from cells transformed with linear plasmid over those transformed with uncut plasmid (Figure 3.8).

Firstly, the mutants which exhibited significantly increased GC in the DSB assay were analysed. *set2*Δ and *mst2*Δ cells showed at least a 50% decreased level of plasmid-rejoining with both the PstI (3' overhang) and EcoRI (5' overhang) cut substrates compared to wildtype (Figure 3.9B and C). *set1*Δ and *set3*Δ cells also showed a reduced level of plasmid-rejoining compared to wildtype, but this was only observed in the PstI cut substrate (Figure 3.9A and E). This suggests that Set1 and Set3 are required for NHEJ repair of 3' overhang substrates only. Both *sir2*Δ and *set11*Δ mutants showed no impairment in their ability to repair a break by NHEJ compared to wildtype (Figure 3.9D and F), indicating that the significant decrease in NHEJ/SCC in the DSB assay for *sir2*Δ is likely due to loss of SCC.

Figure 3.7

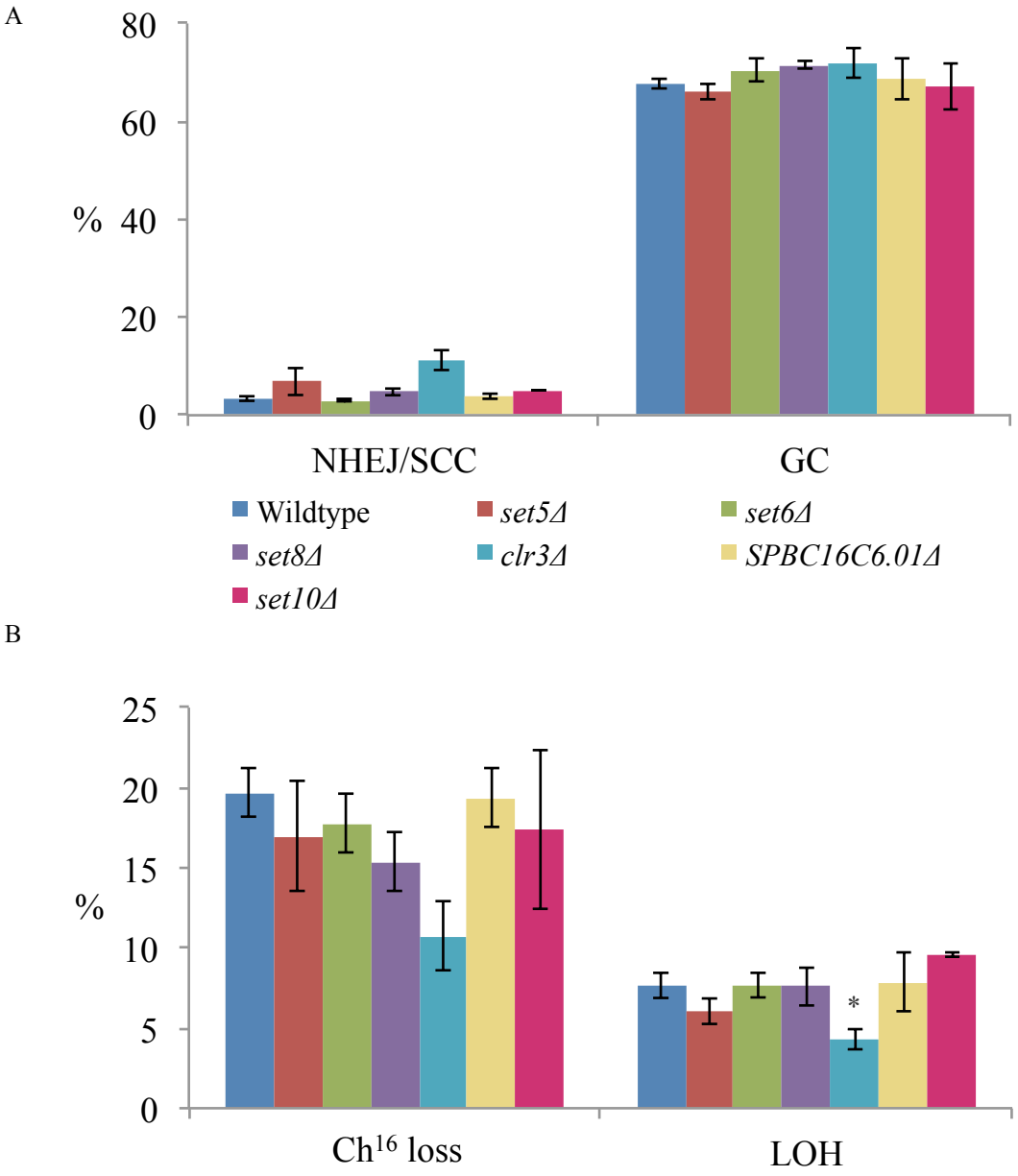


Figure 3.7 A subset of histone-modifying mutants show no significant difference compared to wildtype in their ability to repair a DSB (A) Percentage DSB-induced marker loss in wildtype (4104), *set5*Δ (5342-4), *set6*Δ (5311-3), *set8*Δ (5319, 5478-9), *clr3*Δ (3865-7), *SPBC16C6.01*Δ (5619-21) and *set10*Δ (5627-9) containing Ch^{16}-RMYAH. The levels of NHEJ/SCC and GC are shown. **(B)** Percentage DSB-induced marker loss in wildtype *set5*Δ, *set6*Δ, *set8*Δ, *clr3*Δ, *SPBC16C6.01*Δ and *set10*Δ containing Ch^{16}-RMYAH. The levels of Ch^{16} loss and LOH are shown. Data are the mean of three experiments and error bars (± SE) are shown. * indicates statistical significance.

Figure 3.8

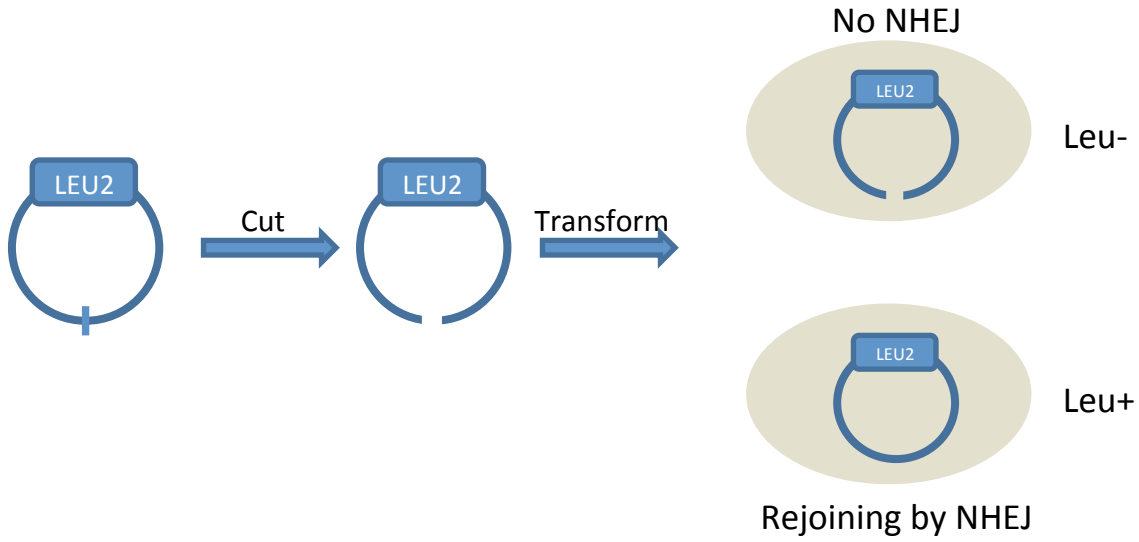


Figure 3.8 Non-homologous end-joining (NHEJ) plasmid-rejoining assay A plasmid containing LEU2 was linearised with EcoRI or PstI. Logarithmically growing cells were transformed with 1 µg of uncut control plasmid or linearised plasmid. NHEJ frequency was calculated as the percentage of *leu+* colonies arising from cells transformed with linear plasmids over those transformed with undigested DNA.

Several of the mutants that exhibited increased GC also had impaired NHEJ (Figure 3.9H). It is feasible that there is competition between HR and NHEJ repair such that when NHEJ is compromised, those cells that would have repaired by end-joining undergo HR, leading to an increased level of HR (Allen *et al*, 2003; Fukushima *et al*, 2001; Paques & Haber, 1999; Pierce *et al*, 2001). Consistent with this, *lig4*Δ cells, which cannot repair a break by NHEJ (Figure 3.9A-F) also showed a significant increase in GC compared to wildtype (61%; p=0.03; Figure 3.9G). It would be interesting to investigate whether there is a genome wide correlation between failed NHEJ and increased HR, but this was not the focus of this study.

Analysis of repair by NHEJ was also carried out for the mutants that showed other repair profiles in the DSB assay. As expected, *gcn5*Δ, which showed a significant increase in NHEJ/SCC in the DSB assay was proficient at plasmid-rejoining (Figure 3.10). In the PstI cut plasmid, the percentage rejoining was in fact 2.5-fold greater than in wildtype, suggesting that the increase in NHEJ/SCC may be due to NHEJ. To confirm this, DSB repair by a *gcn5*Δ*lig4*Δ mutant was analysed and is discussed in Chapter 7. Unfortunately it was not possible to analyse *elp3*Δ using the plasmid-rejoining assay, despite repeated efforts.

Finally the group that had impaired repair by GC (*hat1*Δ, *set13*Δ and *clr4*Δ) were analysed using the plasmid-rejoining assay. Both *hat1*Δ and *set13*Δ cells had at least wildtype levels of rejoining (Figure 3.11), indicating they can repair a break by NHEJ. In fact the *hat1*Δ cells exhibited plasmid-rejoining that was higher than wildtype, especially with the EcoRI cut plasmid, suggesting a possible role for Hat1 in inhibiting NHEJ. *clr4*Δ could not be analysed using this assay, as the transformation efficiency was not high enough, which may reflect its inability to maintain episomal DNA in the cell.

Figure 3.9

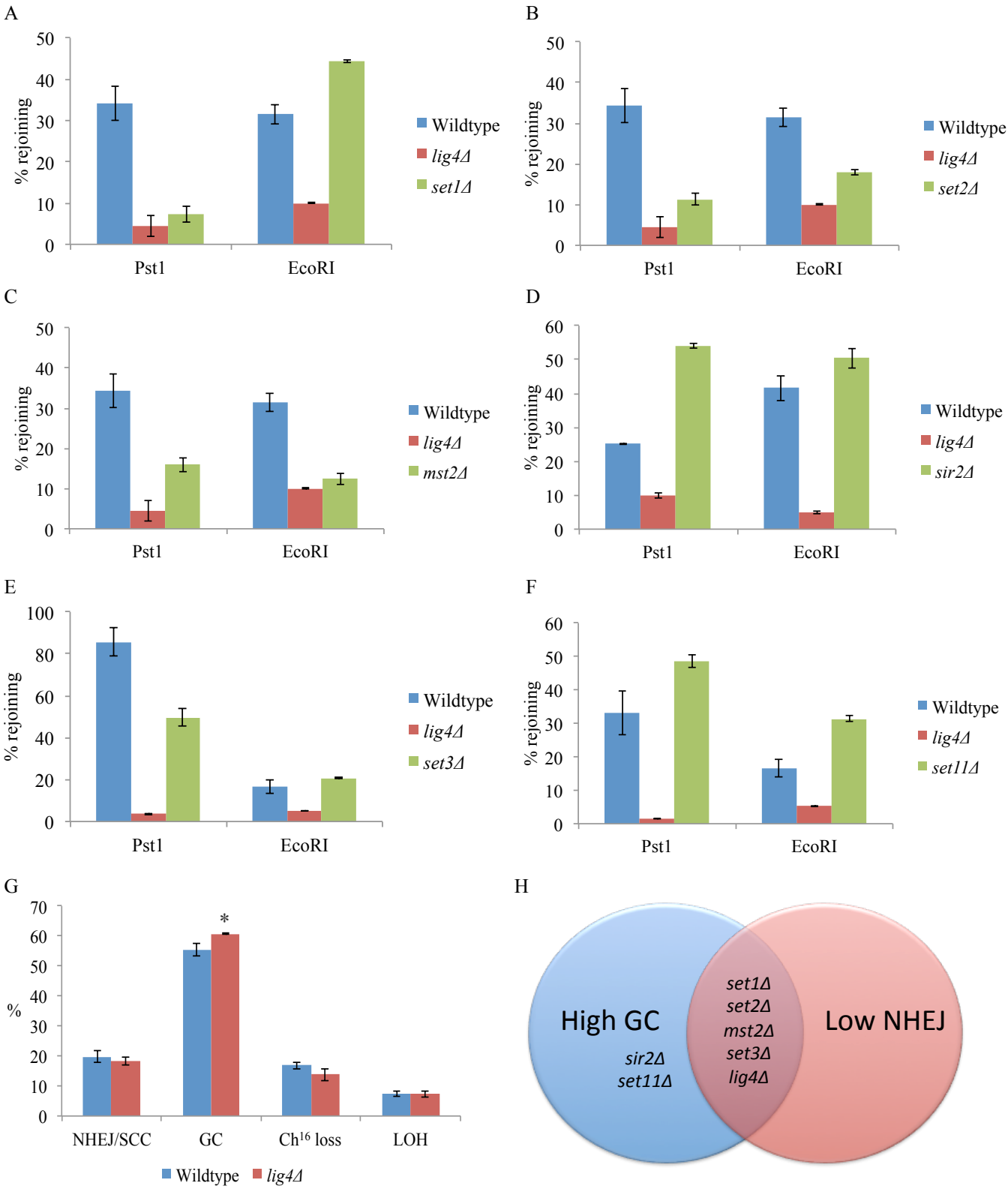


Figure 3.9 High levels of DSB repair by GC are frequently associated with low levels of NHEJ in histone-modifying mutants Outcome of NHEJ plasmid-rejoining assay for **(A)** *set1*Δ (3270)**, (B)** *set2*Δ (3271), **(C)** *mst2*Δ (3771), **(D)** *sir2*Δ (3518), **(E)** *set3*Δ (5469) and **(F)** *set11*Δ (5464). Data are the mean of three experiments and error bars (± SE) are shown. **(G)** Percentage DSB-induced marker loss in wildtype (2131) and *lig4*Δ (3568-70) containing Ch^{16}-RMGAH. The levels of NHEJ/SCC, GC, Ch^{16} loss and LOH are shown. Data are the mean of three experiments and error bars (± SE) are shown. * indicates statistical significance. **(H)** Venn diagram showing relationship between high GC and low NHEJ in histone-modifying mutants.

Figure 3.10

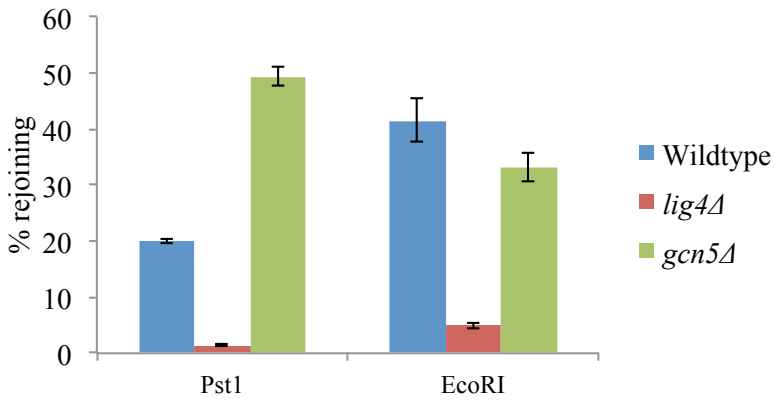


Figure 3.10 *gcn5*Δ is proficient at non-homologous end-joining
Outcome of NHEJ plasmid-rejoining assay for *gcn5*Δ (3718) cells. Data are the mean of three experiments and error bars (± SE) are shown.

Figure 3.11

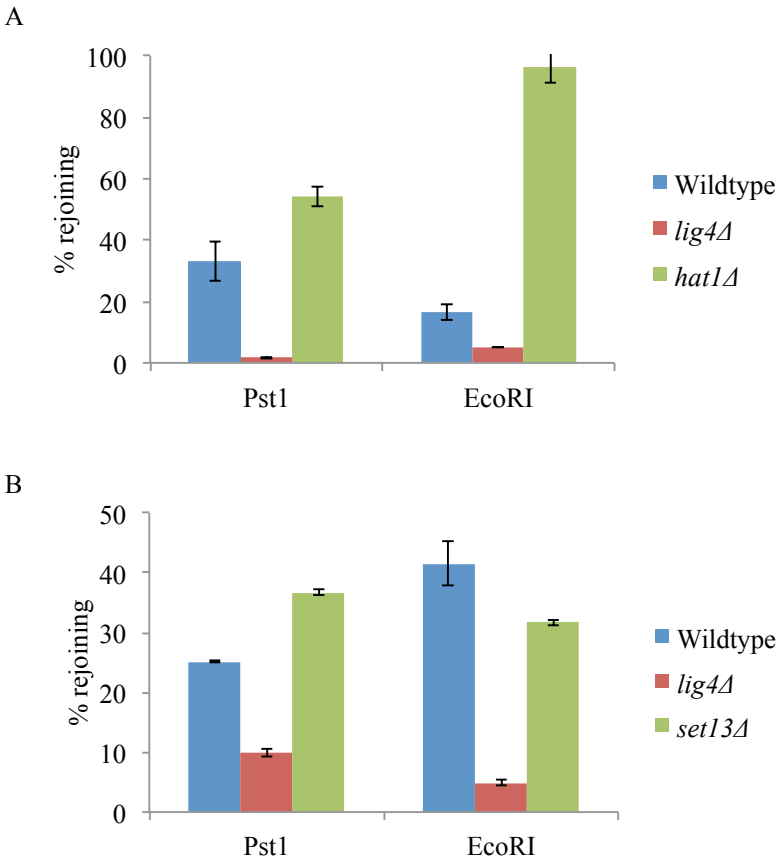


Figure 3.11 *hat1*Δ and *set13*Δ are proficient at non-homologous end-joining Outcome of NHEJ plasmid-rejoining assay for **(A)** *hat1*Δ (5465) and **(B)** *set13*Δ (5468) cells. Data are the mean of three experiments and error bars (± SE) are shown.

3.2.4 Hat1 and Set13 are required for efficient HR repair

3.2.4.1 *hat1*Δ displays a genetic interaction with *rad3*Δ

The analysis above suggests that Hat1 and Set13 are required for efficient HR repair. Further preliminary investigation of their role is discussed here. Analysis of the genetic interactions between mutants has been used as a way to further understand gene function (Nijman, 2011). Genetic interactions can be identified when the phenotypic effects of a mutation in one gene are changed by a mutation in a second gene; this phenomenon is termed epistasis. These alterations can be both positive (e.g. suppression), which can identify pairs of genes whose products are physically associated and/or function in the same pathway, and negative (e.g. synthetic sickness/lethality) which can identify genes which act in parallel pathways (reviewed in Dixon *et al*, 2009). For example, the DNA damage checkpoint has been demonstrated to be essential when HR is compromised, evident by the synthetic lethality associated with $rad3^{+}$ deletion in HR deficient backgrounds, e.g. *rhp51*Δ (Smeets *et al*, 2003).

To further define the role of Hat1 and Set13 in DSB repair, their genetic interaction with *rad3*Δ was investigated. The mutants were crossed to *rad3*Δ and their viability before and after exposure to bleomycin assessed. The double mutant of *rad3*Δ*hat1*Δ showed increased sensitivity to bleomycin compared to the single mutants alone (Figure 3.12). This suggests that Hat1 has a role in a pathway parallel to that of Rad3, which contributes to genome stability following DNA damage. On the other hand, the double mutant of *rad3*Δ*set13*Δ showed no interaction, as there was no altered viability compared to the single mutants (Figure 3.12). This indicates that Set13 functions downstream Rad3, or has no genetic interaction with *rad3*Δ.

Figure 3.12

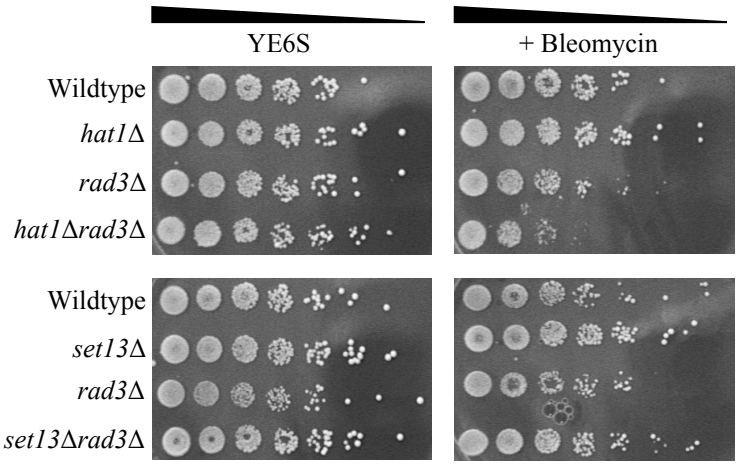


Figure 3.12 Response of *hat1*Δ*rad3*Δ and *set13*Δ*rad3*Δ to the IR-mimetic bleomycin 5-fold serial dilutions of wildtype (2094), *hat1*Δ (5465), *set13*Δ (5468), *rad3*Δ (2799), *hat1*Δ*rad3*Δ (6316) and *set13*Δ*rad3*Δ (6315) were spotted onto YE6S and YE6S + 1 μg/ml bleomycin.

3.2.4.2 *hat1*Δ and *set13*Δ cells are checkpoint proficient

Previous work in this laboratory has characterised the DSB repair profiles of DNA damage checkpoint mutants (Prudden *et al*, 2003; H. Tinline-Purvis, unpublished data). These mutants often exhibit significantly reduced GC and significantly increased Ch^{16} loss and LOH (H. Tinline-Purvis, unpublished data), a repair profile similar to that of *hat1*Δ and *set13*Δ cells. Therefore, the checkpoint response of *hat1*Δ and *set13*Δ cells was investigated by analysing cell length in response to treatment with hydroxyurea (HU). Treatment with HU, inhibits ribonucleotide reductase (RNR), disrupting dNTP synthesis. Checkpoint proficient cells arrest cell division, resulting in an elongated phenotype. On the other hand, checkpoint defective cells, such as *rad3*Δ, undergo aberrant mitosis and are therefore short and often display a 'cut' (cell untimely torn) phenotype (Figure 3.13). Following six hours treatment with HU, both *hat1*Δ and *set13*Δ displayed an elongated cell phenotype, indicating a proficient checkpoint (Figure 3.13). Given the response of *set13*Δ*rad3*Δ to bleomycin, this result suggests that Set13 has no genetic interaction with *rad3*Δ in a checkpoint pathway.

3.2.4.3 *hat1*Δ and *set13*Δ cells display aberrant Rhp51 foci kinetics

Following detection of a DSB and 5'-3' resection, Rhp51 binds to ssDNA forming a nucleofilament which is required for subsequent homology search, strand invasion and D-loop formation. The presence of Rhp51 at a break site can be visualised as distinct foci within the nucleus, when Rhp51 is fluorescently tagged (Figure 3.14A). To investigate whether Hat1 and Set13 act pre- or post-synaptically during HR, the kinetics of Rhp51-CFP foci were analysed in *hat1*Δ and *set13*Δ backgrounds following treatment with IR.

Cells in which *hat1*$^+$ is deleted exhibited a slightly reduced level of Rhp51-CFP foci immediately following treatment with IR, compared to wildtype (Figure 3.14B), indicating there is reduced recruitment of Rhp51 to ssDNA. There was also a delay in restoration to background levels of foci in the *hat1*Δ cells; at 90 minutes following treatment, there was still

Figure 3.13

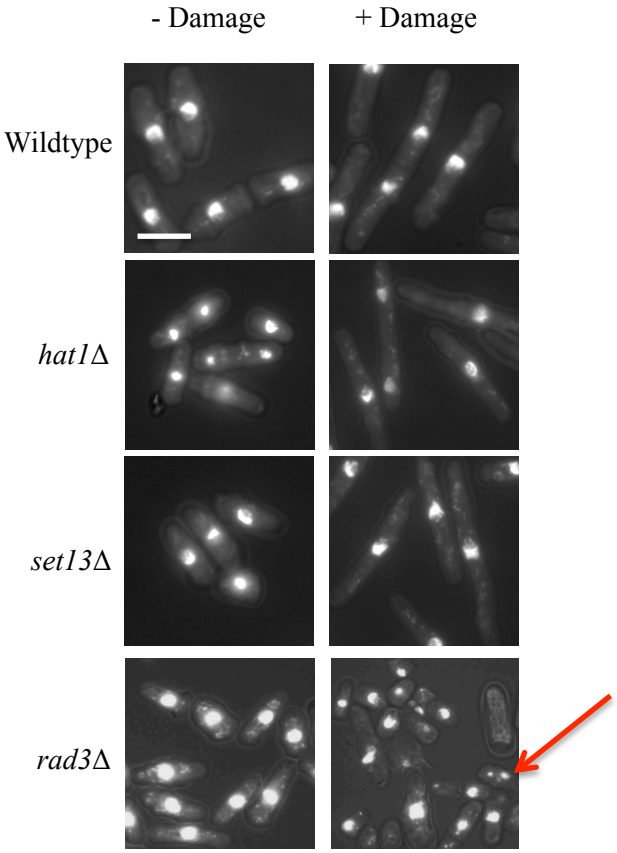


Figure 3.13 *hat1*Δ and *set13*Δ are checkpoint proficient Images of DAPI-stained wildtype (2094), *rad3*Δ (2799), *set13*Δ (5468) and *hat1*Δ (5465) cells are shown. Cells were imaged before (-Damage) and following 6 hours treatment with 10 mM HU (+Damage). Arrow indicates "cut" phenotype. Scale bar, 10 µm.

approximately the same percentage of cells with foci (27%) as at 30 minutes, whereas in wildtype, there was already a significant reduction in the percentage of cells with foci by 90 minutes (from 35% to 20%). The re-establishment of Rhp51-CFP foci at background levels was not achieved by 300 minutes in *hat1*Δ cells, unlike in wildtype. This data suggests that *hat1*Δ cells, although still able to recruit Rhp51, do so less effectively than wildtype cells, indicating a presynaptic role for Hat1. In addition, given Rhp51 foci do not disappear in *hat1*Δ cells with the same kinetics as wildtype there is likely a further postsynaptic role for Hat1 in HR repair. To further address a possible presynaptic role for Hat1, it would be interesting to determine whether the recruitment of upstream HR factors, such as the RPA subunit Rad11, is affected in the *hat1*Δ cells. Given the apparent involvement of Hat1 in HR both pre- and post-synaptically it may be that acetylation by Hat1 is required for generating an open chromatin structure that allows the repair machinery to access the break, and allows efficient strand invasion and D-loop formation. Alternatively, acetylation of specific residues by Hat1 may lead to recruitment of factors that are required throughout the repair process.

In contrast, *set13*Δ cells displayed efficient recruitment of Rhp51-CFP to the break, 30 minutes after IR treatment (Figure 3.14C). However, the kinetics of Rhp51-CFP removal in *set13*Δ cells differed from wildtype; in *set13*Δ cells Rhp51 foci remained high 90 minutes following treatment, and never returned to the same background level as wildtype. This profile indicates a postsynaptic role for Set13 in HR, as initial recruitment of Rhp51 is efficient. Set13 is little characterised; it contains a SET domain and is therefore capable of methylation. However, to date it has only been shown to methylate ribosomal protein L42 at lysine 55 (Shirai *et al*, 2010), and not histone proteins. This methylation has been shown to be required for cell proliferation control, but no involvement in DSB repair has been identified.

Figure 3.14

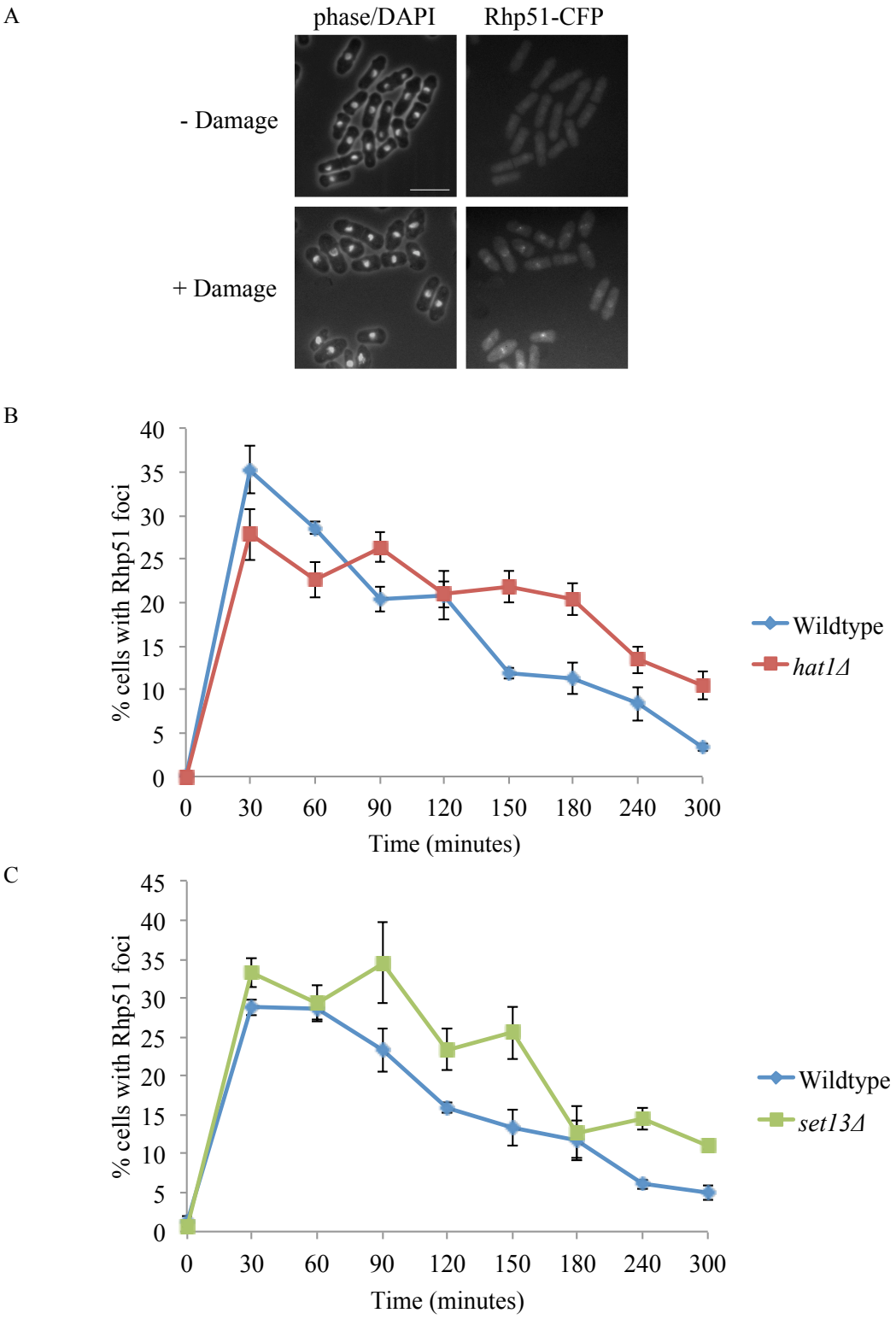


Figure 3.14 *hat1*Δ and *set13*Δ cells display aberrant Rhp51-CFP foci (A) Representative pictures of Rhp51-CFP foci in wildtype (3608) cells before (-Damage) and after (+Damage) exposure to 50 Gy IR. Scale bar, 10 µm. **(B)** Quantification of Rhp51-CFP foci in wildtype (blue; 3608) and *hat1*Δ (red; 6314) cells at the time indicated (minutes) following exposure to 50 Gy IR. **(C)** Quantification of Rhp51-CFP foci in wildtype (blue; 3608) and *set13*Δ (green; 6313) cells at the time indicated (minutes) following exposure to 50 Gy IR.

3.3 DISCUSSION

DSBs are potentially lethal lesions and consequently their efficient detection and repair is essential for cell survival. Failure to correctly repair DSBs can lead to chromosomal rearrangements that are precursors to genome instability and tumourigenesis. Chromatin structure has a key role in DSB repair as the compaction of the DNA can influence the accessibility of the DNA to repair proteins. In addition, histone modifications can lead to the recruitment of specific repair factors.

The work presented in this chapter describes a screen to identify histone-modifying enzymes that are required for efficient DSB repair in *S. pombe*. Results identify eleven proteins shown to be required either directly or indirectly for normal DSB repair.

3.3.1 The relationship between DNA damage sensitivity and DSB repair outcome in histone-modifying mutants

3.3.1.1 Fifteen mutants are associated with increased resistance to bleomycin

An initial screen of the nineteen histone-modifying mutants identified fifteen that exhibited an increased resistance to bleomycin compared to wildtype. Strikingly although bleomycin is considered a radiomimetic, these fifteen mutants did not show the same resistance in response to IR. This inconsistency may reflect the relative damaging capacity of the doses of bleomycin and IR used. Alternatively, additional damage may result from using bleomycin as an alternative to IR. Previous work from this laboratory has shown that there is not complete overlap between an individual mutant's response to these two agents. Although most mutants that are IR sensitive are also bleomycin sensitive, there are mutants that show altered viability in response to bleomycin, but not IR (J. Moss, unpublished data).

Mutations in genes that are required for the repair of DSBs often confer a change in sensitivity to DNA damaging agents. For example, mutations in genes that are essential for

HR, such as *rhp51*Δ show a striking sensitivity to DSB inducing agents such as bleomycin. Therefore, it might be expected that the fifteen mutants showing increased resistance to bleomycin have an increased ability to repair a DSB. Of the fifteen mutants, five did show significantly increased repair by GC in the DSB assay, associated with a significant decrease in LOH and/or Ch^{16} loss (*set1*Δ, *set2*Δ, *mst2*Δ, *sir2*Δ and *set11*Δ). This may reflect that repair by HR is considered to be error-free; if HR is the dominant repair mechanism in these mutants there may be an increase in the proportion of surviving cells in response to bleomycin. However, a significant proportion of the fifteen mutants showing increased resistance to bleomycin did not have a repair profile showing increased repair by GC.

Two of the mutants showing resistance to bleomycin, *hst2*Δ and *set9*Δ could not be analysed using the DSB assay, as they are present on chromosome III. However, Set9 is required for methylation of H4K20, which leads to recruitment of the checkpoint protein Crb2 to sites of DNA damage (Sanders *et al*, 2004) and lack of Set9 impairs genome integrity (Greeson *et al*, 2008). *set9*Δ cells have been shown to be sensitive to UV, CPT and IR and thus sensitivity to bleomycin and IR in this work would be expected; however, the previous study showed sensitivity to IR only at doses above 600 Gy (Greeson *et al*, 2008). Therefore, in this work, perhaps sensitivity to IR and bleomycin would have been observed in the *set9*Δ cells, had a higher dose been used.

Six of the fifteen mutants showing resistance to bleomycin showed no significant difference to wildtype in the DSB assay (*set5*Δ, *set6*Δ, *set8*Δ, *set10*Δ, *clr3*Δ and *SPBC16C6.01*Δ). In *S. cerevisiae* Set5 has been shown to monomethylate H4 lysines 5, 8 and 12 and is thought to functionally interact with the Set1-containing COMPASS complex and the NuA4 complex in the control of growth under stress conditions (Green *et al*, 2012). *set5* cells were shown to grow at least as well as wildtype in response to a number of DNA damaging agents including

MMS, HU, cycloheximide and rapamycin (Green *et al*, 2012). Given the proposed role of Set5 in growth control it is plausible that the resistance seen to bleomycin in this mutant reflects a change in growth rate. It would be interesting to analyse the growth rate of *set5*Δ cells with and without DNA damage conditions to determine if growth is altered compared to wildtype in *S. pombe*.

Three of the six mutants are predicted to be HMTs based on homology or the presence of a SET domain (the catalytic methylation domain; *set6*Δ, *set8*Δ and *SPBC16C6.01c*Δ) and one (*set10*Δ) is a predicted ribosomal lysine methyltransferase and also contains a SET domain. Given their lack of characterisation it is difficult to conclude why these mutants exhibit resistance to bleomycin. However, analysis of the growth rate of these mutants would show if the resistance could be attributed to this. Another possibility is that altered histone modification in these mutants may lead to a more compact chromatin state that is less prone to the damaging effects of bleomycin.

The final mutant that showed resistance to bleomycin, but no significant difference to wildtype in the DSB assay was *clr3*Δ. Clr3 is a class-II HDAC, which specifically deacetylates H3K14 and is required for silencing in heterochromatic regions; it is also implicated in the transcription of stress related genes through an antagonistic interaction with Gcn5 in the modification of H3K14 (Bjerling *et al*, 2002; Johnsson *et al*, 2009; Wiren *et al*, 2005). Given the importance of the acetylation state of H3K14 in the adaptation to stress, through transcription (Johnsson *et al*, 2009), it is possible that in the absence of Clr3, increased levels of H3K14ac lead to an increase in the transcription of stress response genes which results in improved survival in response to bleomycin.

Perhaps the most surprising group of mutants that were resistant to bleomycin are those that show decreased levels of GC in the DSB assay (*hat1*Δ and *set13*Δ). However, given the role

of Set9 in DSB repair and the lack of sensitivity of *set9*Δ cells to bleomycin at the concentration used, it is possible that in mutants which are not essential for HR (i.e. GC levels in *hat1*Δ and *set13*Δ are only reduced by 10-20%) higher concentrations are required to observe any sensitivity. This idea is consistent with results in *S. cerevisiae* that show a *HAT1* deletion mutant exhibiting sensitivity to MMS, but only at high concentrations (0.04%) compared to well characterised DNA repair mutants e.g. *rad52* which show sensitivity at much lower concentrations (0.005%; Qin & Parthun, 2002). In *S. pombe* a *hat1*$^{+}$ deletion mutant has also been shown to be sensitive to MMS but at concentrations higher than normally used (Benson *et al*, 2007). It would be interesting to look at the response of these mutants to a variety of DNA damaging agents, over a range of concentrations.

3.3.1.2 *elp3*Δ cells show sensitivity to bleomycin and IR

One mutant, *elp3*Δ showed sensitivity to both bleomycin and IR. Elp3 is the catalytic component of the Elongator HAT complex, which was originally purified as interacting with hyperphosphorylated forms of RNAP II (Wittschieben *et al*, 1999). The Elongator complex is postulated to have a role in the maintenance of genome integrity and DNA replication through an interaction with PCNA, and in *S. cerevisiae* deletion mutants of *ELP3* show sensitivity to HU and moderate levels of MMS (Li *et al*, 2009), consistent with results shown here. However, surprisingly, the *elp3*Δ DSB assay did not show any decrease in GC, but a significant increase in NHEJ/SCC and a significant decrease in Ch^{16} loss and LOH (Figure 3.5). However, this profile could be a reflection of increased time spent in S phase as shown in previous studies (Li *et al*, 2009). In this scenario, there may be increased use of the sister chromatid, which during S phase will be in closer proximity than chromosome III, resulting in increased levels of SCC.

3.3.2 *gcn5*Δ and *elp3*Δ mutants show increased levels of NHEJ/SCC

Two mutants, *elp3*Δ and *gcn5*Δ exhibited increased levels of NHEJ/SCC in the DSB assay. The potential role of Elp3 has been discussed above, and further analysis of the role of Gcn5 in DSB repair is addressed in Chapter 7. Briefly, Gcn5 is an evolutionarily conserved HAT that acetylates a number of residues including H3K9, H3K14 and H3K18, and is the catalytic subunit of several complexes including the SAGA co-activator complex (reviewed in Baker & Grant, 2007). It is involved in transcriptional initiation where is it recruited to promoters and also has a role in transcriptional elongation. In addition, acetylation of H3K14 by Mst2 and Gcn5 has recently been shown to be required for activation of the DNA damage checkpoint in fission yeast (Wang *et al*, 2012).

It is interesting, given both *elp3*Δ and *gcn5*Δ show increased NHEJ/SCC, that the C-terminal of Elp3 is structurally similar to the catalytic domain of Gcn5 (Winkler *et al*, 2002). In addition, budding yeast cells lacking Elp3 exhibit severe growth defects in the absence of Gcn5 (Kristjuhan *et al*, 2003) and overlapping functions between Elongator and Gcn5-containing SAGA complexes have been observed in *S. cerevisiae* (Wittschieben *et al*, 2000). Given these similarities it would be interesting to determine whether the increase in NHEJ/SCC is attributable to the same factor in both of these mutants, which could be achieved by analysing the DSB profile in cells which have SCC disabled, through deletion of *rhp51*$^{+}$. It is possible that the high levels of NHEJ/SCC could be due to low expression of the HO endonuclease in these genetic backgrounds or inefficient cutting, resulting from an altered chromatin state.

3.3.3 Hat1, Set13 and Clr4 are required for efficient HR

Three mutants, *hat1*Δ, *set13*Δ and *clr4*Δ showed decreased levels of GC associated with changes in LOH and/or Ch^{16} loss in the DSB assay (Figure 3.5). In the *clr4*Δ mutant, the low

levels of GC and exquisitely high levels of spontaneous Ch[16] loss likely reflect the key role of Clr4 in heterochromatin formation (Rea *et al*, 2000; Shankaranarayana *et al*, 2003). In the absence of Clr4, there will be little methylation of H3K9, resulting in inefficient recruitment of Swi6 and unsuccessful heterochromatin formation, which would likely cause chromosomal instability.

Further analysis of the *hat1*Δ and *set13*Δ mutants showed increased sensitivity of *hat1*Δ*rad3*Δ cells to bleomycin, and a role for Hat1 and Set13 in correct Rhp51 foci formation following DNA damage. However, both *hat1*Δ and *set13*Δ cells were checkpoint proficient.

Little is known about Set13 and there has been no suggested role for it in DSB repair. Set13 has been identified as a methyltransferase for lysine 55 of the ribosomal protein Rpl42 (Shirai *et al*, 2010). Methylation of ribosomal proteins appears conserved among a number of organisms (Carroll *et al*, 2008; Odintsova *et al*, 2003); however, its physiological significance remains largely unknown. The ribosome plays a key role in the adaptation to environmental stress and this methyl mark in particular is involved in regulating stress-adapted cell growth. It is suggested that methylation of Rpl42 may contribute to a particular step in the peptidyltransferase reaction (Shirai *et al*, 2010). Given the potential implications on translation efficiency, it would be interesting to determine whether the levels of proteins required for DSB repair are normal in the *set13*Δ mutant, as an indirect effect on the levels of HR proteins may explain the repair phenotype seen. In particular, given the postsynaptic role indicated by the Rhp51 kinetics, it would be important to address the levels of proteins involved in the steps following nucleofilament formation such as invasion, branch migration and resolution.

Hat1 is a B type HAT that has been characterised mostly in budding yeast. It is a member of two complexes: in the cytoplasm as HAT-B that is involved in acetylation of newly

synthesised histones (Parthun *et al*, 1996); and in the nucleus as NuB4 that contains a histone chaperone (Ai & Parthun, 2004; Poveda *et al*, 2004). In budding yeast, Hat1 has been shown to be involved in recombinational DSB repair (Qin & Parthun, 2002) where it is recruited to the DSB and acetylates H4K12 (Qin & Parthun, 2006). However, the role of this modification at the break site remains unknown. It is possible that this modification leads to recruitment of a specific repair factor. On the other hand, given the results shown in this chapter indicate that Hat1 has both a pre- and post-synaptic role in HR, perhaps this modification is required to provide an appropriate chromatin structure in which HR repair can progress. Further, Hat1 is required for chromatin reassembly following DSB repair (Ge *et al*, 2011) and this could explain its postsynaptic role in HR. It would be of interest to see if Hat1 is localised to the break site in fission yeast, by either visualising fluorescently tagged Hat1 or by chromatin immunoprecipitation.

3.3.4 Increased DSB repair by GC is frequently associated with inefficient NHEJ in histone-modifying mutants

Analysis of the histone-modifying mutants identified six mutants (*set1*Δ, *set2*Δ, *set3*Δ, *set11*Δ, *sir2*Δ and *mst2*Δ) that showed a significant increase in GC associated with a significant reduction in Ch^{16} loss and/or LOH (Figure 3.4), an unusual phenotype that suggests more efficient repair than wildtype cells. Given that controlling the choice of repair by HR or NHEJ is a key decision, which can affect repair fidelity, the NHEJ efficiency in these mutants was addressed. Four of the six mutants that exhibited high levels of GC also exhibited inefficient NHEJ (*set1*Δ, *set2*Δ, *set3*Δ and *mst2*Δ). This finding supports the existence of a competitive relationship between the mechanisms of DSB repair, which may help maintain genome stability.

3.3.4.1 A role for Set11 and Sir2 in DSB repair

The two mutants in which NHEJ was not compromised, were *sir2*Δ and *set11*Δ. Set11 has been shown to methylate ribosomal protein Rpl12; however, the functional significance of

this is not understood, although overexpression of Set11 does result in a growth defect (Sadaie *et al*, 2008). As discussed with the *set13*Δ mutant above, given the potential implications on translation, it would be interesting to address the levels of proteins involved in DSB repair.

The second mutant with increased GC, but efficient NHEJ is *sir2*Δ. Sir2 is a HDAC that deacetylates H3K9 and H4K16 and has an important role in silencing at mating type loci, telomeric and centromeric regions (Shankaranarayana *et al*, 2003). Deacetylation of H3K9 is required for subsequent methylation of this residue and recruitment of the Swi6 heterochromatic factor. Sir2 is also implicated in DSB repair; in budding yeast, Sir2 is recruited to a HO-induced break three hours after induction, consistent with a decrease in H3K9ac and H4K16ac at the break site (Tamburini & Tyler, 2005). Sir proteins have also been suggested to play a role in repair by NHEJ (Jackson, 1997; Tsukamoto *et al*, 1997), although further work has suggested this may be a minor role, caused by the effect of these mutations on mating type (Astrom *et al*, 1999; Lee *et al*, 1999). Certainly in this work, deletion of *sir2*$^{+}$ did not impart any defect in the ability of the cells to repair a DSB by NHEJ. It would be interesting to see if Sir2 is also localised to the break site in *S. pombe*. In the absence of Sir2, it is possible that the chromatin structure is more open, allowing steps required for efficient HR, such as resection and invasion, to proceed more efficiently, thus increasing the proportion of cells that repair using this mechanism.

3.3.4.2 A role for Set1, Set2, Set3 and Mst2 in promoting efficient NHEJ

The four mutants which showed increased levels of repair by GC, and inefficient NHEJ were *set1*Δ, *set2*Δ, *set3*Δ and *mst2*Δ. Two of these (Set1 and Set2) are HMTs, Mst2, is a HAT and Set3 is a member of a HDAC complex. Mst2 is a member of the Moz-Ybf2/Sas3-Sas2-Tip60 (MYST) family of acetyltransferases and acetylates H3K14 (Wang *et al*, 2012). It is involved as a negative regulator in telomeric heterochromatin formation and RNAi mediated

heterochromatin formation (Gomez *et al*, 2005; Reddy *et al*, 2011). Mst2 functions in conjunction with Gcn5 to regulate the global levels of H3K14ac (Nugent *et al*, 2010). The levels of this modification play a role in transcription (Pokholok *et al*, 2005; Wang *et al*, 2008) and activation of the DNA damage checkpoint through the recruitment of the RSC chromatin remodeling complex (Wang *et al*, 2012).

As with all histone modifiers that have a potential role in transcription it would be essential to determine whether the expression of DSB repair genes is altered in the *mst2*Δ mutant. Although H3K14 has been linked to the DNA damage checkpoint, the phenotypes were only observed when both Gcn5 and Mst2 were absent; given the strikingly different repair phenotypes of the two mutants it seems unlikely that these phenotypes relate to loss of H3K14 acetylation.

Despite the presence of a SET domain in Set3, which is often associated with HMT activity (Rea *et al*, 2000) no methyltransferase activity has been associated with Set3. In fact, in budding yeast Set3 forms a complex with HDACs Hos2 and Hst1 (Pijnappel *et al*, 2001), which is recruited to H3K4 dimethylated by Set1, consequently deacetylating histones in 5' transcribed regions (Kim & Buratowski, 2009). This is striking given that *set1*Δ cells exhibit the same repair phenotype as *set3*Δ cells. The homologue of the Set3 complex in fission yeast is required for the successful completion of cytokinesis (Rentas *et al*, 2012). In this work the authors showed that there is little change in the transcription of genes between a *set3*Δ mutant and wildtype under normal conditions, but following treatment with latrunculin A, a drug that impedes constriction of the actomyosin ring, the transcription of genes involved in the stress response was impaired. Given that in budding yeast, Set3 has also been shown to be requried for the correct response to secretory stress (Cohen *et al*, 2008) there may be a conserved role for Set3 in mounting an effective stress response. It would be interesting to investigate any transcriptional changes in this mutant following treatment with a DSB inducing agent such as

bleomycin, to see if the genes required for a timely response to this agent are transcribed in a manner different to wildtype.

The link between Set1 and Set3 in budding yeast is interesting given that in this work, *set1*Δ and *set3*Δ mutants both show increased levels of GC associated with impaired NHEJ. Set1 is a conserved H3K4 HMT that has important roles in transcription, telomeric and centromeric silencing (although it is suggested that a role for Set1 in gene silencing exists only in budding yeast), and a more recently identified function in DNA repair (Faucher & Wellinger, 2010; Kanoh *et al*, 2003; Noma *et al*, 2001; Schramke *et al*, 2001; Sollier *et al*, 2004). In yeast and mammalian cells, Set1 is part of a multi-component complex, known as Set1C (Lee & Skalnik, 2005; Roguev *et al*, 2003; Roguev *et al*, 2001; Wysocka *et al*, 2003). H3K4 methylation is associated with euchromatic regions of the genome (Noma *et al*, 2001), and methylation is enriched over transcripton start sites and the 5' end of transcribed genes (Kim & Buratowski, 2009). Studies have shown that in a *set1* mutant in budding yeast, there are global changes in gene expression (Boa *et al*, 2003; Schramke *et al*, 2001). One fission yeast study suggested the repair genes *rhp51*$^{+}$ and *suc22*$^{+}$ are not differentially expressed in a *set1*Δ mutant (Kanoh *et al*, 2003) but it would be essential to check the expression level of a wider range of DSB repair genes. However, during the course of this study, work published by Faucher and Wellinger has identified a role for Set1 in DSB repair by NHEJ in budding yeast (Faucher & Wellinger, 2010). They demonstrated that Set1 is normally recruited to a DSB in an RSC complex dependent manner, where it methylates H3K4; the presence of Set1 and H3K4me at the break site is required for the normal recruitment of Ku80. Given these findings it is possible that the NHEJ defect seen in the *set1*Δ mutant in this work is due to lack of recruitment of Ku to the break; this possibility could be addressed by chromatin immunoprecipitation.

*set2*Δ is the final mutant that exhibited significantly increased GC and deficient NHEJ. Set2 is a specific H3K36 HMT that is associated with euchromatic regions and transcription, where it interacts with elongating RNAP II (Morris *et al*, 2005). Further analysis of the role of Set2 in DSB repair was undertaken and is discussed in the subsequent chapters of this thesis.

3.3.4.3 A relationship between inefficient NHEJ and increased HR

The choice of DSB repair pathway is carefully regulated. The cell cycle is an key factor in this regulation; in haploid organisms HR can only be utilised in S and G2 phases when there is a sister chromatid, the preferred template for HR repair (Kadyk & Hartwell, 1992). In G1, a homologous chromosome could be used for HR repair, but this would result in LOH, and thus HR is restricted to S and G2 phase. In this work, four mutants have been identified that exhibit increased levels of repair by GC associated with inefficient NHEJ, suggesting a competitive interaction between NHEJ and HR. The idea of competition between DSB repair pathways was first suggested by early studies showing that plasmid DNA transfected into cells could be repaired by either NHEJ or HR (Roth & Wilson, 1985). Indeed several studies have demonstrated that when NHEJ is compromised there is an increase in repair by HR (Allen *et al*, 2003; Fukushima *et al*, 2001; Paques & Haber, 1999; Pierce *et al*, 2001). Whilst complete understanding of this has not been revealed, there is competition between Ku and the MRN complex for binding DNA ends (Mimitou & Symington, 2010; Shim *et al*, 2010) and if Ku is bound, resection is blocked, thus preventing repair by HR. Studies in DT40 cells by Adashi *et al*, demonstrated this competition in S phase by identifying an increased resistance to camptothecin in cells lacking Ku70 compared to wildtype (Adachi *et al*, 2004); presumably this resistance reflects that in wildtype cells, Ku binding to DSBs in S phase results in error-prone repair and consequently, some cell death. This phenotype mimics the increased viability to bleomycin observed in a number of the histone-modifying mutants in this work, including those with impaired NHEJ.

It would be interesting to complete a genome wide analysis of the relationship between NHEJ and HR; however, a more high-throughput method of analysing repair outcome would be required. Nevertheless, all the NHEJ defective mutants identified in this chapter, in addition to *lig4*Δ and *ku70*Δ mutants, exhibit increased levels of GC, supporting the existence of a competitive relationship between NHEJ and HR repair.

3.4 SUMMARY

To conclude, this chapter led to the identification of eleven genes required for efficient DSB repair.

- Preliminary characterisation of the role of eleven genes in DSB repair was described.
- A relationship between increased levels of DSB repair by HR and inefficient NHEJ was demonstrated.

Consequently, evidence has been presented to suggest a role for Set1, Set2, Mst2, Sir2, Set3, Set11, Hat1, Set13, Clr4, Gcn5 and Elp3 in DSB repair.

CHAPTER 4
A role for Set2 in DSB repair by non-homologous end-joining

4.1 INTRODUCTION

In Chapter 3, a screen of the histone-modifying mutants in a Bioneer deletion library identified four mutants, *set1*Δ*, set2*Δ*, set3*Δ and *mst2*Δ that exhibited significantly increased levels of GC associated with significantly decreased levels of Ch^{16} loss and/or LOH, and impaired NHEJ following a DSB. Thus, a potential role for these genes in controlling DSB repair was identified. Further investigation into the role of Set1, Set2 and Mst2 in DSB repair was undertaken in this chapter, with a particular focus on Set2.

4.2 RESULTS

4.2.1 Set1, Set2 and Mst2 are required for normal DNA double-strand break repair

As described in Chapter 3, quantification of DSB repair in *set1*$^+$*, set2*$^+$, *set3*$^+$ and *mst2*$^+$ deletion mutants was achieved by introduction of a minichromosome into the strains, and assessment of DSB-induced marker loss using the DSB assay (see Materials and Methods 2.10.1). This analysis identified all four mutants as having significantly increased levels of GC, associated with significantly decreased levels of Ch^{16} loss and/or LOH (Figure 3.4). Using a plasmid-rejoining assay, the ability of these mutants to repair a DSB by NHEJ was assessed, and was found to be impaired (Figure 3.9).

To further assess the role of Set1, Set2 and Mst2 in DSB repair, the response of *set1*$^+$*, set2*$^+$ and *mst2*$^+$ deletion mutants to various doses of IR was analysed. At lower doses of between 100 and 400 Gy, all three mutants were more resistant to IR than wildtype (Figure 4.1A). As

the dose increased from 500 to 1000 Gy, *set1*Δ and *mst2*Δ cells remained more resistant than wildtype. However at doses of 500 Gy or greater, *set2*Δ cells were as sensitive as wildtype. Given the resistance that all three mutants showed to bleomycin (Figure 3.1) this suggests that the 1 μg/ml bleomycin concentration used in the serial dilution assay corresponds to an IR dose not greater than 500 Gy.

To determine if the increased level of GC observed in *set1*$^{+}$, *set2*$^{+}$ and *mst2*$^{+}$ deletion mutants was associated with any increase in chromosomal rearrangements, LOH and GC colonies from the DSB assay were taken and the levels of crossovers were analysed by pulsed field gel electrophoresis (PFGE). On a pulsed field gel, crossovers between chromosome 16 and chromosome III (ChX; Figure 4.1B) appear as an intermediate band between chromosome III and chromosome 16 (Figure 4.1C). Quantification of crossover levels showed no significant difference between wildtype, *set1*Δ, *set2*Δ and *mst2*Δ cells (Figure 4.1D), indicating the increased ability to repair a DSB by GC is not associated with an increased level of chromosomal rearrangements.

4.2.2 *set2*$^{+}$ deletion does not result in resistance to all DNA damaging agents

Set2 is the only H3K36 HMT in *S. pombe* and is the homologue of SETD2, a human H3K36 HMT that has recently been identified as a tumour suppressor in renal cell carcinoma and breast cancer (Al Sarakbi *et al*, 2009; Dalgliesh *et al*, 2010; Duns *et al*, 2010). It was therefore decided to focus further on a detailed analysis of the role of Set2 in DSB repair.

Mutants of genes involved in DSB repair often exhibit an altered viability in response to a range of DNA damaging agents (Jackson & Bartek, 2009). To investigate whether *set2*Δ cells show an increased resistance to a range of DNA damaging agents or whether it is only to bleomycin and low doses of IR, serial dilution assays analysing the viability of *set2*Δ cells in

Figure 4.1

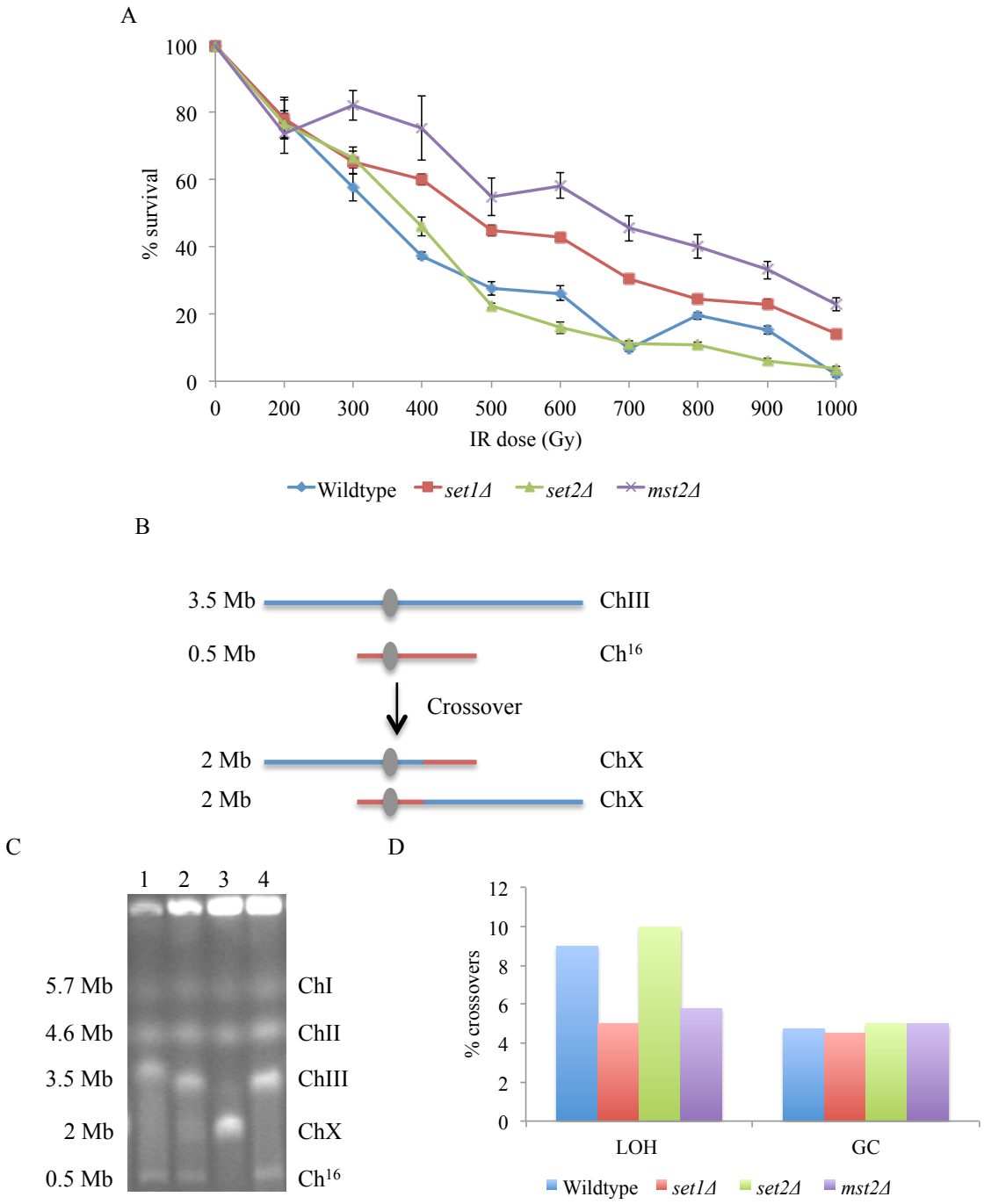


Figure 4.1 Increased GC is not associated with increased chromosomal rearrangements
(A) Ionising-radiation survival curve for wildtype (2094), *set1*Δ (3270), *set2*Δ (3271) and *mst2*Δ (3771) strains. Irradiations performed by Carol Walker. **(B)** Schematic showing formation of ChX by crossover of Ch^{16} and ChIII. **(C)** Example of crossovers (ChX) seen on pulsed-field gel: 1) wildtype, 2) *set1*Δ, 3) *set2*Δ, 4) *mst2*Δ. **(D)** Quantification of crossover levels in wildtype, *set1*Δ, *set2*Δ and *mst2*Δ cells in LOH and GC populations.

response to other agents were performed. The viability in response to methyl methanesulphonate (MMS), an alkylating agent, camptothecin (CPT), an inhibitor of topoisomerase I and hydroxyurea (HU) an inhibitor of ribonucleotide reductase (RNR) was analysed.

*set2*Δ cells showed a similar viability to wildtype in response to MMS and CPT, unlike *ctp1*Δ, a mutant in a key HR gene, which is sensitive to both agents (Figure 4.2). However, *set2*Δ cells did show an increased resistance to HU. HU inhibits RNR, resulting in a depletion of nucleotide pools and S phase arrest. This resistance may reflect HR being the predominant repair mechanism in S phase; the increased levels of repair by HR in *set2*Δ cells may be advantageous if longer is spent in this phase of the cell cycle (see Chapter 6). However, this somewhat depends of the extent of depletion of nucleotide pools, as a significant level of nucleotides would be required for the gap-filling stage of HR.

4.2.3 *set2*$^{+}$ deletion is epistatic with NHEJ mutants

In the plasmid-rejoining assay, *set2*Δ showed severely compromised NHEJ levels. If Set2 is required for NHEJ, then a *set2*Δ mutant should phenocopy mutants in key NHEJ factors. To this end, double mutants of *set2*Δ with *lig4*Δ and *ku70*Δ were created and their viability in response to bleomycin observed. Both *set2*Δ*lig4*Δ and *set2*Δ*ku70*Δ exhibited the same viability as the single mutants alone (Figure 4.3A), indicating that they do function in the same pathway, as expected. It would also be expected that if Set2 is required for NHEJ, then a double mutant with a key HR factor such as *rhp51*Δ should severely compromise the ability of the cells to survive treatment with a DNA damaging agent. This is indeed the case; a *set2*Δ*rhp51*Δ double mutant was exquisitely sensitive to bleomycin compared to both single mutants (Figure 4.3A).

Figure 4.2

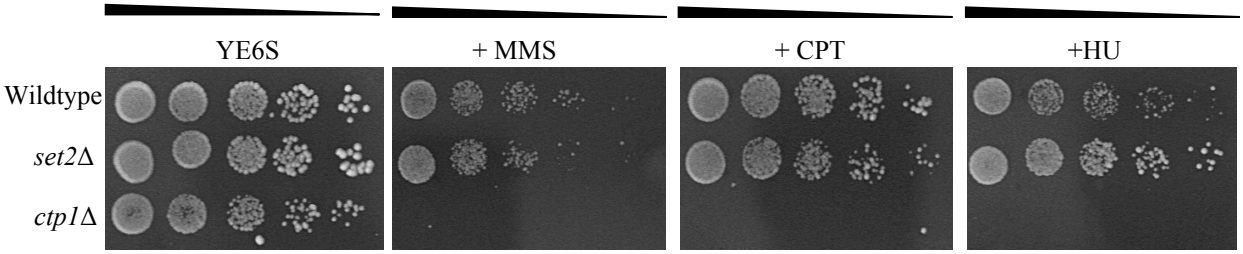


Figure 4.2 *set2*Δ cells do not exhibit increased resistance to all DNA damaging agents 5-fold serial dilutions of wildtype (2094), *set2*Δ (3271) and *ctp1*Δ (3423) cells were grown on YE6S, YE6S + 0005% MMS, YE6S + 5 μM camptothecin (CPT) and YE6S + 5 mM hydroxyurea (HU).

Given the qualitative nature of the serial dilution assay, the survival of wildtype, *set2*Δ, *ku70*Δ and *set2*Δ*ku70*Δ cells in response to varying doses of bleomycin was also assessed using a survival curve. This confirmed that the *set2*Δ*ku70*Δ double mutant was no more sensitive to bleomycin than the single mutants (Figure 4.3B). Interestingly, in this experiment in which cells are treated with bleomycin whilst growing in liquid culture, *set2*Δ cells did not show a resistance to bleomycin compared to wildtype cells. Perhaps this reflects the damaging capability of bleomycin to cells in liquid compared to on solid media. It is possible that the cells in the serial dilution assay quickly reach stationary phase compared to the cells in liquid. In stationary phase they may be less prone to damage, thus the concentration of bleomycin on solid media may be equivalent to a lower concentration in liquid.

To further this analysis, *lig4*Δ and *ku70*Δ strains containing Ch^{16}-RMGAH were analysed using the DSB assay. *lig4*Δ cells showed an increased level of GC compared to wildtype (60%, p=0.03); all other outcomes were reduced but not significantly, compared to wildtype (Figure 4.3C). *ku70*Δ cells showed a similar phenotype to *set2*Δ cells; GC was significantly increased compared to wildtype (82%, p=0.02), and LOH and Ch^{16} loss were significantly reduced (1%, p=0.04 and 2%, p=0.01; Figure 4.3C). Double mutants of *ku70*Δ or *lig4*Δ with *set2*Δ were also analysed using the DSB assay. Both *set2*Δ*ku70*Δ and *set2*Δ*lig4*Δ double mutants had similar phenotypes to *set2*Δ alone. The *set2*Δ*ku70*Δ double mutant had increased levels of GC (81%, p=0.07) and decreased Ch^{16} loss (8%, p=0.03) whilst the *set2*Δ*lig4*Δ double mutant had increased GC (69%, p<0.01) and significantly decreased LOH and Ch^{16} loss (2%, p=0.01 and 1%, p<0.01; Figure 4.3D and E). These data align with the hypothesis that these genes act in the same pathway.

4.2.4 *set2*$^{+}$ deletion exhibits negative genetic interactions with early-acting HR mutants

If Set2 acts in NHEJ, then a negative genetic interaction with mutations in genes whose products are involved in HR would be anticipated in response to DNA damage. In addition to the double mutant of *set2*Δ*rhp51*Δ already tested (Figure 4.3A) double mutants of *set2*Δ with other HR mutants were created and their viability in response to bleomycin assessed using the serial dilution assay.

A key requirement for HR is 5'-3' resection of the DNA flanking the DSB, which creates single-strand tracts that can be bound by RPA. RPA is displaced by Rhp51, which forms a nucleofilament that initiates strand invasion and homology search. Given this key requirement for DNA resection in HR, double mutants of *set2*Δ with factors involved in resection were constructed and analysed. Initial short tract resection is performed by the MRN complex, in concert with Ctp1 (Limbo *et al*, 2007; Paques & Haber, 1999). This is followed by long tract resection; in *S. pombe*, the majority of long tract resection is performed by Exo1, with the helicase Rqh1 playing an additional role (Langerak *et al*, 2011).

Firstly the requirement of long tract DNA resection in a *set2*Δ mutant was analysed. The double mutant of *set2*Δ*exo1*Δ showed sensitivity to bleomycin compared to the single mutants alone (Figure 4.4A) suggesting that in the absence of *set2*$^{+}$, resection by Exo1 becomes essential for survival following treatment with bleomycin. As shown previously, *set2*Δ is epistatic with *ku70*Δ; deletion of *exo1*$^{+}$ in this background still led to the sensitivity observed in the *set2*Δ*exo1*Δ mutant. In keeping with this sensitivity, the double mutant cells exhibited an elongated phenotype in response to bleomycin, compared to the single mutants, indicating a cell cycle arrest (Figure 4.4B). Quantitative analysis of the relative sensitivities of *set2*Δ,

Figure 4.3

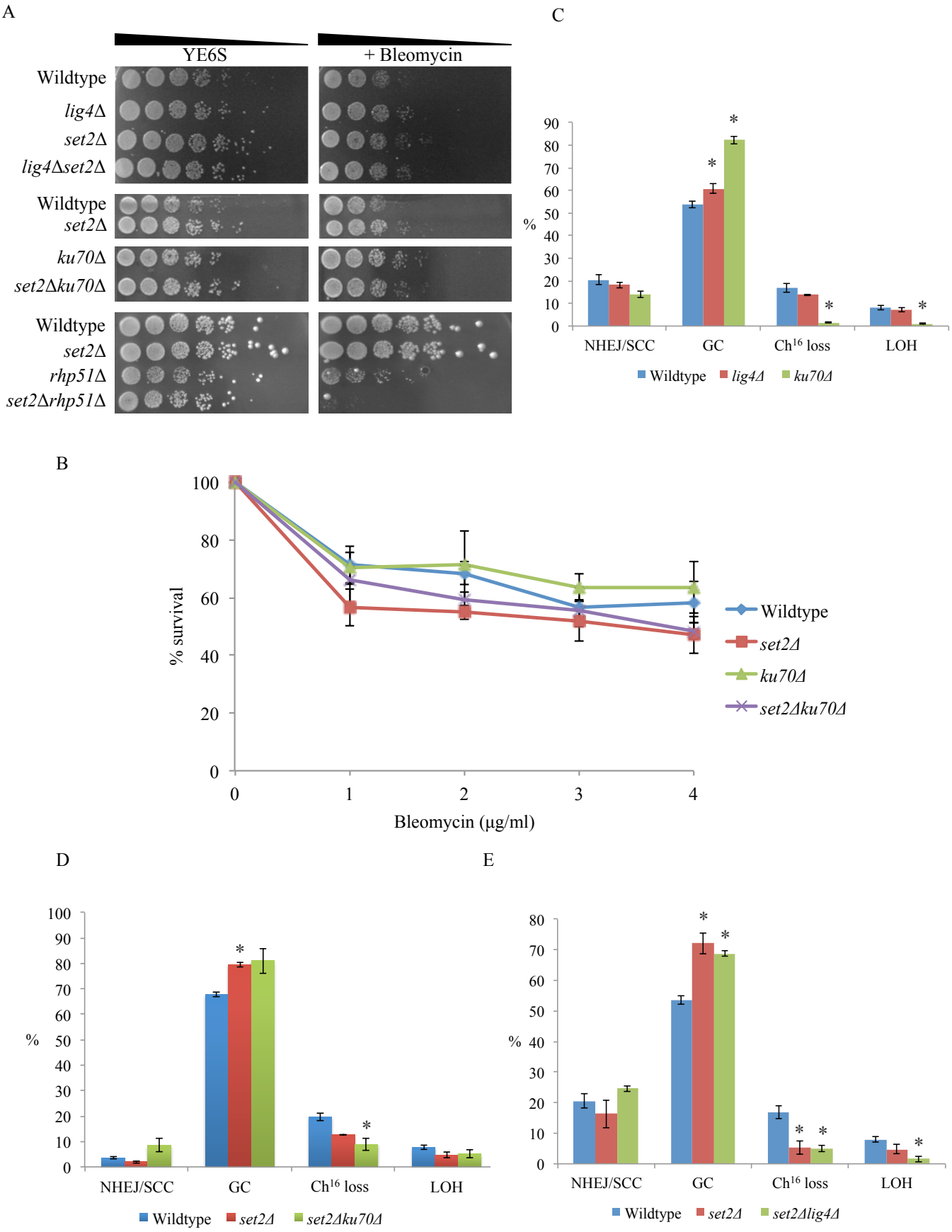

A
YE6S
+ Bleomycin
Wildtype
lig4Δ
set2Δ
lig4Δset2Δ
Wildtype
set2Δ
ku70Δ
set2Δku70Δ
Wildtype
set2Δ
rhp51Δ
set2Δrhp51Δ
C
%
NHEJ/SCC
GC
Ch16 loss
LOH
Wildtype
lig4Δ
ku70Δ
B
% survival
Bleomycin (µg/ml)
Wildtype
set2Δ
ku70Δ
set2Δku70Δ
D
%
NHEJ/SCC
GC
Ch16 loss
LOH
Wildtype
set2Δ
set2Δku70Δ
E
%
NHEJ/SCC
GC
Ch16 loss
LOH
Wildtype
set2Δ
set2Δlig4Δ

Figure 4.3 *set2*$^{+}$ deletion is epistatic with NHEJ gene deletions (A) 5-fold serial dilutions of wildtype (2094), *lig4*Δ (1069), *set2*Δ (3271), *lig4*Δ*set2*Δ (5376), *ku70*Δ (5593), *set2*Δ*ku70*Δ (5654), *rhp51*Δ (3992) and *set2*Δ*rhp51*Δ (5153) cells were grown on YE6S and YE6S + 1 µg/ml bleomycin (top 2 panels) or 0.3 µg/ml bleomycin (bottom panel). **(B)** Bleomycin survival curve for wildtype, *set2*Δ, *ku70*Δ and *set2*Δ*ku70*Δ cells. **(C)** Percentage DSB-induced marker loss in wildtype (2131), *lig4*Δ (3568-70), and *ku70*Δ (4766-7, 4762) containing Ch^{16}-RMGAH. The levels of NHEJ/SCC, GC, Ch^{16} loss and LOH are shown. **(D)** Percentage DSB-induced marker loss in wildtype (4104), *set2*Δ (6549-51) and *set2*Δ*ku70*Δ (5770, 5772, 6853) containing Ch^{16}-RMYAH. The levels of NHEJ/SCC, GC, Ch^{16} loss and LOH are shown. **(E)** Percentage DSB-induced marker loss in wildtype (2131), *set2*Δ (3841-3) and *set2*Δ*lig4*Δ (5988-90) containing Ch^{16}-RMGAH. The levels of NHEJ/SCC, GC, Ch^{16} loss and LOH are shown. Data are the mean of three experiments and error bars (± SE) are shown. * indicates statistical significance.

*exo1*Δ and the double mutant using a survival curve confirmed the finding that the double mutant is more sensitive than either of the single mutants alone (Figure 4.4C). To address whether an absence of Rqh1 also conferred this sensitivity in the *set2*Δ mutant, the response of a *set2*Δ*rqh1*Δ double mutant to bleomycin was analysed using the serial dilution assay. Although the *set2*Δ*rqh1*Δ showed a slight increased sensitivity to bleomycin compared to the single mutants, it was not as striking as seen in the *set2*Δ*exo1*Δ (Figure 4.4A). This likely reflects the predominance of Exo1 in long tract resection in fission yeast.

To further this analysis, Ch^{16}-RMGAH was introduced into *exo1*Δ and *set2*Δ*exo1*Δ cells and break-induced marker loss analysed using the DSB assay. It would be expected, in the absence of Exo1, that HR would be less efficient. However, surprisingly *exo1*Δ cells showed a repair profile not dissimilar to *set2*Δ cells; significantly increased levels of GC (66%, p=0.02) and significantly decreased levels of NHEJ/SCC (8%, p=0.02), compared to wildtype (Figure 4.4D). Given only 200 bases of ssDNA are required for efficient HR between two episomal plasmids (Liskay *et al*, 1987; Rubnitz & Subramani, 1984), Exo1 may not be essential for repair in this context. The double *set2*Δ*exo1*Δ mutant showed a similar repair profile to the single *set2*Δ mutant; increased, although not significantly, levels of GC (66%, p=0.28), and reduced levels of Ch^{16} loss (9%, p=0.02) and LOH (3%, p=0.18; Figure 4.4D).

Following this initial analysis of the requirement for long tract DNA resection in a *set2*Δ mutant, short tract resection by the MRN complex and Ctp1 was investigated. The viability of *set2*Δ double mutants with MRN complex members in response to bleomycin was analysed using the serial dilution assay. Deletion mutants of $rad50^+$, $rad32^+$ and $nbs1^+$ in a *set2*Δ background showed a striking sensitivity to bleomycin, similar to that seen in the *set2*Δ*exo1*Δ mutant, indicating that short tract resection is required in a *set2*Δ background (Figure 4.5A).

Figure 4.4

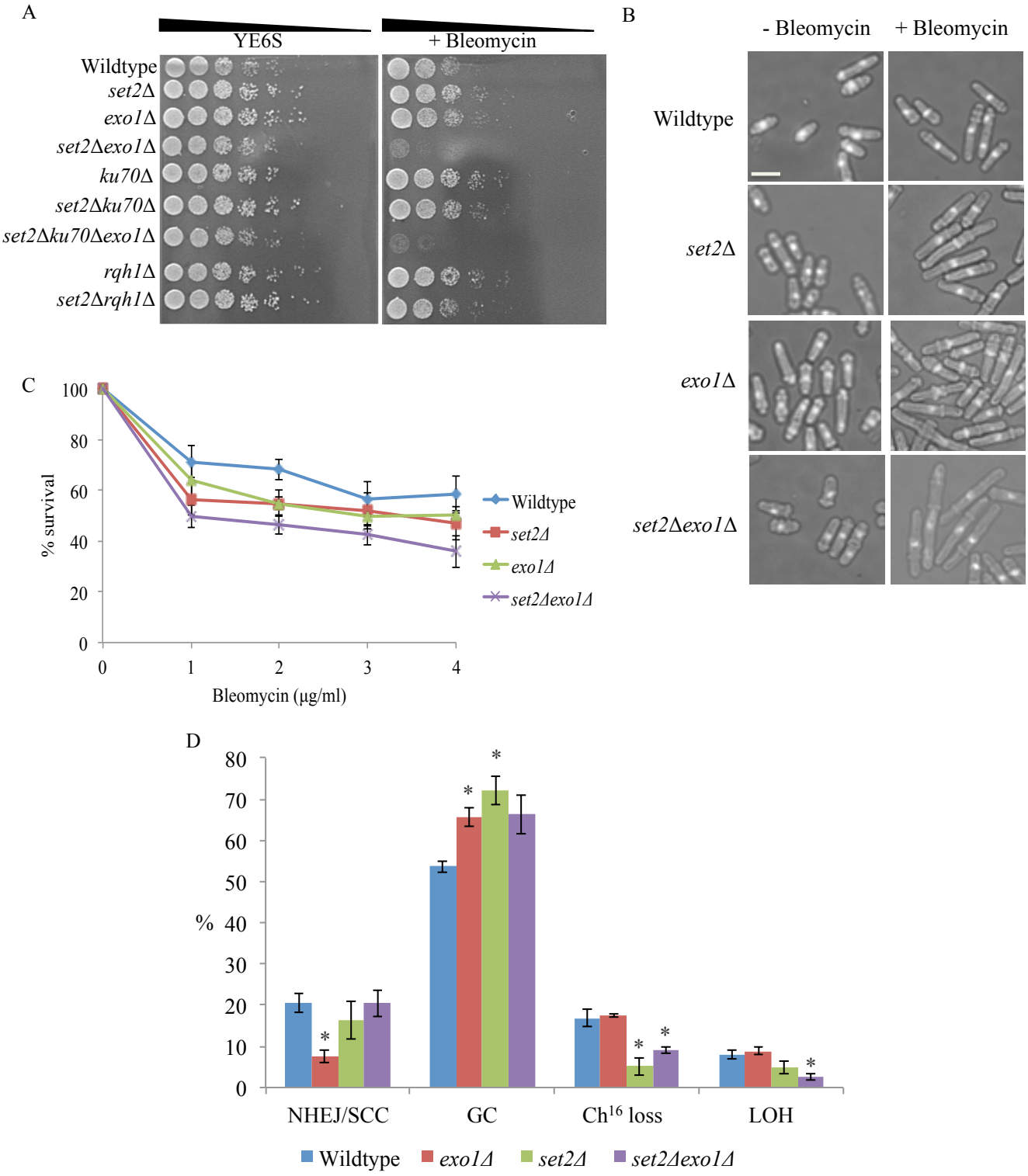


Figure 4.4 *set2*Δ cells are sensitive to bleomycin in combination with early-acting HR genes (A) 5-fold serial dilutions of wildtype (2094), *set2*Δ (3271), *exo1*Δ (5310), *set2*Δ*exo1*Δ (4999), *ku70*Δ (5593), *set2*Δ*ku70*Δ (5654), *set2*Δ*ku70*Δ*exo1*Δ (6199), *rqh1*Δ (DL1.6A9) and *set2*Δ*rqh1*Δ (6197) cells were grown on YE6S and YE6S + 1 µg/ml bleomycin. **(B)** Wildtype, *set2*Δ, *exo1*Δ and *set2*Δ*exo1*Δ cells were grown to mid-log phase in YE6S and samples taken for microscopy before and after 3 hours treatment with 5 µg/ml bleomycin. Scale bar, 10 µm. **(C)** Bleomycin survival curve for wildtype, *set2*Δ, *exo1*Δ and *set2*Δ*exo1*Δ cells. **(D)** Percentage DSB-induced marker loss in wildtype (2131), *exo1*Δ (3378-80), *set2*Δ (3841-3) and *set2*Δ*exo1*Δ (7091-4) containing Ch^{16}-RMGAH. The levels of NHEJ/SCC, GC, Ch^{16} loss and LOH are shown. Data are the mean of three experiments and error bars (± SE) are shown. * indicates statistical significance.

Due to the sensitivity of the single *rad50*$^{+}$, *rad32*$^{+}$ and *nbs1*$^{+}$ deletion mutants, bleomycin concentration was used at a third of the normal level, which explains the lack of resistance shown in the *set2*Δ strain compared to wildtype in this instance. In keeping with this sensitivity, the double mutants showed a further elongated phenotype following treatment with bleomycin, compared to the single mutants (Figure 4.5B). Ctp1 has been shown to be essential for initiation of resection in *S. pombe* (Limbo *et al*, 2007). Therefore, viability of a *set2*Δ*ctp1*Δ double mutant following bleomycin treatment was also analysed. *set2*Δ*ctp1*Δ cells exhibited a striking sensitivity to bleomycin, similar to that seen when Exo1, or members of the MRN complex were deleted in a *set2*Δ background (Figure 4.5C).

Collectively, this genetic analysis suggests resection is essential for *set2*Δ cells to survive following bleomycin treatment. This supports a role for Set2 in a HR-independent DNA repair pathway.

4.2.5 *lig4*$^{+}$ and *ku70*$^{+}$ are not equivalent to *set2*$^{+}$ in their interaction with *exo1*Δ

As shown above, *set2*Δ cells are very sensitive to bleomycin in combination with mutants involved in resection. Presumably this is because *set2*Δ cells have compromised repair by NHEJ; therefore, inhibiting DNA resection by introducing deletion mutants in *exo1*$^{+}$, *rad50*$^{+}$, *rad32*$^{+}$, *nbs1*$^{+}$or *ctp1*$^{+}$ in a *set2*Δ background should compromise repair by both HR and NHEJ, which would explain the sensitivity in these mutants. However, contradictory to this, is the finding that *exo1*Δ and *exo1*Δ*set2*Δ cells do not exhibit reduced GC in the DSB assay.

To investigate this, double mutants of *exo1*Δ with NHEJ factor mutants (*lig4*Δ and *ku70*Δ) were constructed to determine whether the sensitivity of the *set2*Δ*exo1*Δ double mutant is due to defective NHEJ in a *set2*Δ background. First, the viability of the double mutants in

Figure 4.5

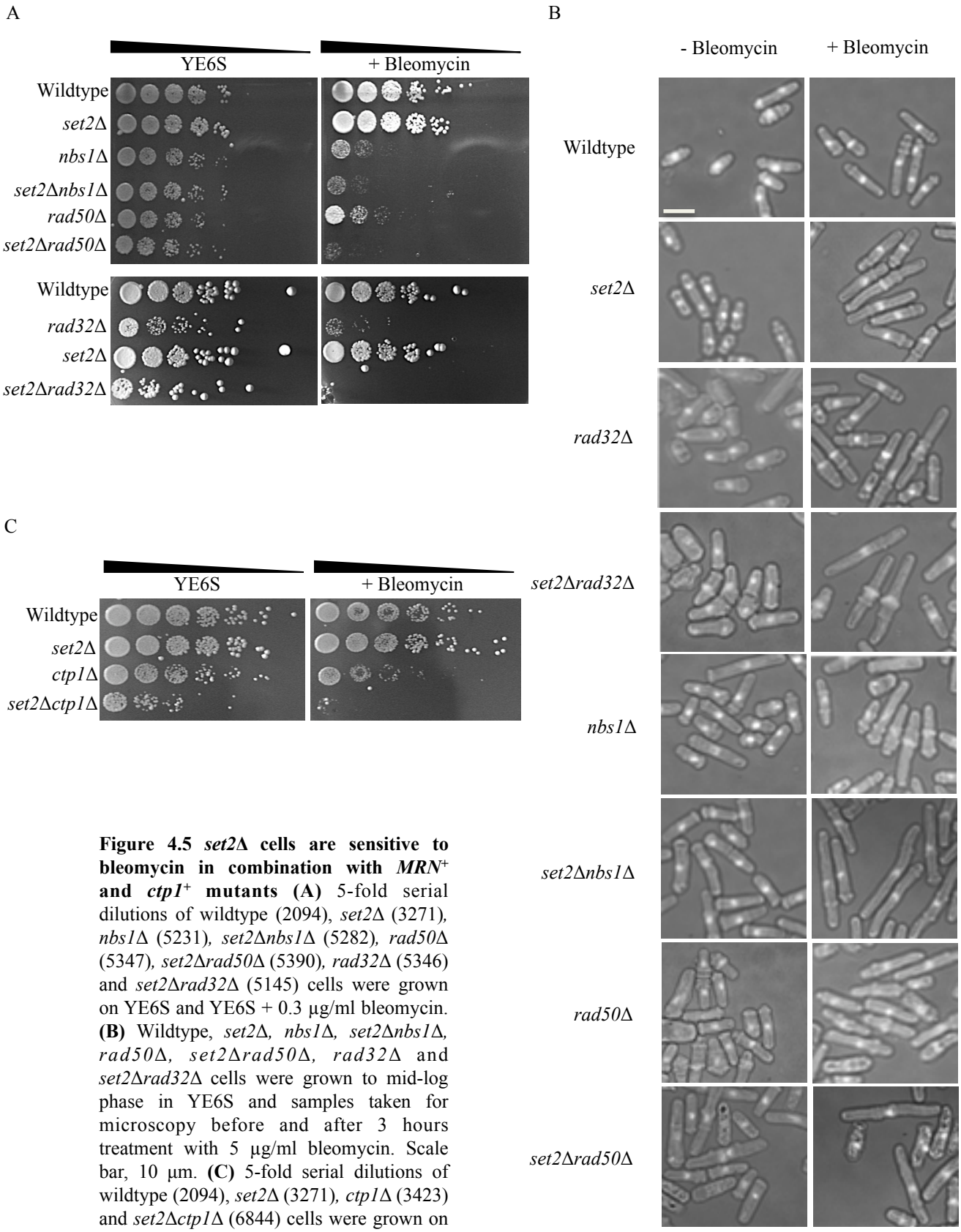


Figure 4.5 *set2*Δ cells are sensitive to bleomycin in combination with *MRN*$^+$ and *ctp1*$^+$ mutants (A) 5-fold serial dilutions of wildtype (2094), *set2*Δ (3271), *nbs1*Δ (5231), *set2*Δ*nbs1*Δ (5282), *rad50*Δ (5347), *set2*Δ*rad50*Δ (5390), *rad32*Δ (5346) and *set2*Δ*rad32*Δ (5145) cells were grown on YE6S and YE6S + 0.3 µg/ml bleomycin. **(B)** Wildtype, *set2*Δ, *nbs1*Δ, *set2*Δ*nbs1*Δ, *rad50*Δ, *set2*Δ*rad50*Δ, *rad32*Δ and *set2*Δ*rad32*Δ cells were grown to mid-log phase in YE6S and samples taken for microscopy before and after 3 hours treatment with 5 µg/ml bleomycin. Scale bar, 10 µm. **(C)** 5-fold serial dilutions of wildtype (2094), *set2*Δ (3271), *ctp1*Δ (3423) and *set2*Δ*ctp1*Δ (6844) cells were grown on YE6S and YE6S + 0.3 µg/ml bleomycin.

response to bleomycin was addressed using the serial dilution assay. The *lig4*Δ*exo1*Δ double mutant was no more sensitive than the *lig4*Δ mutant alone, which shows an increased resistance to bleomycin similar to that seen in *set2*Δ cells (Figure 4.6A). A similar response was seen with the *ku70*Δ*exo1*Δ mutant: the same sensitivity in the double mutant as *ku70*Δ cells alone, which shows an increased resistance compared to wildtype (Figure 4.6A). In fact, deletion of $ku70^{+}$ or $lig4^{+}$ in an *exo1*Δ background rescued any sensitivity to bleomycin observed in *exo1*Δ cells alone (Figure 4.6A). This result was confirmed quantitatively using a survival curve with varying doses of bleomycin; *set2*Δ*exo1*Δ was the most sensitive strain as expected, with *ku70*Δ alone showing an increased resistance to bleomycin, compared to wildtype and *exo1*Δ*ku70*Δ showing a similar response to *ku70*Δ alone (Figure 4.6B). These data suggest that the sensitivity observed in the *set2*Δ*exo1*Δ mutant is not due to the NHEJ defect of the $set2^{+}$ deletion strain, and indicates an additional role for Set2.

4.2.6 Altering phosphorylation of RNAP II CTD does not result in the same repair phenotype as a $set2^{+}$ deletion mutant

Set2 interacts with the C-terminal domain (CTD) of elongating RNAP II (Kizer *et al*, 2005; Li *et al*, 2003; Schaft *et al*, 2003; Xiao *et al*, 2003) and methylated H3K36 is enriched over actively transcribed genes (Buratowski, 2003; Phatnani & Greenleaf, 2006; Pokholok *et al*, 2005). Set2 binds to serine 2 and 5 phosphorylated RNAP II, through an interaction mediated by a C-terminal domain of Set2, named SRI (Set2-Rpb1 interacting domain; Kizer *et al*, 2005; Vojnic *et al*, 2006; Xiao *et al*, 2003). Fission yeast Cdk9 is the essential orthologue of metazoan P-TEFb which phosphorylates the CTD of RNAP II and is required for coordination of capping and elongation of RNAP II transcripts (Garriga & Grana, 2004). In fission yeast, Cdk9 is also involved in phosphorylating the CTD of RNAP II and is activated by phosphorylation of T212 by the CDK activating kinase (CAK) Csk1 (Pei *et al*, 2006).

Figure 4.6

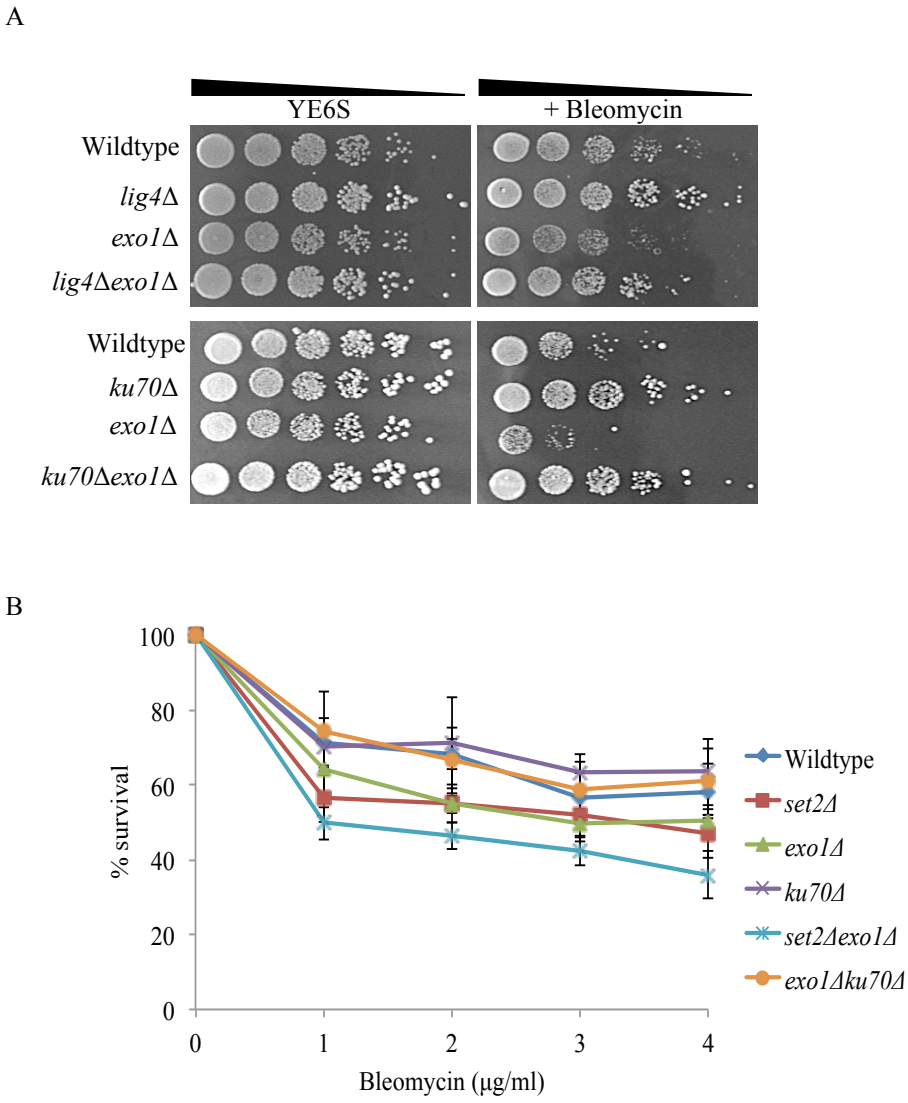


Figure 4.6 Deletion of *set2*$^{+}$ is not equivalent to deletion of NHEJ genes in its interaction with HR mutants (A) 5-fold serial dilutions of wildtype (2094), *lig4*Δ (1069), *exo1*Δ (5310), *lig4*Δ*exo1*Δ (6360), *ku70*Δ (5593) and *ku70*Δ*exo1*Δ (6657) cells were grown on YE6S and YE6S + 1 µg/ml bleomycin. **(B)** Bleomycin survival curve for wildtype, *set2*Δ, *exo1*Δ, *ku70*Δ, *set2*Δ*ku70*Δ and *ku70*Δ*exo1*Δ cells.

To address whether an interaction with RNAP II is required for the role of Set2 in DNA repair, mutations in Csk1 and Cdk9 were utilised. A *csk1*$^{+}$ deletion mutant, and *cdk9-T212A* and *cdk9-T212E* point mutants were used to determine if phosphorylation of RNAP II and thus interaction with Set2 is required for the role of Set2 in NHEJ. In the *csk1*Δ mutant, Cdk9 activity will not be enhanced, the *cdk9-T212A* shows reduced phosphorylation of RNAP II whereas *cdk9-T212E* is constitutively active and RNAP II will be phosphorylated to a greater extent. If phosphorylation of RNAP II by Cdk9 is required for the role of Set2 in repair, *csk1*Δ and *cdk9-T212A* may be phenotypically similar to Set2.

The viability of *csk1*Δ, *cdk9-T212A* and *cdk9-T212E* cells in response to bleomycin was assessed using the serial dilution assay. *csk1*Δ and *cdk9-T212A* cells were both mildly sensitive to bleomycin compared to wildtype and *set2*Δ cells, whereas *cdk9-T212E* cells were resistant to bleomycin, as seen in *set2*Δ cells (Figure 4.7A). To address DSB repair more quantitatively, Ch^{16}-RMYAH was introduced into the mutants and break-induced marker loss analysed. Unfortunately, in the *csk1*Δ background, high levels of spontaneous chromosome rearrangements were observed. Therefore marker loss could not be counted and a repair profile could not be generated for this mutant. In the *cdk9-T212A* mutant, significant cell death occurred when the cells were grown for 48 hours during the DSB assay, and therefore no repair profile could be obtained for this mutant. This suggests that this residue is important for normal growth. The *cdk9-T212E* mutant was also slow growing; however it did grow sufficiently to allow the DSB assay to be performed. Results showed a significant decrease in GC compared to wildtype (20%, p=0.02) and a significant increase in Ch^{16} loss (68%, p=0.04; Figure 4.7B). This suggests a role for Cdk9 T212 in promoting efficient HR repair. This is surprising given the increased resistance to bleomycin seen in the *cdk9-T212E* mutant; it would be interesting to address this resistance more quantitatively by generating survival

curves using a number of DSB-inducing drugs, over a range of concentrations. It is possible that using higher concentrations of drugs would result in the sensitivity expected.

Without the results for the *csk1*Δ and *cdk9-T212E* DSB assay it is difficult to definitively conclude whether phosphorylation of RNAP II by Cdk9 is required for the role of Set2 in DSB repair. However, the DSB result for *cdk9-T212E* cells indicates that Cdk9 is required for maintenance of genome integrity in a different way to Set2. In addition, the serial dilution assay shows the opposite result to that expected if phosphorylation of RNAP II and subsequent interaction with Set2 was required for the role of Set2 in NHEJ.

4.2.7 The Clr6 HDAC complex is not required for the role of Set2 in NHEJ

Co-transcriptional methylation of H3K36 by Set2 leads to recruitment of HDAC complexes; in *S. cerevisiae* the reduced potassium dependency 3 small (Rpd3S) HDAC, which leads to deacetylation of histones in the wake of elongating RNAP II (Keogh *et al*, 2005). This prevents spurious transcriptional initiation within coding sequences (Carrozza *et al*, 2005; Li *et al*, 2007; Lickwar *et al*, 2009). In *S. pombe*, the homolog of Rpd3, Clr6, deacetylates several lysines of H3 and H4 (Bjerling *et al*, 2002) and forms two active complexes (Nicolas *et al*, 2007); complex II is homologous to the Rpd3(S) complex in budding yeast, which is also involved in deacetylation of coding regions and suppression of aberrant transcription. On the other hand, complex I is involved in deacetylation of promoters. Complex II comprises Alp13, a chromodomain containing protein, which is required for binding methylated histones, Pst2, Prw1 and Cph1 and Cph2 (Nakayama *et al*, 2003; Nicolas *et al*, 2007). In *S. pombe*, deletion of $set2^{+}$ results in an increase in aberrant transcription, but this is a milder phenotype than seen in an *alp13*Δ mutant, suggesting that these genes at least in part act in different pathways (Nicolas *et al*, 2007); this is consistent with the observation that a *set2*Δ mutant in fission yeast does not have a substantial effect on the acetylation levels of histones

Figure 4.7

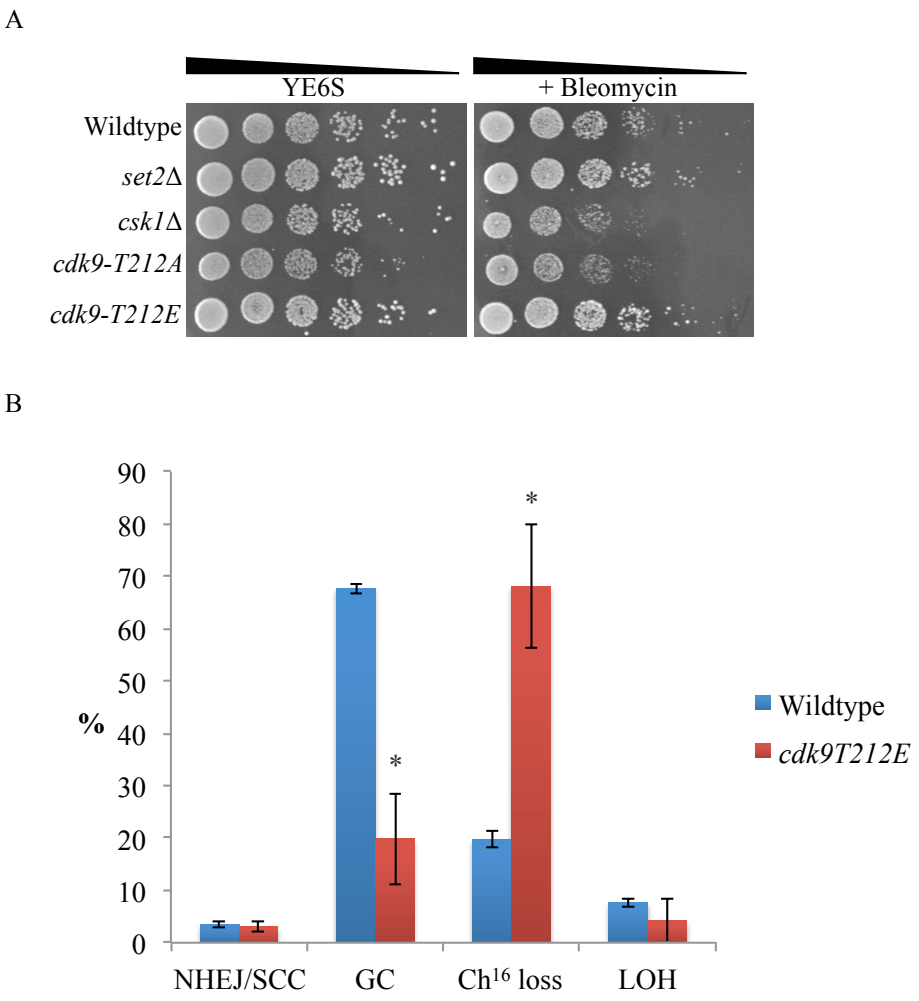


Figure 4.7 Cdk9 T212 is required for efficient DSB repair by GC (A) 5-fold serial dilutions of wildtype (2094), *set2*Δ (3271), *csk1*Δ (1228), *cdk9-T212A* (6108) and *cdk9-T212E* (6109) cells were grown on YE6S and YE6S + 1 µg/ml bleomycin. **(B)** Percentage DSB-induced marker loss in wildtype (4104) and *cdk9-T212E* (6846-8) cells containing Ch^{16}-RMYAH. The levels of NHEJ/SCC, GC, Ch^{16} loss and LOH are shown. Data are the mean of three experiments and error bars (± SE) are shown. * indicates statistical significance.

(Morris *et al*, 2005). It is suggested that although H3K36 methylation may recruit the Clr6 HDAC complex in fission yeast, there are likely other factors involved (Nicolas *et al*, 2007). Despite this complexity, whether recruitment of this complex is required for efficient NHEJ was addressed, by analysing an *alp13*Δ mutant and a *clr6-1* temperature sensitive mutant.

As *set2*Δ cells show an increased resistance to bleomycin in the serial dilution assay, the viability of *alp13*Δ and *alp13*Δ*set2*Δ cells to bleomycin was investigated. In agreement with Nakayama *et al*., (2003) *alp13*Δ cells were extremely sensitive to bleomycin and the double mutant was even more sensitive (Figure 4.8A). Given this different phenotype in *alp13*Δ compared to *set2*Δ cells, and the sensitivity to bleomycin in the double mutant, it seems unlikely that Alp13 is required for the repair role of Set2. In agreement, *clr6-1*, a temperature sensitive mutant, whose HDAC activity is significantly reduced from 25°C to 32°C, failed to exhibit any NHEJ defect compared to wildtype, when analysed with the plasmid-rejoining assay (Figure 4.8B). These data suggest that the Clr6 HDAC complex is not required for the role of Set2 in NHEJ.

Figure 4.8

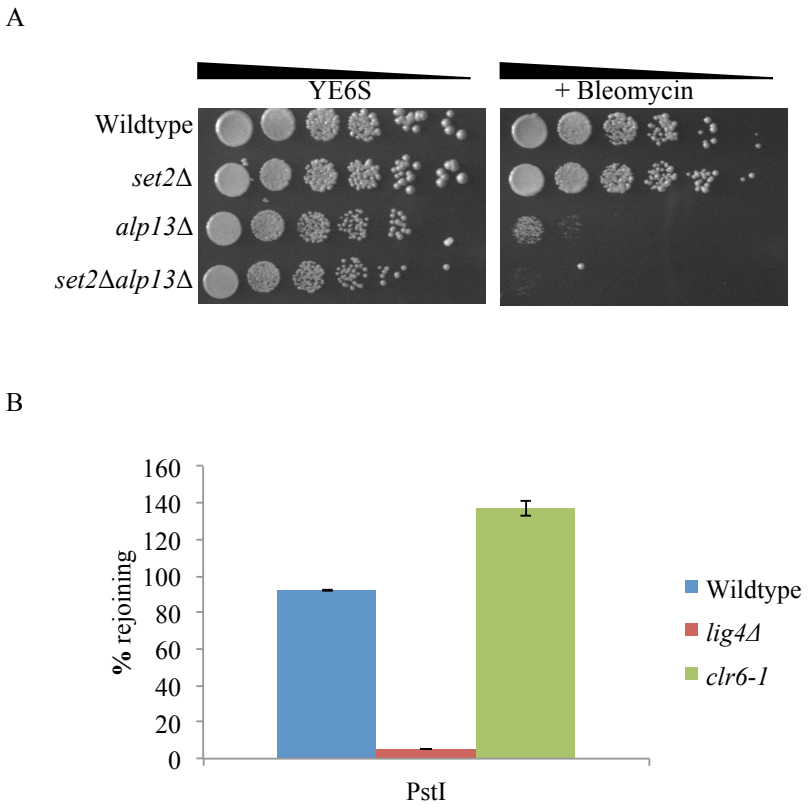


Figure 4.8 The Clr6 HDAC complex is not required for the role of Set2 in NHEJ (A) 5-fold serial dilutions of wildtype (2094), *alp13*Δ (5591), *set2*Δ (3271) and *alp13*Δ*set2*Δ (6525) cells were grown on YE6S and YE6S + 1 µg/ml bleomycin. **(B)** Outcome of NHEJ plasmid-rejoining assay for *clr6-1* (3274) cells. Cells were grown at the restrictive temperature of 32°C. Data are the mean of three experiments and error bars (± SE) are shown.

4.3 DISCUSSION

In Chapter 3, a screen for histone-modifying enzymes that function in DSB repair identified a *set2*$^{+}$ deletion mutant as exhibiting increased levels of repair by GC and inefficient NHEJ. In this chapter, further work supports a role for Set2 in promoting efficient NHEJ. Results suggest that this role is independent of RNAP II phosphorylation by Cdk9 and recruitment of the Clr6 HDAC complex.

4.3.1 An essential role for resection in a *set2*$^{+}$ deletion mutant

Analysis in Chapter 3 showed that *set2*Δ cells exhibit increased levels of DSB repair by GC and impaired NHEJ. Further analysis in this chapter indicated that deletion of *set2*$^{+}$ phenocopies mutations in NHEJ factors. *set2*Δ is epistatic with *lig4*Δ and *ku70*Δ in the response to bleomycin and IR, and analysis using the DSB assay showed that *ku70*Δ and *lig4*Δ mutants exhibit a similar profile to *set2*Δ cells, increased GC, supporting the concept of competition between NHEJ and HR. Analysis of the genetic interactions between mutants has been used as a way to further understand gene function (Nijman, 2011), and genetic analysis suggests that Set2 functions in the NHEJ pathway (Figure 4.3).

Further analysis of *set2*Δ cells showed that efficient resection is essential in a *set2*$^{+}$ deletion background, as double mutants with *exo1*Δ, *rad50*Δ, *rad32*Δ, *nbs1*Δ and *ctp1*Δ are all exquisitely sensitivity to bleomycin. The dependence of *set2*Δ cells on resection for survival in response to bleomycin presumably reflects an increased dependence on HR when NHEJ is deficient, as a *set2*Δ*rhp51*Δ double mutant was also sensitive. This is consistent with results in budding yeast that show a *set1rad50* mutant is more sensitive to bleomycin than the single mutants alone (Faucher & Wellinger, 2010). In accordance with the *ku70*Δ and *lig4*Δ DSB profiles, this suggests that in the absence of NHEJ, use of HR to repair DSBs is essential. However, contradictory to this is the finding that *exo1*Δ and *exo1*Δ*set2*Δ show increased

repair by GC. This finding is in agreement with other data that shows Exo1 is required for long-tract resection, but not for efficient homologous recombination, possibly explaining why the *exo1*Δ mutant does not show particular sensitivity to bleomycin or IR (Clerici *et al*, 2006; Fiorentini *et al*, 1997; Llorente & Symington, 2004). On the other hand, loss of any component of the MRN complex results in a striking decrease in GC and increase in Ch^{16} loss and LOH in the DSB assay (Tinline-Purvis *et al*, 2009) suggesting that short tract but not long tract resection is required for efficient HR. It is possible that the key role of long ssDNA tracts is to efficiently activate the ATR-mediated checkpoint response and G2/M arrest (Chung *et al*, 2010; Zhu *et al*, 2008; Zou & Elledge, 2003). A possible explanation for the increased HR and decreased NHEJ/SCC in the *exo1*Δ mutant is that in the absence of Exo1, HR repair utilises the homologous chromosome III, rather than the sister chromatid. However, this would be unexpected, given that the sister chromatid is likely to be in closer proximity than the homologue, and so shorter, not longer, Rhp51-coated ssDNA might be required for efficient strand invasion of the sister chromatid.

Another finding contrary to the suggestion that the bleomycin sensitivity of the *set2*Δ double mutants with resection genes is due to loss of both HR and NHEJ pathways is the finding that *lig4*Δ*exo1*Δ or *ku70*Δ*exo1*Δ mutants do not show the same sensitivity. This implies the sensitivity of *set2*Δ with HR mutants is not due to the role of Set2 in NHEJ, and suggests Set2 has an additional NHEJ-independent role.

4.3.2 A Cdk9-independent role for Set2

Further analysis sought to address whether an interaction with RNAP II was required for the role of Set2 in NHEJ. Analysis of *csk1*Δ, *cdk9-T212A* and *cdk9-T212E* cells suggest that Cdk9 and Csk1 are required for efficient DSB repair, but unlike *set2*Δ cells, *cdk9-T212E* cells showed significantly decreased GC associated with significantly increased Ch^{16} loss. This data supports a previous study that showed Csk1 is sensitive to a variety of genotoxic agents

and is required for efficient HR (Gerber *et al*, 2008). This was suggested to be partially due to function through Cdk9, which could explain the DSB repair phenotype of the *cdk9-T212E* mutant. However, results suggest it is likely that Csk1 also has another target with respect to its role in DNA repair (Gerber *et al*, 2008); given Csk1 also activates Cdc2, this could be the additional target, given Cdc2 has been shown to regulate HR in budding and fission yeast (Aylon *et al*, 2004; Caspari *et al*, 2002; Ira *et al*, 2004). However, it also seems likely, given the high levels of spontaneous chromosome rearrangements seen when the *csk1*Δ mutant was analysed using the DSB assay, that Csk1 is required for maintaining chromosome integrity under normal conditions. Given Csk1 is a CAK that activates all of three essential CDKs in fission yeast, it is difficult to predict how it may be exerting this effect. However, it is clearly important in maintaining genomic integrity, both under normal conditions and in response to DNA damage.

The lack of DSB assay data for *csk1*Δ and *cdk9-T212A* cells make it difficult to definitively conclude whether Cdk9 is required for the role of Set2 in DSB repair; however, given the phenotype of *cdk9-T212E* and the viability data it does seem unlikely. The literature regarding RNAP II CTD phosphorylation in fission yeast is inconclusive. Some studies suggest that Cdk9 is required for phosphorylation of both Ser2 and Ser5 (Guiguen *et al*, 2007; Pei *et al*, 2006; Viladevall *et al*, 2009). However, other studies show that in an *lsk1*Δ mutant Ser2 and Ser5 phosphorylation is abolished, suggesting Lsk1 is the major kinase (Karagiannis & Balasubramanian, 2007). In addition, phosphorylation of Ser5 by Mcs6 has been shown to prime the CTD for recruitment and further phosphorylation by Cdk9 (Viladevall *et al*, 2009). Further, in various mutant combinations, Ser5 phosphorylation is still observed; given the importance of these modifications it is likely that compensation between kinases exists (Pei *et al*, 2006). Although it is suggested that Cdk9 is required for both Ser2 and Ser5 phosphorylation, and so is likely to be important in the recruitment of Set2 it would be useful

to look at the DSB response in combinations of these mutants to see if any additional conclusions could be made. However, this would be further complicated by the fact that these proteins have various targets, for example Mcs6 is also a CAK that activates Cdc2 (Gerber *et al*, 2008; Lee *et al*, 1999). In addition, phosphorylation of Ser2 and Ser5 creates binding sites for many accessory factors, such as mRNA processing machinery and chromatin modifying enzymes (including Set1), and so any results would have to be confirmed to be due to an affect on Set2 recruitment (reviewed in Phatnani & Greenleaf, 2006). Further, studies in budding yeast have shown that disrupting the interaction between Set2 and RNAP II results in destabilised Set2 protein levels (Fuchs *et al*, 2012; Youdell *et al*, 2008) so any results may be due to reduced protein levels. Despite the complexities of this analysis, given that Cdk9 appears to be required for efficient GC, it is unlikely that Cdk9 is also required for the role of Set2 in NHEJ.

4.3.3 A Clr6-independent role for Set2

In budding yeast, the recruitment of the Rpd3(S) HDAC complex to dimethylated H3K36, through the chromodomain of Eaf3, has been extensively characterised (Carrozza *et al*, 2005; Joshi & Struhl, 2005; Keogh *et al*, 2005; Li *et al*, 2007; Youdell *et al*, 2008). This deacetylation of histones in the wake of elongating RNAP II is required to re-establish chromatin structure between rounds of transcription and also prevents spurious transcription from cryptic start sites (Cheung *et al*, 2008; Kaplan *et al*, 2003; Li *et al*, 2007; Lickwar *et al*, 2009). Thus, in a *set2* mutant in budding yeast, there is a striking increase in the histone acetylation levels and an associated increase in spurious transcript levels (Li *et al*, 2007). The Rpd3 homologue in fission yeast, Clr6, forms two distinct complexes, of which complex II is equivalent to Rpd3(S) (Nicolas *et al*, 2007); however, there is some uncertainty as to whether H3K36me is the only recruiting factor for the Clr6 complex II, as deletion of $set2^{+}$ in *S. pombe* does not result in the same striking increase in histone acetylation (Morris *et al*, 2005). However, there is an increase in spurious transcription in a *set2*Δ mutant, suggesting that Set2

has at least some role in recruiting Clr6 complex II (Nicolas *et al*, 2007). Therefore an analysis of *alp13*Δ and *clr6-1* cells was performed. *alp13*Δ cells exhibited a striking sensitivity to bleomycin, compared to wildtype, which is consistent with previous studies which also showed sensitivity of *clr6-1* cells to MMS and CPT (Nakayama *et al*, 2003; Nicolas *et al*, 2007). The *alp13*Δ*set2*Δ mutant was even more sensitive than the single *alp13*Δ mutant suggesting that they function in different pathways in the response to DNA damage. Therefore it is unlikely that Set2 and Alp13 are working in the same pathway with respect to NHEJ repair. In agreement with this, is the NHEJ proficiency of the *clr6-1* mutant.

The sensitivity of *alp13*Δ cells to bleomycin suggests a role for Clr6 complex II in maintaining genome stability; this role has also been identified in work by Nicolas *et al* (2007) and Nakayama *et al*, (2003). Further, in budding yeast, Rpd3 is also linked to DNA repair (Jazayeri *et al*, 2004; Tamburini & Tyler, 2005). It would be interesting to analyse *alp13*Δ cells using the DSB assay, but unfortunately when this was attempted the mutant accumulated suppressor mutations. The sensitivity of *alp13*Δ cells to bleomycin may reflect that in the presence of functional HDAC complexes, the closed chromatin structure caused by deacetylation prevents the accessibility of DNA damaging agents. On the other hand, Nicolas *et al* (2007) suggest that given the increase in antisense transcripts observed when the Clr6 complex is absent, R-loops may form, which have been shown to lead to an increase in DNA lesions and genomic instability (Li & Manley, 2006). It would be interesting to further analyse the role of this complex in maintaining genome integrity; however, it was not performed as it was out of the scope of this study.

4.4 SUMMARY

To conclude, the work presented in this chapter:

- Supports a role for Set2 in efficient DSB repair by NHEJ.
- Suggests the role for Set2 in NHEJ does not require recruitment of the Clr6 HDAC complex.
- Suggests the role for Set2 in NHEJ does not require Cdk9.
- Suggests an additional NHEJ-independent role for Set2.

CHAPTER 5

Microarray analysis of a *set2*$^{+}$ deletion mutant

5.1 INTRODUCTION

Analysis in Chapters 3 and 4 showed that *set2*Δ cells repair ineffectively by NHEJ and have an increased proportion of cells repairing by HR. In both *S. cerevisiae* and *S. pombe*, Set2 has been shown to interact with elongating RNAP II (Gerber & Shilatifard, 2003; Hampsey & Reinberg, 2003; Morris *et al*, 2005). H3K36 methylation has also been shown to be highly enriched over transcribed regions of active genes, and absent in non-transcribed regions of telomeric and mating type loci (Krogan *et al*, 2003; Morris *et al*, 2005; Schaft *et al*, 2003; Xiao *et al*, 2003b). Given this involvement in transcription, it is possible that the repair phenotype seen in the *set2*Δ cells is due to an indirect effect, through up-regulation of HR genes or down-regulation of NHEJ genes. To address this, a microarray analysis of *set2*Δ cells was undertaken and is described in this chapter.

5.2 RESULTS

5.2.1 Microarray analysis of wildtype and *set2*Δ cells

Given the involvement of Set2 in transcription, it is possible that the repair phenotype seen in the *set2*Δ cells is due to up-regulation of HR genes or down-regulation of NHEJ genes. Consequently a microarray analysis of wildtype and *set2*Δ cells before and after treatment with bleomycin was performed, in collaboration with Jürg Bähler (UCL). Cells were grown to log phase and treated with 5 μg/ml bleomycin for 30 minutes; samples were taken before and after treatment. Two repeats of the microarray were performed using independently extracted RNA.

Results from the microarray were split into groups. Firstly, those genes that were up- or down-regulated in wildtype cells following bleomycin treatment were analysed. Secondly, the transcript levels prior to bleomycin treatment in wildtype and *set2*Δ cells were compared; these were split into two categories: those that are higher in *set2*Δ cells compared to wildtype (i.e. genes that require Set2 for repression) and those that are higher in wildtype compared to *set2*Δ cells (i.e. genes that require Set2 for induction). Finally, the differences between wildtype and *set2*Δ cells following bleomycin treatment were analysed.

5.2.2 The expression of fifty-nine transcripts is altered following bleomycin treatment in wildtype cells

5.2.2.1 Seventeen transcripts are at least 1.5-fold up-regulated in wildtype cells following treatment with bleomycin

Seventeen transcripts were found to be at least 1.5-fold up-regulated in wildtype cells treated with bleomycin for 30 minutes, compared to untreated cells (Table 5.1). Approximately 80% of the *S. pombe* genome has been assigned a Gene Ontology (GO) term, which describes the biological process in which it functions. These GO terms have been assigned based on experimental data, sequence alignment, a non-traceable author statement or inferred by the curator based on other GO annotations (Aslett & Wood, 2006). Analysis of the GO terms of the seventeen up-regulated transcripts showed that only ten had an associated GO term, presumably due to the presence of up-regulated antisense and intergenic RNAs. There were five over-represented GO terms, when compared to the genome wide representation; perhaps unsurprisingly, these were response to stress, DNA metabolic process, response to DNA damage, response to heat and response to stimulus (Table 5.2).

Table 5.1 Transcripts at least 1.5 fold up-regulated in wildtype cells following bleomycin treatment compared to untreated cells

Transcript	Fold increase	Description
cdt2	2.44	WD repeat protein Cdt2
SPNCRNA.1696	1.93	antisense RNA (predicted)
kpa1	1.83	DinB translesion DNA repair polymerase, pol kappa
rev1	1.81	deoxycytidyl transferase Rev1 (predicted)
ams2	1.77	cell cycle regulated GATA-type transcription factor Ams2
SPNCRNA.564	1.75	antisense RNA (predicted)
SPNCRNA.1037	1.70	antisense RNA (predicted)
SPNCRNA.1654	1.66	antisense RNA (predicted)
SPBC4F6.17c	1.65	mitochondrial heatshock protein Hsp78 (predicted)
rhp54	1.64	Rad54 homolog Rhp54
SPNCRNA.863	1.58	intergenic RNA (predicted)
rhp51	1.57	recombinase Rhp51
slt1	1.57	sequence orphan Slt1
SPNCRNA.1187	1.57	intergenic RNA (predicted), possible alternative UTR
psi1	1.54	DNAJ domain protein, involved in translation initiation Psi1
SPBC3B9.01	1.52	Hsp70 nucleotide exchange factor (predicted)
SPNCRNA.1435	1.51	antisense RNA (predicted)

Table 5.2 Over-represented GO terms in the up-regulated subset in wildtype cells following bleomycin treatment compared to untreated cells

GO term	% in genome	% in upregulated subset	p value
Response to stress	13.6	80.0	5.1×10^{-4}
DNA metabolic process	7.1	60.0	2.7×10^{-3}
Response to DNA damage	4.1	50.0	3.1×10^{-3}
Response to heat	0.6	30.0	3.7×10^{-3}
Response to stimulus	19.8	80.0	9.5×10^{-3}

5.2.2.2 Forty-two transcripts are at least 1.5-fold down-regulated in wildtype cells following treatment with bleomycin

Forty-two transcripts were found to be at least 1.5-fold down-regulated in wildtype cells treated with bleomycin for 30 minutes, compared to untreated cells (Table 5.3). Analysis of the GO terms of the forty-two transcripts showed that seven did not have an associated GO term; these were intergenic or antisense RNAs. There were four over-represented GO terms, which were cytokinesis, cell division, polysaccharide metabolism and cell wall organisation (Table 5.4).

5.2.3 The expression of 186 transcripts is altered in untreated *set2*Δ cells compared to wildtype

5.2.3.1 140 transcripts are over 2-fold higher in untreated *set2*Δ cells compared to wildtype

140 transcripts were found to be at least 2-fold higher in untreated *set2*Δ cells compared to wildtype (Appendix V). Analysis of the GO terms of the 140 transcripts showed that only 27.5% of these had an associated GO term (Figure 5.1A). This is likely due to the presence of non-coding and antisense RNAs analysed in the microarray. Of the 27.5%, the functional groupings included vacuole processing, cell adhesion, amino acid metabolism, DNA recombination, signaling, meiosis, transport, response to stress, carbohydrate metabolism, DNA repair, lipid metabolism and cytoskeleton organisation (Figure 5.1B). However, the only over-represented GO term was cell adhesion (Figure 5.1C). The transcript in the DNA recombination group was *tlh1*$^{+}$, a RecQ type helicase proposed to have a role in telomerase independent telomere maintenance (Mandell *et al*, 2005). In the DNA repair group were three transcripts; *SPAC977.06*$^{+}$, a DUF999 family protein; *pol4*$^{+}$, a polymerase X family gene; and *rdh54*$^{+}$, a DNA helicase involved in meiotic DNA recombination (Catlett & Forsburg, 2003).

5.2.3.2 Forty-six transcripts are at least two-fold lower in untreated *set2*Δ cells compared to wildtype

Forty-six transcripts were at least 2-fold lower in untreated *set2*Δ cells compared to wildtype (Appendix VI). Of these, 50% had an associated GO term (Figure 5.2A); the functional groupings included ascospore formation, vitamin metabolism, chromatin modification, amino acid metabolism, transport, response to stress and cytoskeleton organisation. The only over-represented functional grouping was response to stress (Figure 5.2B). The transcript in the chromatin modification group was *bub1*$^{+}$, which encodes a protein kinase, which is required for correct localization of Bub3 and Mad3 to the kinetochore (Vanoosthuyse *et al*, 2004).

Table 5.3 Forty-two transcripts that are at least 1.5-fold down-regulated in wildtype cells following bleomycin treatment compared to untreated cells

Transcript	Fold change	Description
gas1	0.65	cell wall protein Gas1, 1,3-beta-glucanosyltransferase (predicted)
SPNCRNA.1193	0.65	intergenic RNA (predicted)
SPCC757.12	0.64	alpha-amylase homolog (predicted)
cdm1	0.63	DNA polymerase delta subunit Cdm1
cdc15	0.63	extended Fer/CIP4 (EFC) domain protein Cdc15
SPCC1322.10	0.63	cell wall protein Pwp1
myp2	0.63	myosin II heavy chain Myo3
SPAC15A10.09c	0.62	SUR7 family protein (predicted)
chs2	0.61	chitin synthase homolog Chs2
ecm33	0.61	cell wall protein Ecm33
SPBPB7E8.01	0.60	sequence orphan
etd1	0.60	ethanol-hypersensitive mutant protein Etd1
rho4	0.60	Rho family GTPase Rho4
SPNCRNA.1210	0.60	antisense RNA (predicted)
SPBC31F10.17c	0.60	sequence orphan
rid1	0.59	GTPase binding protein Rid1 (predicted)
SPAC644.05c	0.59	deoxyuridine 5'-triphosphate nucleotidohydrolase (predicted)
bet1	0.59	SNARE Bet1 (predicted)
SPNCRNA.1447	0.56	antisense RNA (predicted)
SPBC651.04	0.55	sequence orphan
mid2	0.55	medial ring protein Mid2
SPAC212.12	0.55	S. pombe specific GPI anchored protein family
gas5	0.54	cell wall protein Gas5, 1,3-beta-glucanosyltransferase (predicted)
mik1	0.54	mitotic inhibitor kinase Mik1
pxl1	0.50	paxillin-like protein Pxl1
adg3	0.49	beta-glucosidase Adg3 (predicted)
SPNCRNA.1278	0.47	intergenic RNA (predicted)
SPNCRNA.80	0.47	non-coding RNA (predicted)
chr1	0.44	chitin synthase regulatory factor Chr1 (predicted)
agn1	0.42	glucan endo-1,3-alpha-glucosidase Agn1
slp1	0.40	sleepy homolog Slp1
SPNCRNA.1609	0.39	intergenic RNA (predicted)
SPAC869.01	0.39	amidase (predicted)
spo12	0.39	Spo12 family protein
adg1	0.35	sequence orphan
adg2	0.31	conserved fungal protein Adg2
exg1	0.30	glucan 1,6-beta-glucosidase Exg1
uds1	0.28	septation protein Uds1
SPCC306.11	0.27	sequence orphan
eng1	0.27	endo-1,3-beta-glucanase Eng1
SPAPB1E7.04c	0.25	chitinase (predicted)
ace2	0.24	transcription factor Ace2

Table 5.4 Over-represented GO terms in the down-regulated subset in wildtype cells following bleomycin treatment compared to untreated cells

GO term	% in genome	% in upregulated subset	p value
Cytokinesis	2.2	31.0	3.3×10^{-10}
Cell division	3.1	31.0	3.9×10^{-8}
Polysaccharide metabolism	1.4	19.0	2.0×10^{-5}
Cell wall organisation	2.5	21.4	1.2×10^{-4}

5.2.4 Transcription levels of genes involved in NHEJ and HR repair are not significantly changed in untreated s*et2*Δ cells

Specifically, it was important to analyse the transcription levels of genes involved in HR and NHEJ repair; if these are significantly different it could explain the repair phenotype of *set2*Δ cells. First the key genes involved in NHEJ were analysed; *pku70*$^+$, *pku80*$^+$ and *lig4*$^+$ transcript levels were not lowered in *set2*Δ compared to wildtype (Figure 5.3A). In fact, levels of all three were slightly higher than observed in wildtype (*pku70*$^+$ 1.25, *pku80*$^+$ 1.15 and *lig4*$^+$ 1.05; the number relates to the level compared to that of wildtype cells, which is 1.0). In *S. pombe*, Xlf1, an XRCC4 like factor is also involved in NHEJ; however, microarray data was not obtained for *xlf1*$^+$ expression. Genes that are required for HR repair were also analysed; the levels of all transcripts analysed were found to be close to wildtype levels (Figure 5.3B). These data suggest that the repair phenotype seen in the *set2*Δ cells is unlikely to be due to an indirect effect caused by altered transcription of genes required for repair.

5.2.5 The level of 250 transcripts is altered in *set2*Δ cells compared to wildtype following treatment with bleomycin

Although there is no evidence of a change in the expression of genes required for HR or NHEJ repair in *set2*Δ cells prior to DNA damage it is possible that the expression of the genes may be altered compared to wildtype, following DNA damage. Therefore, transcript levels were analysed 30 minutes following treatment with bleomycin.

Figure 5.1

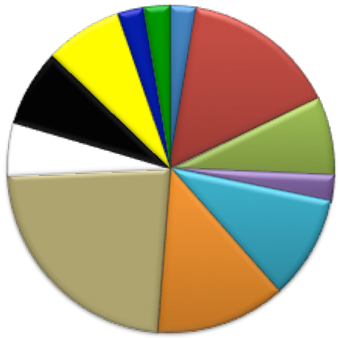
A



Known GO Terms
No annotation

	% of upregulated subset
Known GO Terms	27.5
No annotation	72.5

B



Vacuole Processing
Cell adhesion
Amino acid metabolic process
DNA recombination
Signalling
Meiosis
Transport
Response to stress
Carbohydrate metabolic process
DNA repair
Lipid metabolic process
Cytoskeleton organisation

Principle GO term	% of upregulated subset
Vacuole Processing	0.7
Cell adhesion	4.2
Amino acid metabolic process	2.1
DNA recombination	0.7
Signalling	2.8
Meiosis	3.5
Transport	6.3
Response to stress	1.4
Carbohydrate metabolic process	2.1
DNA repair	2.1
Lipid metabolic process	0.7
Cytoskeleton organisation	0.7

C

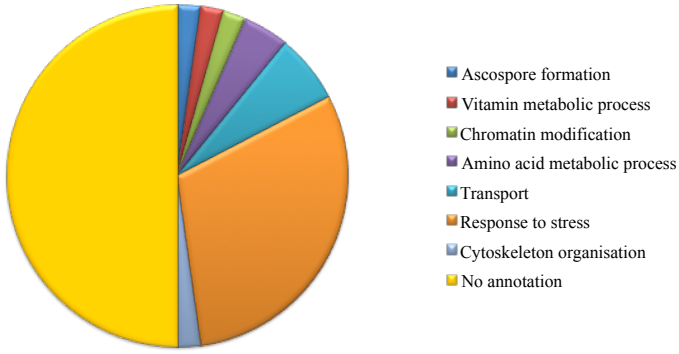
Over-represented GO terms

GO term	% in genome	% in upregulated subset	p value
Cell adhesion	0.5	8.1	5×10^{-4}

Figure 5.1 140 transcripts are over 2-fold up-regulated in untreated *set2*Δ cells compared to wildtype **(A)** Pie chart representation of those up-regulated transcripts which have a known GO term (blue), or no known annotation (red). **(B)** Pie chart representation of functional groupings assigned to up-regulated transcripts in untreated *set2*Δ cells (3271). Functional groupings assigned according to Gene Ontology Consortium (www.geneontology.org). **(C)** Over-represented GO terms associated with up-regulated transcripts in untreated *set2*Δ cells. The p value indicates significance of over representation.

Figure 5.2

A



Principle GO term	% of downregulated subset
Ascospore formation	2.2
Vitamin metabolic process	2.2
Chromatin modification	2.2
Amino acid metabolic process	4.3
Transport	6.5
Response to stress	30.4
Cytoskeleton organisation	2.2
No annotation	50.0

B

Over-represented GO terms

GO term	% in genome	% in downregulated subset	p value
Response to stress	14.2	53.6	5×10^{-4}

Figure 5.2 Forty-six transcripts are down-regulated in untreated *set2*Δ cells compared to wildtype **(A)** Pie chart representation of functional groupings assigned to down-regulated transcripts in untreated *set2*Δ cells (3271). Functional groupings assigned according to Gene Ontology Consortium (www.geneontology.org). **(C)** Over-represented GO terms associated with down-regulated transcripts in untreated *set2*Δ cells. The p value indicates significance of over representation.

Figure 5.3

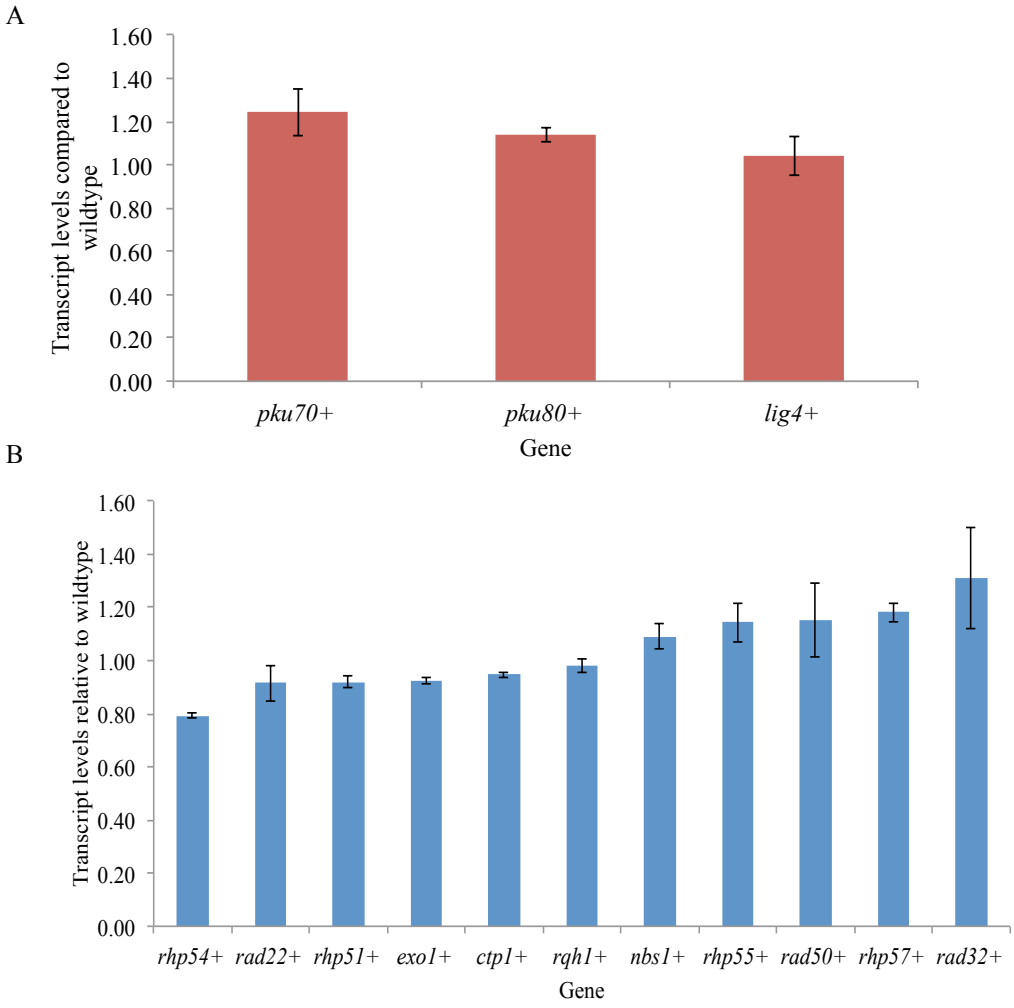


Figure 5.3 HR and NHEJ gene expression is not significantly changed in untreated *set2*Δ cells **(A)** NHEJ gene expression levels in untreated *set2*Δ cells (3271) relative to wildtype (2094), where the level in wildtype cells is 1.0. **(B)** HR gene expression levels in untreated *set2*Δ cells relative to wildtype, where the level in wildtype cells is 1.0. Data represent the mean of two experiments with independently derived RNA and error bars are (±SE) are shown.

A scatter diagram showing the relative transcript levels compared to the level before treatment in wildtype and *set2*Δ cells, showed that in the majority of cases, the change in expression was similar in wildtype and *set2*Δ cells (Figure 5.4). However, there were a number of transcripts that were higher in *set2*Δ cells compared to wildtype and fewer that were lower.

The differences between wildtype and *set2*Δ cells following bleomycin treatment were analysed and the results split into six categories: 1. Increased after treatment in wildtype, increased less in *set2*Δ cells (i.e. require Set2 for up-regulation); 2. Increased after treatment in wildtype, decreased after treatment in *set2*Δ cells (i.e. require Set2 for up-regulation); 3. Decreased after treatment in wildtype, decreased further in *set2*Δ cells; 4. Increased after treatment in *set2*Δ cells, increased less in wildtype (i.e. requires Set2 for repression); 5. Decreased after treatment in wildtype, increased after treatment in *set2*Δ cells (i.e. require Set2 for down-regulation); and 6. Decreased after treatment in wildtype, decreased less in *set2*Δ cells (i.e. requires Set2 for down-regulation).

5.2.5.1 Thirty transcripts are increased in wildtype cells following bleomycin treatment, and increased less in *set2*Δ cells

In the first grouping (increased after treatment in wildtype, increased less in *set2*Δ cells) there are thirty transcripts (Appendix VII category 1, Figure 5.5); however, twenty-one of these are non coding, intergenic RNAs. Of the other nine, three are sequence orphans (*SPAPB18E9.04c*$^{+}$, *mug95*$^{+}$, *SPBC8E4.02c*$^{+}$), one is a conserved hypothetical protein (*SPAC11D3.01c*$^{+}$), two are involved in membrane transport (*SPAC212.08c*$^{+}$ and *SPAC1002.16c*$^{+}$), two are transcription factors (*atf31*$^{+}$ and *ams2*$^{+}$) and one is involved in S phase control (*cdt2*$^{+}$).

Figure 5.4

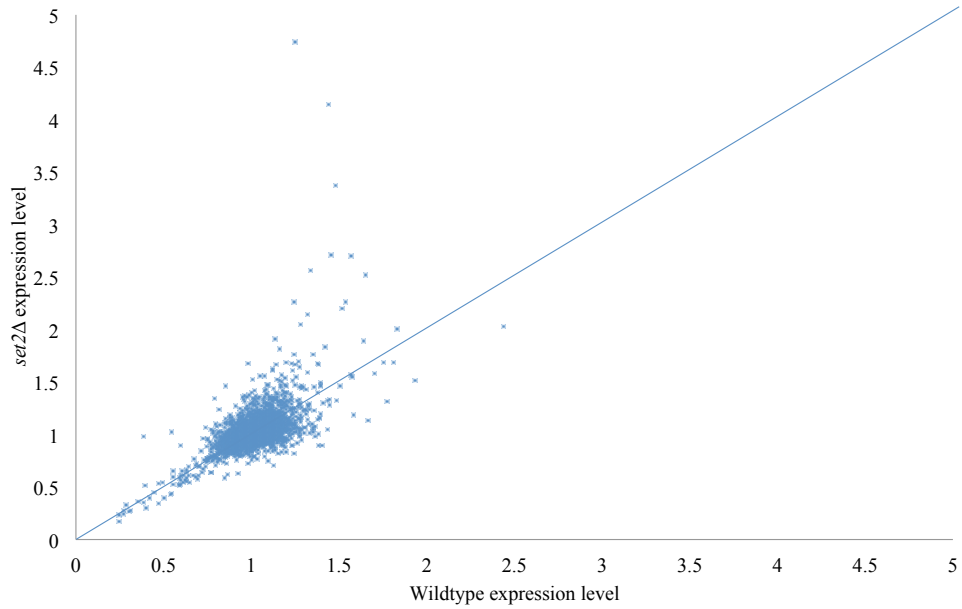


Figure 5.4 Comparison of transcript levels in wildtype (2094) and *set2*Δ (3271) cells following 30 minutes of treatment with 5 µg/ml bleomycin

Figure 5.5

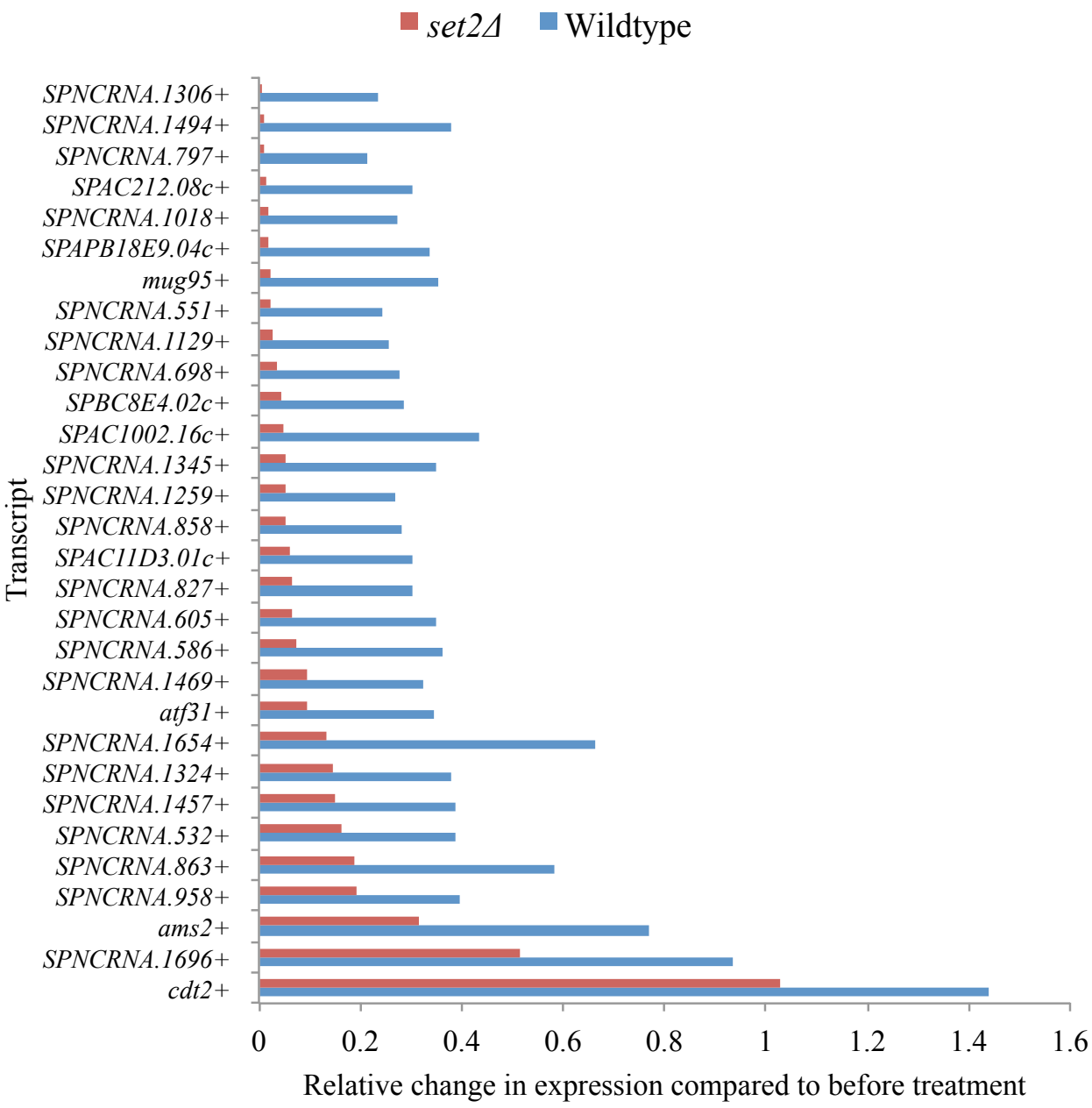


Figure 5.5 The levels of thirty transcripts that are increased after bleomycin treatment in wildtype, but increased less in *set2*Δ cells The change in levels of thirty transcripts in wildtype (blue; 2094) and *set2*Δ (red; 3271) cells following 30 minutes treatment with 5 μg/ml bleomycin, where the level before treatment is 0. Data represent the mean of two experiments with independently derived RNA.

5.2.5.2 Fifty-six transcripts are increased in wildtype cells following bleomycin treatment, and decreased following treatment in *set2*Δ cells

In the second group (increased after treatment in wildtype, but decreased after treatment in *set2*Δ cells) there were fifty-six transcripts, of which forty-seven were non-coding, intergenic RNAs (Appendix VII category 2, Figure 5.6). The other nine included a replication licensing factor (*cdc18*$^+$), an iron permease (*fip1*$^+$), two sequence orphans (*SPAPB18E9.05c*$^+$ and *SPCC569.04*$^+$), two hypothetical proteins (*SPAC5H10.04*$^+$ and *SPBC557.05*$^+$), a P-type ATPase (*pma2*$^+$), a 40S ribosomal protein (*rps3002*$^+$) and an RNA binding protein (*seb1*$^+$).

5.2.5.3 Six transcripts are decreased in wildtype cells following bleomycin treatment, and further decreased following treatment in *set2*Δ cells

In the third grouping (decreased after treatment in wildtype, and decreased further in *set2*Δ cells) there were only six transcripts (Appendix VII category 3, Figure 5.7). These included an S phase transcription factor (*SPAP14E8.02*$^+$ or *tos4*$^+$), a replication licensing factor (*cdt1*$^+$), the large subunit of RNR (*cdc22*$^+$), a copper oxidase (*fio1*$^+$), a 60S ribosomal protein (*rpl22*$^+$) and superoxide dismutase (*sod1*$^+$). Interestingly, in this subset are three gene transcripts that are involved in S phase and cell cycle progression (*tos4*$^+$, *cdt1*$^+$ and *cdc22*$^+$).

5.2.5.4 Ninety-one transcripts are increased in *set2*Δ cells following bleomycin treatment, and increased less in wildtype

Ninety-one transcripts fall into the fourth category (increased after treatment in *set2*Δ cells, but increased less in wildtype); of these, fifty-four are protein-coding genes (Appendix VII category 4, Figure 5.8). However, ten of the transcripts are hypothetical proteins and ten are sequence orphans. Seven of the fifty-four are heat shock proteins and five are involved in carbohydrate metabolism. Only one, *rhp54*$^+$ is involved in DNA repair; there is approximately an additional 25% up-regulation of *rhp54*$^+$ transcript levels in *set2*Δ cells following DNA damage compared to wildtype.

Figure 5.6

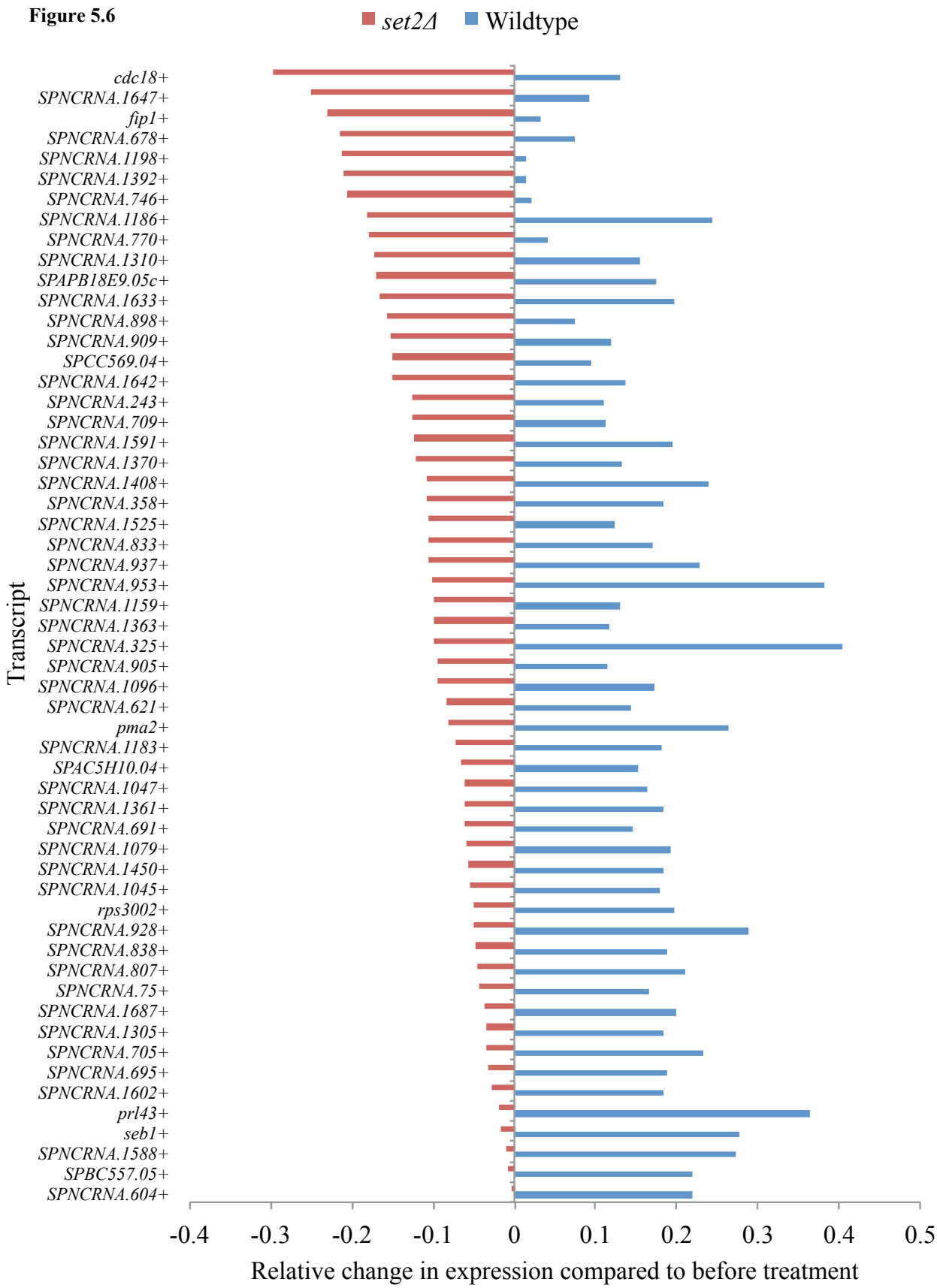


Figure 5.6 Fifty-six transcripts are increased after bleomycin treatment in wildtype, but decreased in *set2*Δ cells The change in levels of fifty-six transcripts in wildtype (blue; 2094) and *set2*Δ (red; 3271) cells following 30 minutes treatment with 5 μg/ml bleomycin, where the level before treatment is 0. Data represent the mean of two experiments with independently derived RNA.

Figure 5.7

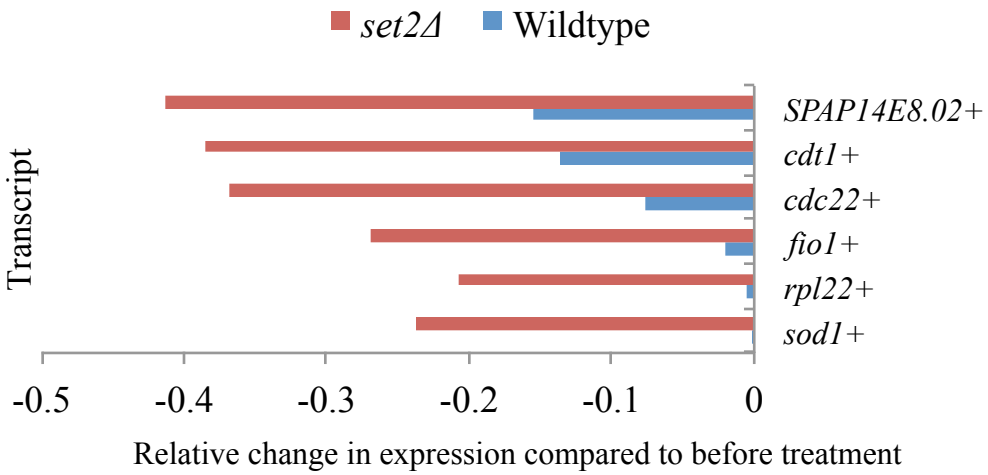


Figure 5.7 Six transcripts are decreased after bleomycin treatment in wildtype, but further decreased in *set2*Δ cells The change in levels of six transcripts in wildtype (blue; 2094) and *set2*Δ (red; 3271) cells following 30 minutes treatment with 5 µg/ml bleomycin, where the level before treatment is 0. Data represent the mean of two experiments with independently derived RNA.

Figure 5.8

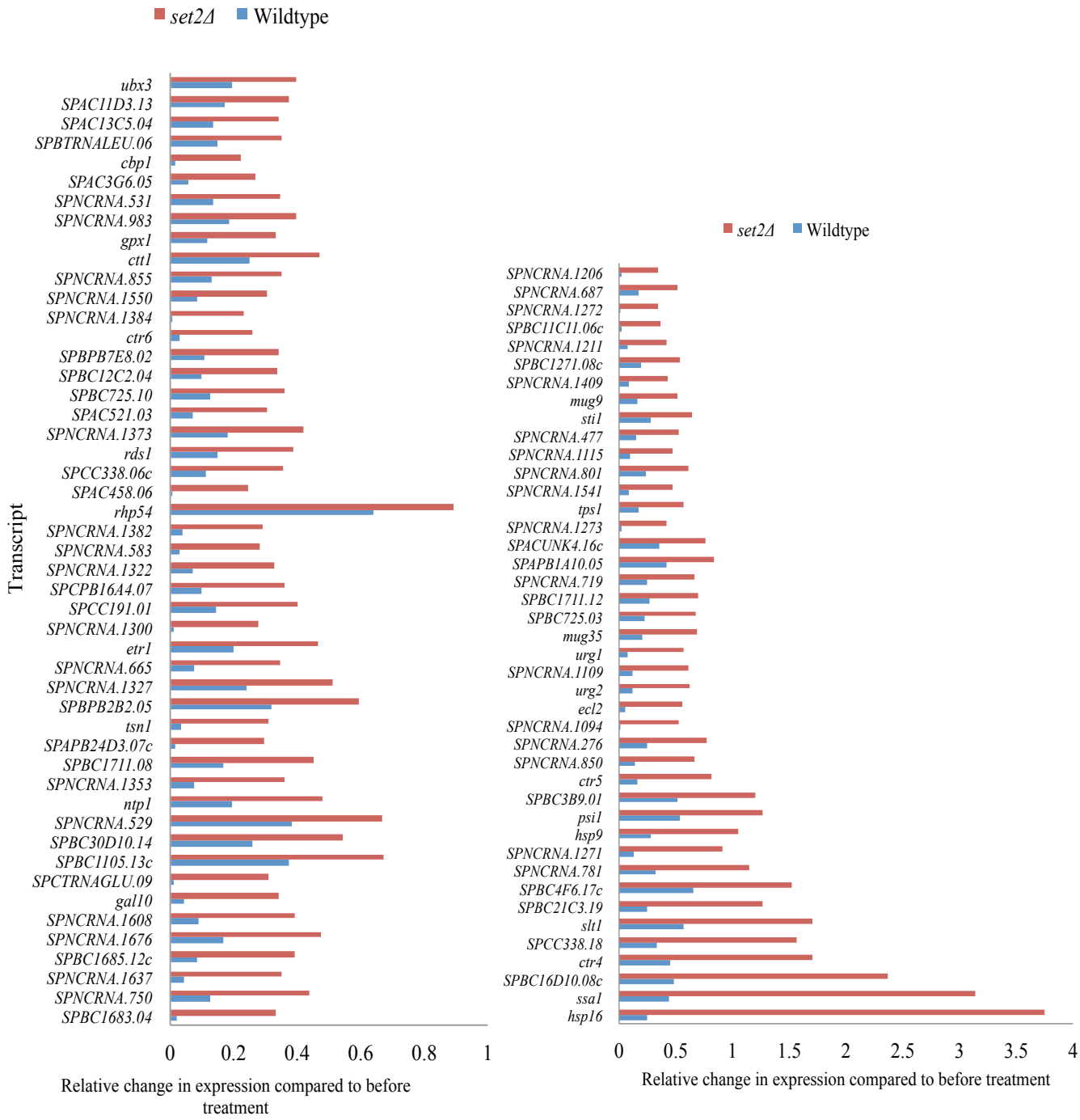


Figure 5.8 Ninety-one transcripts are further increased following bleomycin treatment in *set2*Δ cells compared to wildtype The change in levels of ninety-one transcripts in wildtype (blue; 2094) and *set2*Δ (red; 3271) cells following 30 minutes treatment with 5 µg/ml bleomycin, where the level before treatment is 0. Data represent the mean of two experiments with independently derived RNA.

5.2.5.5 Sixty-two transcripts are decreased in wildtype cells following bleomycin treatment, but increased following treatment in *set2*Δ cells

In the fifth category (decreased after treatment in wildtype, increased after treatment in *set2*Δ cells) there were sixty-two transcripts, of which twenty-seven were transcripts of protein coding genes (Appendix VII category 5, Figure 5.9A). Of the twenty-seven, five were sequence orphans and four hypothetical proteins. None of the transcripts in this category had any role in DNA repair.

5.2.5.6 Five transcripts are decreased after treatment in wildtype, but decreased less in *set2*Δ cells

In the sixth category (decreased after treatment in wildtype, decreased less in *set2*Δ cells) there were five transcripts; two were for protein coding genes; one was a hypothetical protein (*SPAC869.01*$^+$) and the other an eIF2 kinase (*hri1*$^+$), which is involved in mediating down-regulation of protein synthesis in response to stress conditions (Appendix VII category 6, Figure 5.9B).

5.3 DISCUSSION

Given the well-documented role for histone-modifying enzymes in the control of transcription, the work in this chapter sought to address whether the repair phenotype of *set2*Δ cells reflected altered transcription of DNA repair genes. Fifty-nine transcripts showing altered expression in wildtype cells following treatment with bleomycin were identified by microarray analysis. There was no significant change in the transcription of NHEJ and HR genes in *set2*Δ cells compared to wildtype under normal conditions. However, two repair genes, *rhp54*$^+$ and *cdt2*$^+$ with a significant change in *set2*Δ cells compared to wildtype following treatment with bleomycin were identified. In addition, a cluster of genes that were down-regulated in *set2*Δ cells compared to wildtype was identified; these genes play key roles in S phase control.

Figure 5.9

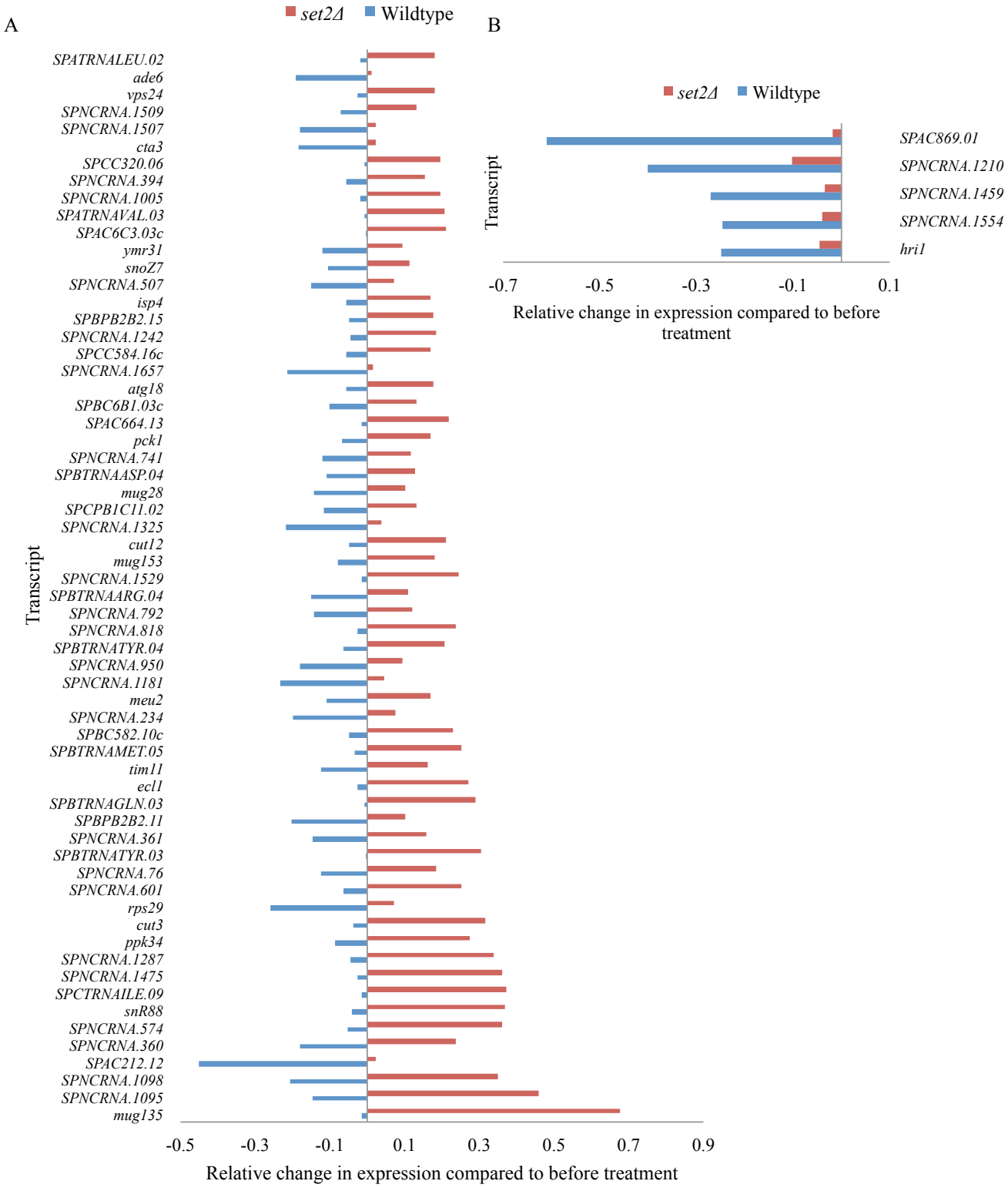


Figure 5.9 Sixty-seven transcripts that show altered response to bleomycin in *set2*Δ cells compared to wildtype (A) The change in levels of sixty-two transcripts in wildtype (blue; 2094) and *set2*Δ (red; 3271) cells following 30 minutes treatment with 5 µg/ml bleomycin, where the level before treatment is 0. **(B)** The change in levels of five transcripts in wildtype (blue) and *set2*Δ (red) cells following 30 minutes treatment with 5 µg/ml bleomycin, where the level before treatment is 0. Data represent the mean of two experiments with independently derived RNA.

5.3.1 Fifty-nine transcripts show altered expression following DNA damage in wildtype cells

An evolutionary conserved way in which the DNA damage response is regulated is at the level of gene expression. In fission yeast, many genes show increased transcription in response to DNA damage including the key HR gene *rhp51*$^{+}$ (Park *et al*, 1998; Shim *et al*, 2000) and genes involved in the UV response (Davey *et al*, 1997). Transcriptional changes in response to DNA damage are coordinated through activation of the DNA damage checkpoint and stress-kinase pathways. The *S. pombe* Sty1 stress-kinase is activated in response to a range of environmental stresses including UV and MMS and is involved in controlling the transcriptional response to these stresses (Degols & Russell, 1997; Shiozaki & Russell, 1995; Takeda *et al*, 1995). For example, a central role for Sty1 is the coordination of the core environmental stress response (CESR), in which a group of genes are transcriptionally up-regulated in response to environmental stresses (Chen *et al*, 2003).

In this study, the expression of fifty-nine transcripts was altered following 30 minutes treatment with bleomycin in wildtype cells. Seventeen transcripts were at least 1.5-fold up-regulated, and forty-two transcripts were at least 1.5-fold down-regulated compared to untreated cells. These transcripts fall into a variety of functional categories; as expected, the up-regulated subset contains significant enrichment of DNA repair and stress-response factors. A previous study which analysed the global gene expression responses of fission yeast to IR identified 204 genes whose levels were significantly altered (at least twofold) in response to 500 Gy (Watson *et al*, 2004). Although far fewer altered transcripts were observed in this work, this is likely because in the previous study, the transcript levels were observed at 60 and 160 minutes following DNA damage. Had the RNA samples been taken at a later time point in this work, is probable that an increased number of altered transcripts would have been observed.

All ten protein-coding genes that were up-regulated in response to bleomycin in this study, were also up-regulated following treatment with IR in the work by Watson *et al*, confirming the validity of the results in this chapter. These included repair genes known to be up-regulated in response to DNA damage: *rhp51*$^{+}$, *rhp54*$^{+}$ and *cdt2*$^{+}$. In the down-regulated subset, nineteen out of the thirty-six protein-coding genes that were down-regulated in response to bleomycin in this work, were also down-regulated in response to IR in the study by Watson *et al*. This difference may reflect a different cutoff for significant change between the two studies; Watson *et al*. showed genes which were at least 2-fold down-regulated whereas this work analysed genes at least 1.5-fold down-regulated. In agreement with this, the majority of genes (12/17) down-regulated in this work but not in the Watson *et al*. study fell between 1.5- and 2-fold down-regulated.

The comparison of results from this work and the study by Watson *et al*. confirms that bleomycin elicits similar transcriptional responses to IR and highlights the validity of the use of bleomycin as a radiomimetic throughout this work.

5.3.2 Two transcripts that are significantly altered in *set2*Δ cells compared to wildtype following treatment with bleomycin are involved in DNA repair

Microarray analysis showed that prior to DNA damage there were no DNA repair genes that were significantly up- or down-regulated in *set2*Δ cells compared to wildtype. Following treatment with bleomycin, one gene involved in DNA repair was up-regulated less in *set2*Δ cells compared to wildtype; this was *cdt2*$^{+}$ (Cdc10-dependent transcript 2), which is postulated to have a role in DNA repair, and is normally expressed in G1 and S phase (Hofmann & Beach, 1994) and following DNA damage (Liu *et al*, 2005). Cdt2 is part of the Ddb1-Cul4^{Cdt2} E3 ubiquitin ligase whose activity is required for the degradation of Spd1, an

inhibitor of RNR in fission yeast (Holmberg *et al*, 2005; Liu *et al*, 2005; Liu *et al*, 2003). Degradation of Spd1 is required following DNA damage to allow activation of RNR leading to nucleotide production for subsequent DNA synthesis. Work done by this laboratory has shown that a *cdt2*$^{+}$ deletion mutant shows impaired repair by HR and sensitivity to DNA damaging agents (Moss *et al*, 2010), a repair profile dissimilar to that seen in the *set2*$^{+}$ deletion strain. Therefore it is unlikely that the lower levels of *cdt2*$^{+}$ transcription are resulting in the *set2*Δ repair phenotype observed. Nevertheless, it would be interesting to see if the lower levels of *cdt2*$^{+}$ transcript are also observed at the protein level.

There was also one repair gene that showed further increased transcript levels following bleomycin treatment in *set2*Δ cells compared to wildtype; this was *rhp54*$^{+}$, which exhibited an approximate 25% increased up-regulation following DNA damage in *set2*Δ cells compared to wildtype. During HR, Rhp54 interacts with Rhp51, stabilising the nucleofilament and promoting D-loop formation (Heyer *et al*, 2006; Mazin *et al*, 2003). Studies in *S. cerevisiae* show that overexpression of *RAD54* from the strong *ADH1* promoter, which results in significantly increased protein levels, does not alter DSB-induced HR levels (Kim *et al*, 2002). Therefore it seems unlikely that the modest increase in *rhp54*$^{+}$ transcript levels observed here in *set2*Δ cells would result in the increased level of HR seen in this genetic background. It would however be interesting to moderately increase the levels of Rhp54 and see if any affect on DSB repair is observed in our system.

5.3.3 A role for Set2 in the efficient transcription of MBF-regulated genes

Notably, there were a cluster of four transcripts involved in DNA replication and S phase progression that are consistently lower in *set2*Δ cells compared to wildtype following DNA damage: *cdc18*$^{+}$, *cdt1*$^{+}$, *cdc22*$^{+}$ and *tos4*$^{+}$. *cdc18*$^{+}$ was increased following bleomycin treatment in wildtype cells, but decreased in *set2*Δ cells. *cdt1*$^{+}$, *cdc22*$^{+}$ and *tos4*$^{+}$ were slightly decreased following bleomycin treatment in wildtype cells, but further decreased in *set2*Δ

cells. Cdt1 and Cdc18 are replication initiation factors (Nishitani *et al*, 2000), Cdc22 is the regulatory unit of RNR which catalyses dNTP synthesis (Fernandez Sarabia *et al*, 1993) and Tos4 has been characterised in budding yeast and is a putative forkhead domain containing G1/S transcription factor (Horak *et al*, 2002), and a checkpoint effector (Bastos de Oliveira *et al*, 2012). Interestingly the expression of all four of these genes is cell cycle regulated by the MBF (MCB binding factor) complex; expression is high in G1 phase and low in G2 phase (Hofmann & Beach, 1994; Lowndes *et al*, 1992). MBF comprises Cdc10, Res1, Res2, Rep1 and Rep2 (Caligiuri & Beach, 1993; Lowndes *et al*, 1992; Nakashima *et al*, 1995; Sugiyama *et al*, 1994; Whitehall *et al*, 1999; Zhu *et al*, 1994); it binds a cis-acting promoter element called MCB (*Mlu*I cell-cycle box) which can either be present as a single copy (ACGCG) or in tandem (ACGCG(A/T)CGCG; Lowndes *et al*, 1992; Oliva *et al*, 2005; Rustici *et al*, 2004; Tanaka *et al*, 1992). Negative regulators, Cig2, Nrm1 and Yox1 control the activity of MBF, allowing its timely repression, and thus effective cell cycle control of transcription (Aligianni *et al*, 2009; Ayte *et al*, 2001; Caetano *et al*, 2011; de Bruin *et al*, 2008; de Bruin *et al*, 2006). In addition to controlling transcription at G1/S, phosphorylation of Cdc10 by Cds1, following replication checkpoint activation by treatment with HU, leads to transcription of MBF genes, improving survival in response to replication stress (Dutta *et al*, 2008).

Interestingly, the fission yeast G1/S transcriptional programme comprises approximately twenty genes, with roles in DNA replication, DNA repair and cell cycle control, which are transcribed in an MBF-dependent manner (Oliva *et al*, 2005; Peng *et al*, 2005; Rustici *et al*, 2004). In addition to the cluster of four genes discussed above, two other genes showed reduced transcription compared to wildtype following bleomycin treatment: $cdt2^+$ and $ams2^+$. However, other MBF-dependent genes such as $ctp1^+$ and $mrc1^+$ showed no alteration in transcription compared to wildtype. Given that all MBF-dependent genes are similarly regulated it is curious that correct transcription of only a subset of these is dependent on Set2.

However, although all MBF-dependent genes contain at least one MCB motif, these vary in complexity. For example the *cdc22*$^{+}$ gene contains two clusters of four MCB motifs, in addition to another single MCB motif; loss of either cluster affects transcription (Maqbool *et al*, 2003). However, one cluster is required for constitutive expression whereas the other is required for G1/S dependent transcription. *cdc18*$^{+}$, *cdt1*$^{+}$ and *cdt2*$^{+}$ have similarly complex MCB arrangements; therefore, it is possible that Set2 only affects expression of genes whose promoters contain these complex arrangements of MCB motifs.

Given the differences between wildtype and *set2*Δ cells were only seen following treatment with bleomycin, it is possible that Set2 is involved particularly in the MBF transcriptional response to stress. On the other hand, given fission yeast spends the majority of the cell cycle in G2, when the levels of these genes are low, perhaps differences are only observed following DNA damage, when cell cycle arrest occurs. It would be interesting to look at transcript levels of these genes in synchronised *set2*Δ cells to see if the transcription is lower in cells that have not been damaged.

5.4 SUMMARY

To conclude, microarray analysis of wildtype and *set2*Δ cells identified:

- Fifty-nine genes showing altered expression in wildtype cells following bleomycin treatment.
- No significant change in HR and NHEJ gene expression prior to DNA damage in *set2*Δ cells.
- Altered expression of *rhp54*$^{+}$ and *cdt2*$^{+}$ in *set2*Δ cells following DNA damage.
- An additional role for Set2 in controlling expression of a subset of MBF-regulated genes.

CHAPTER 6
A role for Set2 in efficient DNA replication

6.1 INTRODUCTION

In Chapter 4, a *set2*Δ mutant was shown to be epistatic with NHEJ mutants, in keeping with a role for Set2 in repair by NHEJ. In addition, *set2*Δ cells showed an acute sensitivity to bleomycin in combination with a number of HR mutants, suggesting that Set2 functions in a HR-independent pathway. Microarray analysis showed no significant difference in the expression levels of NHEJ or HR genes that would explain the repair phenotype observed in *set2*Δ cells. However, a cluster of genes whose products are involved in DNA replication were found to be down-regulated following DNA damage in *set2*Δ cells. Further investigation into the significance of this finding was undertaken and is described in this chapter.

6.2 RESULTS

6.2.1 *cdc18*$^+$, *cdt1*$^+$, *cdc22*$^+$ and *tos4*$^+$ are down-regulated following DNA damage in *set2*Δ cells

As described in Chapter 5, microarray analysis of wildtype and *set2*Δ cells before and after treatment with bleomycin identified a cluster of genes that were consistently down-regulated in *set2*Δ cells compared to wildtype, following DNA damage. The products of two of these genes, Cdt1 and Cdc18 are members of the pre-RC, and their efficient binding to an origin of replication is required for replication licensing (Nishitani *et al*, 2000). The third, Cdc22, is the large subunit of RNR whose interaction with Suc22 (the small subunit) is required for dNTP production (Fernandez Sarabia *et al*, 1993) and the fourth, Tos4, is a putative forkhead domain containing G1/S transcription factor which has recently been shown to be an effector of the replication checkpoint (Bastos de Oliveira *et al*, 2012; Horak *et al*, 2002). The transcript levels for all four genes were reduced following 30 minutes of treatment with

bleomycin, compared to wildtype (Figure 6.1A and B). Given the apparent involvement of all four genes in DNA replication or S phase control, a cell cycle analysis of *set2*Δ cells was performed.

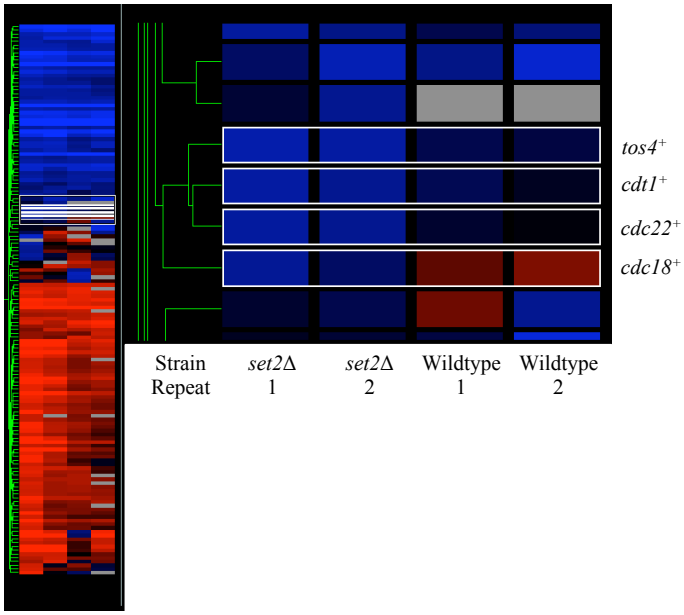
6.2.2 *set2*Δ cells show perturbed progression through S phase

To analyse the cell cycle progression of *set2*Δ cells, double mutants with *cdc25-22* were constructed. Cdc25 is a dual specificity phosphatase, which dephosphorylates Cdc2 allowing entry to mitosis (Coleman & Dunphy, 1994). Growth of the *cdc25-22* point mutant at the restrictive temperature of 35°C allows arrest at the G2/M transition, therefore synchronising the cells.

cdc25-22 and *set2*Δ*cdc25-22* cells were grown at 25°C, shifted to 35°C for 4 hours, and then released, and samples for flow cytometry and microscopy taken every 20 minutes for 5 hours. Following release, the *cdc25-22* cells showed progression to a 1C peak, having undergone mitosis, by 120 minutes, followed by DNA replication and a 2C peak by 240 minutes. A further 1C peak was observed at 240-260 minutes after release (Figure 6.2A); thus progression through two cell cycles is observed. The cells were visualised at each time point, and the number of binucleate cells (stained with DAPI) and septated cells (stained with methyl blue) counted. In keeping with the flow cytometry analysis, in the *cdc25-22* cells following release from the G2/M block, two peaks of binucleate cells were seen at 120 minutes and 240 minutes post release (Figure 6.2B). The percentage of septated cells exhibited a similar profile with peaks at 120 minutes and 240 minutes following release (Figure 6.2C). However, the *set2*Δ*cdc25-22* cells showed a different phenotype. Although formation of the initial 1C peak was similar to that observed in *cdc25-22* cells, further progression to a 2C peak, was not seen by flow cytometry, even 300 minutes following release, when the *cdc25-22* cells have formed a 1C peak for the second time (Figure 6.2A).

Figure 6.1

A



B

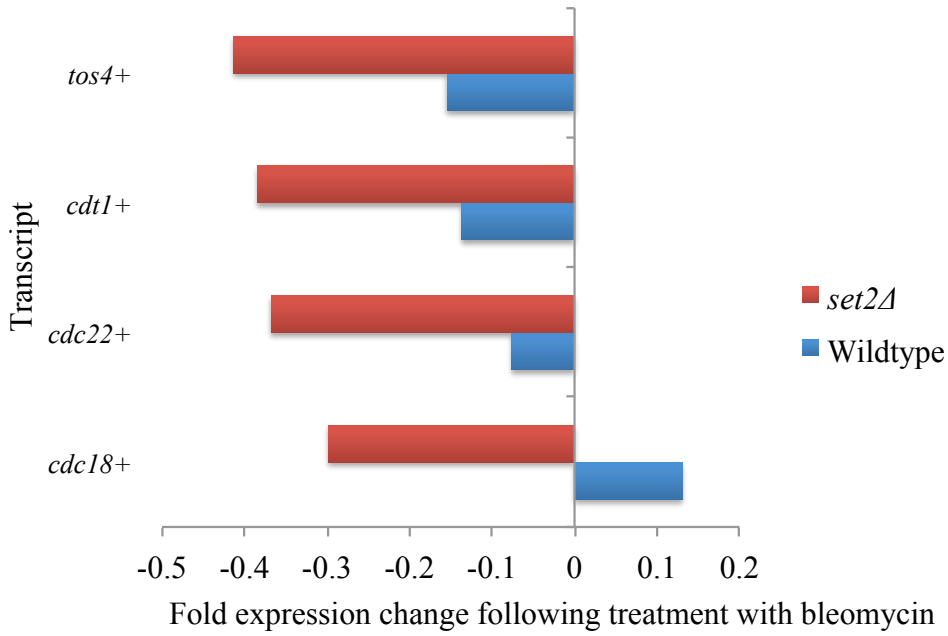


Figure 6.1 *set2*Δ cells have low levels of transcription of a cluster of DNA replication genes following DNA damage (A) Heat map depicting *cdc18*$^{+}$, *cdt1*$^{+}$, *cdc22*$^{+}$ and *tos4*$^{+}$ transcript levels in wildtype (2094) and *set2*Δ (3271) cells following 30 minutes of treatment with 5 µg/ml bleomycin. Blue depicts downregulated compared to before damage, red depicts upregulated compared to before damage. **(B)** Quantification of *cdc18*$^{+}$, *cdt1*$^{+}$, *cdc22*$^{+}$ and *tos4*$^{+}$ transcript levels in wildtype (blue) and *set2*Δ (red) cells following 30 minutes of treatment with 5 µg/ml bleomycin. Data represent mean of two experiments with independently derived RNA.

The percentage of binucleate and septated *set2*Δ*cdc25-22* cells are in keeping with this delay in cell cycle progression, as although there was a peak of both binucleate and septated cells 140 minutes following release, following the decrease, the percentage of binucleate and septated cells remained low until 300 minutes when there was a slight increase (Figure 6.2B and C). These results suggest that although *set2*Δ cells undergo mitosis effectively, the following round of DNA replication is delayed.

It is possible that introducing another mutation (i.e. *cdc25-22*) into *set2*Δ cells could result in other interactions. Therefore, to confirm the cell cycle delay seen in the *set2*Δ cells, nitrogen starvation was used to synchronise the cells. The cells were nitrogen starved for 16 hours, by which time all the cells are in a G0 state; on re-feeding with nitrogen, the cells re-join the cell cycle in G1. In the wildtype cells, an increasing 2C population was observed at 3 hours following re-feeding and by 4 hours, the entire population was 2C, indicating successful DNA replication (Figure 6.3A). However, in the *set2*Δ cells, at 3 hours following re-feeding the population was almost entirely still a 1C peak, and even 6 hours following re-feeding there was a proportion of the cells with a 1C peak, indicating a striking delay in DNA replication (Figure 6.3A).

Given *set2*Δ cells take longer to progress through S phase, this may reflect the repair profile of high HR and low NHEJ, as these repair mechanisms are cell cycle controlled (Ferreira & Cooper, 2004). As *set1*Δ cells also exhibited high levels of HR and low NHEJ (Chapter 3), the cell cycle progression in this background was also addressed using nitrogen starvation. However, the *set1*Δ cells did not show any perturbation in cell cycle progression compared to wildtype (Figure 6.3B), suggesting the cell cycle delay is not observed in all mutants exhibiting this repair profile.

Figure 6.2

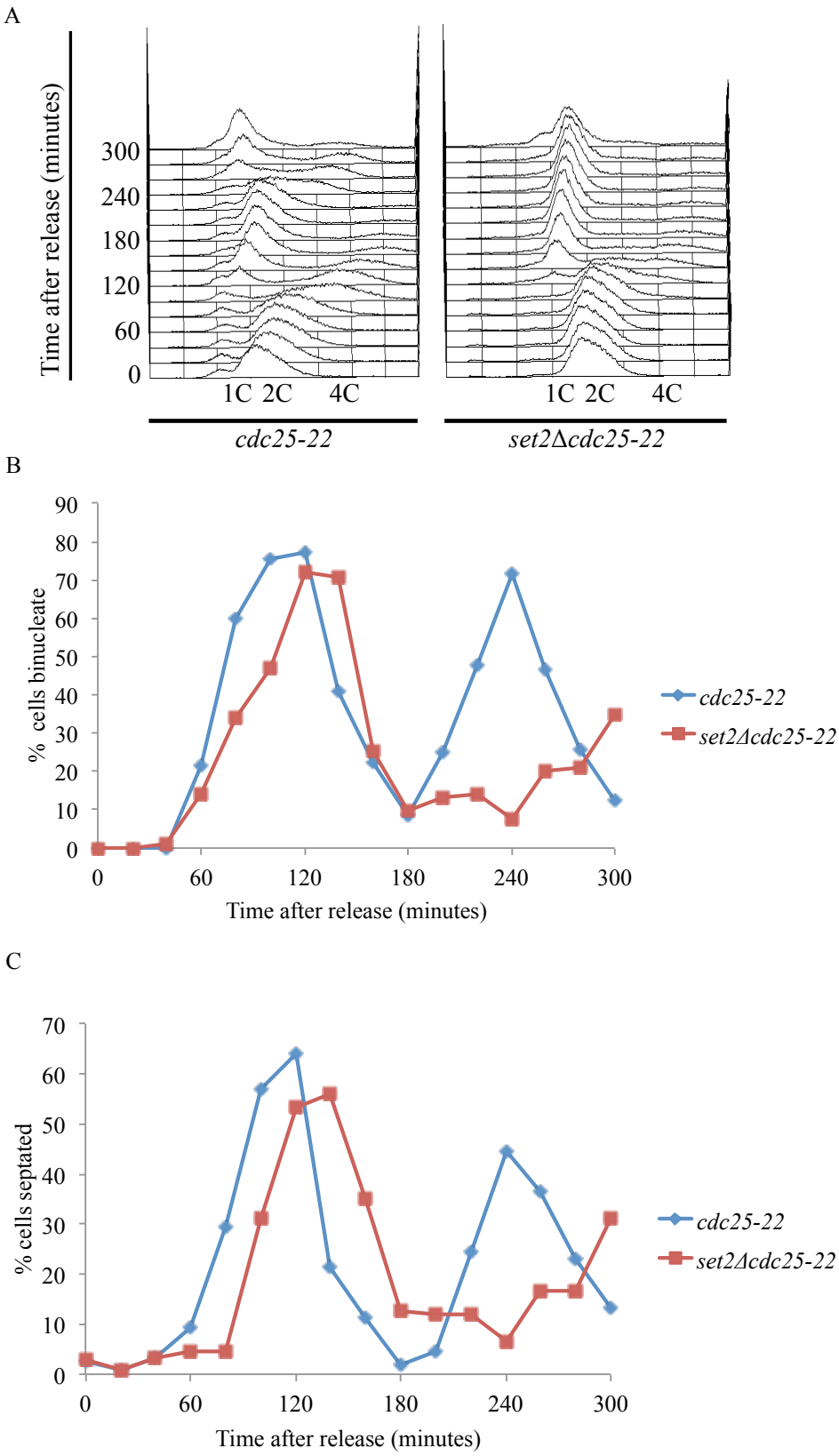
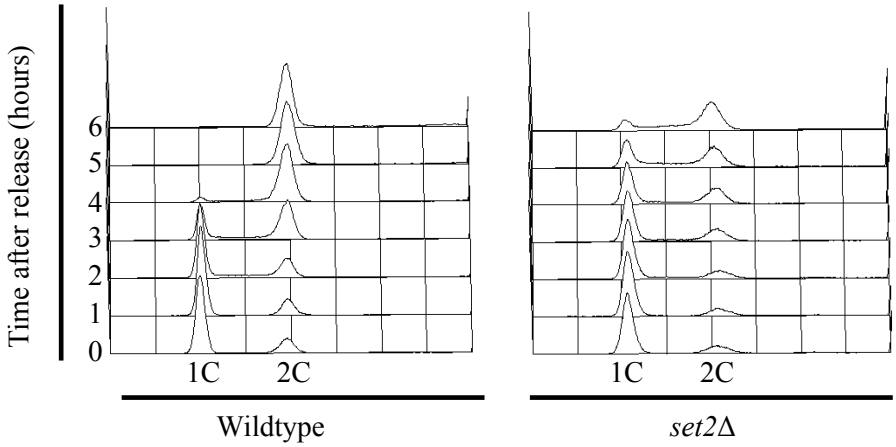


Figure 6.2 *set2*Δ cells show perturbed progression through S phase (A) Flow cytometry analysis of *cdc25-22* (1543) and *set2*Δ*cdc25-22* (6707) cells following release from *cdc25-22* block (35.5°C; 4 hours). **(B)** Percentage of binucleate cells following release from *cdc25-22* block. **(C)** Percentage of septated cells following release from *cdc25-22* block.

Figure 6.3

A



B

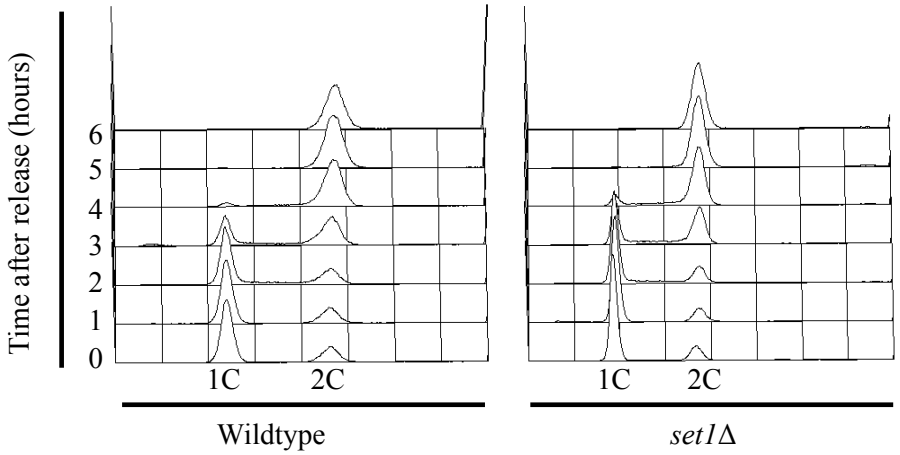


Figure 6.3 *set2*Δ but not *set1*Δ cells show perturbed progression through S phase following release from G1 arrest (A) Flow cytometry analysis of wildtype (6877) and *set2*Δ (6919) cells following release from nitrogen starvation. **(B)** Flow cytometry analysis of wildtype (6877) and *set1*Δ (6916) cells following release from nitrogen starvation.

6.2.3 *tos4*Δ cells exhibit normal cell cycle progression

Of the cluster of four genes which have significantly decreased transcript levels in response to bleomycin in *set2*Δ cells, three are required for efficient replication (Cdt1, Cdc18 and Cdc22) (Fernandez Sarabia *et al*, 1993; Nishitani *et al*, 2000; Zhao *et al*, 2001). The fourth, Tos4, has been identified in *S. cerevisiae* as a putative transcription factor (Horak *et al*, 2002), and has recently been shown to be involved as an effector of the replication checkpoint (Bastos de Oliveira *et al*, 2012a). Given the replication delay seen in *set2*Δ cells and the involvement of the other three members of the cluster in efficient DNA replication, the cell cycle progression of *tos4*Δ cells was analysed.

A *tos4*Δ*cdc25-22* double mutant was created and release from a G2/M *cdc25-22* block observed by flow cytometry and microscopy. In the *cdc25-22* mutant, on release from the block, a 1C population could be observed by 120 minutes, followed by DNA replication and formation of a 2C peak by 210-240 minutes and mitosis resulting in another 1C peak by 270 minutes (Figure 6.4A). A similar profile was observed in the *tos4*Δ*cdc25-22* cells, indicating that there is no significant delay in the cell cycle in cells lacking Tos4 (Figure 6.4A). In keeping with this, the percentage of binucleate and septated *cdc25-22* and *tos4*Δ*cdc25-22* cells peaked and troughed at the same time (Figure 6.4B and C). A recognisable difference was that the percentage of binucleate and septated cells was lower in the *tos4*Δ*cdc25-22* cells than the *cdc25-22* cells (binucleate cells at t=120 minutes, 60% compared to 78%; septated cells at t=120 minutes, 58% compared to 70%). However, this likely reflects a less effective synchronisation in the *tos4*Δ*cdc25-22* cells.

6.2.4 Cdt1 and Cdc18 are misregulated in *set2*Δ cells

DNA replication must only occur once per cell cycle to ensure the viability of the cell is maintained. To ensure this, recruitment of the minichromosome maintenance 2-7 complex

Figure 6.4

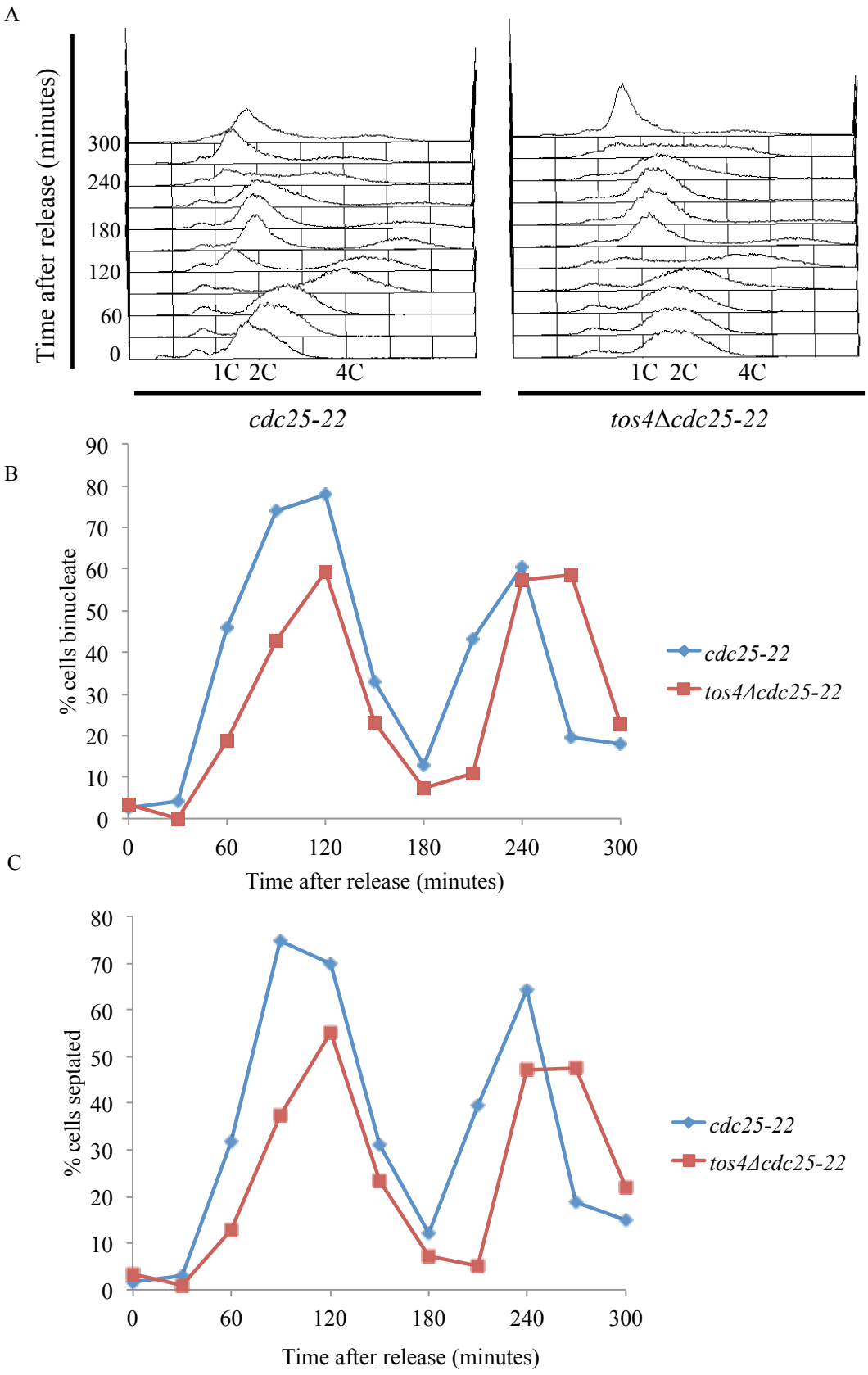


Figure 6.4 *tos4*Δ cells progress normally through S phase (A) Flow cytometry analysis of *cdc25-22* (1543) and *tos4*Δ*cdc25-22* (6932) cells following release from *cdc25-22* block (35.5°C; 4 hours). **(B)** Percentage of cells binucleate following release from *cdc25-22* block. **(C)** Percentage of cells septated following release from *cdc25-22* block.

(Mcm2-7) facilitated by Cdt1 and Cdc18 (Cdc6 in budding yeast and metazoa; Donovan *et al*, 1997; Tanaka *et al*, 1997), resulting in origin licensing and pre-RC formation, occurs only in G1 phase. This precise regulation requires cell cycle fluctuation of Cdt1 and Cdc18 levels.

Given the central role in replication of Cdt1 and Cdc18, the low levels of transcripts of these genes following DNA damage in *set2*Δ cells and the defective cell cycle observed, the regulation of Cdt1 and Cdc18 in *set2*Δ cells was analysed. Cells were synchronised and Cdt1 and Cdc18 protein levels analysed throughout the cell cycle by western blotting. TAP-tagged Cdt1 or Cdc18 was introduced into *cdc25-22* or *set2*Δ*cdc25-22* cells, the population synchronised at G2/M by growth at the restrictive temperature, and samples taken for protein extraction and flow cytometry every 30 minutes for 3 hours.

Before release from the *cdc25-22* block, the cells are arrested at the G2/M boundary. Given Cdt1 is degraded in S phase, and is not transcribed until late M/G1, Cdt1 levels were low at this point (Figure 6.5A, left panel). On release, *cdc25-22* cells enter mitosis and a 1C peak indicating complete mitosis was evident 120 minutes following release (Figure 6.5B, left panel); consistent with this, Cdt1 levels increased up to 90 minutes (Figure 6.5A, left panel). Conversely, in the *set2*Δ*cdc25-22* cells, Cdt1-TAP levels were lower than in *cdc25-22* cells prior to release from the block and remained low up to 90 minutes following release (Figure 6.5A, right panel), in keeping with the flow cytometry profile which showed delayed formation of a 1C peak (Figure 6.5B, right panel).

In the Cdc18-TAP tagged cells, a similar profile was seen; in the *cdc25-22* cells Cdc18 levels were low prior to release from the block, followed by an increase up to 90 minutes following release, presumably reflecting transcription of $cdc18^{+}$ in late M phase (Figure 6.6A and B, left

Figure 6.5

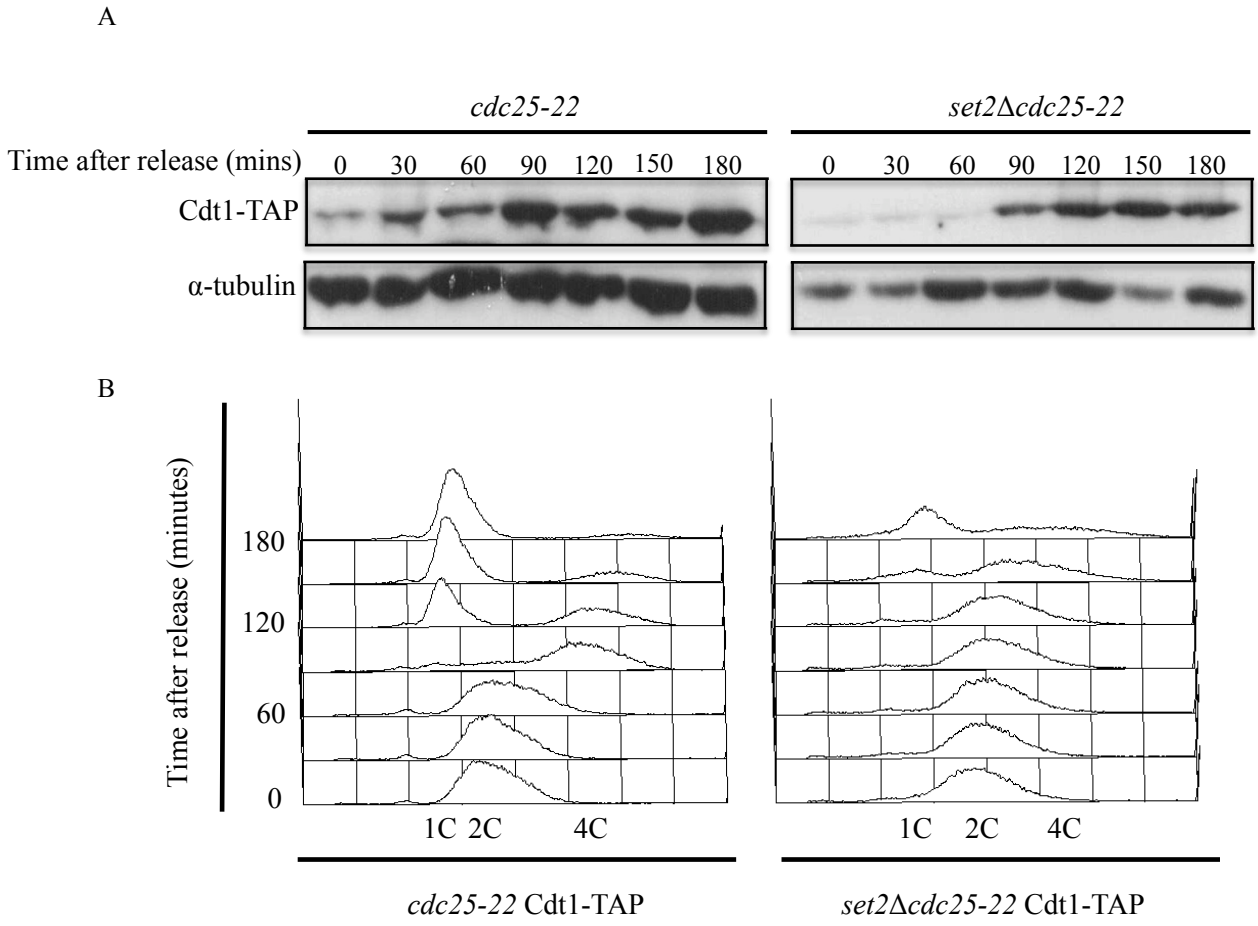


Figure 6.5 Cdt1 is misregulated in *set2*Δ cells (A) Western blot analysis of Cdt1-TAP levels following release from a *cdc25-22* block (35.5°C; 4 hours) in *cdc25-22* (6895) and *set2*Δ*cdc25-22* (6935) cells. **(B)** Flow cytometry profiles of *cdc25-22* and *set2*Δ*cdc25-22* cells following release from a *cdc25-22* block (35.5°C; 4 hours).

panel). The abundance of Cdc18 then decreased, in line with entry into S phase and subsequent degradation. However, in the *set2*Δ*cdc25-22* cells, levels of Cdc18 did not rise until 90 minutes following release indicating a delay in mitosis, confirmed by flow cytometry (Figure 6.6A and B, right panel). These results are consistent with the cell cycle defect observed in *set2*Δ cells.

6.2.5 Cdc22 levels are lower, but do not show cell cycle changes in *set2*Δ cells

To address whether Cdc22 also showed aberrant regulation, GFP tagged Cdc22 was introduced into *cdc25-22* or *set2*Δ*cdc25-22* cells and Cdc22 levels throughout the cell cycle analysed by western blot. In the *cdc25-22* cells there appeared to be no cell cycle specific regulation of Cdc22; the levels were consistent throughout (Figure 6.7A and B, left panel). Similarly, in the *set2*Δ*cdc25-22* cells there was no cell cycle specific change in the Cdc22 levels, although they do appear slightly lower than in *cdc25-22* cells, fitting with the microarray data (Figure 6.7A and B, right panel). It would however, be interesting to directly compare the Cdc22 levels in non-synchronised wildtype and *set2*Δ cells.

6.2.6 Ectopic expression of *cdt1* and *cdc18* does not rescue the cell cycle defect of *set2*Δ cells

To see if the cell cycle defect in *set2*Δ cells could be rescued by increasing the expression of *cdt1* and *cdc18*, the genes were ectopically expressed from a REP81X plasmid in *cdc25-22* and *set2*Δ*cdc5-22* cells. Cells were grown in the presence (+T) or absence of thiamine (-T) to induce expression from the plasmids, synchronised at G2/M using the *cdc25-22* block and samples for flow cytometry taken every 30 minutes following release. Increasing the expression of *cdc18* and *cdt1* in the *cdc25-22* background seemed to prevent the cells cycling, and a 2C peak was observed throughout the timecourse (Figure 6.8, top right panel). In a *set2*Δ*cdc25-22* background the cells grown in the absence of thiamine had a similar profile to those grown in its presence, indicating ectopic expression does not rescue the cell cycle defect

Figure 6.6

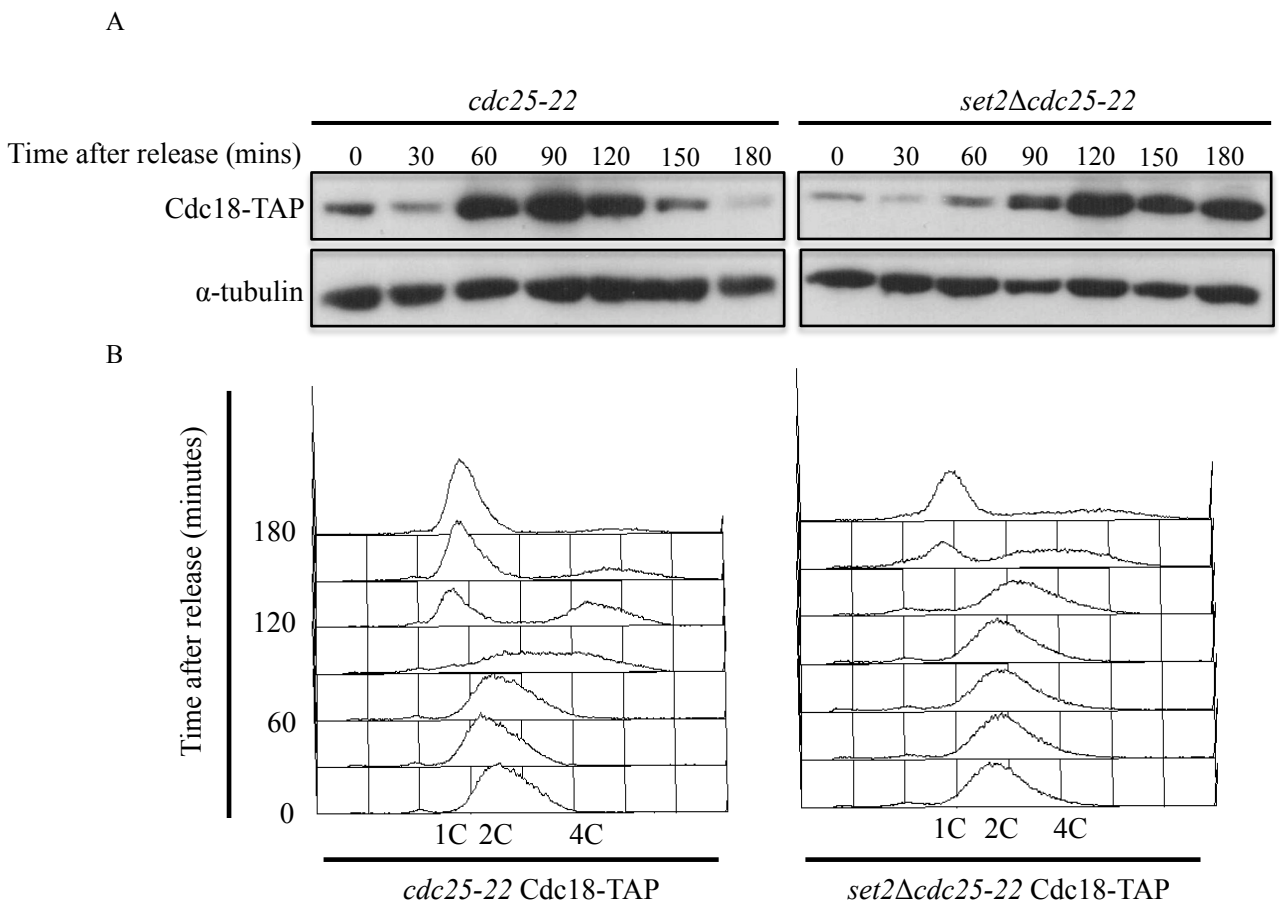


Figure 6.6 Cdc18 is misregulated in *set2*Δ cells (A) Western blot analysis of Cdc18-TAP levels following release from a *cdc25-22* block (35.5°C; 4 hours) in *cdc25-22* (6959) and *set2*Δ*cdc25-22* (7011) cells. **(B)** Flow cytometry profiles of *cdc25-22* and *set2*Δ*cdc25-22* cells following release from a *cdc25-22* block (35.5°C; 4 hours).

Figure 6.7

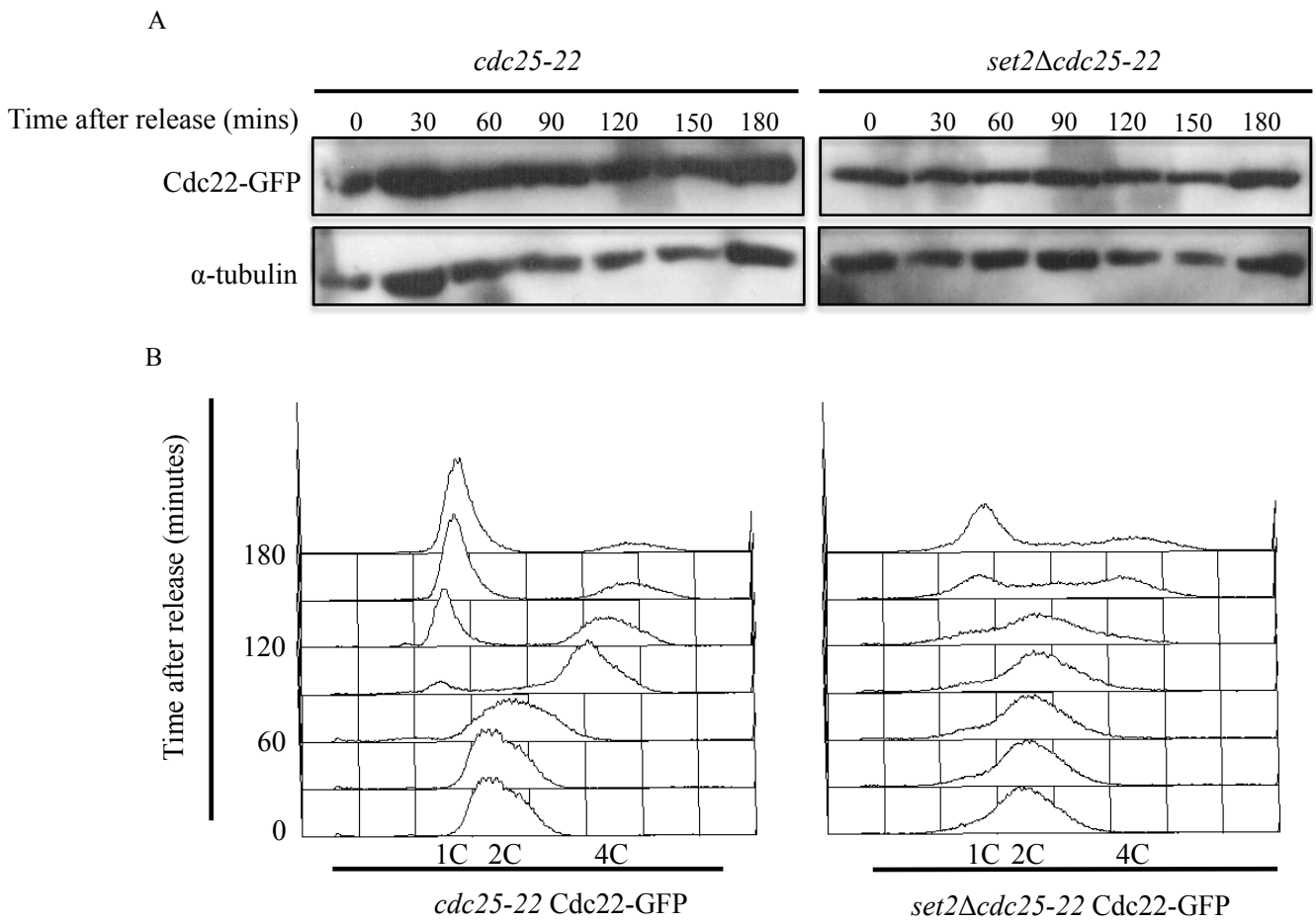


Figure 6.7 Cdc22 levels are low in *set2*Δ cells (A) Western blot analysis of Cdc22-GFP levels following release from a *cdc25-22* block (35.5°C; 4 hours) in *cdc25-22* (7018) and *set2*Δ*cdc25-22* (6986) cells. **(B)** Flow cytometry profiles of *cdc25-22* and *set2*Δ*cdc25-22* cells following release from a *cdc25-22* block (35.5°C; 4 hours).

(Figure 6.8). Given that expression of *cdc18* in G2 can lead to re-replication, which is potentiated by expression of *cdt1* (Yanow *et al*, 2001), it was unlikely that this approach would result in a normal cell cycle. This was evident by the fact that the *cdc25-22* cells in the absence of thiamine did not show normal cell cycling; the widening of this 2C peak though the timecourse may be indicative of some re-replication.

6.2.7 *cdt1-19* shows some phenotypic similarity to *set2*Δ cells

Given the mechanisms of HR and NHEJ are favoured at different stages of the cell cycle it is possible that the low levels of *cdc18* and *cdt1* transcripts are responsible for the cell cycle and repair phenotypes seen in *set2*Δ cells. To address this, temperature sensitive alleles of *cdc18* and *cdt1* were utilised. Both *cdt1-19* and *cdc18-K46* showed striking sensitivity when grown at 35°C compared to wildtype (Figure 6.9A).

Given that Cdc18 and Cdt1 are required for replication initiation, it would be expected that temperature sensitive mutants would show a cell cycle defect. To investigate this, the cells were nitrogen starved and samples taken for flow cytometry following re-feeding at the restrictive temperature of 35°C. The *cdt1-19* mutant showed a slight delay in formation of the 2C peak compared to wildtype; the 1C population was only completely absent in *cdt1-19* cells 6 hours after re-feeding whereas in wildtype this was seen at 5 hours (Figure 6.9B). However, in the *cdc18-K46* mutant there was no delay in progression to a 2C peak (Figure 6.9C). Although surprising, given the role of Cdc18 in replication initiation, this is consistent with initial studies of the *cdc18-K46* mutant which showed it could complete its function early in the cell cycle but then arrested with a 2C DNA content (Nasmyth & Nurse, 1981). Further, following 6 hours growth at the restrictive temperature, chromosomes from *cdc18-K46* entered a pulsed-field gel with reduced efficiency compared to wildtype, similar to HU treated cells (Kelly *et al*, 1993), suggesting chromosome structure is somehow altered. It is suggested that the flow cytometry profiles observed for this mutant reflect that although DNA

Figure 6.8

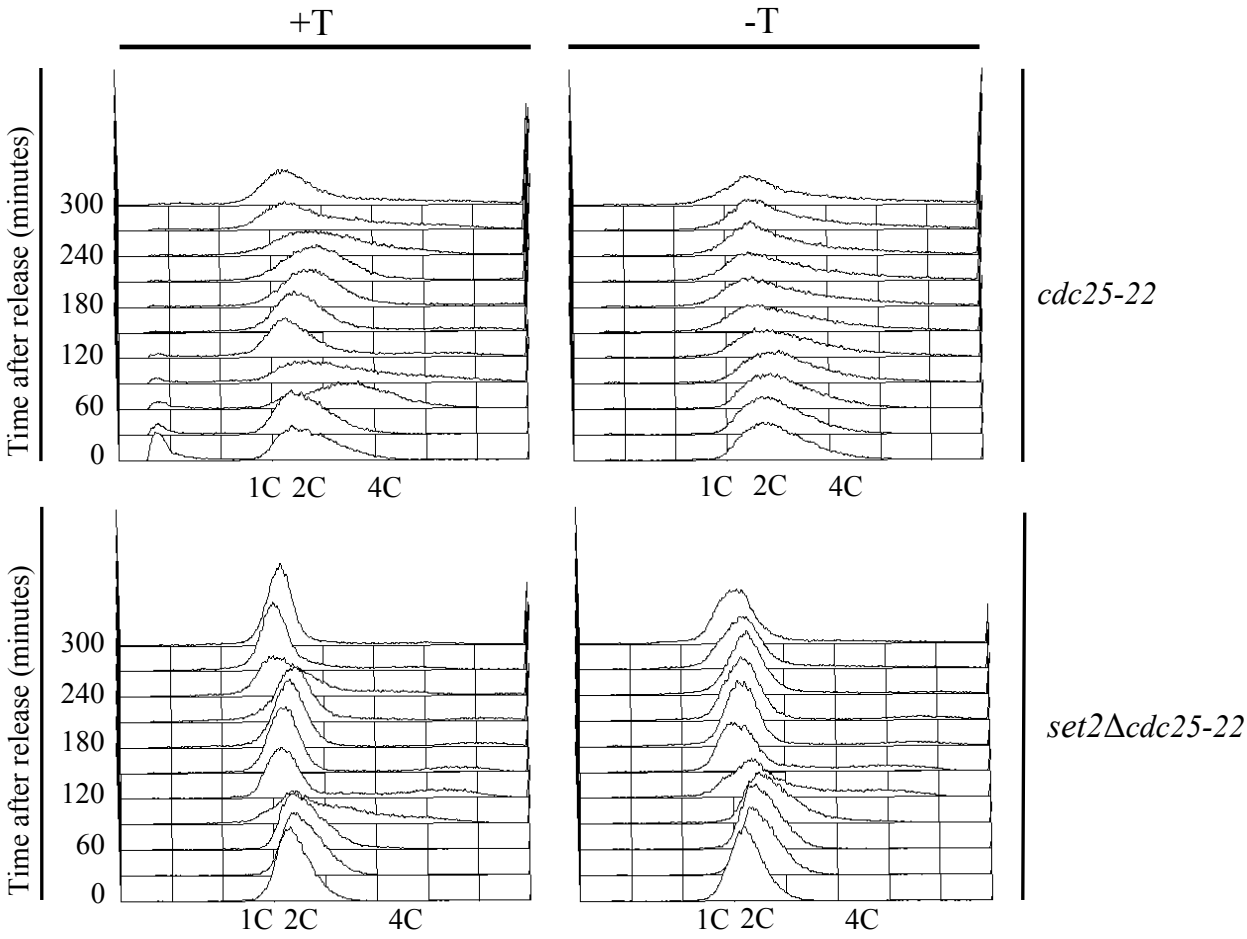


Figure 6.8 Ectopic expression of *cdc18* and *cdt1* does not rescue the cell cycle defect of *set2*Δ cells
Flow cytometry analysis of *cdc25-22* (7002) and *set2*Δ*cdc25-22* (6999) cells with (-thiamine (T)) and without (+thiamine (T)) ectopic expression of *cdt1* and *cdc18* from a REP81X plasmid following release from *cdc25-22* block (35.5°C; 4 hours).

Figure 6.9

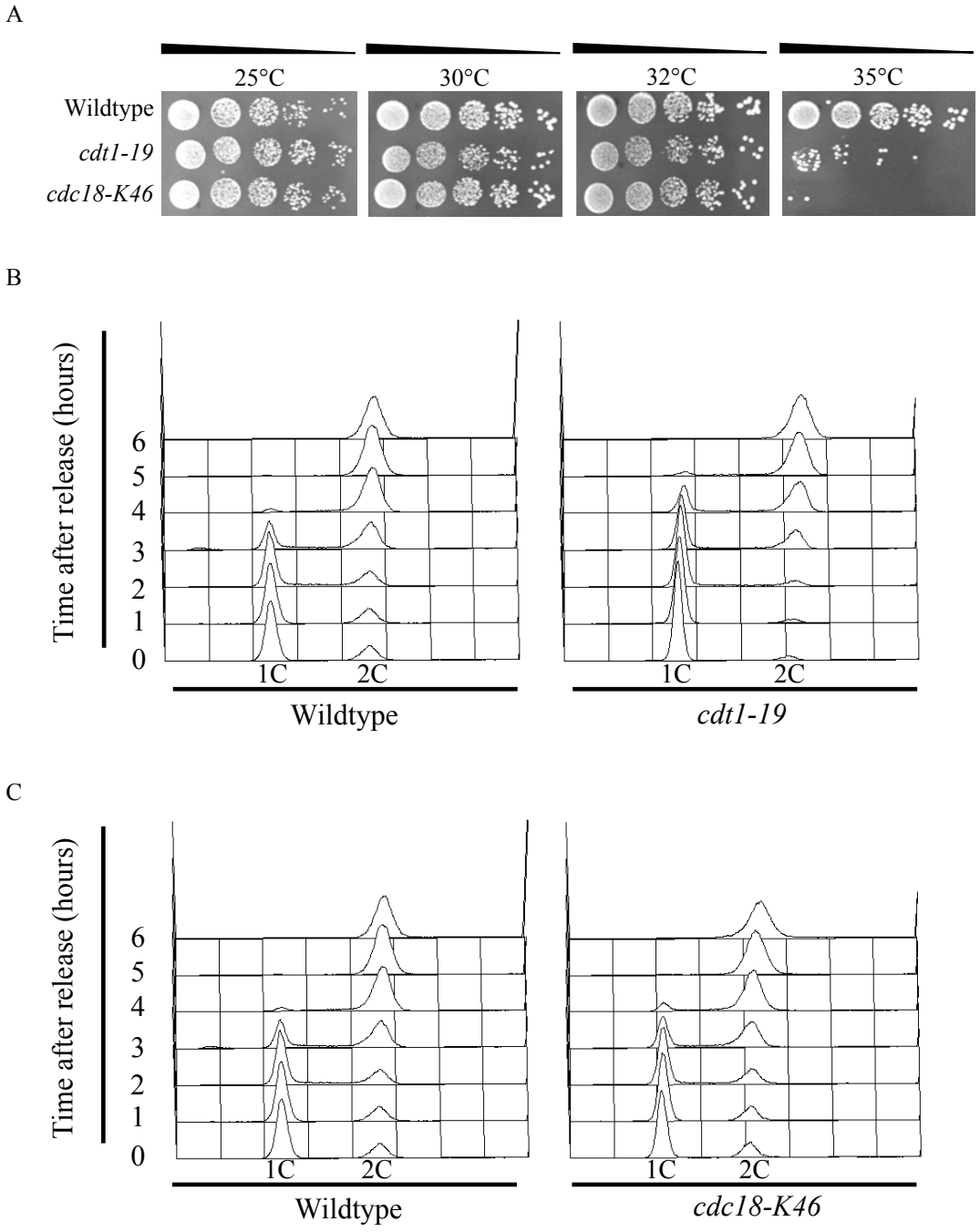


Figure 6.9 *cdt1-19* and *cdc18-K46* cells are temperature sensitive (A) 5-fold serial dilutions of wildtype (2094), *cdt1-19* (6961) and *cdc18-K46* (6960) were grown on YE6S at 25°C, 30°C, 32°C and 35°C. **(B)** Flow cytometry analysis of wildtype (6877) and *cdt1-19* (7118) cells following release from nitrogen starvation at 35°C. **(C)** Flow cytometry analysis of wildtype (6877) and *cdc18-K46* (6960) cells following release from nitrogen starvation at 35°C.

replication is defective in this genetic background, there is some leakiness, so that the DNA content approaches a 2C level (Kelly *et al*, 1993).

To see if either point mutant could phenocopy *set2*Δ with regards to DNA repair, double mutants with *exo1*Δ were created and the viability in response to bleomycin addressed. Similar to the *set2*Δ*exo1*Δ double mutant, the *cdt1-19exo1*Δ cells showed exquisite sensitivity to bleomycin (Figure 6.10), which suggests that the repair phenotype seen in *set2*Δ cells may be due to lower levels of $cdt1^{+}$ expression. Surprisingly, the *cdc18-K46exo1*Δ mutant showed an increased resistance to bleomycin compared to the single mutants (Figure 6.10), a phenotype opposite to the *set2*Δ*exo1*Δ mutant. Therefore although *cdt1-19* mutant does phenocopy *set2*Δ in its negative genetic interaction with *exo1*Δ, the *cdc18-K46* mutant does not. However, this may simply reflect the leaky nature of the mutant.

6.2.8 Increasing the G1 population of *set2*Δ cells does not rescue the NHEJ defect

To investigate whether the NHEJ defect observed in *set2*Δ cells was due to the cells spending longer in S and G2 phase where they will have a sister chromatid that can be used as a template for repair by HR, and therefore possibly less time in G1 where they will preferentially repair by NHEJ, the cell cycle distribution of *set2*Δ cells was perturbed to give them longer in G1.

The initial approach involved making a double mutant of *set2*Δ with *wee1-50*, a point mutant in the Wee1 kinase that influences cell size by inhibiting entry into mitosis, through phosphorylation and inhibition of Cdc2 (Coleman & Dunphy, 1994; Rhind *et al*, 1997). The mutant has a shorter G2 phase as entry into mitosis is not inhibited, and thus cells spend longer in G1 allowing them to reach the minimum size requirement for entry to S phase.

Figure 6.10

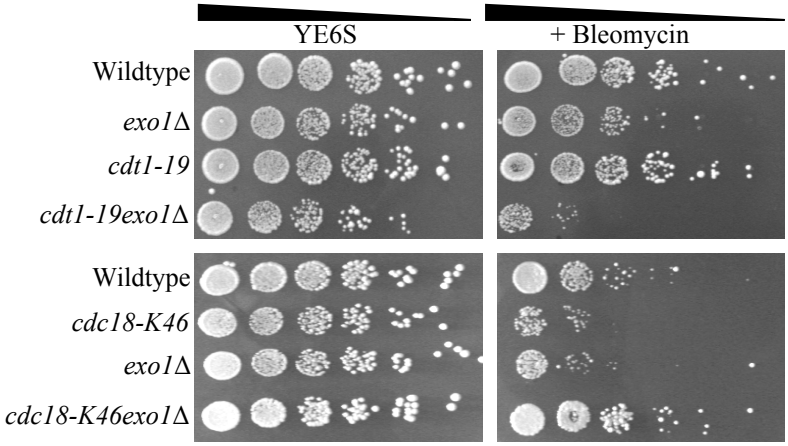


Figure 6.10 *cdt1-19* is equivalent to *set2*Δ 5-fold serial dilutions of wildtype (2094), *cdt1-19* (6961), *exo1*Δ (5310), *cdt1-19exo1*Δ (7014), *cdc18-K46* (6960) and *cdc18-K46exo1*Δ (7039) cells were grown on YE6S and YE6S + 1 μg/ml bleomycin at 32°C.

The growth of the *set2*Δ*wee1-50* mutant at the restrictive temperature was analysed using a serial dilution assay. On growth in EMM at the restrictive temperature of 35°C, the double mutant was synthetic lethal (Figure 6.11A). To address why this cell death was occurring, images of DAPI stained wildtype, *set2*Δ, *wee1-50* and *set2*Δ*wee1-50* cells, grown at the restrictive temperature were analysed. As expected, the *wee1-50* cells were very small, reflecting their early progression into mitosis (Figure 6.11B). Interestingly, the *set2*Δ*wee1-50* cells exhibited a 'cut' (cell untimely torn) phenotype, indicating an aberrant mitosis (Figure 6.11B), and explaining the synthetic lethal phenotype seen in this mutant. Mutants exhibiting a 'cut' phenotype are often checkpoint-defective and checkpoint mutants are often synthetic lethal with *wee1-50*; thus, the checkpoint response of *set2*Δ was investigated by analysis of cell length following treatment with HU. When treated with HU, which disrupts DNA synthesis through inhibition of RNR, checkpoint-proficient cells cease DNA synthesis and arrest cell division, resulting in an elongated cell phenotype. On the other hand, checkpoint-deficient cells, such as *rad3*Δ, exhibit a 'cut' phenotype (Figure 6.11C). Following HU treatment, the *set2*Δ cells exhibited an elongated cell phenotype similar to wildtype, indicating a proficient checkpoint response (Figure 6.11C).

Given the synthetic lethal phenotype of the *set2*Δ*wee1-50* mutant, increasing the G1 population by nitrogen starvation was attempted. Nitrogen starvation in usually done in prototrophic strains to allow cell survival; however, to address whether perturbing the cell cycle affects NHEJ repair, a *leu1-32* mutant had to be utilised, to allow transformation with the LEU2 plasmid. The cells were therefore nitrogen starved for only 8 hours, which increased the population of G1 cells to approximately 30% (Figure 6.12A), re-fed with nitrogen for one hour, and then transformed with the NHEJ assay plasmid. 12 hours following re-feeding, the cells exhibited a normal cell cycle distribution (Figure 6.12A), showing the cells had survived the nitrogen starvation and returned to a normal 2C DNA content. The

Figure 6.11

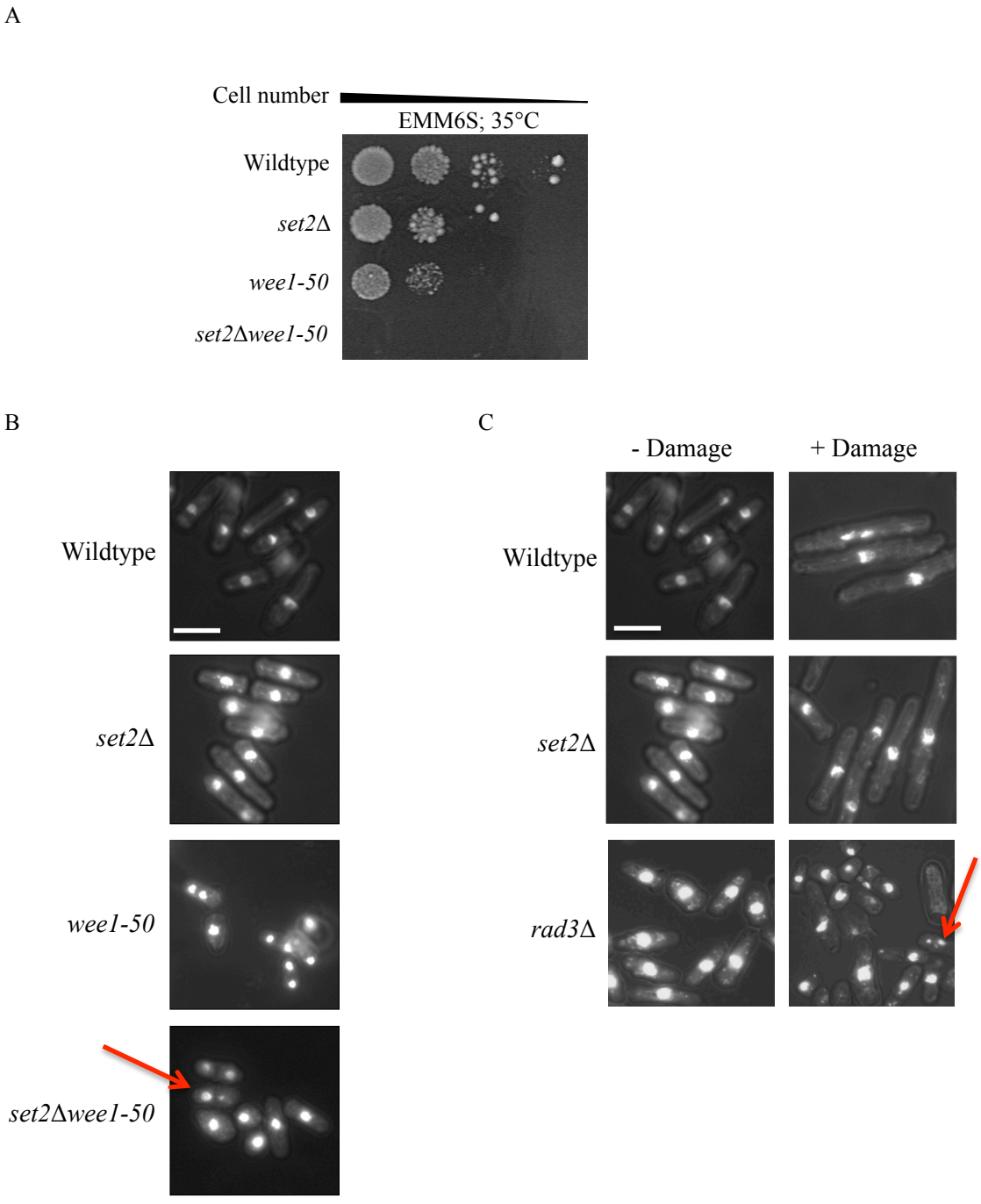


Figure 6.11 *set2Δwee1-50* exhibits a 'cut' phenotype (A) 5-fold serial dilutions of wildtype (2094), *set2*Δ (3271), *wee1-50* (7024) and *set2Δwee1-50* (7121) were grown on EMM6S at 35°C. **(B)** Images of DAPI stained wildtype, *set2*Δ, *wee1-50* and *set2Δwee1-50* cells are shown. Arrow indicates "cut" phenotype. Scale bar, 10 µm. **(C)** Images of DAPI stained wildtype, *rad3*Δ (2799) and *set2*Δ cells are shown. Cells were imaged before (-Damage) and 6 hours following treatment with 10 mM HU (+Damage). Scale bar, 10 µm.

plasmid-rejoining assay in nitrogen starved *set2*Δ cells still showed a decrease in NHEJ compared to wildtype (Figure 6.12B) suggesting that the NHEJ defect in cells lacking Set2 is not due to an aberrant cell cycle.

6.3 DISCUSSION

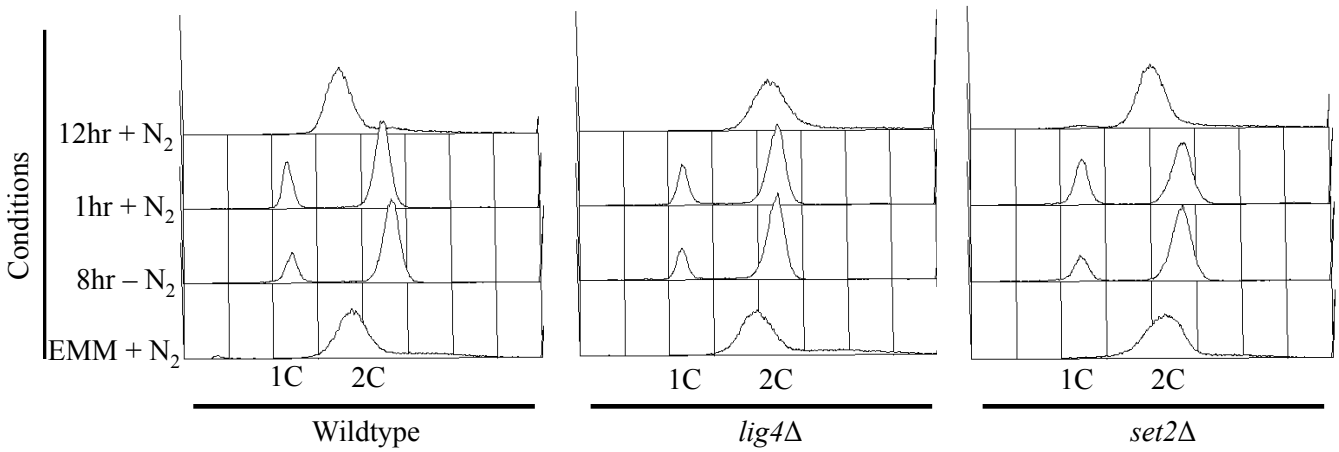
Microarray analysis in Chapter 5 identified a cluster of genes that were consistently down-regulated in *set2*Δ cells compared to wildtype following treatment with bleomycin. These genes all shared a role in DNA replication and S phase control. Therefore, work in this chapter sought to determine whether there was any associated change in cell cycle progression in *set2*Δ cells. A defect in S phase progression was identified in the *set2*Δ cells, consistent with misregulation of Cdc18 and Cdt1, the replication initiation factors. Results suggest that this impaired S phase progression does not result in the NHEJ defect identified in *set2*Δ cells.

6.3.1 Set2 is required for efficient DNA replication

Analysis of the cell cycle progression of *set2*Δ cells, by synchronising the cells using nitrogen starvation or a *cdc25-22* block, identified a delay in the completion of DNA replication, of at least one hour, compared to wildtype. Initiation of DNA replication in eukaryotes is dependent on licensing of the origins of replication by formation of the pre-RC. This requires ORC, Cdc18 and Cdt1 loading onto the origin, which results in recruitment of the Mcm2-7 replicative helicase. Activation of Mcm2-7 on entry to S phase, by activity of CDKs and DDKs leads to the recruitment of additional replication factors, and subsequent replication initiation (reviewed in Bell & Dutta, 2002). Microarray analysis of *set2*Δ cells showed decreased transcript levels of a number of MBF-regulated genes including *cdc18*$^{+}$ and *cdt1*$^{+}$, following treatment with bleomycin, compared to wildtype. Analysis of the corresponding protein levels in synchronised cells showed that levels of Cdc18 and Cdt1 took longer to increase in *set2*Δ cells compared to wildtype following release from a G2/M block. This may

Figure 6.12

A



B

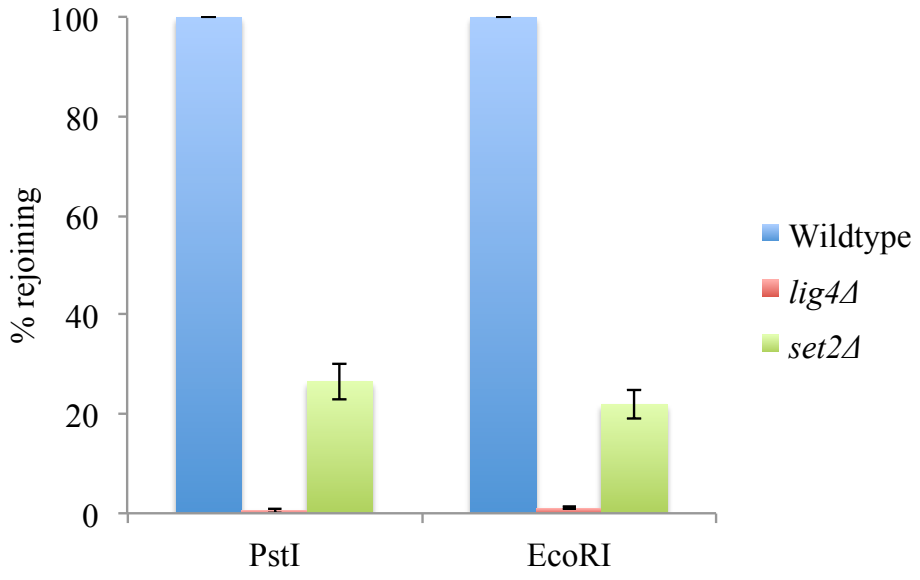


Figure 6.12 Biasing *set2*Δ cells to G1 does not rescue the NHEJ defect (A) Flow cytometry analysis of wildtype (244), *lig4*Δ (1069) and *set2*Δ (7152) cells following 8 hour nitrogen starvation and release. **(B)** Outcome of NHEJ plasmid-rejoining assay for wildtype, *lig4*Δ and *set2*Δ cells 1 hour after release from 8 hours of nitrogen starvation. Data are the mean of two experiments and error bars (±SE) are shown.

explain the slower progression of *set2*Δ cells through S phase, as cells partially depleted of Cdt1 in budding yeast replicate DNA from fewer origins (Devault *et al*, 2002), thus lengthening the time taken to complete DNA replication. Interestingly a study in budding yeast identified a delay in Cdc45 binding to origins in *set2* cells associated with a delayed S phase progression (Pryde *et al*, 2009). Given the results from this work, one could imagine that delayed expression of $cdt1^{+}$ and $cdc18^{+}$ in *set2*Δ cells could result in fewer pre-RC complexes formed, at fewer origins, delaying the recruitment of additional replication factors required for initiation of replication, such as Cdc45, which may result in slower progression through S phase. It would be interesting to test this model by investigating whether there are a reduced number of origins firing in the *set2*Δ cells; this could be addressed using DNA combing.

An attempt to rescue the S phase delay by ectopically expressing *cdc18* and *cdt1* was unsuccessful. However, given the intricacies of regulation of Cdt1 and Cdc18 levels and that expression of *cdc18* in G2 can lead to re-replication, which is potentiated by expression of *cdt1* (Yanow *et al*, 2001), this is perhaps unsurprising. Given that increasing the levels of these proteins too far, can result in re-replication and genomic instability, to see a rescuing effect the genes may need to be expressed at the appropriate stages of the cell cycle and to exact levels.

The study by Pryde *et al*. (2009) showed a decrease in H3K36me3 and an increase in H3K36me1 concurrent with binding of Cdc45, which they suggested may reflect differing functions of these modifications during replication. Trimethylation correlates with highly expressed genes (Pokholok *et al*, 2005) and dimethylation reflects whether a gene is expressed (Rao *et al*, 2005); both forms require interaction between Set2 and RNAP II (Du *et al*, 2008; Youdell *et al*, 2008). On the other hand, monomethylation is independent of RNAP

II phosphorylation and it is suggested histones may be monomethylated before deposition, although there is no evidence to support this (Du *et al*, 2008). Given the dynamics of transcription and resulting changes in DNA topology, transcription may interfere with successful establishment of the repliosome (Osborne & Guarente, 1988; Pederson & Morse, 1990). Thus, a decrease in trimethylation compared to monomethylation on binding of Cdc45 to the replication complex may reflect some regulatory pathway whereby transcription is prevented in regions about to undergo DNA replication.

The S phase delay could also be due to reduced levels of Cdc22, the large subunit of RNR, which is required for dNTP production (Fernandez Sarabia *et al*, 1993). Cells make just enough dNTPs in S phase for efficient replication, and an increase or decrease can be mutagenic (Bebenek *et al*, 1992; Chabes *et al*, 2003). In addition, reduced dNTP levels can cause slower replication (Zhao *et al*, 2001). Although the transcription of *cdc22*$^{+}$ is MBF controlled and thus varies through the cell cycle, analysis of Cdc22 protein levels show its presence throughout the cell cycle in both wildtype and *set2*Δ cells. Although there is perhaps a slight decrease in *set2*Δ cells compared to wildtype, it is not as striking as the Cdt1 and Cdc18 protein levels. A partial depletion of Cdc22 would help ascertain whether the S phase delay in *set2*Δ cells could be due to reduced Cdc22. On the other hand, the levels of Cdc22 could be increased through ectopic expression in the *set2*Δ background to see if this could rescue the S phase delay. Further, it would be interesting to compare the dNTP levels in wildtype and *set2*Δ cells, to see if there is any striking difference.

6.3.2 An interaction between replication initiation factors and Exo1

To address whether the repair phenotype of *set2*Δ was attributable to reduced levels of Cdt1 or Cdc18, double mutants of *cdt1*-19 or *cdc18*-K46 with *exo1*Δ were analysed for response to bleomycin. Interestingly, the double mutant of *cdt1-19exo1*Δ phenocopied *set2*Δ*exo1*Δ in

exhibiting sensitivity to bleomycin compared to the single mutants alone. In Chapter 4, results showed that the sensitivity to bleomycin in the *set2*Δ*exo1*Δ cells was not due to lack of both HR and NHEJ pathways, suggesting an additional role for Set2. Given the similar interaction between *cdt1-19* and *set2*Δ it is possible that this additional role relates to the proper transcriptional regulation of $cdt1^{+}$ and thus a role in DNA replication. However, converse to this is the finding that deletion of $exo1^{+}$ in a *cdc18-K46* mutant actually suppresses its sensitivity to bleomycin.

Studies of the *cdc18-K46* mutant suggest that although the cells can progress through replication, there is likely altered chromosome structure, which could reflect increased fork stalling and collapse (Kelly *et al*, 1993; Nasmyth & Nurse, 1981). In response to stalled forks or replication stress, checkpoint kinases can prevent inappropriate recombination events occurring at replication forks by controlling the activity of nucleases. Consequently, resection of DSBs is slower when the S phase checkpoint is activated and Exo1 is negatively regulated by checkpoint kinases to prevent potentially harmful effects of long tract resection by Exo1 at stalled forks (Alabert *et al*, 2009; El-Shemerly *et al*, 2008; Morin *et al*, 2008). Thus in the *exo1*Δ*cdc18-K46* mutant, $exo1^{+}$ deletion may result in a decrease in the deleterious consequences of resecting stalled forks, increasing survival in response to bleomycin.

A similar response of both *cdt1-19* and *cdc18-K46* double mutants with *exo1*Δ to bleomycin might be expected given their shared function. However, results indicate there is likely to be an additional function for Cdt1. Cdt1 has been implicated in DNA repair; it is recruited to UV and laser irradiated damage sites in G1, and although one study suggests this recruitment is purely to promote its timely degradation (Ishii *et al*, 2010), another suggests that its quick recruitment is indicative of another role (Roukos *et al*, 2011). Given the presence of Cdt1 in

G1, Roukos *et al*., (2011) suggest that Cdt1 could be a marker for signalling repair by NHEJ, however, there is no evidence to support this.

HR plays a major role in restarting stalled and collapsed replication forks but whereas GC can be used to repair stalled forks, BIR is used to restart collapsed one-ended replication forks (reviewed in Allen *et al*, 2011; Haber, 1999; Lydeard *et al*, 2010; Michel, 2000). Interestingly, Cdt1 has been shown to be required for BIR in budding yeast, whereas Cdc6 (Cdc18) is not (Lydeard *et al*, 2010). Therefore it is possible that in the absence of both *exo1*$^{+}$ and *cdt1*$^{+}$ normal repair of stalled and collapsed forks may not occur. There have also been suggestions that NHEJ plays a minor role in the recovery of stalled forks (Allen *et al*, 2011), but use of this pathway could lead to large scale deletions. Perhaps in the *exo1*Δ*cdt1-19* mutant, recovery of stalled forks occurs by NHEJ resulting in increased cell death.

6.3.3 Slower DNA replication in *set2*Δ cells does not result in NHEJ deficiency

Given the choice between DSB repair pathways is cell cycle controlled, and *set2*Δ cells exhibit a delay in progression through S phase, further work sought to determine whether the NHEJ defect in *set2*Δ cells was due to changes in cell cycle distribution. However, results suggest that even when 30-40% of the *set2*Δ cell population is present in G1 phase, NHEJ is still impaired, indicative of a more direct role for Set2 in NHEJ repair.

One of the approaches to increase the G1 population of *set2*Δ cells was to make a *set2*Δ*wee1-50* double mutant. Interestingly, this mutant was synthetic lethal due to aberrant mitosis. Such synthetic lethality with Wee1 mutants is usually seen in checkpoint mutants. Treatment of *set2*Δ cells with HU suggested they do have a functional checkpoint. However, cell cycle arrest is not the only feature of an efficient checkpoint response. One important function of the S phase checkpoint is the stabilisation of stalled replication forks, so that cells can resume

replication once the replication stress is removed. Several proteins are required to prevent fork collapse upon HU arrest (Paulsen & Cimprich, 2007). In addition, careful control of recombination on checkpoint activation prevents inappropriate fork modification. Further, in budding yeast and human cells, inhibition of late firing origins in response to checkpoint activation slows replication (Duncker *et al*, 2002; Santocanale & Diffley, 1998; Syljuasen *et al*, 2005). Another key feature of the S phase checkpoint is the regulation of RNR; expression increases in response to DNA damage or replication defects (Elledge *et al*, 1993) through activation of checkpoint kinases which block RNR repression (de Bruin & Wittenberg, 2009). In fission yeast, this is achieved through inhibition of the MBF-associated transcriptional corepressors, Nrm1 and Yox1 in a Cds1-dependent manner (Caetano *et al*, 2011; de Bruin *et al*, 2008). Inhibition of Nrm1 and Yox1 allows subsequent accumulation of transcripts required for re-initiation of stalled forks and resumption of DNA replication. This group of transcripts includes *cdc22*$^{+}$, but also *cdt1*$^{+}$ and *cdc18*$^{+}$; this is striking given that in a *set2*Δ mutant the regulation of these genes is altered. Given the interaction with *wee1-50*, this suggests a possible role for Set2 in an efficient transcriptional checkpoint response.

Interestingly a study in fission yeast suggests a role for Set2 in the DNA damage checkpoint through interaction with Clr4 (Kim *et al*, 2008), in proper HU-induced up-regulation of *mik1*$^{+}$, a gene encoding a kinase which phosphorylates and inactivates Cdc2, resulting in cell cycle arrest (Boddy *et al*, 1998; Lindsay *et al*, 1998). However, in the Kim *et al* (2008) study, phenotypes including sensitivity to HU, reduced Cdc2 phosphorylation and reduced Mik1 levels were only significant in the *set2*Δ*clr4*Δ double mutant and not the *set2*Δ mutant alone. *set2*Δ cells were not sensitive to HU in this work (Chapter 4) and the microarray analysis in Chapter 5 showed no change in expression of *mik1*$^{+}$, consistent with the efficient cell cycle arrest seen in *set2*Δ cells in this chapter. Nonetheless, given that efficient transcription of

cdc22^{+}, *cdt1*$^{+}$ and *cdc18*$^{+}$ forms an important part of the checkpoint response, perturbation of this regulation in the *set2*Δ cells could explain the synthetic lethal interaction of *set2*Δ*wee1-50*.

The synthetic lethal interaction between Wee1 and checkpoint mutants is currently being exploited for the treatment of cancer; several combinations of Wee1 and checkpoint inhibitors are currently in clinical trial (Bridges *et al*, 2011; Davies *et al*, 2011; Leijen *et al*, 2010; Rajeshkumar *et al*, 2011). There are several instances in which defects in the genes that control H3K36 methylation in humans result in developmental defects and disease; SETD2 is a tumour suppressor in clear renal cell carcinoma and breast cancer (Duns *et al*, 2010; Newbold & Mokbel, 2010), and defects in NSD family members have been implicated in multiple diseases and cancer types (Bianco-Miotto *et al*, 2010; Hudlebusch *et al*, 2011; Kassambara *et al*, 2009; Marango *et al*, 2008; Rosati *et al*, 2002; Wang *et al*, 2007). Therefore the finding that *set2*Δ*wee1-50* is synthetic lethal is of significant interest and could be exploited to create novel approaches for treatment of Set2-related disease.

6.4 SUMMARY

To conclude, work in this chapter has shown:

- Set2 is required for efficient DNA replication.
- Cdt1 and Cdc18 are misregulated in a *set2*Δ mutant.
- The NHEJ defect in *set2*Δ cells is not due to aberrant DNA replication.

CHAPTER 7
A role for H3K36 modification is controlling DSB repair pathway choice

7.1 INTRODUCTION

In Chapter 6, Set2 was shown to be required for efficient DNA replication, as in the absence of *set2*$^{+}$, transcription of *cdt1*$^{+}$, *cdc18*$^{+}$ and *cdc22*$^{+}$ was low and there was delayed progression of S phase. Further investigation showed that biasing the cell cycle of *set2*Δ cells to have a greater G1 proportion did not rescue the NHEJ defect; therefore it is unlikely the role of Set2 in DSB repair is due to its cell cycle defect. Consequently, in this chapter, further analysis was undertaken to determine whether modification of H3K36 by Set2 is required for its role in NHEJ.

7.2 RESULTS

7.2.1 Set2 methyltransferase activity is required for its role in DSB repair and replication

Fission yeast Set2 comprises 798 amino acids of which amino acids 179-301 form the catalytic SET domain (Figure 7.1). Regions of the SET domain are highly conserved and in *S. cerevisiae*, the highly conserved arginine 195 and cysteine 201 have been shown essential for methyltransferase activity (Strahl *et al*, 2002). Homologous residues have also been shown to be important for the methyltransferase activity of SUV39H1 (Rea *et al*, 2000). To investigate whether the methyltransferase activity of Set2 is required for its role in DSB repair and replication, a mutation corresponding to *S. cerevisiae* arginine 195 to glycine was created (R255G in fission yeast; see Appendix VIII for strain construction details; Figure 7.1B and 7.2A).

Figure 7.1

A



B

MQTASSLSVLTPLNEENVDRKSSWSKDTIAVQAVGSSPSSSSSH
DFESKEDAEGMNKDESAPSPSTSSPSSASSRSQSKYVRKEALP
PQLFHHLDSAKDKALTTFEEIQECQYASANIGKPPENEAMICDCR
PHWVDGVNVACGHGSNCINRMTSIECTDEDNVCGPSCQNQRFQ
RHEFAKVDVFLTEKKGFGLRADANLPKDTFVYEYIGEVIPEQKFR
KRMRQYDSEGIKHFYFMMLQKGEYIDATKRGSLARFCNHSCRPN
CYVDKWMVGDKLRMGIFCKRDIIRGEELTFDYNVDRYGAQAQPC
YCGEPCCVGYIGGKTQTEAQSKLPENVREALGIEDEEDSWENIT
ARRQRRKKGIDETSKIIEEVQPTPLTSESATKVIGVLLQTKDDLLTR
KLMERIFLTSDPSVCRSIIALRGYNIFGLMLKKFSIDIEFILRSIKTML
SWPRLTRNKIQDSNIEPVVQEFCDHENEEVKDHAKTLLKEWESL
EIAYRIPRRKPGQVAPQSTNAEPSNNQSNPPLRDQEPQRGDKGD
IKSAINNSTEDLSKKHPALHSSRPSDSRSRSKFGNDYQSHSKHNL
FRKNSFPKRRRLSNSDTPSETTTPNNEQEQVSNQANKVDLNKIIS
AAMESVNQKNVLKAQKEEEERIAQQKREEKRRLAYEESLKRHAK
KLHEKKTKSSQDATIDHHLTSHSPESIAFKAVLAKFFANKTARYQE
KLGKAEFKLRVKKMTEIILKKHIQLVLSKKEKALPDELSDSQQR
KLRVWAFRYLDTVVSRSGTATTTPTDSPSIGESPKKAA

Figure 7.1 Set2 structure in *S. pombe* **(A)** Schematic of Set2 structure. Red pentagon = associated with SET (AWS) domain, blue circle = SET domain, green triangle = post-SET domain and purple diamond = coiled coil domain. Adapted from Morris *et al*., 2005. **(B)** Amino acid sequence of Set2. Blue letters indicate SET domain. Red letter indicates arginine residue mutated in SET domain in *set2-R255G* mutant.

To address whether this residue is required for the methyltransferase activity of Set2 in fission yeast, western blot analysis of H3K36me3 levels in nuclear extracts of wildtype, *set2*Δ and *set2-R255G* cells was performed. As expected, in the *set2*Δ cells, there is no H3K36me3, as Set2 is essential for methylation of this residue. In the *set2-R255G* mutant, there is a very low level of H3K36me3, indicating that this residue is required for optimal H3K36 methylation (Figure 7.2B). To determine whether this mutation has any impact on DSB repair, the viability of the *set2-R255G* cells in response to bleomycin was addressed using a serial dilution assay. The *set2-R255G* cells were as resistant to bleomycin as wildtype, to a similar degree to that seen in the *set2*Δ cells (Figure 7.2C). Further analysis of DSB repair in this mutant background was undertaken using the DSB assay and NHEJ plasmid-rejoining assay. Similarly to the *set2*Δ cells, *set2-R255G* cells showed a significant increase in the levels of GC (70%, $p<0.01$) associated with a significant decrease in LOH (5%, $p<0.01$; Figure 7.2D). In addition, the plasmid-rejoining assay indicated that like *set2*Δ cells, a *set2-R255G* mutant has an impaired ability to repair by NHEJ (Figure 7.2E). Collectively, these data suggest that the methyltransferase activity of Set2 is required for its role in DSB repair by NHEJ.

To determine if loss of the methyltransferase activity also leads to a negative genetic interaction with HR factors, double mutants of *set2-R255G* with *exo1*Δ, *rad32*Δ, *rad50*Δ and *nbs1*Δ were generated and their viability in response to bleomycin analysed. Unlike the *set2*Δ*exo1*Δ mutant, the *set2-R255Gexo1*Δ double mutant did not show sensitivity to bleomycin compared to the single mutants (Figure 7.3A). Similar to deletion of $ku70^{+}$, the *set2-R255G* mutant actually suppressed the sensitivity of *exo1*Δ cells to bleomycin. Likewise, the *set2-R255Grad32*Δ, *set2-R255Grad50*Δ and *set2-R255Gnbs1*Δ did not show an increased sensitivity compared to the single mutants (Figure 7.3A). This data indicates that although arginine 255 is required for the role of Set2 in NHEJ, loss of it does not lead to

Figure 7.2

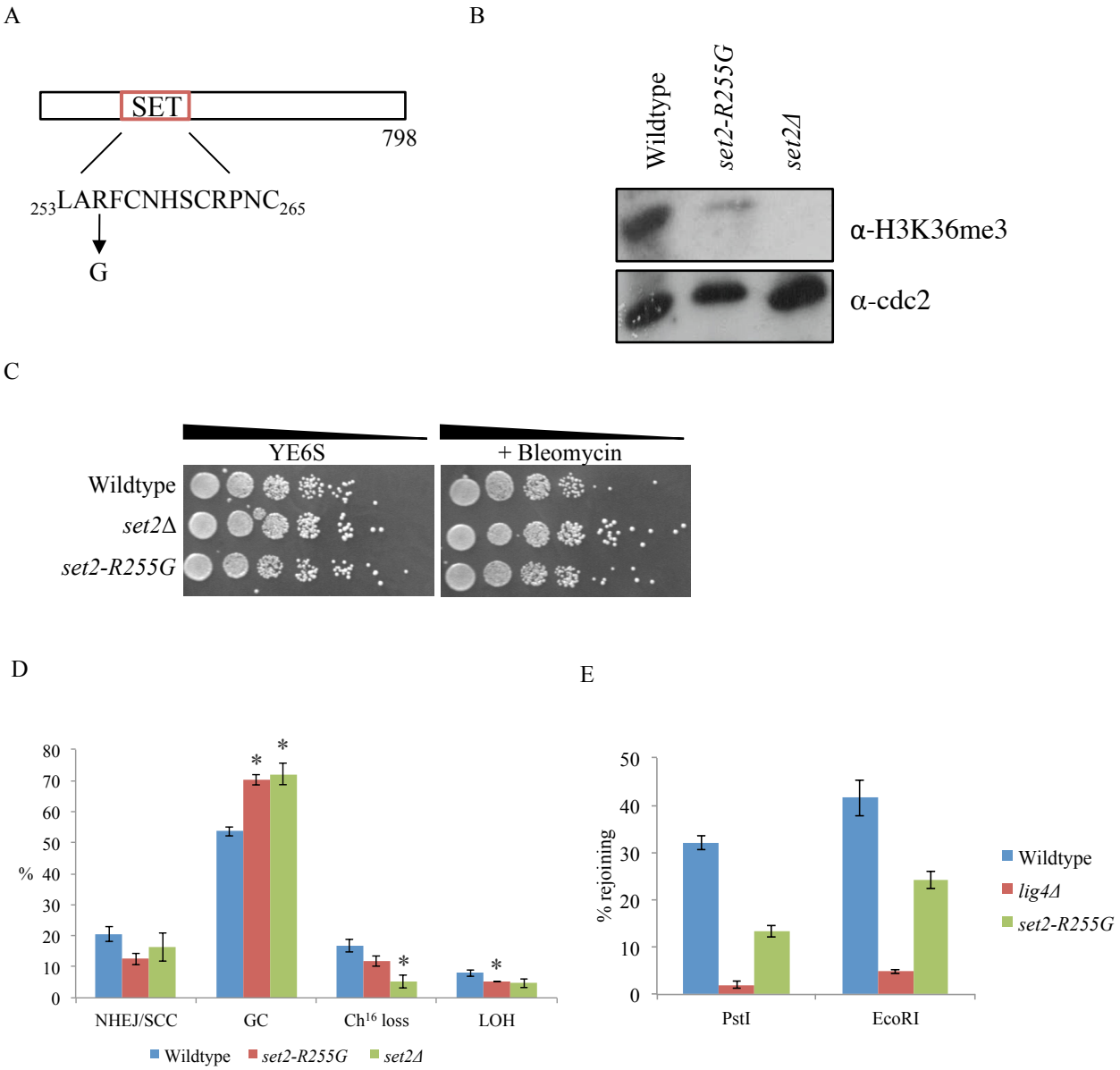


Figure 7.2 Set2 methyltransferase activity is required for its role in DSB repair (A) Schematic of *set2-R255G* mutant. **(B)** Western blot analysis of H3K36me3 levels in wildtype (2094), *set2*Δ (3271) and *set2-R255G* (6367) cells. **(C)** 5-fold serial dilutions of wildtype (2094), *set2*Δ (3271) and *set2-R255G* (6367) cells were grown on YE6S and YE6S + 1 µg/ml bleomycin. **(D)** Percentage DSB-induced marker loss in wildtype (2131), *set2*Δ (3841-3), and *set2-R255G* (6397, 6415-7) containing Ch^{16}-RMGAH. The levels of NHEJ/SCC, GC, Ch^{16} loss and LOH are shown. Data are the mean of three experiments and error bars (± SE) are shown. * indicates statistical significance. **(E)** Outcome of NHEJ plasmid-rejoining assay for wildtype (2094), *lig4*Δ (1069) and *set2-R255G* (6367) strains. Data are the mean of three experiments and error bars (± SE) are shown.

exquisite sensitivity to bleomycin in combination with HR mutants, suggesting loss of an alternate Set2 function is responsible for the sensitivity to bleomycin seen.

To address if methylation was required for DNA replication, the cell cycle profile of *set2-R255G* cells following nitrogen starvation and refeeding was analysed. Compared to wildtype, the *set2-R255G* cells showed a delay in progression to a 2C peak; a similar profile to that seen in *set2*Δ cells (Figure 7.3B). This indicates that the methyltransferase activity of Set2 is also required for efficient DNA replication.

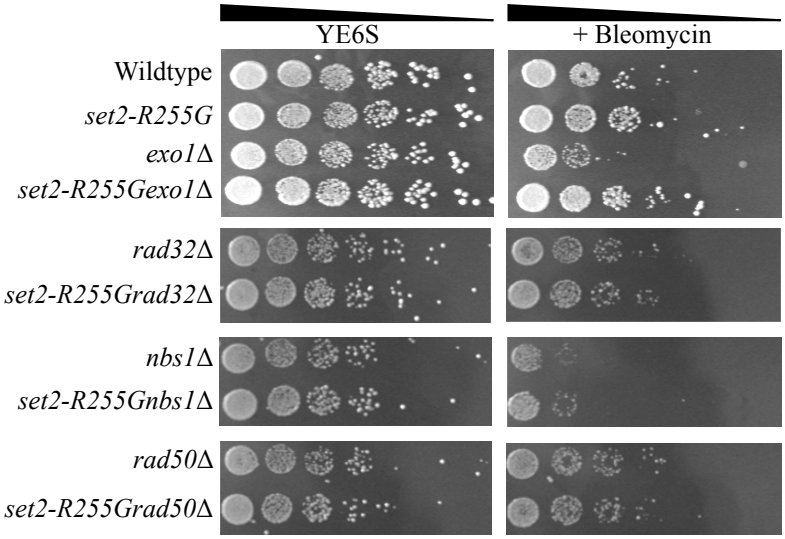
7.2.2 Lysine 36 of histone H3 is essential for survival following a DSB

If methylation of H3K36 by Set2 is required for efficient DSB repair by NHEJ, a *H3K36R* mutant would be expected to show a similar phenotype to *set2*Δ cells. Due to the essential nature of histones, there are three copies of H3 in *S. pombe* (*h3.1*, *h.3.2* and *h3.3*); in the *H3K36R* mutant, two copies are deleted and one mutated. The nature of these deletions means that the cells' viability is poor, and therefore cells in which two copies of H3 are deleted were used as a control.

To address the viability of the *H3K36R* mutant in response to DSB-inducing agents, an IR survival curve was completed. Compared to the H3 double delete (*H3ΔΔ),* the *H3K36R* mutant was very sensitive to doses of IR as low as 100 Gy and remained more sensitive up to 1000 Gy (Figure 7.4A). The viability of the *H3K36R* mutant in response to bleomycin was also addressed using a serial dilution assay. This confirmed the exquisite sensitivity of the *H3K36R* point mutant compared to both wildtype and the H3 double delete (Figure 7.4B); in fact, the sensitivity of the *H3K36R* mutant is equivalent to that of *rhp51*Δ (Figure 7.4B). This striking sensitivity of *H3K36R* cells compared to *set2*Δ cells indicates that there is likely to be another function of H3K36 in DSB repair.

Figure 7.3

A



B

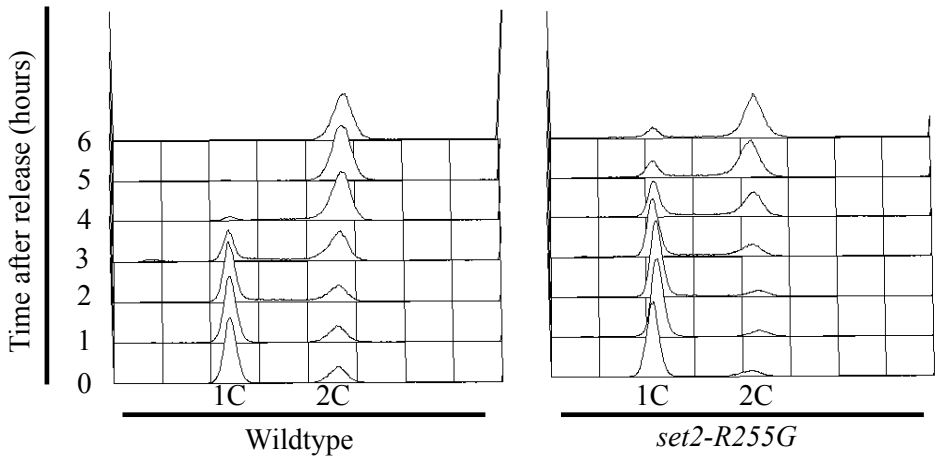
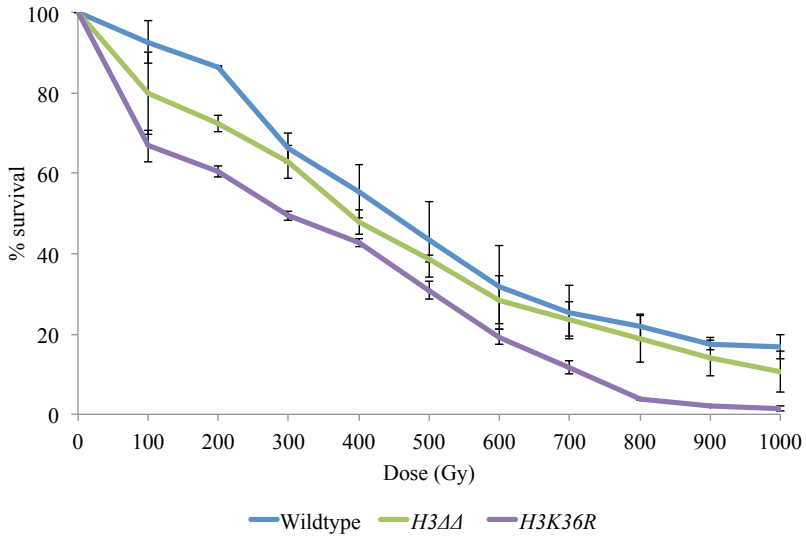


Figure 7.3 Set2 methyltransferase activity is required for its role in DNA replication (A) 5-fold serial dilutions of wildtype (2094), *set2-R255G* (6367), *exo1*Δ (5310), *set2-R255Gexo1*Δ (6835), *rad32*Δ (5346), *set2-R255Grad32*Δ (6842), *nbs1*Δ (5231), *set2-R255Gnbs1*Δ (6843), *rad50*Δ (5347) and *set2-R255Grad50*Δ (6841) cells were grown on YE6S and YE6S + 1 μg/ml bleomycin (top panel) or 0.3 μg/ml bleomycin (bottom panels). **(B)** Flow cytometry analysis of wildtype (6877) and *set2-R255G* (7131) cells following release from nitrogen starvation.

Figure 7.4

A



B

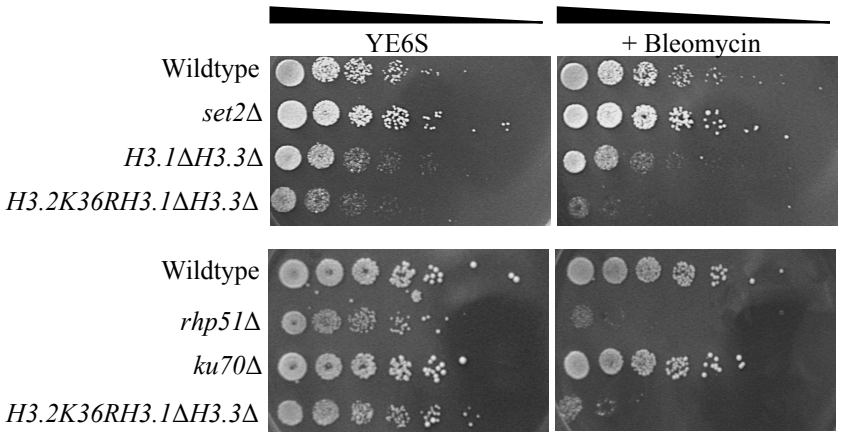


Figure 7.4 Lysine 36 of histone H3 is essential for survival following a DSB (A) Ionising-radiation survival curve for wildtype (2094), *H3.1ΔH3.3Δ* (*H3ΔΔ*; 6238) and *H3.2K36RH3.1ΔH3.3Δ* (*H3K36R*; 6241) cells. Data are the mean of three experiments and error bars (± SE) are shown. Irradiations performed by Carol Walker. **(B)** 5-fold serial dilutions of wildtype (2094), *set2Δ* (3271), *H3.1ΔH3.3Δ* (6238), *H3.2K36RH3.1ΔH3.3Δ* (6241), *rhp51Δ* (3992) and *ku70Δ* (5593) cells were grown on YE6S and YE6S + 1 µg/ml bleomycin.

7.2.3 Gcn5 is required for repair of a DSB by HR

In addition to modification by methylation, H3K36 can also be acetylated; in budding yeast, Gcn5 is postulated to be the HAT (Morris *et al*, 2007). In Chapter 3, initial characterisation of a *gcn5*$^{+}$ deletion mutant was performed. Strikingly, analysis by the DSB assay showed *gcn5*Δ cells exhibit a significant decrease in GC (45%, $p<0.01$), associated with a significant increase in NHEJ/SCC (33%, $p<0.01$) and a slight, but significant decrease in LOH (6%, $p=0.04$; Figure 7.5A). Further analysis by the plasmid-rejoining assay showed that *gcn5*Δ cells are proficient at NHEJ (Figure 7.5B). This phenotype is striking in that it is the converse of *set2*Δ cells.

Checkpoint mutants often exhibit significantly reduced GC and significantly increased Ch^{16} loss and LOH (Tinline-Purvis, unpublished data), a repair profile similar to that of *gcn5*Δ cells. Therefore, the checkpoint response of *gcn5*Δ cells was investigated by analysing cell length in response to treatment with HU. Following six hours treatment with HU, the *gcn5*Δ cells exhibited an elongated phenotype similar to wildtype, indicating a proficient G2/M checkpoint (Figure 7.5C).

7.2.4 *gcn5*Δ cells display aberrant Rhp51 foci kinetics

Following detection of a DSB and 5'-3' resection, Rhp51 binds to ssDNA forming a nucleofilament which is required for subsequent homology search, strand invasion and D-loop formation. The presence of Rhp51 at a break site can be visualised as distinct foci within the nucleus, when Rhp51 is fluorescently tagged. To investigate whether Gcn5 acts pre- or post-synaptically during HR, the kinetics of Rhp51-CFP foci were analysed in *gcn5*Δ cells following treatment with IR.

Figure 7.5

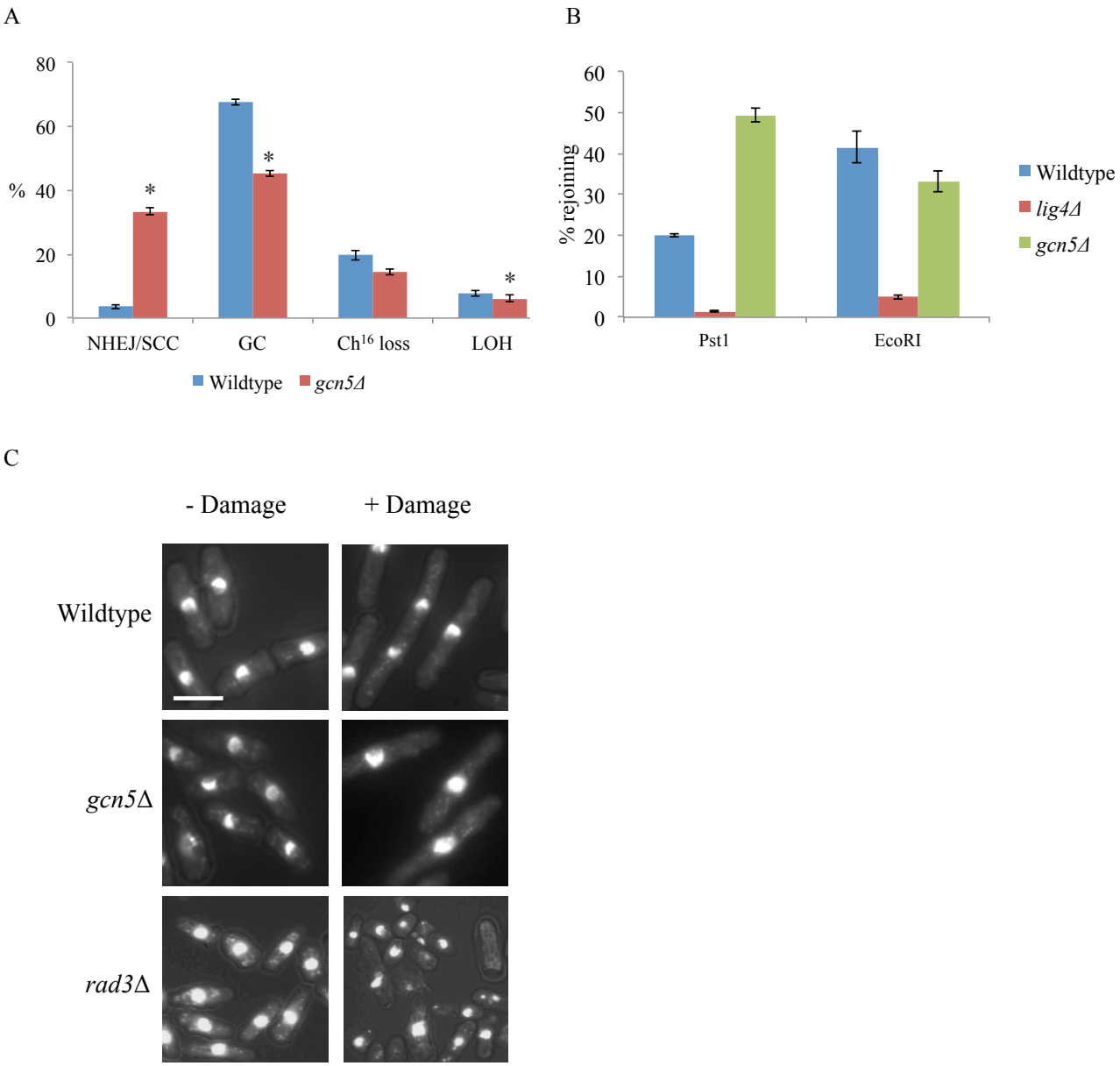


Figure 7.5 Gcn5 is required for repair of a DSB by homologous recombination (A) Percentage DSB-induced marker loss in wildtype (4104), and *gcn5*Δ (3864, 6338-9) cells containing Ch^{16}-RMYAH. The levels of NHEJ/SCC, GC, Ch^{16} loss and LOH are shown. Data are the mean of three experiments and error bars (± SE) are shown. * indicates statistical significance. **(B)** Outcome of NHEJ plasmid-rejoining assay for wildtype (2094), *lig4*Δ (1069) and *gcn5*Δ (3718) cells. Data are the mean of three experiments and error bars (± SE) are shown. **(C)** Images of DAPI stained wildtype (2094), *rad3*Δ (2799) and *gcn5*Δ (3718) cells are shown. Cells were imaged before (-Damage) and 6 hours following treatment with 10 mM HU (+Damage). Scale bar, 10 µm.

Cells in which *gcn5*$^{+}$ is deleted exhibited a striking reduced level of Rhp51-CFP foci immediately following treatment with IR, compared to wildtype (Figure 7.6), indicating there is reduced recruitment of Rhp51 to ssDNA. The percentage of cells containing Rhp51-CFP foci began to decline in the *gcn5*Δ cells following the initial peak at 30 minutes, as observed in wildtype. However, following this initial decline, the percentage of cells containing Rhp51-CFP foci increased again at 120 minutes following damage. It is possible that misrepair of the initial damage results in repair intermediates that require subsequent Rhp51 recruitment. Following this second peak, the percentage of cells containing Rhp51-CFP foci were restored to background levels with similar kinetics to wildtype (Figure 7.6). This data suggests that *gcn5*Δ cells, although still able to recruit Rhp51, do so much less effectively than wildtype cells, indicating a presynaptic role for Gcn5. To further address a possible presynaptic role for Gcn5, it would be interesting to determine whether the recruitment of upstream HR factors, such as the RPA subunit Rad11, is affected in the *gcn5*Δ cells. It is possible that in cells lacking Gcn5, resection is impaired, and thus subsequent Rhp51 nucleofilament formation is decreased, resulting in the reduced Rhp51-CFP foci seen.

7.2.5 NHEJ is increased in *gcn5*Δ cells

Although the plasmid-rejoining assay showed that NHEJ was proficient in *gcn5*Δ cells, and higher than wildtype in substrates containing a 3' overhang, using the DSB assay, the proportion of NHEJ cannot be accurately discerned, as repair by SCC, or failure to induce the break also results in the same marker retention (see Figure 1.4). Therefore, to address whether the high proportion of NHEJ/SCC in the *gcn5*Δ mutant is due to NHEJ or SCC, a *gcn5*Δ*lig4*Δ mutant, in which NHEJ is abolished, was generated and its repair ability assessed using the DSB assay. In the *gcn5*Δ*lig4*Δ mutant, NHEJ/SCC was significantly increased (23%, $p<0.01$) compared to wildtype (Figure 7.7). This was associated with a significant decrease in GC (56%, $p=0.02$) and LOH (6%, $p=0.03$) compared to wildtype. To determine if NHEJ is

Figure 7.6

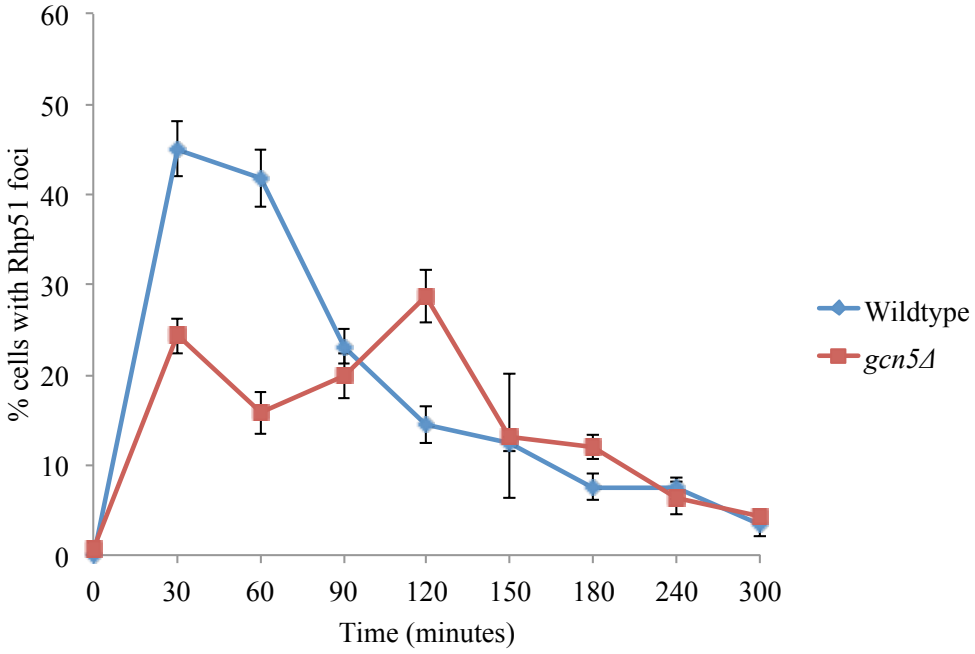


Figure 7.6 *gcn5*Δ cells display aberrant Rhp51-CFP foci Quantification of Rhp51-CFP foci in wildtype (blue; 3608) and *gcn5*Δ (red; 7289) cells at the times indicated (minutes) following exposure to 50 Gy IR.

significantly increased in the *gcn5*Δ mutant, the DSB results from the *gcn5*Δ and *gcn5*Δ*lig4*Δ cells were compared (Table 7.1; Figure 7.7).

Table 7.1 Comparison of *gcn5*Δ and *gcn5*Δ*lig4*Δ DSB results. To determine NHEJ level in *gcn5*Δ cells the difference in NHEJ/SCC between *gcn5*Δ and *gcn5*Δ*lig4*Δ cells was compared to the wildtype level. The p value represents the difference between wildtype and the actual NHEJ levels in *gcn5*Δ cells. Data are the mean of three experiments.

	***gcn5*Δ**	***gcn5*Δ*lig4*Δ**	**Difference**	**Wildtype**	**p value**
NHEJ/SCC	33%	23%	-10%	4%	<0.01
GC	45%	56%	+11%	67%	-

There is a 10% decrease in NHEJ/SCC between *gcn5*Δ and *gcn5*Δ*lig4*Δ which represents the level of NHEJ in the *gcn5*Δ mutant (Table 7.1; Figure 7.7). This level is significantly greater than the NHEJ/SCC level in wildtype cells ($p<0.01$). Thus, even if wildtype NHEJ/SCC comprised entirely NHEJ, this would represent a significant increase in NHEJ in the *gcn5*Δ mutant. The proportion no longer repairing by NHEJ in the *gcn5*Δ*lig4*Δ mutant repair instead by GC, reflecting the 11% increase in GC compared to *gcn5*Δ cells (Table 7.1; Figure 7.7).

7.2.6 *set2*Δ*gcn5*Δ cells exhibit wildtype DSB repair

Given Set2 and Gcn5 both modify H3K36, and mutation of these genes confer opposing phenotypes, it is plausible that alternate modification of this residue could be directing the repair mechanism utilised in response to a DSB. To address this, a *set2*Δ*gcn5*Δ mutant was generated and its viability in response to bleomycin and its repair profile in the DSB assay analysed. If Set2 is required for NHEJ and Gcn5 is required for HR, one might hypothesise that a double mutant may be inefficient at both NHEJ and HR and thus extremely sensitive to DSB inducing agents such as bleomycin. The *set2*Δ*gcn5*Δ mutant was slightly more sensitive to bleomycin than the single mutants alone, consistent with Set2 and Gcn5 functioning in different pathways (Figure 7.8A). However, the sensitivity was not as striking as one would expect if repair by both NHEJ and HR was abrogated. In fact, analysis of the *set2*Δ*gcn5*Δ

Figure 7.7

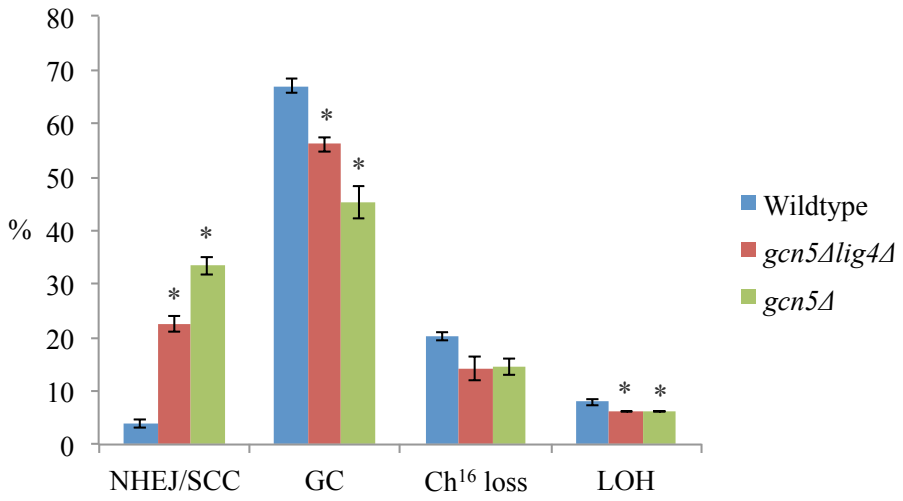


Figure 7.7 DSB repair by *gcn5*Δ*lig4*Δ cells
Percentage DSB-induced marker loss in wildtype (4104), *gcn5*Δ (3864, 6338-9) and *gcn5*Δ*lig4*Δ (6973-6) cells containing Ch[16]-RMYAH. The levels of NHEJ/SCC, GC, Ch[16] loss and LOH are shown. Data are the mean of three experiments and error bars (± SE) are shown. * indicates statistical significance.

mutant using the DSB assay showed that GC levels were similar to wildtype cells (71%, p=0.65; Figure 7.8B). Compared to wildtype, the levels of NHEJ/SCC in the *set2*Δ*gcn5*Δ mutant were still increased (21%, p<0.01). However, compared to *gcn5*Δ, there was a 12% decrease, similar to the decrease seen in the *gcn5*Δ*lig4*Δ mutant, which suggests deletion of *set2*$^{+}$ is equivalent to deletion of *lig4*$^{+}$ in reducing NHEJ levels. In addition, both Ch^{16} loss and LOH are significantly decreased in the *set2*Δ*gcn5*Δ mutant compared to wildtype (5% Ch^{16} loss, p=0.01; 2% LOH, p<0.01). This indicates that in the absence of Set2, Gcn5 is no longer required for efficient repair by HR.

Interestingly the *gcn5*Δ*set2*Δ cells exhibited a similar repair phenotype to the *gcn5*Δ*lig4*Δ cells with approximately 20% NHEJ/SCC that presumably corresponds to SCC levels. Given this is not seen in the *set2*Δ or *set2*Δ*lig4*Δ cells these results suggest that deletion of *gcn5*$^{+}$, in addition to increasing NHEJ levels, also increases the proportion of SCC. Perhaps more compact chromatin in the *gcn5*Δ mutant leads to preferential repair by SCC, as there may be reduced resection, leading to the sister chromatid rather than the homologous chromosome being utilised. On the other hand, it is possible that in the absence of *gcn5*$^{+}$ there could be decreased expression of HO, resulting in cutting of only one of the sister chromatids, and thus favouring repair by SCC.

7.2.7 Overexpression of *gcn5* results in increased repair by GC

If differential modification of H3K36 by Set2 and Gcn5 results in different DSB repair pathways being utilised, then altering the levels of Gcn5 or Set2 may alter the DSB repair profile. For example, if methylation of H3K36 by Set2 is required for NHEJ, overexpression of *set2* may result in high NHEJ and low HR. Equally, if acetylation by Gcn5 is required for HR, then overexpression of *gcn5* may result in high HR and low NHEJ. To address this, REP3X overexpression vectors were created (see Appendix I) and transformed into minichromosome containing strains for analysis by the DSB assay. The REP3X

Figure 7.8

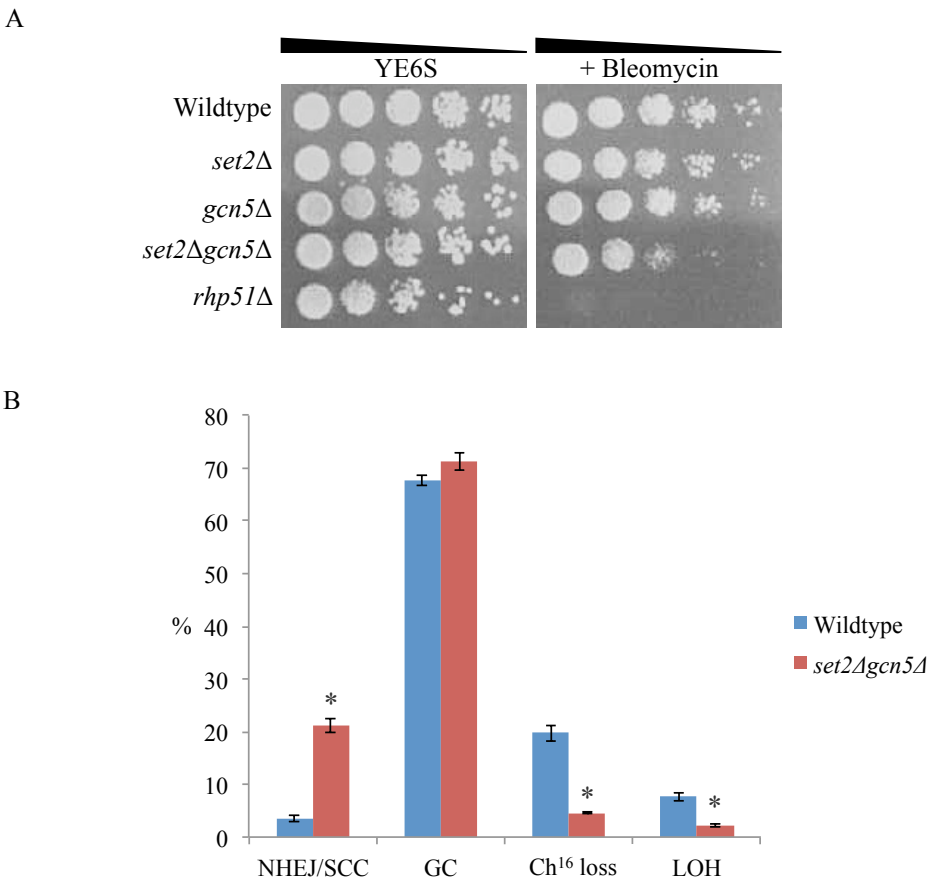


Figure 7.8 *set2*Δ*gcn5*Δ cells exhibit wildtype repair (A) 5-fold serial dilutions of wildtype (2094), *set2*Δ (3271), *gcn5*Δ (3718), *set2*Δ*gcn5*Δ (6318) and *rhp51*Δ (3992) cells were grown on YE6S and YE6S +1 µg/ml bleomycin. **(B)** Percentage DSB-induced marker loss in wildtype (4104) and *set2*Δ*gcn5*Δ (6545-7) cells containing Ch^{16}-RMYAH. The levels of NHEJ/SCC, GC, Ch^{16} loss and LOH are shown. Data are the mean of three experiments and error bars (± SE) are shown. * indicates statistical significance.

overexpression vectors contained a LEU2 marker, and so a plasmid containing REP81X-HO-URA4 instead of LEU2 was used for break induction.

When *gcn5* was overexpressed in a *gcn5*Δ background, a striking phenotype of significantly increased GC (92%, $p<0.01$) and decreased NHEJ/SCC (4%, $p<0.01$), Ch^{16} loss (2%, $p<0.01$) and LOH (0%, $p<0.01$) was observed (Figure 7.9). This is a similar profile to *set2*Δ cells, and is consistent with the hypothesis that acetylation by Gcn5 promotes HR.

A *set2* REP3X overexpression vector was also created and the DSB assay attempted in a wildtype background containing this vector. Five different isolates were analysed; unfortunately the repair profile varied between isolates, and when the experiment was repeated, the results were again varied, with the individual isolates behaving differently on each occasion. In four repeats, the marker loss indicated a repair profile similar to *set2*Δ cells; in three repeats a wildtype repair profile was observed; in the remaining three repeats a repair profile similar to *gcn5*Δ was observed. If the hypothesis that methylation leads to increase NHEJ is correct, overexpression of *set2* should result in increased NHEJ (a *gcn5*Δ phenotype), which was observed on three repeats. Differential expression could explain observation of wildtype and a *gcn5*Δ cell phenotype. However, this cannot account for a *set2*Δ cell phenotype seen in a number of the repeats. Given these varied and unrepeatable outcomes, unfortunately no conclusions could be drawn. It is possible that integration of the overexpression cassette may result in a more uniform expression of *set2*, and this may give more consistent results.

Figure 7.9

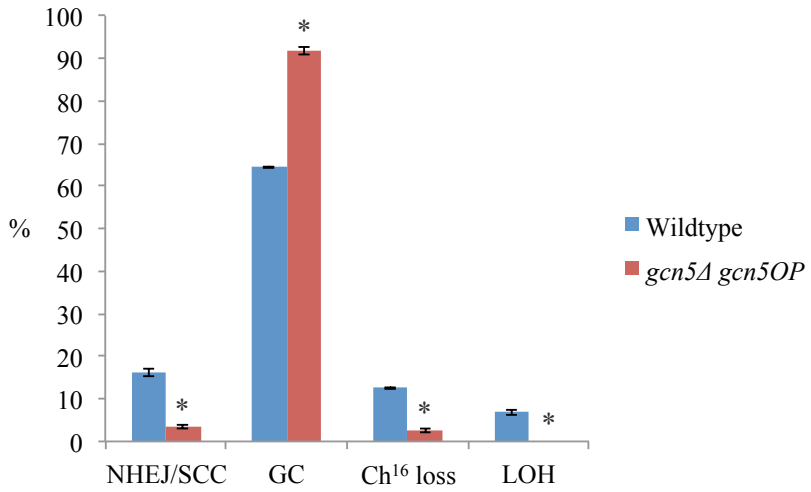


Figure 7.9 *gcn5* overexpression results in high levels of DSB repair by homologous recombination Percentage DSB-induced marker loss in wildtype (6815) and *gcn5*Δ (6799, 6802, 6817-8) cells containing Ch^{16}-RMYAH. In the *gcn5*Δ cells *gcn5* is overexpressed using a REP3X promoter (p255). The levels of NHEJ/SCC, GC, Ch^{16} loss and LOH are shown. Data are the mean of three experiments and error bars (± SE) are shown. * indicates statistical significance.

7.2.8 Methylation and acetylation of H3K36 are mutually inhibitory

Given that acetylation and methylation are mutually exclusive on any given H3K36 residue, a prediction might be that in the absence of one modification the other may increase, as there will be more available substrate. Therefore, the levels of acetylation and methylation in wildtype, *set2*Δ and *gcn5*Δ cells was analysed by western blot. As expected, in the *set2*Δ nuclear extract there was no H3K36me3, consistent with Set2 being essential for H3K36 methylation (Figure 7.10A). Strikingly, in the *gcn5*Δ nuclear extract, the level of H3K36me3 was much higher than in wildtype (Figure 7.10A). This is consistent with the hypothesis that in the absence of one type of modification, there may be an increase in the other, and suggests that acetylation of H3K36 may be inhibitory to methylation.

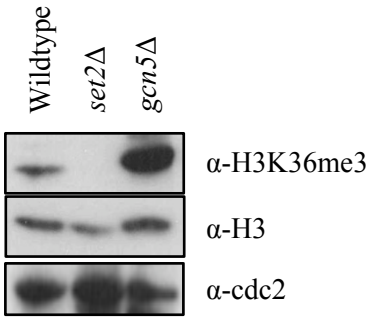
In the *gcn5*Δ nuclear extract, there was no H3K36ac, as expected if Gcn5 is the HAT as in budding yeast (Figure 7.10B; Morris *et al*, 2007). In the absence of Set2, the levels of H3K36ac were increased compared to wildtype cells (Figure 7.10B), although it is not as striking as the increase in methylation in the *gcn5*Δ mutant. These data correspond with the hypothesis that in the absence of one modification, there will be an increase in the other, and suggests that acetylation and methylation of H3K36 are mutually inhibitory. This likely reflects availability of substrate given that these modifications are mutually exclusive on any given H3K36 residue.

7.2.9 Methylation and acetylation of H3K36 occur in a cell cycle dependent manner

Given the cell cycle defect of *set2*Δ cells, and the cell cycle specific utilisation of DSB repair mechanisms, the levels of acetylation and methylation of H3K36 in different stages of the cell cycle was addressed. To do this, cells were nitrogen starved and released as in previous experiments and samples taken for nuclear extraction when the population has a 1C DNA content (t=0) and on progression to S phase (t=3; Figure 7.11C shows cell cycle analysis of cells upon release from nitrogen starvation). When the cells had an entirely 1C DNA content,

Figure 7.10

A



B

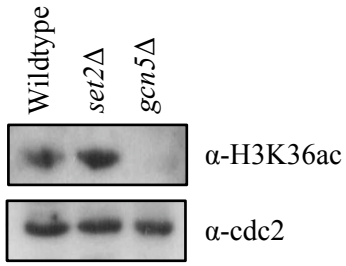


Figure 7.10 Methylation and acetylation of H3K36 are mutually inhibitory (A) Western blot analysis of H3K36me3 in wildtype (2094), *set2*Δ (3271) and *gcn5*Δ (3718) nuclear extract. **(B)** Western blot analysis of H3K36ac in wildtype, *set2*Δ and *gcn5*Δ nuclear extract.

Figure 7.11

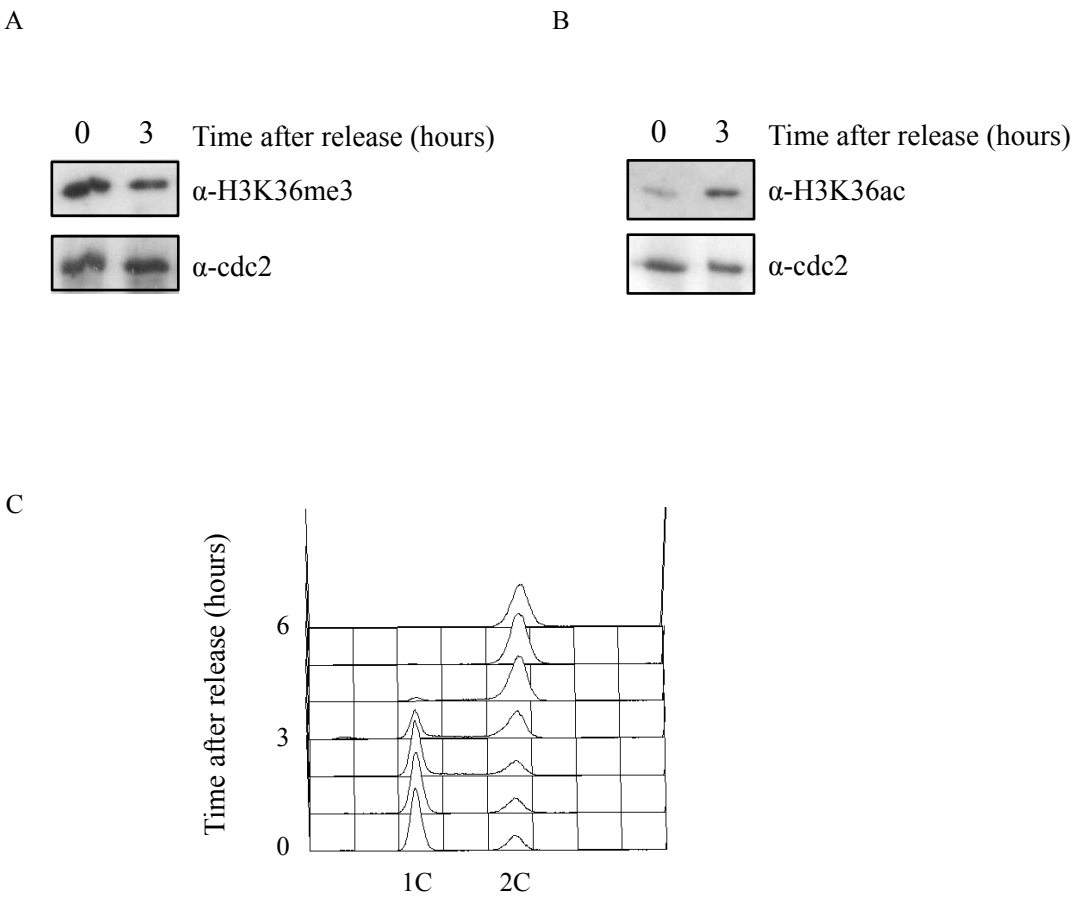


Figure 7.11 Methylation and acetylation of H3K36 change in a cell cycle dependent manner **(A)** Western blot analysis of H3K36me3 in wildtype (2094) nuclear extract at the times shown following release from nitrogen starvation. **(B)** Western blot analysis of H3K36ac in wildtype nuclear extract following release from nitrogen starvation. **(C)** Flow cytometry analysis of wildtype cells following release from nitrogen starvation.

the H3K36me3 levels were high and the H3K36ac levels were fairly low (Figure 7.11A and B). However, three hours following re-feeding when cells are progressing through S phase, H3K36me3 appeared lower (Figure 7.11A) and the H3K36ac levels increased (Figure 7.11B). This result indicates that modification of this residue may be cell cycle controlled. The peak of methylation in a 1C population and acetylation in S phase is consistent with methylation being required for NHEJ, which is the predominant repair mechanism in G1, and acetylation being required for HR, which is the predominant repair mechanism in S/G2.

7.2.10 *gcn5*Δ cells exhibit a slight cell cycle delay

Given the cell cycle distribution of H3K36 methylation and acetylation and the S phase defect in *set2*Δ cells, the cell cycle in *gcn5*Δ cells was analysed following nitrogen starvation and re-feeding. *gcn5*Δ cells showed a slightly slowed progression through S phase, compared to wildtype (Figure 7.12). However, it is not as striking as seen in the *set2*Δ cells, which did not show a complete 2C peak even 6 hours following re-feeding (Figure 6.3A).

7.2.11 Global methylation and acetylation of H3K36 are unchanged following DNA damage

If methylation and acetylation are required for DSB repair, a change in the global levels of these modifications may be expected in response to DNA damage. To investigate this, wildtype cells were treated with bleomycin and samples for nuclear extraction taken before treatment and at 15, 30, 45 and 60 minutes after treatment. There was no obvious global increase in methylation or acetylation of H3K36 in response to bleomycin treatment (Figure 7.13). However, it may be that any changes are directly at the site of the damage. In addition, given the levels of methylation and acetylation are already high in the cell, any small change may not be observed by western blot.

Figure 7.12

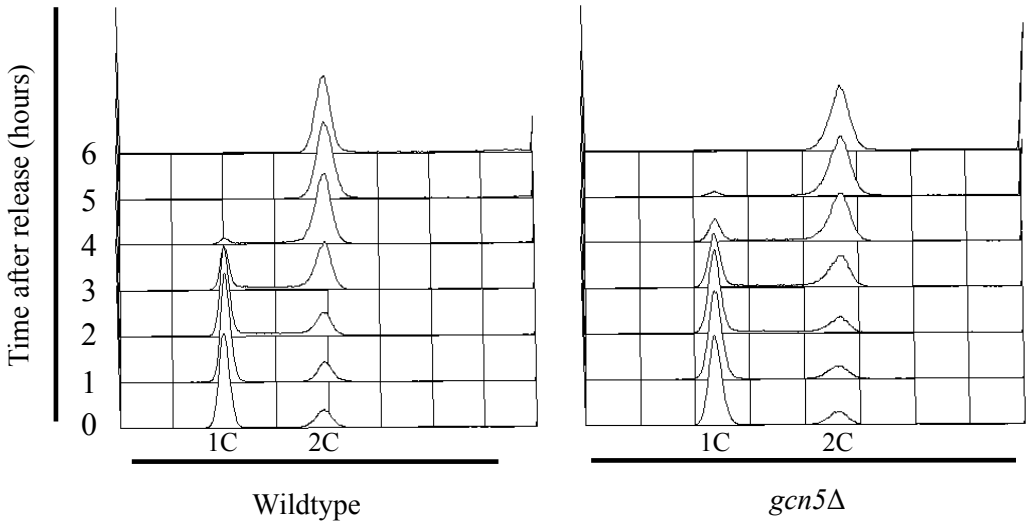
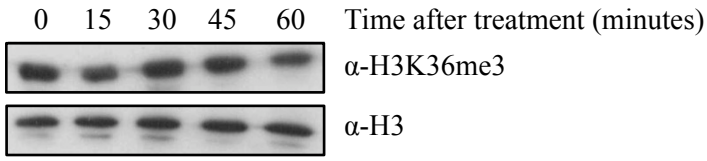


Figure 7.12 *gcn5*Δ cells show slight S phase delay Flow cytometry analysis of wildtype (6877) and *gcn5*Δ (7042) cells following release from nitrogen starvation.

Figure 7.13

A



B

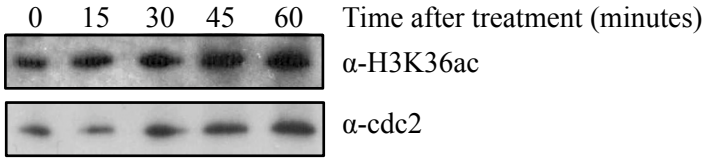


Figure 7.13 Global methylation and acetylation of H3K36 are unchanged following DNA damage (A) Western blot analysis of H3K36me3 levels in wildtype (2094) nuclear extract following treatment with 5 μg/ml bleomycin at the times shown (minutes). **(B)** Western blot analysis of H3K36ac levels in wildtype nuclear extract following treatment with 5 μg/ml bleomycin at the times shown (minutes).

7.2.12 Gcn5 levels increase following treatment with bleomycin

Given the apparent role of Set2 and Gcn5 in efficient DSB repair, they may have a role directly at the break site. To investigate this, GFP-tagged versions of Set2 and Gcn5 were obtained (Hayashi *et al*, 2009) and their subcellular localisation before and after DNA damage was assessed. GFP-tagged Rad22 was used as a positive control, with which distinct foci were observed following treatment with bleomycin (Figure 7.14A). Gcn5 did not form foci following treatment with bleomycin; however, there did appear to be an increased level of Gcn5, compared to the untreated cells, particularly 120 minutes following treatment (Figure 7.14B). This is in keeping with data in *S. cerevisiae*, which showed recruitment of Gcn5 to a DSB two hours following break induction (Tamburini & Tyler, 2005). This is not due to an increase in transcription as the microarray undertaken in Chapter 5 showed no increase in *gcn5*$^{+}$ transcript levels following treatment with bleomycin in wildtype cells. Visualising GFP-tagged Gcn5 may not be a sensitive enough technique to visualise foci, as the presence at the break site may be too transient, or the background level of Gcn5 too high to observe specific foci.

There were no Set2-GFP foci observed at any time point following bleomycin treatment; nor was there any obvious increase in the levels of Set2 (Figure 7.14C). However, as stated above, this does not necessarily rule out a role for Set2 at the break site. A more sensitive method, such as chromatin immunoprecipitation (ChIP) could be used to determine whether Set2 and Gcn5 are recruited to the break, and if methylation and acetylation are enriched at these locations. Attempts were made to perform this analysis by ChIP, but were unfortunately unsuccessful.

7.3 DISCUSSION

Work in previous chapters has shown a role for Set2 in maintaining efficient NHEJ, and that this is not dependent on altered transcription or altered progression through S phase. Further

Figure 7.14

A

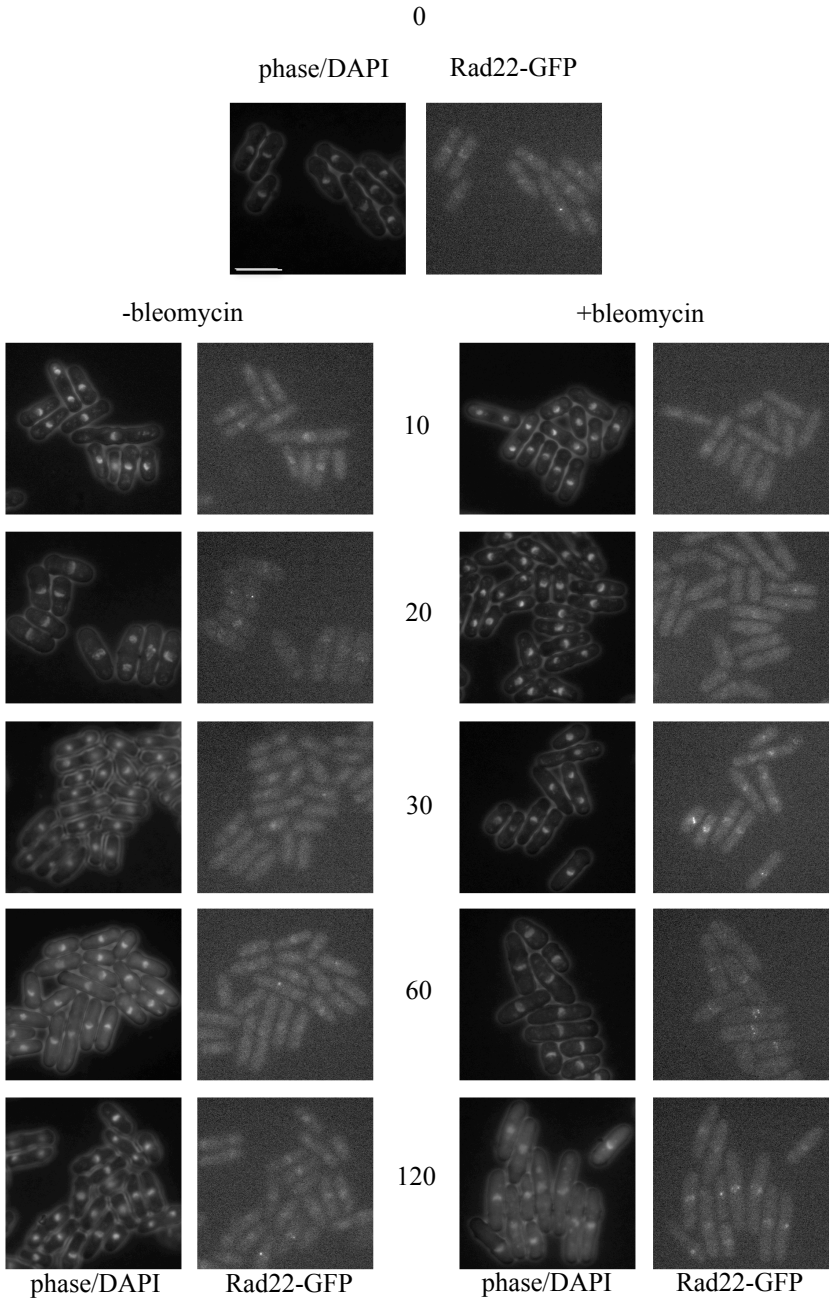


Figure 7.14 Gcn5 is enriched following DNA damage Representative images of methanol fixed samples of asynchronous Rad22-GFP (2148) **(A)**, Gcn5-GFP (7140) **(B)** or Set2-GFP (4823) **(C)** wildtype cells imaged at time indicated (minutes) following exposure to 5 μg/ml bleomycin. Merged phase and DAPI images are shown in addition to GFP images. Scale bar, 10 μm.

Figure 7.14 continued

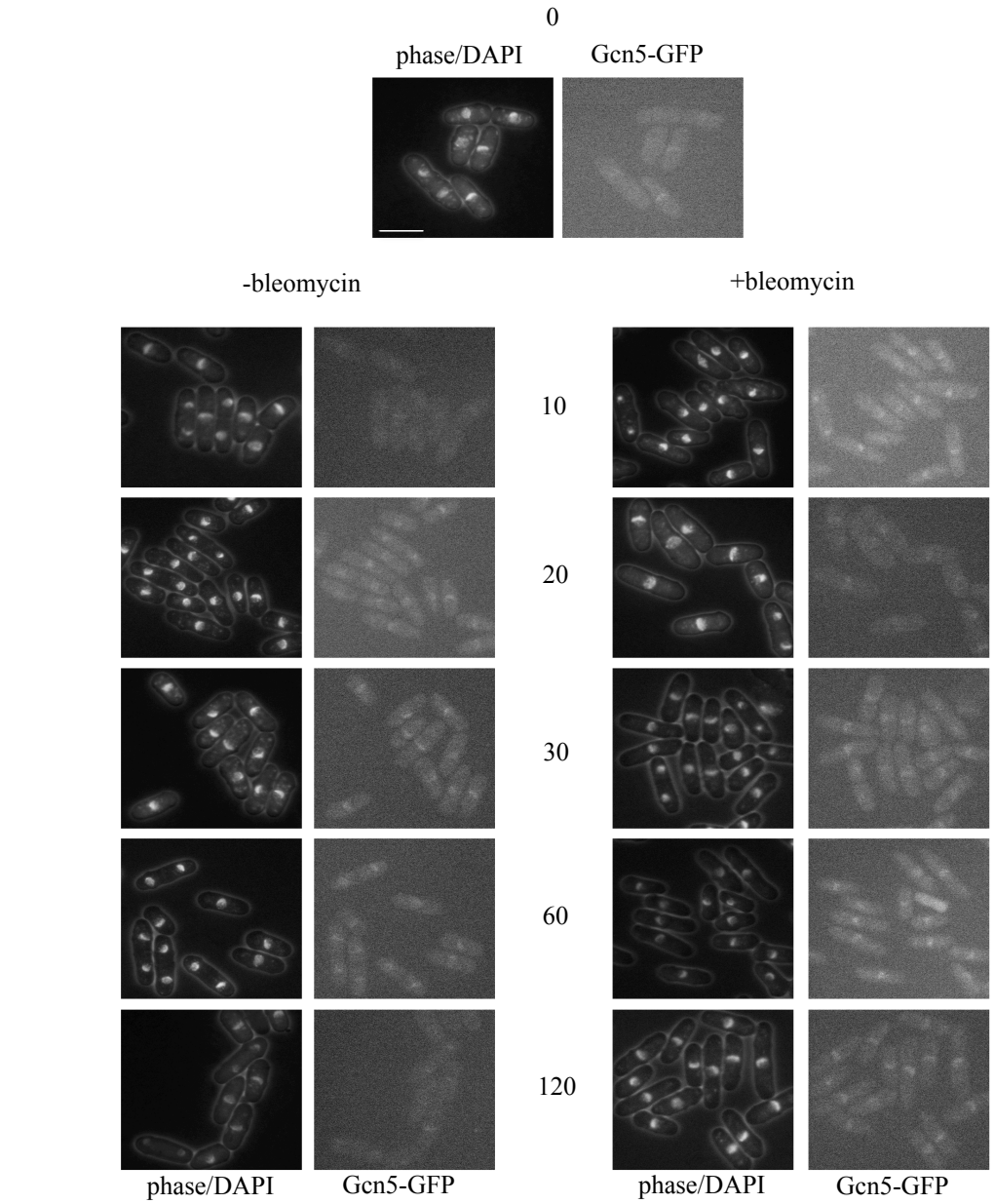
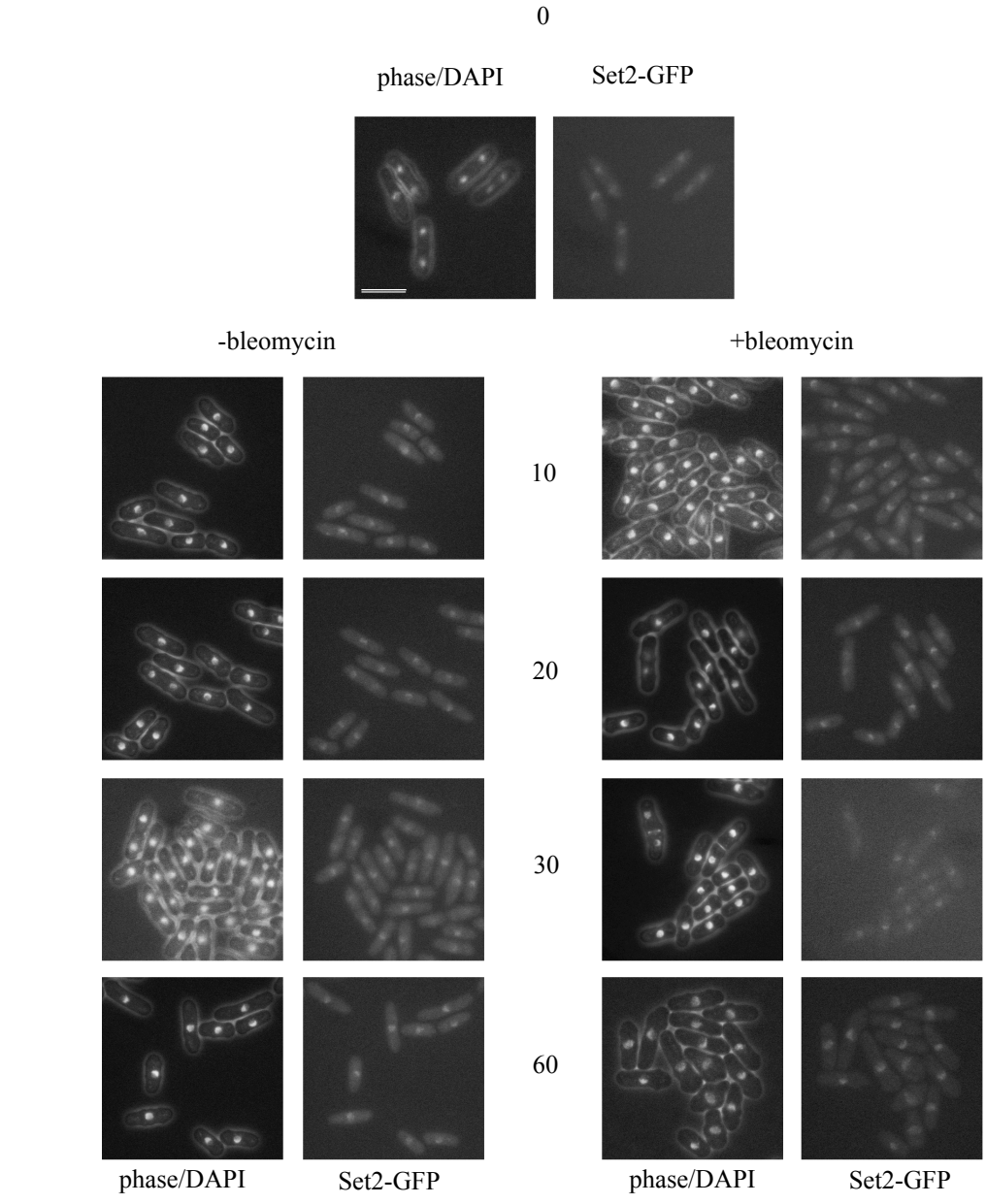


Figure 7.14 continued

C



investigation in this chapter showed that the methyltransferase activity of Set2 is required for its role in both NHEJ and DNA replication. However, an additional role for H3K36 in DSB repair was identified; Gcn5 acetylates this residue and a *gcn5*Δ mutant exhibits decreased repair by HR. As a result, a model is proposed whereby if H3K36 is methylated by Set2 in G1, repair occurs by NHEJ; however, if H3K36 is acetylated by Gcn5 in S phase, repair occurs by HR (Figure 7.15).

7.3.1 Methylation of H3K36 by Set2 is required for efficient NHEJ and DNA replication

To determine if the role for Set2 in DSB repair was dependent on methylation of H3K36 a *set2-R255G* point mutant was created. Analysis showed that this residue is essential for methylation of H3K36 and lack of methylation is associated with increased levels of GC and impaired NHEJ.

Whereas in yeast, Set2 performs mono-, di- and trimethylation of H3K36, in higher eukaryotes these different methylation states require different enzymes. There are at least eight SET domain containing proteins that methylate H3K36 in metazoa (Table 7.2; reviewed in Wagner & Carpenter, 2012).

During the course of this study, H3K36 dimethylation by METNASE was shown to be required for efficient NHEJ in mammalian cells (Fnu *et al*, 2011). The authors showed a global and local increase in H3K36me2 in response to IR and recruitment of METNASE to the break site; this was required for effective recruitment of Ku70 and NBS1. Interestingly, the authors only observed a global increase in H3K36me2, and not H3K36me3, consistent with the data here, which showed no global change in H3K36me3 levels in response to bleomycin treatment. Given the increased association of Ku70 and NBS1 with the break in the presence of METNASE, it would be interesting to see if there is reduced recruitment of

Figure 7.15

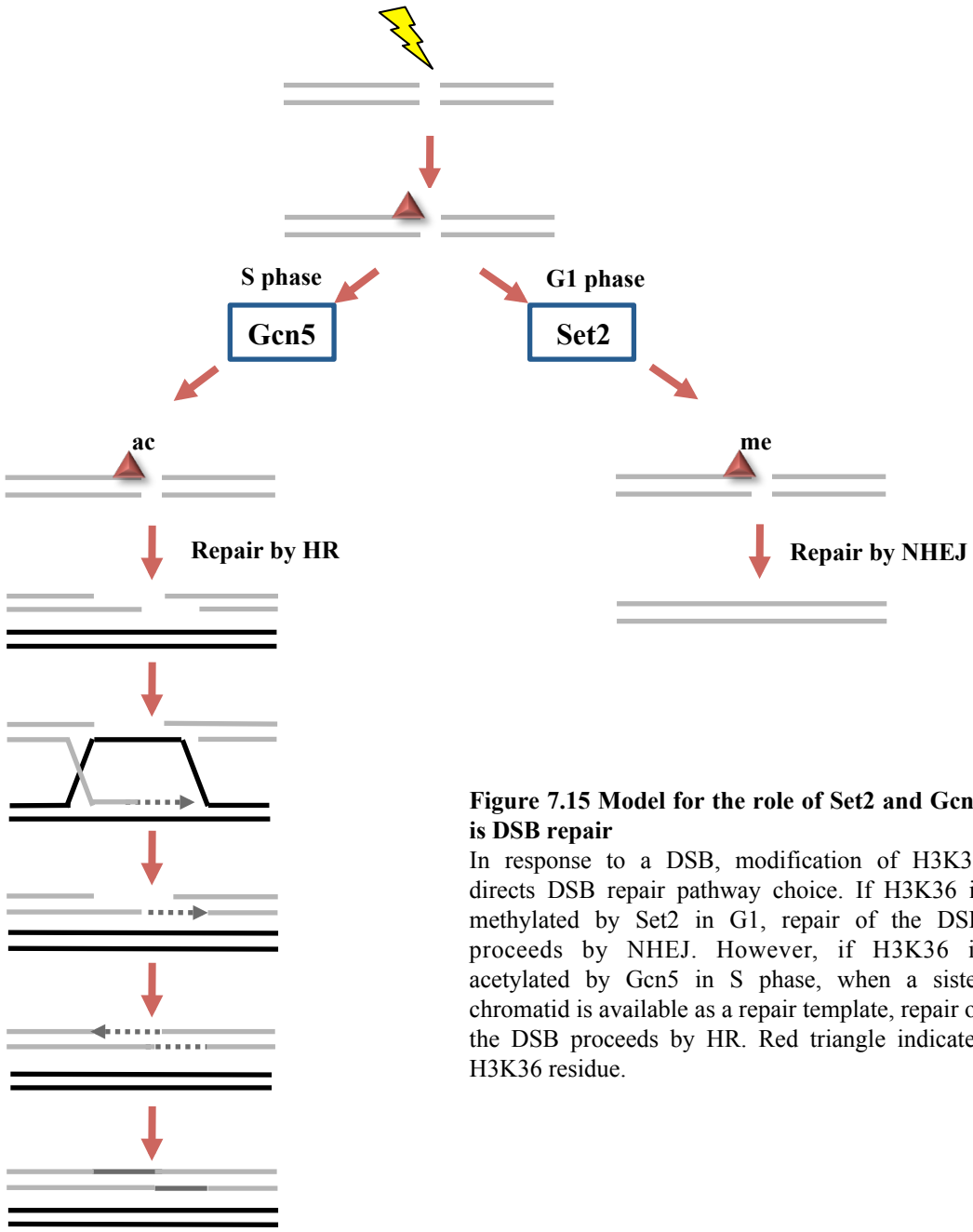


Figure 7.15 Model for the role of Set2 and Gcn5 is DSB repair

In response to a DSB, modification of H3K36 directs DSB repair pathway choice. If H3K36 is methylated by Set2 in G1, repair of the DSB proceeds by NHEJ. However, if H3K36 is acetylated by Gcn5 in S phase, when a sister chromatid is available as a repair template, repair of the DSB proceeds by HR. Red triangle indicates H3K36 residue.

Table 7.2 H3K36 methyltransferases in higher eukaryotes and their specificities

Enzyme	K36-K36me1	K36me1-K36me2	K36me2-K36me3
NSD1	✓	✓	
NSD2	✓	✓	
NSD3	✓	✓	
ASH1L	✓	✓	
METNASE	✓	✓	
SMYD1	✓	✓	
SMYD2	✓	✓	
SETD2			✓

Ku70 in a *set2*Δ mutant in *S. pombe* and if so, whether the recruitment of Ku70 is specific to dimethylation of H3K36. A recent study in mammalian cells showed that JMJD2A, a H3K9 and H3K36 demethylase, is degraded via the proteasome in a RNF8-dependent manner during the DDR, which is required for efficient 53BP1 recruitment (Mallette *et al*, 2012). This may facilitate the accumulation of H3K36 methylation in response to DNA damage. Given higher eukaryotes utilise NHEJ as their predominant repair mechanism, this may promote the activity of NHEJ in response to a DSB, and supports a conserved role for H3K36 methylation in promoting NHEJ repair.

Analysis of cell cycle progression in the *set2-R255G* mutant, indicated that methylation of H3K36 is also required for efficient progression through S phase. In Chapter 6, the regulation of levels of Cdt1 and Cdc18 was shown to be impaired in *set2*Δ cells, which is likely to cause the S phase delay observed in this mutant. Given the result in this chapter, this suggests that H3K36 methylation is required for efficient transcriptional control of $cdt1^{+}$ and $cdc18^{+}$. It would be interesting to confirm this, by analysing cell cycle levels of Cdt1 and Cdc18 in the

set2-R255G mutant, and also determining whether there are any transcriptional changes in this genetic background. This would support the hypothesis that transcriptional changes are the cause of the S phase delay seen.

Loss of Set2 in both budding and fission yeast results in increased levels of spurious transcription, due to lack of HDAC recruitment (Li *et al*, 2007; Nicolas *et al*, 2007). However, a study in budding yeast has shown that dimethylation of H3K36 is sufficient for recruitment of Rpd3(S) and repression of spurious transcripts (Youdell *et al*, 2008) which suggests an additional uncharacterised role for trimethylation in the transcription process. Given the association of trimethylation with highly expressed genes (Pokholok *et al*, 2005) it is possible that H3K36me3 may be required for efficient transcription of genes involved in S phase progression, which may explain the S phase delay in the *set-R255G* and *set2*Δ mutants.

Intriguingly, the *set2-R255G* mutant phenocopied the *set2*Δ mutant in all aspects apart from the interaction with resection mutants. Whereas *set2*Δ was exquisitely sensitive to bleomycin in combination with mutants in factors required for both short and long tract resection, *set2-R255G* did not show this interaction; this separates the sensitivity of *set2*Δ with mutants in resection factors away from the role in DNA replication and NHEJ. In fact, the *set2-R255G* mutant suppressed the sensitivity of *exo1*Δ cells to bleomycin; this suppression was also seen by *ku70*Δ (Chapter 4). In all aspects addressed, *set2-R255G* phenocopied *ku70*Δ; increased DSB repair by GC, inefficient NHEJ, and suppression of *exo1*Δ sensitivity to bleomycin. The repression of *exo1*Δ sensitivity by *ku70*Δ may reflect its role in end-protection; Ku70 binds and protects DNA ends following a DSB, and loss of Ku70 results in increased resection at the break site (Lee *et al*, 1998). Thus, deletion of $ku70^{+}$can suppress the reduced resection observed in an *exo1*Δ mutant (Limbo *et al*, 2007; Tomita *et al*, 2003). This indicates a

possible role for methylation of H3K36 in end-protection, perhaps through recruitment of Ku70, as observed in mammalian cells (Fnu *et al*, 2011).

In addition, these results indicate a methylation-independent role for Set2, which when lost results in exquisite sensitivity with *exo1*Δ cells. Set2 contains an associated with SET (AWS) domain, a SET domain, a post-SET domain and a C-terminal coiled-coil domain (Figure 7.1A). It would be interesting to address if loss of a particular region or domain of Set2 is responsible for the sensitivity to bleomycin observed in the *set2*Δ*exo1*Δ mutant; this could be achieved by creating various truncations, and analysing their interaction with *exo1*Δ cells.

7.3.2 A role for Gcn5 in efficient HR repair

Analysis of a *H3K36R* mutant identified an additional role for this residue in DSB repair, as unlike the *set2*Δ and *set2-R255G* mutants, these cells exhibited marked sensitivity to bleomycin. H3K36 is also acetylated by Gcn5 (Morris *et al*, 2007), and so further work focussed on DSB repair in g*cn5*Δ cells. Strikingly, the DSB profile was the converse of *set2*Δ cells: significantly decreased levels of GC associated with a significant increase in NHEJ/SCC, suggesting a role for Gcn5 in repair of DSBs by HR. In addition, Rhp51 foci formation was impaired in *gcn5*Δ cells, indicating a presynaptic role for Gcn5 in HR repair.

Histone acetylation is well documented to be important in the DNA damage response and mutations of H3 lysine residues or deletion of the genes whose products modify these residues, compromises repair outcome (Bird *et al*, 2002; Murr *et al*, 2006; Qin & Parthun, 2002; Tamburini & Tyler, 2005). Consistent with this, is the finding that *H3K36R* cells exhibit a striking sensitivity to bleomycin and IR. A number of studies have identified roles for Gcn5 in DNA repair in both mammalian cells and yeast. A study in budding yeast showed increased acetylation of H3 and H4 lysine residues adjacent to a HO-induced break

(Tamburini & Tyler, 2005), coincident with recruitment of Gcn5. This increase in acetylation was suggested to occur during HR and was dependent on the HR machinery, as in *rad52* cells increased acetylation was no longer observed. Further, a study in mammalian cells showed a role for Gcn5 in promoting DSB repair through efficient formation of phosphorylated H2AX, and recruitment of the SWI/SNF chromatin remodeler (Lee *et al*, 2010). They propose a model whereby initial binding of Gcn5 to nucleosomes containing γH2AX, results in acetylation of H3 and subsequent recruitment of SWI/SNF through BRG1, promoting chromatin remodelling and further phosphorylation of H2AX. Blocking this interaction of BRG1 with acetylated H3, results in a reduction in phosphorylated H2AX and subsequent DSB repair. It would be interesting to investigate whether H2A phosphorylation is altered in the *gcn5*Δ mutant in fission yeast. In addition, histone acetylation by Gcn5 following UV treatment is required for chromatin remodelling and the efficient recruitment of factors for efficient nucleotide excision repair (Guo *et al*, 2011; Yu *et al*, 2011). Further, in fission yeast, H3K14 acetylation by Gcn5 and Mst2 has been shown to be critical for DNA damage checkpoint activation through recruitment of the RSC complex (Wang *et al*, 2012), although deletion of *gcn5*$^{+}$ alone did not exhibit a significant effect, in agreement with results in this chapter that showed *gcn5*Δ cells exhibited a proficient cell cycle arrest in response to HU treatment.

Given these roles for Gcn5 in DNA repair, and the results in this chapter that show significantly reduced repair by GC in a *gcn5*Δ mutant, it is surprising that cells lacking *gcn5*$^{+}$ did not show a greater sensitivity to bleomycin and IR. However, as discussed with regard to Hat1 and Set13 in Chapter 3, given the levels of GC are only reduced by 20%, higher concentrations of bleomycin or increased doses of IR may be required to observe any sensitivity. In this respect, the results from this study are consistent with others; *gcn5* cells only show mild sensitivity to consistent HO expression in budding yeast (Tamburini & Tyler,

2005) and only slight sensitivity to bleomycin (double the concentration used here) in fission yeast (Wang *et al*, 2012). A bleomycin or IR survival curve would help determine whether *gcn5*Δ cells exhibit sensitivity to these agents when the concentration or dose is increased.

Gcn5 is well conserved from yeast to mammalian cells and is found in several transcription related complexes such as SAGA (reviewed in Baker & Grant, 2007; Grant *et al*, 1997). Gcn5 is found associated with both promoter and coding regions where it is required for nucleosome eviction (Johnsson *et al*, 2009; Rosaleny *et al*, 2007). However, whereas in budding yeast, Gcn5-dependent genes show depletion of RNAP II from the promoters, this is not observed in fission yeast (Sanso *et al*, 2011). Rather, Gcn5 is required for acetylation and subsequent histone eviction in coding regions and is required for efficient transcription elongation in fission yeast (Johnsson *et al*, 2009; Sanso *et al*, 2011). This difference is suggested to reflect the differential promoter nucleosome structure in budding and fission yeasts; whereas in fission yeast Gcn5-dependent genes are devoid of nucleosomes around the transcription start site (TSS) under basal conditions, in budding yeast nucleosomes are present in the promoter region and have to be mobilised for efficient transcription initiation (Sanso *et al*, 2011; Wippo *et al*, 2009). Despite these differences it is clear that Gcn5 is an important transcriptional regulator.

Under normal conditions in fission yeast, only forty-one out of over four thousand genes are differentially expressed in a *gcn5*Δ mutant (Johnsson *et al*, 2006). However, Gcn5 is essential in the transcriptional response to stress in both budding and fission yeast (Huisinga & Pugh, 2004; Johnsson *et al*, 2006; Xue-Franzen *et al*, 2010) and although the role of Gcn5 in mammalian cells is not well understood, it is required for differential transcription in response to alcohol (Choudhury *et al*, 2011). Although the microarray study of *gcn5*Δ cells in fission yeast did not identify any alteration in the transcription of repair genes (Johnsson *et al*, 2006),

it would be important to confirm this, and look at any transcriptional changes in response to DSB induction in this mutant, compared to wildtype.

Given acetylation of histones results in a more open chromatin structure, another consideration is whether lack of acetylation resulting from deletion of *gcn5*$^{+}$ may result in reduced accessibility of the DNA to the HO endonuclease and therefore less cutting. A study in *S. pombe* showed reduced efficiency of HO-induced breaks in a *gcn5*Δ*mst2*Δ double mutant (Wang *et al*, 2012) and so this possibility should be addressed. However, given the role for Gcn5 in DSB repair in budding yeast, and the increased NHEJ observed in this study, it is likely that the DSB profile does reflect decreased repair by HR.

7.3.3 A model for the role of differential modification of H3K36 in directing DSB repair pathway choice

Given the striking converse phenotypes of *set2*Δ and *gcn5*Δ mutants, and the ability of both enzymes to modify H3K36, a hypothesis whereby differential modification of this residue can determine DSB repair pathway choice was investigated. However, although the *set2*Δ*gcn5*Δ mutant showed some increased sensitivity to bleomycin, it was not as striking as the *H3K36R* mutant, and the *set2*Δ*gcn5*Δ cells were proficient at repair by GC in the DSB assay, suggesting that in the absence of Set2, Gcn5 is no longer required for efficient GC. This may reflect the predominance of HR as a repair mechanism in *S. pombe* (Ferreira & Cooper, 2004). Given the essential requirement for efficient DSB repair in maintaining genome integrity, modification of this residue is unlikely to be a sole indicator for repair, but rather an additional layer of control. Results in this chapter have shown that deletion of *gcn5*$^{+}$ results in increased methylation, whereas deletion of *set2*$^{+}$ results in increased acetylation. If methylation promotes NHEJ and acetylation promotes HR, then the repair phenotypes of the single mutants are not surprising; increased methylation in the *gcn5*Δ cells leads to increased NHEJ and increased acetylation in *set2*Δ cells leads to increased GC. Consistent with this, is

the finding that overexpression of *gcn5* results in extremely high levels of repair by GC. In the double mutant, in the absence of both modifications, this layer of control is lost, but other mechanisms of controlling DSB repair are still present, resulting in a wildtype repair phenotype, whereby HR predominates.

Interestingly, analysis of the levels of H3K36 acetylation and methylation in G1 and S phase cells suggests that methylation is increased in G1 phase, when repair occurs preferentially by NHEJ, and acetylation is increased in S phase, when repair occurs preferentially by HR. This cell cycle regulation is interesting; in addition to the proposed role for Set2 in DNA replication in Chapter 6, mutants in which $gcn5^{+}$ is deleted also show a slight delay in DNA replication. Gcn5 has previously been shown to be required for efficient cell cycle progression; in budding yeast, Gcn5 is required for efficient pre-RC formation (Espinosa *et al*, 2010) and *gcn5* mutants have been shown to accumulate in G2/M (Burgess *et al*, 2010; Zhang *et al*, 1998). The reason for this is unclear: some studies suggest Gcn5 is required for efficient replication coupled nucleosome assembly (Burgess *et al*, 2010) whereas others show physical interaction with origins and reduced recruitment of replication factors in its absence, possibly through chromatin structure alterations or a direct role in recruitment (Espinosa *et al*, 2010). Interestingly in mammalian cells, GCN5 is involved in controlling the stability of CDC6, which it acetylates leading to its re-localisation in S phase (Paolinelli *et al*, 2009). Interestingly, the study by Paolinelli *et al* (2009) shows that the levels of GCN5 protein peak in S phase, consistent with the observation here showing increased H3K36 acetylation in S phase compared to G1. Recently, a study in mammalian cells has shown that GCN5 levels are controlled by the $CRL4^{Cdt2}$ E3 ubiquitin ligase (Li *et al*, 2011), which also controls the levels of CDT1 and SET8 by promoting their degradation in S phase and following DNA damage. It would be very interesting to see if the levels of Gcn5 in fission yeast are controlled in a cell cycle manner, to co-ordinate a peak of H3K36ac in S phase. There is no evidence of Set2

protein levels being cell cycle controlled, but this may reflect the ability of NHEJ to repair DSBs throughout the cell cycle; a peak of Gcn5 protein levels in S phase would lead to competition between these modifications, allowing HR to compete with NHEJ when a sister chromatid is present as a repair template.

Analysis of the levels of global H3K36 methylation and acetylation following bleomycin treatment showed no significant change. In addition, analysis of GFP-tagged Set2 showed no increase in abundance or formation of foci following treatment with bleomycin. However, analysis of GFP-tagged Gcn5 suggested a slight increase in abundance following treatment with bleomycin. This is not reflected at the level of transcription, as *gcn5*$^{+}$ transcript was not up-regulated in response to bleomycin in wildtype cells (Chapter 5). However, as GCN5 levels are controlled through degradation in mammalian cells (Li *et al*, 2011), it is possible a similar level of control exists in fission yeast.

To determine if Set2 and Gcn5 do function directly at the break site in fission yeast, it will be essential to perform ChIP analysis. Looking at the levels of H3K36 methylation and acetylation at the break site would also be of interest; given the increase in acetylation of a number of other residues on H3 at the break site, one might expect an associated increase in H3K36 acetylation.

If Gcn5 and Set2 are recruited to the break, a key unanswered question is whether their function in DSB repair is through direct recruitment of repair factors, or creating an appropriate chromatin environment in which repair can proceed. The study in mammalian cells that shows H3K36me2 is required for recruitment of Ku70 provides a good starting point (Fnu *et al*, 2011), and it would be worthwhile assessing Ku70 recruitment in the absence of Set2. If H3K36 methylation is required for recruitment of Ku70, it may be that in the

presence of acetylation, NHEJ factors are not efficiently recruited, which precludes NHEJ, thus promoting HR. The reduced Rhp51 foci formation in the *gcn5*Δ cells is consistent with this, as in the absence of acetylation, more methylation may result in increased recruitment of Ku70, increasing end-protection and NHEJ, and reducing resection and thus Rhp51 nucleofilament formation and HR. In addition, acetylation of this residue may reduce chromatin compaction, further promoting HR.

The function of histone modifications is often difficult to determine. Lysine residues are subject to various modifications (Kouzarides, 2007), as demonstrated by the acetylation and methylation of H3K36, and histone-modifying enzymes often target more than one residue. Thus, mutating the histone residue will give information about loss of various modifications, and mutating the enzyme will give information about loss of modification of a number of residues. In this regard, a key outstanding question in this study is whether the repair phenotype of *gcn5*Δ relates to loss of acetylation of H3K36. One way to address this would be to overexpress *gcn5* in a *H3K36R* background; if the same phenotype as when *gcn5* is overexpressed in a wildtype background was observed, the phenotype would not be due to H3K36 modification. However, this approach is problematic, as the *H3K36R* mutant has poor viability, and attempts to introduce a minichromosome into this strain to perform the DSB assay were unsuccessful.

7.4 SUMMARY

To conclude, the data in this chapter suggest a role for differential modification of H3K36 in determining DSB repair pathway choice.

- The methyltransferase activity of Set2 is required for its role in efficient NHEJ and DNA replication.
- Gcn5 is required for efficient repair by HR.
- H3K36 modification by Set2 and Gcn5 is mutually inhibitory and is regulated through the cell cycle.

These findings support a model in which methylation of H3K36 by Set2 results in repair by NHEJ and acetylation by Gcn5 results in repair by HR.

CHAPTER 8
General Discussion

This study has described the identification and characterisation of a role for H3K36 modification in DSB repair. Initial analysis of nineteen histone-modifying mutants identified eleven genes that are required for efficient DSB repair: *set1*$^+$, *set2*$^+$, *mst2*$^+$, *sir2*$^+$, *set3*$^+$, *set11*$^+$, *hat1*$^+$, *set13*$^+$, *clr4*$^+$, *gcn5*$^+$ and *elp3*$^+$. Deletion of these genes resulted in aberrant repair compared to wildtype. A novel function for Hat1 and Set13 in efficient HR repair in *S. pombe* was identified, and further analysis, as discussed in Chapter 3 may help to elucidate their exact roles in DSB repair. Further work focussed on characterising Set2; in addition to a requirement for Set2 in efficient NHEJ, a role in DNA replication was identified. This is likely through correct regulation of genes required for pre-RC formation. Further, the methyltransferase activity of Set2 was shown to be required for its role in NHEJ and DNA replication. Evidence provided here shows that in addition to being methylated by Set2, H3K36 can also be acetylated by Gcn5. Analysis of these modifications in combination with the opposing DSB repair profiles of *set2*Δ and *gcn5*Δ mutants led to a proposed model whereby differential modification of H3K36 dictates the DSB repair pathway utilised. The work presented highlights the importance of histone modification in effective DSB repair and maintaining genome integrity, and implies that differential modification of lysine residues can function as a 'chromatin switch' that controls distinct biological effects.

8.1 The importance of histone modification in control of DNA-templated processes

Histone modifications have been implicated in numerous biological processes including DNA repair, DNA replication and transcription (reviewed in Kouzarides, 2007). These processes often require access of large enzyme complexes to the DNA, and so chromatin structure and thus histone modification are of key importance, through controlling DNA compaction. The work presented in this thesis further highlights the importance of histone modification in

DNA-templated processes as lack of Set2 results in impaired DNA repair (Chapters 3, 4 and 7), changes in normal transcriptional processes (Chapter 5) and defective DNA replication (Chapter 6). The role in DNA repair and DNA replication is due to loss of Set2 methyltransferase activity, as a *set2-R255G* mutant, in which H3K36 methylation is abrogated also exhibited impaired NHEJ and DNA replication. Given the documented role for H3K36 methylation in transcription elongation it is likely the same transcriptional changes would also be observed in the *set2-R255G* mutant. There is evidence in other organisms for a single histone-modifying enzyme being implicated in diverse DNA-templated processes. For example, in budding yeast, Set1 is required for both efficient transcription and DNA repair (Boa *et al*, 2003; Faucher & Wellinger, 2010) and in mammalian cells, PR-SET7 is involved in the DNA damage response and DNA replication (Oda *et al*, 2010; Tardat *et al*, 2010). Thus, utilising histone-modifying enzymes to promote distinct biological processes is a conserved mechanism. Conceivably the presence of a modification in distinct locations at distinct times may allow one modification to promote varying processes. Further, given lysine residues can be mono-, di- and tri-methylated, changing the extent of modification of a residue may alter the biological outcome.

8.2 A conserved role for histone methylation in NHEJ

Work in previous studies, in addition to the results presented in this thesis, suggest that methylation of histones is likely a conserved mechanism for promoting NHEJ. In mammalian cells, methylation of H3K36 by METNASE is required for NHEJ through the recruitment of Ku70 to the break site (Fnu *et al*, 2011); in budding yeast, methylation of H3K4 by Set1 performs the same role (Faucher & Wellinger, 2010). As the Ku70-Ku80 heterodimer has such high affinity for DNA ends, Fnu *et al* (2011) suggest it is likely that binding to methyl-lysine residues stabilises the interaction of the heterodimer with DNA ends, preventing its dissociation. Given these findings, and the highly conserved role of the Ku70-Ku80 heterodimer in NHEJ, it is possible that in *S. pombe* methylation of H3K36 by Set2 also

promotes recruitment or retention of the Ku70-Ku80 heterodimer to DNA ends, thus facilitating end protection and NHEJ. Consequently one might expect increased levels of resection in cells lacking H3K36 methylation, which could be investigated by analysing Rad11 (RPA) foci formation following IR treatment in the *set2-R255G* mutant. Increased resection in the *set2-R255G* cells would be consistent with results presented here which show that *ku70*Δ and *set2-R255G* both suppress the sensitivity of *exo1*Δ cells to bleomycin.

The requirement for histone methylation in promoting Ku70-Ku80 binding to DSBs, suggests that the heterodimer may bind directly to methyl-lysine residues. As discussed in Chapter 1, histone modification 'readers' often contain domains that specifically recognise the modified residue. There are many distinct domains that recognise methyl-lysine residues and lead to the recruitment of proteins. These include the 'royal' family of proteins, comprising chromo-, Tudor-, PWWP- and MBT-domains in addition to the PHD fingers (Kim *et al*, 2006a; Maurer-Stroh *et al*, 2003; Shi *et al*, 2006). Given the recruitment of Ku70-Ku80 to methyl-lysine residues in budding yeast and mammalian cells it is tempting to speculate the presence of a methyl-lysine binding domain in the heterodimer. However, there is no documentation of this from structural studies. Creating truncations of Ku70 or Ku80 may help determine which regions of the proteins are required for methyl-lysine binding. Ku70, which is mainly required for the DNA-binding ability of the heterodimer, has two DNA-binding domains, one N-terminal and one C-terminal (Chou *et al*, 1992; Wu & Lieber, 1996). It would be interesting to see if any overlap exists between the regions required for DNA-binding and methyl-lysine binding.

8.3 A role for 'chromatin switches' in directing distinct biological events

Further analysis indicated that Gcn5 acetylates H3K36 in *S. pombe*, as previously shown in budding yeast (Morris *et al*, 2007). The converse repair phenotypes of *set2*Δ and *gcn5*Δ cells

led to a proposed model whereby methylation of H3K36 by Set2 promotes NHEJ and acetylation by Gcn5 promotes HR. If H3K36 methylation is required for Ku70-Ku80 recruitment, then in the presence of Gcn5, H3K36 acetylation would compete with methylation, reducing the presence of Ku70-Ku80 at the DSB and increasing resection, thus promoting repair by HR. Data showing reduced Rhp51-CFP foci in a *gcn5*Δ background compared to wildtype following IR treatment supports this model.

A key question concerns the factors controlling the choice between methylation and acetylation of H3K36 following DSB formation, in order to dictate the repair mechanism used. Preliminary cell cycle analysis of H3K36 trimethylation and H3K36 acetylation levels suggests that methylation is predominant in G1 phase. However, on entry to S phase, a slight decrease in methylation, associated with a striking increase in acetylation, would result in an increase in the ratio of acetylated to methylated H3K36. This would allow competition between NHEJ and HR in S phase, when a sister chromatid is available to act as a repair template. Thus, fluctuating levels of acetylated and methylated H3K36 during the cell cycle may act as a 'chromatin switch', ensuring appropriate repair mechanisms are utilised at the correct stage of the cell cycle, to prevent the accumulation of mutations and maintain genome stability.

H3K36 acetylation is a conserved modification in human cells (Kim *et al*, 2006b; Morris *et al*, 2007). Given H3K36 dimethylation by METNASE is required for NHEJ in mammalian cells (Fnu *et al*, 2011) it would be interesting to determine if differential modification of H3K36 represents a conserved mechanism by which the choice of repair mechanism is controlled.

This work suggests that functional interplay between histone modifications can drive distinct biological effects. Previous evidence of such chromatin switches existing in biology comes from studies of H3K9 modification. H3K9 methylation serves as a binding site for recruitment of HP1, initiating the formation of heterochromatin (Bannister *et al*, 2001). However, acetylation of this residue must be removed prior to methylation (Nicolas *et al*, 2003). Thus, a chromatin switch acts to control the transition between euchromatin and heterochromatin. Further, Morris *et al* (2007) show that in budding yeast H3K36 acetylation is present in the promoters of actively transcribed genes, whereas methylation is present in the body of the actively transcribed genes. The authors suggest that transition between acetylation and methylation may represent a chromatin switch controlling the regulation of gene expression. The work presented in this thesis suggests a novel chromatin switch may exist in fission yeast to help control the choice between NHEJ and HR repair. This chromatin switch combined with the existing complex networks that control DSB repair ensures the fidelity of the DNA is maintained, preventing deleterious chromosomal rearrangements as a consequence of misuse of repair mechanisms. Collectively, the work in this thesis in addition to previous studies implies that the presence of chromatin switches may act to control distinct biological events in the cell, providing an additional fine-tuning mechanism for biological systems.

References

Abbas T, Shibata E, Park J, Jha S, Karnani N, Dutta A (2010) CRL4(Cdt2) regulates cell proliferation and histone gene expression by targeting PR-Set7/Set8 for degradation. Molecular Cell **40:** 9-21

Adachi N, So S, Koyama H (2004) Loss of nonhomologous end joining confers camptothecin resistance in DT40 cells. Implications for the repair of topoisomerase I-mediated DNA damage. The Journal of Biological Chemistry **279:** 37343-37348

Adam M, Robert F, Larochelle M, Gaudreau L (2001) H2A.Z is required for global chromatin integrity and for recruitment of RNA polymerase II under specific conditions. Molecular and Cellular Biology **21**: 6270-6279

Aguilera A, Gomez-Gonzalez B (2008) Genome instability: a mechanistic view of its causes and consequences. Nature Reviews Genetics **9:** 204-217

Ahnesorg P, Smith P, Jackson SP (2006) XLF interacts with the XRCC4-DNA ligase IV complex to promote DNA nonhomologous end-joining. Cell **124:** 301-313

Ai X, Parthun MR (2004) The nuclear Hat1p/Hat2p complex: a molecular link between type B histone acetyltransferases and chromatin assembly. Molecular Cell **14:** 195-205

Akamatsu Y, Dziadkowiec D, Ikeguchi M, Shinagawa H, Iwasaki H (2003) Two different Swi5-containing protein complexes are involved in mating-type switching and recombination repair in fission yeast. Proceedings of the National Academy of Sciences of the United States of America **100:** 15770-15775

Al Sarakbi W, Sasi W, Jiang WG, Roberts T, Newbold RF, Mokbel K (2009) The mRNA expression of SETD2 in human breast cancer: correlation with clinico-pathological parameters. BMC Cancer **9:** 290

Alabert C, Bianco JN, Pasero P (2009) Differential regulation of homologous recombination at DNA breaks and replication forks by the Mrc1 branch of the S-phase checkpoint. The EMBO Journal **28:** 1131-1141

Aligianni S, Lackner DH, Klier S, Rustici G, Wilhelm BT, Marguerat S, Codlin S, Brazma A, de Bruin RA, Bahler J (2009) The fission yeast homeodomain protein Yox1p binds to MBF and confines MBF-dependent cell-cycle transcription to G1-S via negative feedback. PLoS Genetics **5:** e1000626

Allen C, Ashley AK, Hromas R, Nickoloff JA (2011) More forks on the road to replication stress recovery. Journal of Molecular Cell Biology **3:** 4-12

Allen C, Halbrook J, Nickoloff JA (2003) Interactive competition between homologous recombination and non-homologous end joining. Molecular Cancer Research **1:** 913-920

Altaf M, Auger A, Covic M, Cote J (2009) Connection between histone H2A variants and chromatin remodeling complexes. Biochemistry and Cell Biology **87:** 35-50

Arias EE, Walter JC (2006) PCNA functions as a molecular platform to trigger Cdt1 destruction and prevent re-replication. Nature Cell Biology **8:** 84-90

Aslett M, Wood V (2006) Gene Ontology annotation status of the fission yeast genome: preliminary coverage approaches 100%. Yeast **23:** 913-919

Astrom SU, Okamura SM, Rine J (1999) Yeast cell-type regulation of DNA repair. Nature **397:** 310

Aylon Y, Liefshitz B, Kupiec M (2004) The CDK regulates repair of double-strand breaks by homologous recombination during the cell cycle. The EMBO Journal **23:** 4868-4875

Ayte J, Schweitzer C, Zarzov P, Nurse P, DeCaprio JA (2001) Feedback regulation of the MBF transcription factor by cyclin Cig2. Nature Cell Biology **3:** 1043-1050

Baker SP, Grant PA (2007) The SAGA continues: expanding the cellular role of a transcriptional co-activator complex. Oncogene **26:** 5329-5340

Baldinger T, Gossen M (2009) Binding of Drosophila ORC proteins to anaphase chromosomes requires cessation of mitotic cyclin-dependent kinase activity. Molecular and Cellular Biology **29:** 140-149

Bannister AJ, Kouzarides T (2011) Regulation of chromatin by histone modifications. Cell Research **21:** 381-395

Bannister AJ, Zegerman P, Partridge JF, Miska EA, Thomas JO, Allshire RC, Kouzarides T (2001) Selective recognition of methylated lysine 9 on histone H3 by the HP1 chromo domain. Nature **410:** 120-124

Bao Y, Shen X (2007) Chromatin remodeling in DNA double-strand break repair. Current Opinion in Genetics & Development **17:** 126-131

Bao Y, Shen X (2007b) INO80 subfamily of chromatin remodeling complexes. Mutation Research **618**: 18-29

Barlev NA, Poltoratsky V, Owen-Hughes T, Ying C, Liu L, Workman JL, Berger SL (1998) Repression of GCN5 histone acetyltransferase activity via bromodomain-mediated binding and phosphorylation by the Ku-DNA-dependent protein kinase complex. Molecular and Cellular Biology **18:** 1349-1358

Bastos de Oliveira FM, Harris MR, Brazauskas P, de Bruin RA, Smolka MB (2012) Linking DNA replication checkpoint to MBF cell-cycle transcription reveals a distinct class of G1/S genes. The EMBO Journal **31:** 1798-1810

Bebenek K, Roberts JD, Kunkel TA (1992) The effects of dNTP pool imbalances on frameshift fidelity during DNA replication. The Journal of Biological Chemistry **267:** 3589-3596

Bednar J, Horowitz RA, Grigoryev SA, Carruthers LM, Hansen JC, Koster AJ, Woodcock CL (1998) Nucleosomes, linker DNA, and linker histone form a unique structural motif that directs the higher-order folding and compaction of chromatin. Proceedings of the National Academy of Sciences of the United States of America **95:** 14173-14178

Bell SP, Dutta A (2002) DNA replication in eukaryotic cells. Annual Review of Biochemistry **71:** 333-374

Benson LJ, Phillips JA, Gu Y, Parthun MR, Hoffman CS, Annunziato AT (2007) Properties of the type B histone acetyltransferase Hat1: H4 tail interaction, site preference, and involvement in DNA repair. The Journal of Biological Chemistry **282:** 836-842

Bianco PR, Tracy RB, Kowalczykowski SC (1998) DNA strand exchange proteins: a biochemical and physical comparison. Frontiers in bioscience : a journal and virtual library **3:** D570-603

Bianco-Miotto T, Chiam K, Buchanan G, Jindal S, Day TK, Thomas M, Pickering MA, O'Loughlin MA, Ryan NK, Raymond WA, Horvath LG, Kench JG, Stricker PD, Marshall VR, Sutherland RL, Henshall SM, Gerald WL, Scher HI, Risbridger GP, Clements JA, Butler LM, Tilley WD, Horsfall DJ, Ricciardelli C (2010) Global levels of specific histone modifications and an epigenetic gene signature predict prostate cancer progression and development. Cancer epidemiology, biomarkers & prevention : a publication of the American Association for Cancer Research, cosponsored by the American Society of Preventive Oncology **19:** 2611-2622

Bird AW, Yu DY, Pray-Grant MG, Qiu Q, Harmon KE, Megee PC, Grant PA, Smith MM, Christman MF (2002) Acetylation of histone H4 by Esa1 is required for DNA double-strand break repair. Nature **419:** 411-415

Bjerling P, Silverstein RA, Thon G, Caudy A, Grewal S, Ekwall K (2002) Functional divergence between histone deacetylases in fission yeast by distinct cellular localization and in vivo specificity. Molecular and Cellular Biology **22:** 2170-2181

Block WD, Yu Y, Merkle D, Gifford JL, Ding Q, Meek K, Lees-Miller SP (2004) Autophosphorylation-dependent remodeling of the DNA-dependent protein kinase catalytic subunit regulates ligation of DNA ends. Nucleic Acids Research **32:** 4351-4357

Boa S, Coert C, Patterton HG (2003) Saccharomyces cerevisiae Set1p is a methyltransferase specific for lysine 4 of histone H3 and is required for efficient gene expression. Yeast **20:** 827-835

Bochman ML, Schwacha A (2008) The Mcm2-7 complex has in vitro helicase activity. Molecular Cell **31:** 287-293

Boddy MN, Furnari B, Mondesert O, Russell P (1998) Replication checkpoint enforced by kinases Cds1 and Chk1. Science **280:** 909-912

Boddy MN, Gaillard PH, McDonald WH, Shanahan P, Yates JR, 3rd, Russell P (2001) Mus81-Eme1 are essential components of a Holliday junction resolvase. Cell **107:** 537-548

Botuyan MV, Lee J, Ward IM, Kim JE, Thompson JR, Chen J, Mer G (2006) Structural basis for the methylation state-specific recognition of histone H4-K20 by 53BP1 and Crb2 in DNA repair. Cell **127:** 1361-1373

Bowman GD (2010) Mechanisms of ATP-dependent nucleosome sliding. Current Opinion in Structural Biology **20**: 73-81

Bridges KA, Hirai H, Buser CA, Brooks C, Liu H, Buchholz TA, Molkentine JM, Mason KA, Meyn RE (2011) MK-1775, a novel Wee1 kinase inhibitor, radiosensitizes p53-defective human tumor cells. Clinical Cancer Research : an official journal of the American Association for Cancer Research **17:** 5638-5648

Buratowski S (2003) The CTD code. Nature Structural Biology **10:** 679-680

Burgers PM (2009) Polymerase dynamics at the eukaryotic DNA replication fork. The Journal of Biological Chemistry **284:** 4041-4045

Burgess RJ, Zhou H, Han J, Zhang Z (2010) A role for Gcn5 in replication-coupled nucleosome assembly. Molecular Cell **37:** 469-480

Caetano C, Klier S, de Bruin RA (2011) Phosphorylation of the MBF repressor Yox1p by the DNA replication checkpoint keeps the G1/S cell-cycle transcriptional program active. PloS one **6:** e17211

Caligiuri M, Beach D (1993) Sct1 functions in partnership with Cdc10 in a transcription complex that activates cell cycle START and inhibits differentiation. Cell **72:** 607-619

Carroll AJ, Heazlewood JL, Ito J, Millar AH (2008) Analysis of the Arabidopsis cytosolic ribosome proteome provides detailed insights into its components and their post-translational modification. Molecular & Cellular Proteomics : MCP **7:** 347-369

Carrozza MJ, Li B, Florens L, Suganuma T, Swanson SK, Lee KK, Shia WJ, Anderson S, Yates J, Washburn MP, Workman JL (2005) Histone H3 methylation by Set2 directs deacetylation of coding regions by Rpd3S to suppress spurious intragenic transcription. Cell **123:** 581-592

Caspari T, Murray JM, Carr AM (2002) Cdc2-cyclin B kinase activity links Crb2 and Rqh1-topoisomerase III. Genes & Development **16:** 1195-1208

Catlett MG, Forsburg SL (2003) Schizosaccharomyces pombe Rdh54 (TID1) acts with Rhp54 (RAD54) to repair meiotic double-strand breaks. Molecular Biology of the cCll **14:** 4707-4720

Celeste A, Fernandez-Capetillo O, Kruhlak MJ, Pilch DR, Staudt DW, Lee A, Bonner RF, Bonner WM, Nussenzweig A (2003) Histone H2AX phosphorylation is dispensable for the initial recognition of DNA breaks. Nature Cell Biology **5:** 675-679

Centore RC, Havens CG, Manning AL, Li JM, Flynn RL, Tse A, Jin J, Dyson NJ, Walter JC, Zou L (2010) CRL4(Cdt2)-mediated destruction of the histone methyltransferase Set8 prevents premature chromatin compaction in S phase. Molecular Cell **40:** 22-33

Chabes A, Georgieva B, Domkin V, Zhao X, Rothstein R, Thelander L (2003) Survival of DNA damage in yeast directly depends on increased dNTP levels allowed by relaxed feedback inhibition of ribonucleotide reductase. Cell **112:** 391-401

Chailleux C, Tyteca S, Papin C, Boudsocq F, Puget N, Courilleau C, Grigoriev M, Canitrot Y, Trouche D (2010) Physical interaction between the histone acetyl transferase Tip60 and the DNA double-strand breaks sensor MRN complex. The Biochemical Journal **426:** 365-371

Chappell C, Hanakahi LA, Karimi-Busheri F, Weinfeld M, West SC (2002) Involvement of human polynucleotide kinase in double-strand break repair by non-homologous end joining. The EMBO Journal **21:** 2827-2832

Chen CC, Carson JJ, Feser J, Tamburini B, Zabaronick S, Linger J, Tyler JK (2008) Acetylated lysine 56 on histone H3 drives chromatin assembly after repair and signals for the completion of repair. Cell **134:** 231-243

Chen D, Toone WM, Mata J, Lyne R, Burns G, Kivinen K, Brazma A, Jones N, Bahler J (2003) Global transcriptional responses of fission yeast to environmental stress. Molecular Biology of the Cell **14:** 214-229

Chen XB, Melchionna R, Denis CM, Gaillard PH, Blasina A, Van de Weyer I, Boddy MN, Russell P, Vialard J, McGowan CH (2001) Human Mus81-associated endonuclease cleaves Holliday junctions in vitro. Molecular Cell **8:** 1117-1127

Chernikova SB, Dorth JA, Razorenova OV, Game JC, Brown JM (2010) Deficiency in Bre1 impairs homologous recombination repair and cell cycle checkpoint response to radiation damage in mammalian cells. Radiation Research **174:** 558-565

Chernikova SB, Razorenova OV, Higgins JP, Sishc BJ, Nicolau M, Dorth JA, Chernikova DA, Kwok S, Brooks JD, Bailey SM, Game JC, Brown JM (2012) Deficiency in mammalian histone H2B ubiquitin ligase Bre1 (Rnf20/Rnf40) leads to replication stress and chromosomal instability. Cancer Research **72:** 2111-2119

Cheung V, Chua G, Batada NN, Landry CR, Michnick SW, Hughes TR, Winston F (2008) Chromatin- and transcription-related factors repress transcription from within coding regions throughout the Saccharomyces cerevisiae genome. PLoS Biology **6:** e277

Chi P, San Filippo J, Sehorn MG, Petukhova GV, Sung P (2007) Bipartite stimulatory action of the Hop2-Mnd1 complex on the Rad51 recombinase. Genes & development **21:** 1747-1757

Chiani F, Di Felice F, Camilloni G (2006) SIR2 modifies histone H4-K16 acetylation and affects superhelicity in the ARS region of plasmid chromatin in Saccharomyces cerevisiae. Nucleic acids research **34:** 5426-5437

Chou CH, Wang J, Knuth MW, Reeves WH (1992) Role of a major autoepitope in forming the DNA binding site of the p70 (Ku) antigen. The Journal of Experimental Medicine 175: 1677-1684

Choudhury M, Pandey RS, Clemens DL, Davis JW, Lim RW, Shukla SD (2011) Knock down of GCN5 histone acetyltransferase by siRNA decreases ethanol-induced histone acetylation and affects differential expression of genes in human hepatoma cells. Alcohol **45:** 311-324

Chung WH, Zhu Z, Papusha A, Malkova A, Ira G (2010) Defective resection at DNA double-strand breaks leads to de novo telomere formation and enhances gene targeting. PLoS genetics **6:** e1000948

Ciccia A, Elledge SJ (2010) The DNA damage response: making it safe to play with knives. Molecular Cell **40:** 179-204

Clapier CR, Cairns BR (2009) The biology of chromatin remodeling complexes. Annual Review of Biochemistry **78**: 273-304

Clements A, Poux AN, Lo WS, Pillus L, Berger SL, Marmorstein R (2003) Structural basis for histone and phosphohistone binding by the GCN5 histone acetyltransferase. Molecular Cell **12:** 461-473

Clerici M, Mantiero D, Lucchini G, Longhese MP (2006) The Saccharomyces cerevisiae Sae2 protein negatively regulates DNA damage checkpoint signalling. EMBO Reports **7:** 212-218

Cohen TJ, Mallory MJ, Strich R, Yao TP (2008) Hos2p/Set3p deacetylase complex signals secretory stress through the Mpk1p cell integrity pathway. Eukaryotic Cell **7:** 1191-1199

Coleman TR, Dunphy WG (1994) Cdc2 regulatory factors. Current Opinion in Cell Biology **6:** 877-882

Corona DF, Tamkun JW (2004) Multiple roles for ISWI in transcription, chromosome organization and DNA replication. Biochimica et Biophysica Acta **1677**: 113-119

Costantini S, Woodbine L, Andreoli L, Jeggo PA, Vindigni A (2007) Interaction of the Ku heterodimer with the DNA ligase IV/Xrcc4 complex and its regulation by DNA-PK. DNA Repair **6:** 712-722

Cullen JK, Hussey SP, Walker C, Prudden J, Wee BY, Dave A, Findlay JS, Savory AP, Humphrey TC (2007) Break-induced loss of heterozygosity in fission yeast: dual roles for homologous recombination in promoting translocations and preventing de novo telomere addition. Molecular and Cellular Biology **27:** 7745-7757

Dalgliesh GL, Furge K, Greenman C, Chen L, Bignell G, Butler A, Davies H, Edkins S, Hardy C, Latimer C, Teague J, Andrews J, Barthorpe S, Beare D, Buck G, Campbell PJ, Forbes S, Jia M, Jones D, Knott H, Kok CY, Lau KW, Leroy C, Lin ML, McBride DJ, Maddison M, Maguire S, McLay K, Menzies A, Mironenko T, Mulderrig L, Mudie L, O'Meara S, Pleasance E, Rajasingham A, Shepherd R, Smith R, Stebbings L, Stephens P, Tang G, Tarpey PS, Turrell K, Dykema KJ, Khoo SK, Petillo D, Wondergem B, Anema J, Kahnoski RJ, Teh BT, Stratton MR, Futreal PA (2010) Systematic sequencing of renal carcinoma reveals inactivation of histone modifying genes. Nature **463:** 360-363

Das C, Lucia MS, Hansen KC, Tyler JK (2009) CBP/p300-mediated acetylation of histone H3 on lysine 56. Nature **459**: 113-117

Davey S, Nass ML, Ferrer JV, Sidik K, Eisenberger A, Mitchell DL, Freyer GA (1997) The fission yeast UVDR DNA repair pathway is inducible. Nucleic Acids Research **25:** 1002-1008

Davies KD, Cable PL, Garrus JE, Sullivan FX, von Carlowitz I, Huerou YL, Wallace E, Woessner RD, Gross S (2011) Chk1 inhibition and Wee1 inhibition combine synergistically to impede cellular proliferation. Cancer Biology & Therapy **12:** 788-796

Davis AJ, Chen DJ (2010) A role for ATM kinase activity and Mre11 in microhomology-mediated end-joining. Cell Cycle **9:** 3147-3148

de Bruin RA, Kalashnikova TI, Aslanian A, Wohlschlegel J, Chahwan C, Yates JR, 3rd, Russell P, Wittenberg C (2008) DNA replication checkpoint promotes G1-S transcription by inactivating the MBF repressor Nrm1. Proceedings of the National Academy of Sciences of the United States of America **105:** 11230-11235

de Bruin RA, Kalashnikova TI, Chahwan C, McDonald WH, Wohlschlegel J, Yates J, 3rd, Russell P, Wittenberg C (2006) Constraining G1-specific transcription to late G1 phase: the MBF-associated corepressor Nrm1 acts via negative feedback. Molecular Cell **23:** 483-496

de Bruin RA, Wittenberg C (2009) All eukaryotes: before turning off G1-S transcription, please check your DNA. Cell Cycle **8:** 214-217

Degols G, Russell P (1997) Discrete roles of the Spc1 kinase and the Atf1 transcription factor in the UV response of Schizosaccharomyces pombe. Molecular and Cellular Biology **17:** 3356-3363

Deriano L, Stracker TH, Baker A, Petrini JH, Roth DB (2009) Roles for NBS1 in alternative nonhomologous end-joining of V(D)J recombination intermediates. Molecular Cell **34:** 13-25

Detweiler CS, Li JJ (1998) Ectopic induction of Clb2 in early G1 phase is sufficient to block prereplicative complex formation in Saccharomyces cerevisiae. Proceedings of the National Academy of Sciences of the United States of America **95:** 2384-2389

Devault A, Vallen EA, Yuan T, Green S, Bensimon A, Schwob E (2002) Identification of Tah11/Sid2 as the ortholog of the replication licensing factor Cdt1 in Saccharomyces cerevisiae. Current Biology : CB **12:** 689-694

Dhalluin C, Carlson JE, Zeng L, He C, Aggarwal AK, Zhou MM (1999) Structure and ligand of a histone acetyltransferase bromodomain. Nature **399:** 491-496

Dianov GL, O'Neill P, Goodhead DT (2001) Securing genome stability by orchestrating DNA repair: removal of radiation-induced clustered lesions in DNA. BioEssays : news and reviews in molecular, cellular and developmental biology **23:** 745-749

Diffley JF (2004) Regulation of early events in chromosome replication. Current Biology : CB **14:** R778-786

Dixon SJ, Costanzo M, Baryshnikova A, Andrews B, Boone C (2009) Systematic mapping of genetic interaction networks. Annu Rev Genet **43:** 601-625.

Donovan S, Harwood J, Drury LS, Diffley JF (1997) Cdc6p-dependent loading of Mcm proteins onto pre-replicative chromatin in budding yeast. Proceedings of the National Academy of Sciences of the United States of America **94:** 5611-5616

Downs JA, Lowndes NF, Jackson SP (2000) A role for Saccharomyces cerevisiae histone H2A in DNA repair. Nature **408:** 1001-1004

Du HN, Fingerman IM, Briggs SD (2008) Histone H3 K36 methylation is mediated by a trans-histone methylation pathway involving an interaction between Set2 and histone H4. Genes & Development **22:** 2786-2798

Duncker BP, Shimada K, Tsai-Pflugfelder M, Pasero P, Gasser SM (2002) An N-terminal domain of Dbf4p mediates interaction with both origin recognition complex (ORC) and Rad53p and can deregulate late origin firing. Proceedings of the National Academy of Sciences of the United States of America **99:** 16087-16092

Duns G, van den Berg E, van Duivenbode I, Osinga J, Hollema H, Hofstra RM, Kok K (2010) Histone methyltransferase gene SETD2 is a novel tumor suppressor gene in clear cell renal cell carcinoma. Cancer Research **70:** 4287-4291

Dutta C, Patel PK, Rosebrock A, Oliva A, Leatherwood J, Rhind N (2008) The DNA replication checkpoint directly regulates MBF-dependent G1/S transcription. Molecular and Cellular Biology **28:** 5977-5985

Eggler AL, Inman RB, Cox MM (2002) The Rad51-dependent pairing of long DNA substrates is stabilized by replication protein A. The Journal of Biological Chemistry **277:** 39280-39288

El-Shemerly M, Hess D, Pyakurel AK, Moselhy S, Ferrari S (2008) ATR-dependent pathways control hEXO1 stability in response to stalled forks. Nucleic Acids Research **36:** 511-519

Elledge SJ, Zhou Z, Allen JB, Navas TA (1993) DNA damage and cell cycle regulation of ribonucleotide reductase. BioEssays : news and reviews in molecular, cellular and developmental biology **15:** 333-339

Espinosa MC, Rehman MA, Chisamore-Robert P, Jeffery D, Yankulov K (2010) GCN5 is a positive regulator of origins of DNA replication in Saccharomyces cerevisiae. PloS one **5:** e8964

Falbo KB, Shen X (2006) Chromatin remodeling in DNA replication. Journal of Cellular Biochemistry **97:** 684-689

Falck J, Coates J, Jackson SP (2005) Conserved modes of recruitment of ATM, ATR and DNA-PKcs to sites of DNA damage. Nature **434:** 605-611

Fang J, Feng Q, Ketel CS, Wang H, Cao R, Xia L, Erdjument-Bromage H, Tempst P, Simon JA, Zhang Y (2002) Purification and functional characterization of SET8, a nucleosomal histone H4-lysine 20-specific methyltransferase. Current Biology : CB **12:** 1086-1099

Fang R, Barbera AJ, Xu Y, Rutenberg M, Leonor T, Bi Q, Lan F, Mei P, Yuan GC, Lian C, Peng J, Cheng D, Sui G, Kaiser UB, Shi Y, Shi YG (2010) Human LSD2/KDM1b/AOF1 regulates gene transcription by modulating intragenic H3K4me2 methylation. Molecular Cell **39:** 222-233

Faucher D, Wellinger RJ (2010) Methylated H3K4, a transcription-associated histone modification, is involved in the DNA damage response pathway. PLoS Genetics **6**

Fekairi S, Scaglione S, Chahwan C, Taylor ER, Tissier A, Coulon S, Dong MQ, Ruse C, Yates JR, 3rd, Russell P, Fuchs RP, McGowan CH, Gaillard PH (2009) Human SLX4 is a Holliday junction resolvase subunit that binds multiple DNA repair/recombination endonucleases. Cell **138:** 78-89

Feng L, Chen J (2012) The E3 ligase RNF8 regulates KU80 removal and NHEJ repair. Nature Structural & Molecular Biology **19:** 201-206

Fernandez Sarabia MJ, McInerny C, Harris P, Gordon C, Fantes P (1993) The cell cycle genes cdc22+ and suc22+ of the fission yeast Schizosaccharomyces pombe encode the large and small subunits of ribonucleotide reductase. Molecular & General Genetics : MGG **238:** 241-251

Ferreira H, Flaus A, Owen-Hughes T (2007) Histone modifications influence the action of Snf2 family remodelling enzymes by different mechanisms. Journal of Molecular Biology **374**: 563-579

Ferreira MG, Cooper JP (2004) Two modes of DNA double-strand break repair are reciprocally regulated through the fission yeast cell cycle. Genes & Development **18:** 2249-2254

Fiorentini P, Huang KN, Tishkoff DX, Kolodner RD, Symington LS (1997) Exonuclease I of Saccharomyces cerevisiae functions in mitotic recombination in vivo and in vitro. Molecular and Cellular Biology **17:** 2764-2773

Fischle W, Tseng BS, Dormann HL, Ueberheide BM, Garcia BA, Shabanowitz J, Hunt DF, Funabiki H, Allis CD (2005) Regulation of HP1-chromatin binding by histone H3 methylation and phosphorylation. Nature **438:** 1116-1122

Fishman-Lobell J, Rudin N, Haber JE (1992) Two alternative pathways of double-strand break repair that are kinetically separable and independently modulated. Molecular and Cellular Biology **12:** 1292-1303

Fnu S, Williamson EA, De Haro LP, Brenneman M, Wray J, Shaheen M, Radhakrishnan K, Lee SH, Nickoloff JA, Hromas R (2011) Methylation of histone H3 lysine 36 enhances DNA repair by nonhomologous end-joining. Proceedings of the National Academy of Sciences of the United States of America **108:** 540-545

Fuchs SM, Kizer KO, Braberg H, Krogan NJ, Strahl BD (2012) RNA polymerase II carboxyl-terminal domain phosphorylation regulates protein stability of the Set2 methyltransferase and histone H3 di- and trimethylation at lysine 36. The Journal of Biological Chemistry **287:** 3249-3256

Fugger K, Mistrik M, Danielsen JR, Dinant C, Falck J, Bartek J, Lukas J, Mailand N (2009) Human Fbh1 helicase contributes to genome maintenance via pro- and anti-recombinase activities. The Journal of Cell Biology **186:** 655-663

Fukushima T, Takata M, Morrison C, Araki R, Fujimori A, Abe M, Tatsumi K, Jasin M, Dhar PK, Sonoda E, Chiba T, Takeda S (2001) Genetic analysis of the DNA-dependent protein kinase reveals an inhibitory role of Ku in late S-G2 phase DNA double-strand break repair. The Journal of Biological Chemistry **276:** 44413-44418

Gaillard PH, Noguchi E, Shanahan P, Russell P (2003) The endogenous Mus81-Eme1 complex resolves Holliday junctions by a nick and counternick mechanism. Molecular Cell **12:** 747-759

Garriga J, Grana X (2004) Cellular control of gene expression by T-type cyclin/CDK9 complexes. Gene **337:** 15-23

Ge Z, Wang H, Parthun MR (2011) Nuclear Hat1p complex (NuB4) components participate in DNA repair-linked chromatin reassembly. The Journal of Biological Chemistry **286:** 16790-16799

Gell D, Jackson SP (1999) Mapping of protein-protein interactions within the DNA-dependent protein kinase complex. Nucleic Acids Research **27:** 3494-3502

Gerber HB, Pikman Y, Fisher RP (2008) The CDK-activating kinase (CAK) Csk1 is required for normal levels of homologous recombination and resistance to DNA damage in fission yeast. PloS one **3:** e1492

Gerber M, Shilatifard A (2003) Transcriptional elongation by RNA polymerase II and histone methylation. The Journal of Biological Chemistry **278:** 26303-26306

Gomez EB, Espinosa JM, Forsburg SL (2005) Schizosaccharomyces pombe mst2+ encodes a MYST family histone acetyltransferase that negatively regulates telomere silencing. Mol Cell Biol **25:** 8887-8903

Grant PA, Duggan L, Cote J, Roberts SM, Brownell JE, Candau R, Ohba R, Owen-Hughes T, Allis CD, Winston F, Berger SL, Workman JL (1997) Yeast Gcn5 functions in two multisubunit complexes to acetylate nucleosomal histones: characterization of an Ada complex and the SAGA (Spt/Ada) complex. Genes & Development **11:** 1640-1650

Green EM, Mas G, Young NL, Garcia BA, Gozani O (2012) Methylation of H4 lysines 5, 8 and 12 by yeast Set5 calibrates chromatin stress responses. Nature Structural & Molecular Biology **19:** 361-363

Greenberg RA (2011) Histone tails: Directing the chromatin response to DNA damage. FEBS letters **585:** 2883-2890

Greeson NT, Sengupta R, Arida AR, Jenuwein T, Sanders SL (2008) Di-methyl H4 lysine 20 targets the checkpoint protein Crb2 to sites of DNA damage. The Journal of Biological Chemistry **283:** 33168-33174

Groth A, Rocha W, Verreault A, Almouzni G (2007) Chromatin challenges during DNA replication and repair. Cell **128:** 721-733

Gu J, Lu H, Tsai AG, Schwarz K, Lieber MR (2007) Single-stranded DNA ligation and XLF-stimulated incompatible DNA end ligation by the XRCC4-DNA ligase IV complex: influence of terminal DNA sequence. Nucleic Acids Research **35:** 5755-5762

Guarino E, Shepherd ME, Salguero I, Hua H, Deegan RS, Kearsey SE (2011) Cdt1 proteolysis is promoted by dual PIP degrons and is modulated by PCNA ubiquitylation. Nucleic Acids Research **39:** 5978-5990

Guiguen A, Soutourina J, Dewez M, Tafforeau L, Dieu M, Raes M, Vandenhaute J, Werner M, Hermand D (2007) Recruitment of P-TEFb (Cdk9-Pch1) to chromatin by the cap-methyl transferase Pcm1 in fission yeast. The EMBO Journal **26:** 1552-1559

Guirouilh-Barbat J, Huck S, Bertrand P, Pirzio L, Desmaze C, Sabatier L, Lopez BS (2004) Impact of the KU80 pathway on NHEJ-induced genome rearrangements in mammalian cells. Molecular Cell **14:** 611-623

Gunjan A, Paik J, Verreault A (2005) Regulation of histone synthesis and nucleosome assembly. Biochimie **87:** 625-635

Guo R, Chen J, Mitchell DL, Johnson DG (2011) GCN5 and E2F1 stimulate nucleotide excision repair by promoting H3K9 acetylation at sites of damage. Nucleic Acids Research **39:** 1390-1397

Haber JE (1999) DNA recombination: the replication connection. Trends in Biochemical Sciences **24:** 271-275

Hampsey M, Reinberg D (2003) Tails of intrigue: phosphorylation of RNA polymerase II mediates histone methylation. Cell **113:** 429-432

Han L, Yu K (2008) Altered kinetics of nonhomologous end joining and class switch recombination in ligase IV-deficient B cells. The Journal of Experimental Medicine **205:** 2745-2753

Haruta N, Kurokawa Y, Murayama Y, Akamatsu Y, Unzai S, Tsutsui Y, Iwasaki H (2006) The Swi5-Sfr1 complex stimulates Rhp51/Rad51- and Dmc1-mediated DNA strand exchange in vitro. Nature Structural & Molecular Biology **13:** 823-830

Hayashi A, Ding DQ, Tsutsumi C, Chikashige Y, Masuda H, Haraguchi T, Hiraoka Y (2009) Localization of gene products using a chromosomally tagged GFP-fusion library in the fission yeast Schizosaccharomyces pombe. Genes to Cells : devoted to molecular & cellular mechanisms **14:** 217-225

Henikoff S (2008) Nucleosome destabilization in the epigenetic regulation of gene expression. Nature Reviews Genetics **9**: 15-26

Heyer WD, Li X, Rolfsmeier M, Zhang XP (2006) Rad54: the Swiss Army knife of homologous recombination? Nucleic Acids Research **34:** 4115-4125

Heyer WD, Rao MR, Erdile LF, Kelly TJ, Kolodner RD (1990) An essential Saccharomyces cerevisiae single-stranded DNA binding protein is homologous to the large subunit of human RP-A. The EMBO Journal **9:** 2321-2329

Heyer, W.D., Ehmsen, K.T., and Liu, J. (2010). Regulation of homologous recombination in eukaryotes. Annual Review Genetics **44**: 113-139.

Hofmann JF, Beach D (1994) cdt1 is an essential target of the Cdc10/Sct1 transcription factor: requirement for DNA replication and inhibition of mitosis. The EMBO Journal **13:** 425-434

Holmberg C, Fleck O, Hansen HA, Liu C, Slaaby R, Carr AM, Nielsen O (2005) Ddb1 controls genome stability and meiosis in fission yeast. Genes & Development **19:** 853-862

Horak CE, Luscombe NM, Qian J, Bertone P, Piccirrillo S, Gerstein M, Snyder M (2002) Complex transcriptional circuitry at the G1/S transition in Saccharomyces cerevisiae. Genes & Development **16:** 3017-3033

Howe L, Auston D, Grant P, John S, Cook RG, Workman JL, Pillus L (2001) Histone H3 specific acetyltransferases are essential for cell cycle progression. Genes & Development **15:** 3144-3154

Hsu HL, Yannone SM, Chen DJ (2002) Defining interactions between DNA-PK and ligase IV/XRCC4. DNA repair **1:** 225-235

Hu J, Xiong Y (2006) An evolutionarily conserved function of proliferating cell nuclear antigen for Cdt1 degradation by the Cul4-Ddb1 ubiquitin ligase in response to DNA damage. The Journal of Biological Chemistry **281:** 3753-3756

Huang N, vom Baur E, Garnier JM, Lerouge T, Vonesch JL, Lutz Y, Chambon P, Losson R (1998) Two distinct nuclear receptor interaction domains in NSD1, a novel SET protein that exhibits characteristics of both corepressors and coactivators. The EMBO Journal **17:** 3398-3412

Hubscher U, Maga G, Spadari S (2002) Eukaryotic DNA polymerases. Annual Review of Biochemistry **71:** 133-163

Hudlebusch HR, Santoni-Rugiu E, Simon R, Ralfkiaer E, Rossing HH, Johansen JV, Jorgensen M, Sauter G, Helin K (2011) The histone methyltransferase and putative oncoprotein MMSET is overexpressed in a large variety of human tumors. Clinical Cancer Research : an official journal of the American Association for Cancer Research **17:** 2919-2933

Huen MS, Grant R, Manke I, Minn K, Yu X, Yaffe MB, Chen J (2007) RNF8 transduces the DNA-damage signal via histone ubiquitylation and checkpoint protein assembly. Cell **131:** 901-914

Huen MS, Sy SM, van Deursen JM, Chen J (2008) Direct interaction between SET8 and proliferating cell nuclear antigen couples H4-K20 methylation with DNA replication. The Journal of Biological Chemistry **283:** 11073-11077

Huertas P, Cortes-Ledesma F, Sartori AA, Aguilera A, Jackson SP (2008) CDK targets Sae2 to control DNA-end resection and homologous recombination. Nature **455:** 689-692

Huisinga KL, Brower-Toland B, Elgin SC (2006) The contradictory definitions of heterochromatin: transcription and silencing. Chromosoma **115:** 110-122

Huisinga KL, Pugh BF (2004) A genome-wide housekeeping role for TFIID and a highly regulated stress-related role for SAGA in Saccharomyces cerevisiae. Molecular Cell **13:** 573-585

Huyen Y, Zgheib O, Ditullio RA, Jr., Gorgoulis VG, Zacharatos P, Petty TJ, Sheston EA, Mellert HS, Stavridi ES, Halazonetis TD (2004) Methylated lysine 79 of histone H3 targets 53BP1 to DNA double-strand breaks. Nature **432:** 406-411

Iizuka M, Matsui T, Takisawa H, Smith MM (2006) Regulation of replication licensing by acetyltransferase Hbo1. Molecular and Cellular Biology **26:** 1098-1108

Ikura T, Tashiro S, Kakino A, Shima H, Jacob N, Amunugama R, Yoder K, Izumi S, Kuraoka I, Tanaka K, Kimura H, Ikura M, Nishikubo S, Ito T, Muto A, Miyagawa K, Takeda S, Fishel R, Igarashi K, Kamiya K (2007) DNA damage-dependent acetylation and ubiquitination of H2AX enhances chromatin dynamics. Molecular and Cellular Biology **27:** 7028-7040

Ip SC, Rass U, Blanco MG, Flynn HR, Skehel JM, West SC (2008) Identification of Holliday junction resolvases from humans and yeast. Nature **456:** 357-361

Ira G, Malkova A, Liberi G, Foiani M, Haber JE (2003) Srs2 and Sgs1-Top3 suppress crossovers during double-strand break repair in yeast. Cell **115:** 401-411

Ira G, Pellicioli A, Balijja A, Wang X, Fiorani S, Carotenuto W, Liberi G, Bressan D, Wan L, Hollingsworth NM, Haber JE, Foiani M (2004) DNA end resection, homologous recombination and DNA damage checkpoint activation require CDK1. Nature **431:** 1011-1017

Ishii T, Shiomi Y, Takami T, Murakami Y, Ohnishi N, Nishitani H (2010) Proliferating cell nuclear antigen-dependent rapid recruitment of Cdt1 and CRL4Cdt2 at DNA-damaged sites after UV irradiation in HeLa cells. The Journal of Biological Chemistry **285:** 41993-42000

Jackson SP (1997) Genomic stability. Silencing and DNA repair connect. Nature **388:** 829-830

Jackson SP, Bartek J (2009) The DNA-damage response in human biology and disease. Nature **461:** 1071-1078

Jackson WT, Martin GS (2006) Transcription of the Schizosaccharomyces pombe gene cdc18+: roles of MCB elements and the DSC1 complex. Gene **369:** 100-108

Jallepalli PV, Brown GW, Muzi-Falconi M, Tien D, Kelly TJ (1997) Regulation of the replication initiator protein p65cdc18 by CDK phosphorylation. Genes & Development **11:** 2767-2779

Jazayeri A, McAinsh AD, Jackson SP (2004) Saccharomyces cerevisiae Sin3p facilitates DNA double-strand break repair. Proceedings of the National Academy of Sciences of the United States of America **101:** 1644-1649

Jenuwein T, Allis CD (2001) Translating the histone code. Science **293:** 1074-1080

Jenuwein T, Laible G, Dorn R, Reuter G (1998) SET domain proteins modulate chromatin domains in eu- and heterochromatin. Cellular and Molecular Life Sciences : CMLS **54:** 80-93

Jin J, Arias EE, Chen J, Harper JW, Walter JC (2006) A family of diverse Cul4-Ddb1-interacting proteins includes Cdt2, which is required for S phase destruction of the replication factor Cdt1. Molecular Cell **23:** 709-721

Johnsson A, Durand-Dubief M, Xue-Franzen Y, Ronnerblad M, Ekwall K, Wright A (2009) HAT-HDAC interplay modulates global histone H3K14 acetylation in gene-coding regions during stress. EMBO Reports **10:** 1009-1014

Johnsson A, Xue-Franzen Y, Lundin M, Wright AP (2006) Stress-specific role of fission yeast Gcn5 histone acetyltransferase in programming a subset of stress response genes. Eukaryotic Cell **5:** 1337-1346

Jorgensen S, Elvers I, Trelle MB, Menzel T, Eskildsen M, Jensen ON, Helleday T, Helin K, Sorensen CS (2007) The histone methyltransferase SET8 is required for S-phase progression. The Journal of Cell Biology **179:** 1337-1345

Joshi AA, Struhl K (2005) Eaf3 chromodomain interaction with methylated H3-K36 links histone deacetylation to Pol II elongation. Molecular Cell **20:** 971-978

Kabotyanski EB, Gomelsky L, Han JO, Stamato TD, Roth DB (1998) Double-strand break repair in Ku86- and XRCC4-deficient cells. Nucleic Acids Research **26:** 5333-5342

Kadyk LC, Hartwell LH (1992) Sister chromatids are preferred over homologs as substrates for recombinational repair in Saccharomyces cerevisiae. Genetics **132:** 387-402

Kanoh J, Francesconi S, Collura A, Schramke V, Ishikawa F, Baldacci G, Geli V (2003) The fission yeast spSet1p is a histone H3-K4 methyltransferase that functions in telomere maintenance and DNA repair in an ATM kinase Rad3-dependent pathway. J Mol Biol **326:** 1081-1094

Kaplan CD, Laprade L, Winston F (2003) Transcription elongation factors repress transcription initiation from cryptic sites. Science **301:** 1096-1099

Karagiannis J, Balasubramanian MK (2007) A cyclin-dependent kinase that promotes cytokinesis through modulating phosphorylation of the carboxy terminal domain of the RNA Pol II Rpb1p sub-unit. PloS One **2:** e433

Karow JK, Constantinou A, Li JL, West SC, Hickson ID (2000) The Bloom's syndrome gene product promotes branch migration of holliday junctions. Proceedings of the National Academy of Sciences of the United States of America **97:** 6504-6508

Kassambara A, Klein B, Moreaux J (2009) MMSET is overexpressed in cancers: link with tumor aggressiveness. Biochemical and Biophysical Research Communications **379:** 840-845

Kastan MB, Bartek J (2004) Cell-cycle checkpoints and cancer. Nature **432:** 316-323

Kasten M, Szerlong H, Erdjument-Bromage H, Tempst P, Werner M, Cairns BR (2004) Tandem bromodomains in the chromatin remodeler RSC recognize acetylated histone H3 Lys14. The EMBO Journal **23:** 1348-1359

Kearsey SE, Cotterill S (2003) Enigmatic variations: divergent modes of regulating eukaryotic DNA replication. Molecular Cell **12:** 1067-1075

Kelly TJ, Martin GS, Forsburg SL, Stephen RJ, Russo A, Nurse P (1993) The fission yeast cdc18+ gene product couples S phase to START and mitosis. Cell **74:** 371-382

Keogh MC, Kurdistani SK, Morris SA, Ahn SH, Podolny V, Collins SR, Schuldiner M, Chin K, Punna T, Thompson NJ, Boone C, Emili A, Weissman JS, Hughes TR, Strahl BD, Grunstein M, Greenblatt JF, Buratowski

S, Krogan NJ (2005) Cotranscriptional set2 methylation of histone H3 lysine 36 recruits a repressive Rpd3 complex. Cell **123:** 593-605

Kim DU, Hayles J, Kim D, Wood V, Park HO, Won M, Yoo HS, Duhig T, Nam M, Palmer G, Han S, Jeffery L, Baek ST, Lee H, Shim YS, Lee M, Kim L, Heo KS, Noh EJ, Lee AR, Jang YJ, Chung KS, Choi SJ, Park JY, Park Y, Kim HM, Park SK, Park HJ, Kang EJ, Kim HB, Kang HS, Park HM, Kim K, Song K, Song KB, Nurse P, Hoe KL (2010) Analysis of a genome-wide set of gene deletions in the fission yeast Schizosaccharomyces pombe. Nature biotechnology **28:** 617-623

Kim HS, Rhee DK, Jang YK (2008) Methylations of histone H3 lysine 9 and lysine 36 are functionally linked to DNA replication checkpoint control in fission yeast. Biochemical and Biophysical Research Communications **368:** 419-425

Kim J, Daniel J, Espejo A, Lake A, Krishna M, Xia L, Zhang Y, Bedford MT (2006a) Tudor, MBT and chromo domains gauge the degree of lysine methylation. EMBO Reports **7:** 397-403

Kim SC, Sprung R, Chen Y, Xu Y, Ball H, Pei J, Cheng T, Kho Y, Xiao H, Xiao L, Grishin NV, White M, Yang XJ, Zhao Y (2006b) Substrate and functional diversity of lysine acetylation revealed by a proteomics survey. Molecular Cell 23: 607-618

Kim PM, Paffett KS, Solinger JA, Heyer WD, Nickoloff JA (2002) Spontaneous and double-strand break-induced recombination, and gene conversion tract lengths, are differentially affected by overexpression of wild-type or ATPase-defective yeast Rad54. Nucleic Acids Research **30:** 2727-2735

Kim T, Buratowski S (2009) Dimethylation of H3K4 by Set1 recruits the Set3 histone deacetylase complex to 5' transcribed regions. Cell **137:** 259-272

Kizer KO, Phatnani HP, Shibata Y, Hall H, Greenleaf AL, Strahl BD (2005) A novel domain in Set2 mediates RNA polymerase II interaction and couples histone H3 K36 methylation with transcript elongation. Mol Cell Biol **25:** 3305-3316

Klose RJ, Gardner KE, Liang G, Erdjument-Bromage H, Tempst P, Zhang Y (2007) Demethylation of histone H3K36 and H3K9 by Rph1: a vestige of an H3K9 methylation system in Saccharomyces cerevisiae? Molecular and Cellular Biology 27: 3951-396

Klose RJ, Yamane K, Bae Y, Zhang D, Erdjument-Bromage H, Tempst P, Wong J, Zhang Y (2006) The transcriptional repressor JHDM3A demethylates trimethyl histone H3 lysine 9 and lysine 36. Nature 442: 312-316

Kominami K, Toda T (1997) Fission yeast WD-repeat protein pop1 regulates genome ploidy through ubiquitin-proteasome-mediated degradation of the CDK inhibitor Rum1 and the S-phase initiator Cdc18. Genes & Development **11:** 1548-1560

Kotian S, Liyanarachchi S, Zelent A, Parvin JD (2011) Histone deacetylases 9 and 10 are required for homologous recombination. The Journal of Biological Chemistry **286:** 7722-7726

Kouzarides T (2007) Chromatin modifications and their function. Cell **128:** 693-705

Krejci L, Van Komen S, Li Y, Villemain J, Reddy MS, Klein H, Ellenberger T, Sung P (2003) DNA helicase Srs2 disrupts the Rad51 presynaptic filament. Nature **423:** 305-309

Kristjuhan A, Wittschieben BO, Walker J, Roberts D, Cairns BR, Svejstrup JQ (2003) Spreading of Sir3 protein in cells with severe histone H3 hypoacetylation. Proceedings of the National Academy of Sciences of the United States of America **100:** 7551-7556

Krogan NJ, Kim M, Tong A, Golshani A, Cagney G, Canadien V, Richards DP, Beattie BK, Emili A, Boone C, Shilatifard A, Buratowski S, Greenblatt J (2003) Methylation of histone H3 by Set2 in Saccharomyces cerevisiae is linked to transcriptional elongation by RNA polymerase II. Molecular and Cellular Biology **23:** 4207-4218

Krogh BO, Symington LS (2004) Recombination proteins in yeast. Annual Review of Genetics **38:** 233-271

Labib K, Tercero JA, Diffley JF (2000) Uninterrupted MCM2-7 function required for DNA replication fork progression. Science **288:** 1643-1647

Lan F, Zaratiegui M, Villen J, Vaughn MW, Verdel A, Huarte M, Shi Y, Gygi SP, Moazed D, Martienssen RA (2007) S. pombe LSD1 homologs regulate heterochromatin propagation and euchromatic gene transcription. Molecular Cell 26: 89-101

Landry J, Sutton A, Hesman T, Min J, Xu RM, Johnston M, Sternglanz R (2003) Set2-catalyzed methylation of histone H3 represses basal expression of GAL4 in Saccharomyces cerevisiae. Molecular and Cellular Biology **23:** 5972-5978

Langerak P, Mejia-Ramirez E, Limbo O, Russell P (2011) Release of Ku and MRN from DNA ends by Mre11 nuclease activity and Ctp1 is required for homologous recombination repair of double-strand breaks. PLoS Genetics **7:** e1002271

Lee C, Hong B, Choi JM, Kim Y, Watanabe S, Ishimi Y, Enomoto T, Tada S, Cho Y (2004) Structural basis for inhibition of the replication licensing factor Cdt1 by geminin. Nature **430:** 913-917

Lee HS, Park JH, Kim SJ, Kwon SJ, Kwon J (2010) A cooperative activation loop among SWI/SNF, gamma-H2AX and H3 acetylation for DNA double-strand break repair. The EMBO Journal **29:** 1434-1445

Lee JH, Skalnik DG (2005) CpG-binding protein (CXXC finger protein 1) is a component of the mammalian Set1 histone H3-Lys4 methyltransferase complex, the analogue of the yeast Set1/COMPASS complex. The Journal of Biological Chemistry **280:** 41725-41731

Lee JS, Shukla A, Schneider J, Swanson SK, Washburn MP, Florens L, Bhaumik SR, Shilatifard A (2007) Histone crosstalk between H2B monoubiquitination and H3 methylation mediated by COMPASS. Cell **131:** 1084-1096

Lee KJ, Huang J, Takeda Y, Dynan WS (2000) DNA ligase IV and XRCC4 form a stable mixed tetramer that functions synergistically with other repair factors in a cell-free end-joining system. The Journal of Biological Chemistry **275:** 34787-34796

Lee KM, Saiz JE, Barton WA, Fisher RP (1999a) Cdc2 activation in fission yeast depends on Mcs6 and Csk1, two partially redundant Cdk-activating kinases (CAKs). Current Biology : CB **9:** 441-444

Lee SE, Moore JK, Holmes A, Umezu K, Kolodner RD, Haber JE (1998) Saccharomyces Ku70, mre11/rad50 and RPA proteins regulate adaptation to G2/M arrest after DNA damage. Cell **94:** 399-409

Lee SE, Paques F, Sylvan J, Haber JE (1999b) Role of yeast SIR genes and mating type in directing DNA double-strand breaks to homologous and non-homologous repair paths. Current Biology : CB **9:** 767-770

Leijen S, Beijnen JH, Schellens JH (2010) Abrogation of the G2 checkpoint by inhibition of Wee-1 kinase results in sensitization of p53-deficient tumor cells to DNA-damaging agents. Current Clinical Pharmacology **5:** 186-191

Lengauer C, Kinzler KW, Vogelstein B (1998) Genetic instabilities in human cancers. Nature **396:** 643-649

Li B, Gogol M, Carey M, Pattenden SG, Seidel C, Workman JL (2007) Infrequently transcribed long genes depend on the Set2/Rpd3S pathway for accurate transcription. Genes & Development **21:** 1422-1430

Li B, Howe L, Anderson S, Yates JR, 3rd, Workman JL (2003) The Set2 histone methyltransferase functions through the phosphorylated carboxyl-terminal domain of RNA polymerase II. The Journal of Biological Chemistry **278:** 8897-8903

Li Q, Fazly AM, Zhou H, Huang S, Zhang Z, Stillman B (2009) The elongator complex interacts with PCNA and modulates transcriptional silencing and sensitivity to DNA damage agents. PLoS Genetics **5:** e1000684

Li X, Manley JL (2006) Cotranscriptional processes and their influence on genome stability. Genes & Development **20:** 1838-1847

Li Y, Jaramillo-Lambert A, Hao J, Yang Y, Zhu W (2011) The stability of histone acetyltransferase general control non-derepressible (Gcn) 5 is regulated by Cullin4-RING E3 ubiquitin ligase. The Journal of Biological Chemistry **286:** 41344-41352

Lickwar CR, Rao B, Shabalin AA, Nobel AB, Strahl BD, Lieb JD (2009) The Set2/Rpd3S pathway suppresses cryptic transcription without regard to gene length or transcription frequency. PloS One **4:** e4886

Lieber MR (2010) The mechanism of double-strand DNA break repair by the nonhomologous DNA end-joining pathway. Annual Review of Biochemistry **79:** 181-211

Lima-de-Faria A, Jaworska H (1968) Late DNA synthesis in heterochromatin. Nature **217:** 138-142

Limbo O, Chahwan C, Yamada Y, de Bruin RA, Wittenberg C, Russell P (2007) Ctp1 is a cell-cycle-regulated protein that functions with Mre11 complex to control double-strand break repair by homologous recombination. Molecular Cell **28:** 134-146

Lindsay HD, Griffiths DJ, Edwards RJ, Christensen PU, Murray JM, Osman F, Walworth N, Carr AM (1998) S-phase-specific activation of Cds1 kinase defines a subpathway of the checkpoint response in Schizosaccharomyces pombe. Genes & Development **12:** 382-395

Liskay RM, Letsou A, Stachelek JL (1987) Homology requirement for efficient gene conversion between duplicated chromosomal sequences in mammalian cells. Genetics **115:** 161-167

Liu C, Poitelea M, Watson A, Yoshida SH, Shimoda C, Holmberg C, Nielsen O, Carr AM (2005) Transactivation of Schizosaccharomyces pombe cdt2+ stimulates a Pcu4-Ddb1-CSN ubiquitin ligase. The EMBO Journal **24:** 3940-3951

Liu C, Powell KA, Mundt K, Wu L, Carr AM, Caspari T (2003) Cop9/signalosome subunits and Pcu4 regulate ribonucleotide reductase by both checkpoint-dependent and -independent mechanisms. Genes & Development **17:** 1130-1140

Liu J, Renault L, Veaute X, Fabre F, Stahlberg H, Heyer WD (2011) Rad51 paralogues Rad55-Rad57 balance the antirecombinase Srs2 in Rad51 filament formation. Nature **479:** 245-248

Ljungman M (2010) The DNA damage response--repair or despair? Environmental and Molecular Mutagenesis **51:** 879-889

Llorente B, Smith CE, Symington LS (2008) Break-induced replication: what is it and what is it for? Cell Cycle **7:** 859-864

Llorente B, Symington LS (2004) The Mre11 nuclease is not required for 5' to 3' resection at multiple HO-induced double-strand breaks. Molecular and Cellular Biology **24:** 9682-9694

Lowndes NF, McInerny CJ, Johnson AL, Fantes PA, Johnston LH (1992) Control of DNA synthesis genes in fission yeast by the cell-cycle gene cdc10+. Nature **355:** 449-453

Lucio-Eterovic AK, Singh MM, Gardner JE, Veerappan CS, Rice JC, Carpenter PB (2010) Role for the nuclear receptor-binding SET domain protein 1 (NSD1) methyltransferase in coordinating lysine 36 methylation at histone 3 with RNA polymerase II function. Proceedings of the National Academy of Sciences of the United States of America **107:** 16952-16957

Luger K, Mader AW, Richmond RK, Sargent DF, Richmond TJ (1997) Crystal structure of the nucleosome core particle at 2.8 A resolution. Nature **389:** 251-260

Lydeard JR, Lipkin-Moore Z, Sheu YJ, Stillman B, Burgers PM, Haber JE (2010) Break-induced replication requires all essential DNA replication factors except those specific for pre-RC assembly. Genes & Development **24:** 1133-1144

Ma Y, Pannicke U, Schwarz K, Lieber MR (2002) Hairpin opening and overhang processing by an Artemis/DNA-dependent protein kinase complex in nonhomologous end joining and V(D)J recombination. Cell **108:** 781-794

Maga G, Hubscher U (2003) Proliferating cell nuclear antigen (PCNA): a dancer with many partners. Journal of Cell Science **116:** 3051-3060

Mahajan KN, Gangi-Peterson L, Sorscher DH, Wang J, Gathy KN, Mahajan NP, Reeves WH, Mitchell BS (1999) Association of terminal deoxynucleotidyl transferase with Ku. Proceedings of the National Academy of Sciences of the United States of America **96:** 13926-13931

Mahajan KN, Nick McElhinny SA, Mitchell BS, Ramsden DA (2002) Association of DNA polymerase mu (pol mu) with Ku and ligase IV: role for pol mu in end-joining double-strand break repair. Molecular and Cellular Biology **22:** 5194-5202

Maiorano D, Rul W, Mechali M (2004) Cell cycle regulation of the licensing activity of Cdt1 in Xenopus laevis. Experimental Cell Research **295:** 138-149

Mallette FA, Mattiroli F, Cui G, Young LC, Hendzel MJ, Mer G, Sixma TK, Richard S (2012) RNF8- and RNF168-dependent degradation of KDM4A/JMJD2A triggers 53BP1 recruitment to DNA damage sites. The EMBO Journal **31:** 1865-1878

Mandell JG, Goodrich KJ, Bahler J, Cech TR (2005) Expression of a RecQ helicase homolog affects progression through crisis in fission yeast lacking telomerase. The Journal of Biological Chemistry **280:** 5249-5257

Mankouri HW, Hickson ID (2006) Top3 processes recombination intermediates and modulates checkpoint activity after DNA damage. Molecular Biology of the Cell **17:** 4473-4483

Maqbool Z, Kersey PJ, Fantes PA, McInerny CJ (2003) MCB-mediated regulation of cell cycle-specific cdc22+ transcription in fission yeast. Molecular Genetics and Genomics : MGG **269:** 765-775

Marango J, Shimoyama M, Nishio H, Meyer JA, Min DJ, Sirulnik A, Martinez-Martinez Y, Chesi M, Bergsagel PL, Zhou MM, Waxman S, Leibovitch BA, Walsh MJ, Licht JD (2008) The MMSET protein is a histone methyltransferase with characteristics of a transcriptional corepressor. Blood **111:** 3145-3154

Maresca TJ, Heald R (2006) The long and the short of it: linker histone H1 is required for metaphase chromosome compaction. Cell Cycle **5:** 589-591

Marfella CG, Imbalzano AN (2007) The Chd family of chromatin remodelers. Mutation Research **618**: 30-40

Mari PO, Florea BI, Persengiev SP, Verkaik NS, Bruggenwirth HT, Modesti M, Giglia-Mari G, Bezstarosti K, Demmers JA, Luider TM, Houtsmuller AB, van Gent DC (2006) Dynamic assembly of end-joining complexes requires interaction between Ku70/80 and XRCC4. Proceedings of the National Academy of Sciences of the United States of America **103:** 18597-18602

Marmorstein R (2001) Structure of histone acetyltransferases. Journal of Molecular Biology **311:** 433-444

Maurer-Stroh S, Dickens NJ, Hughes-Davies L, Kouzarides T, Eisenhaber F, Ponting CP (2003) The Tudor domain 'Royal Family': Tudor, plant Agenet, Chromo, PWWP and MBT domains. Trends in Biochemical Sciences **28:** 69-74

Mazin AV, Alexeev AA, Kowalczykowski SC (2003) A novel function of Rad54 protein. Stabilization of the Rad51 nucleoprotein filament. The Journal of Biological Chemistry **278:** 14029-14036

McGarry TJ, Kirschner MW (1998) Geminin, an inhibitor of DNA replication, is degraded during mitosis. Cell **93:** 1043-1053

McInerny CJ, Kersey PJ, Creanor J, Fantes PA (1995) Positive and negative roles for cdc10 in cell cycle gene expression. Nucleic Acids Research **23:** 4761-4768

McKinnon PJ, Caldecott KW (2007) DNA strand break repair and human genetic disease. Annual Review of Genomics and Human Genetics **8:** 37-55

McVey M, Lee SE (2008) MMEJ repair of double-strand breaks (director's cut): deleted sequences and alternative endings. Trends in Genetics : TIG **24:** 529-538

Michel B (2000) Replication fork arrest and DNA recombination. Trends in Biochemical Sciences **25:** 173-178

Mickelsen S, Snyder C, Trujillo K, Bogue M, Roth DB, Meek K (1999) Modulation of terminal deoxynucleotidyltransferase activity by the DNA-dependent protein kinase. Journal of Immunology **163:** 834-843

Miller KM, Tjeertes JV, Coates J, Legube G, Polo SE, Britton S, Jackson SP (2010) Human HDAC1 and HDAC2 function in the DNA-damage response to promote DNA nonhomologous end-joining. Nature Structural & Molecular Biology **17:** 1144-1151

Mimitou EP, Symington LS (2008) Sae2, Exo1 and Sgs1 collaborate in DNA double-strand break processing. Nature **455:** 770-774

Mimitou EP, Symington LS (2009) DNA end resection: many nucleases make light work. DNA Repair **8:** 983-995

Mimitou EP, Symington LS (2010) Ku prevents Exo1 and Sgs1-dependent resection of DNA ends in the absence of a functional MRX complex or Sae2. The EMBO Journal **29:** 3358-3369

Miotto B, Struhl K (2008) HBO1 histone acetylase is a coactivator of the replication licensing factor Cdt1. Genes & Development **22:** 2633-2638

Miotto B, Struhl K (2010) HBO1 histone acetylase activity is essential for DNA replication licensing and inhibited by Geminin. Molecular Cell **37:** 57-66

Mohrmann L, Verrijzer CP (2005) Composition and functional specificity of SWI2/SNF2 class chromatin remodeling complexes. Biochimica et Biophysica Acta **1681**: 59-73

Moore JK, Haber JE (1996) Cell cycle and genetic requirements of two pathways of nonhomologous end-joining repair of double-strand breaks in Saccharomyces cerevisiae. Molecular and Cellular Biology **16:** 2164-2173

Moreno S, Klar A, Nurse P (1991) Molecular genetic analysis of fission yeast Schizosaccharomyces pombe. Methods Enzymol **194:** 795-823

Morin I, Ngo HP, Greenall A, Zubko MK, Morrice N, Lydall D (2008) Checkpoint-dependent phosphorylation of Exo1 modulates the DNA damage response. The EMBO Journal **27:** 2400-2410

Morris SA, Rao B, Garcia BA, Hake SB, Diaz RL, Shabanowitz J, Hunt DF, Allis CD, Lieb JD, Strahl BD (2007) Identification of histone H3 lysine 36 acetylation as a highly conserved histone modification. The Journal of Biological Chemistry **282:** 7632-7640

Morris SA, Shibata Y, Noma K, Tsukamoto Y, Warren E, Temple B, Grewal SI, Strahl BD (2005) Histone H3 K36 methylation is associated with transcription elongation in Schizosaccharomyces pombe. Eukaryot Cell **4:** 1446-1454

Mosammaparast N, Shi Y (2010) Reversal of histone methylation: biochemical and molecular mechanisms of histone demethylases. Annual Review of Biochemistry **79:** 155-179

Moss J, Tinline-Purvis H, Walker CA, Folkes LK, Stratford MR, Hayles J, Hoe KL, Kim DU, Park HO, Kearsey SE, Fleck O, Holmberg C, Nielsen O, Humphrey TC (2010) Break-induced ATR and Ddb1-Cul4(Cdt)(2) ubiquitin ligase-dependent nucleotide synthesis promotes homologous recombination repair in fission yeast. Genes & Development **24:** 2705-2716

Moyal L, Lerenthal Y, Gana-Weisz M, Mass G, So S, Wang SY, Eppink B, Chung YM, Shalev G, Shema E, Shkedy D, Smorodinsky NI, van Vliet N, Kuster B, Mann M, Ciechanover A, Dahm-Daphi J, Kanaar R, Hu MC, Chen DJ, Oren M, Shiloh Y (2011) Requirement of ATM-dependent monoubiquitylation of histone H2B for timely repair of DNA double-strand breaks. Molecular Cell **41:** 529-542

Moyer SE, Lewis PW, Botchan MR (2006) Isolation of the Cdc45/Mcm2-7/GINS (CMG) complex, a candidate for the eukaryotic DNA replication fork helicase. Proceedings of the National Academy of Sciences of the United States of America **103:** 10236-10241

Mujtaba S, Zeng L, Zhou MM (2007) Structure and acetyl-lysine recognition of the bromodomain. Oncogene **26:** 5521-5527

Munoz IM, Hain K, Declais AC, Gardiner M, Toh GW, Sanchez-Pulido L, Heuckmann JM, Toth R, Macartney T, Eppink B, Kanaar R, Ponting CP, Lilley DM, Rouse J (2009) Coordination of structure-specific nucleases by human SLX4/BTBD12 is required for DNA repair. Molecular Cell **35:** 116-127

Murr R, Loizou JI, Yang YG, Cuenin C, Li H, Wang ZQ, Herceg Z (2006) Histone acetylation by Trrap-Tip60 modulates loading of repair proteins and repair of DNA double-strand breaks. Nature Cell Biology **8:** 91-99

Nakamura TM, Du LL, Redon C, Russell P (2004) Histone H2A phosphorylation controls Crb2 recruitment at DNA breaks, maintains checkpoint arrest, and influences DNA repair in fission yeast. Molecular and Cellular Biology **24:** 6215-6230

Nakashima N, Tanaka K, Sturm S, Okayama H (1995) Fission yeast Rep2 is a putative transcriptional activator subunit for the cell cycle 'start' function of Res2-Cdc10. The EMBO Journal **14:** 4794-4802

Nakayama J, Xiao G, Noma K, Malikzay A, Bjerling P, Ekwall K, Kobayashi R, Grewal SI (2003) Alp13, an MRG family protein, is a component of fission yeast Clr6 histone deacetylase required for genomic integrity. The EMBO Journal **22:** 2776-2787

Nasmyth K, Nurse P (1981) Cell division cycle mutants altered in DNA replication and mitosis in the fission yeast Schizosaccharomyces pombe. Molecular & General Genetics : MGG **182:** 119-124

Nelson CJ, Santos-Rosa H, Kouzarides T (2006) Proline isomerization of histone H3 regulates lysine methylation and gene expression. Cell **126:** 905-916

Newbold RF, Mokbel K (2010) Evidence for a tumour suppressor function of SETD2 in human breast cancer: a new hypothesis. Anticancer Research **30:** 3309-3311

Nick McElhinny SA, Snowden CM, McCarville J, Ramsden DA (2000) Ku recruits the XRCC4-ligase IV complex to DNA ends. Molecular and Cellular Biology **20:** 2996-3003

Nickoloff JA, Singer JD, Heffron F (1990) In vivo analysis of the Saccharomyces cerevisiae HO nuclease recognition site by site-directed mutagenesis. Molecular and Cellular Biology **10:** 1174-1179

Nicolas E, Yamada T, Cam HP, Fitzgerald PC, Kobayashi R, Grewal SI (2007) Distinct roles of HDAC complexes in promoter silencing, antisense suppression and DNA damage protection. Nature Structural & Molecular Biology **14:** 372-380

Nicolas E, Roumillac C, Trouche D (2003) Balance between acetylation and methylation of histone H3 lysine 9 on the E2F-responsive dihydrofolate reductase promoter. Molecular and Cellular Biology **23**: 1614-1622

Nijman, S.M. (2011). Synthetic lethality: general principles, utility and detection using genetic screens in human cells. FEBS Letters **585**, 1-6.

Nishitani H, Lygerou Z, Nishimoto T, Nurse P (2000) The Cdt1 protein is required to license DNA for replication in fission yeast. Nature **404:** 625-628

Niwa, O., Matsumoto, T., and Yanagida, M. (1986). Construction of a mini-chromosome by deletion and its mitotic and meiotic behaviour in fission yeast. Molecular and General Genetics MGG 203, 397-405.

Noma K, Allis CD, Grewal SI (2001) Transitions in distinct histone H3 methylation patterns at the heterochromatin domain boundaries. Science **293:** 1150-1155

Nugent RL, Johnsson A, Fleharty B, Gogol M, Xue-Franzen Y, Seidel C, Wright AP, Forsburg SL (2010) Expression profiling of S. pombe acetyltransferase mutants identifies redundant pathways of gene regulation. BMC Genomics **11:** 59

Oda H, Hubner MR, Beck DB, Vermeulen M, Hurwitz J, Spector DL, Reinberg D (2010) Regulation of the histone H4 monomethylase PR-Set7 by CRL4(Cdt2)-mediated PCNA-dependent degradation during DNA damage. Molecular Cell **40:** 364-376

Odintsova TI, Muller EC, Ivanov AV, Egorov TA, Bienert R, Vladimirov SN, Kostka S, Otto A, Wittmann-Liebold B, Karpova GG (2003) Characterization and analysis of posttranslational modifications of the human large cytoplasmic ribosomal subunit proteins by mass spectrometry and Edman sequencing. Journal of Protein Chemistry **22:** 249-258

Oliva A, Rosebrock A, Ferrezuelo F, Pyne S, Chen H, Skiena S, Futcher B, Leatherwood J (2005) The cell cycle-regulated genes of Schizosaccharomyces pombe. PLoS Biology **3:** e225

Osborne BI, Guarente L (1988) Transcription by RNA polymerase II induces changes of DNA topology in yeast. Genes & Development **2:** 766-772

Osman F, Dixon J, Barr AR, Whitby MC (2005) The F-Box DNA helicase Fbh1 prevents Rhp51-dependent recombination without mediator proteins. Molecular and Cellular Biology **25:** 8084-8096

Osman F, Fortunato EA, Subramani S (1996) Double-strand break-induced mitotic intrachromosomal recombination in the fission yeast Schizosaccharomyces pombe. Genetics **142:** 341-357.

Owen DJ, Ornaghi P, Yang JC, Lowe N, Evans PR, Ballario P, Neuhaus D, Filetici P, Travers AA (2000) The structural basis for the recognition of acetylated histone H4 by the bromodomain of histone acetyltransferase gcn5p. The EMBO Journal **19:** 6141-6149

Pacek M, Tutter AV, Kubota Y, Takisawa H, Walter JC (2006) Localization of MCM2-7, Cdc45, and GINS to the site of DNA unwinding during eukaryotic DNA replication. Molecular Cell **21:** 581-587

Pacek M, Walter JC (2004) A requirement for MCM7 and Cdc45 in chromosome unwinding during eukaryotic DNA replication. The EMBO Journal **23:** 3667-3676

Paolinelli R, Mendoza-Maldonado R, Cereseto A, Giacca M (2009) Acetylation by GCN5 regulates CDC6 phosphorylation in the S phase of the cell cycle. Nature Structural & Molecular Biology **16:** 412-420

Papamichos-Chronakis M, Watanabe S, Rando OJ, Peterson CL (2011) Global regulation of H2A.Z localization by the INO80 chromatin-remodeling enzyme is essential for genome integrity. Cell **144**: 200-213

Paques F, Haber JE (1999) Multiple pathways of recombination induced by double-strand breaks in Saccharomyces cerevisiae. Microbiology and Molecular Biology Reviews : MMBR **63:** 349-404

Park SD, Jin YH, Jang YK (1998) Regulation of DNA damage inducible rhp51+ gene, a rec A homolog from Schizosaccharomyces pombe. The Journal of Toxicological Sciences **23 Suppl 2:** 110-116

Parthun MR, Widom J, Gottschling DE (1996) The major cytoplasmic histone acetyltransferase in yeast: links to chromatin replication and histone metabolism. Cell **87:** 85-94

Paulsen RD, Cimprich KA (2007) The ATR pathway: fine-tuning the fork. DNA Repair **6:** 953-966

Pederson DS, Morse RH (1990) Effect of transcription of yeast chromatin on DNA topology in vivo. The EMBO Journal **9:** 1873-1881

Pei Y, Du H, Singer J, Stamour C, Granitto S, Shuman S, Fisher RP (2006) Cyclin-dependent kinase 9 (Cdk9) of fission yeast is activated by the CDK-activating kinase Csk1, overlaps functionally with the TFIIH-associated kinase Mcs6, and associates with the mRNA cap methyltransferase Pcm1 in vivo. Molecular and Cellular Biology **26:** 777-788

Peng X, Karuturi RK, Miller LD, Lin K, Jia Y, Kondu P, Wang L, Wong LS, Liu ET, Balasubramanian MK, Liu J (2005) Identification of cell cycle-regulated genes in fission yeast. Molecular Biology of the Cell **16:** 1026-1042

Pfeiffer P, Goedecke W, Obe G (2000) Mechanisms of DNA double-strand break repair and their potential to induce chromosomal aberrations. Mutagenesis **15:** 289-302

Phatnani HP, Greenleaf AL (2006) Phosphorylation and functions of the RNA polymerase II CTD. Genes & Development **20:** 2922-2936

Piatti S, Bohm T, Cocker JH, Diffley JF, Nasmyth K (1996) Activation of S-phase-promoting CDKs in late G1 defines a "point of no return" after which Cdc6 synthesis cannot promote DNA replication in yeast. Genes & Development **10:** 1516-1531

Pierce AJ, Hu P, Han M, Ellis N, Jasin M (2001) Ku DNA end-binding protein modulates homologous repair of double-strand breaks in mammalian cells. Genes & Development **15:** 3237-3242

Pijnappel WW, Schaft D, Roguev A, Shevchenko A, Tekotte H, Wilm M, Rigaut G, Seraphin B, Aasland R, Stewart AF (2001) The S. cerevisiae SET3 complex includes two histone deacetylases, Hos2 and Hst1, and is a meiotic-specific repressor of the sporulation gene program. Genes & Development **15:** 2991-3004

Pokholok DK, Harbison CT, Levine S, Cole M, Hannett NM, Lee TI, Bell GW, Walker K, Rolfe PA, Herbolsheimer E, Zeitlinger J, Lewitter F, Gifford DK, Young RA (2005) Genome-wide map of nucleosome acetylation and methylation in yeast. Cell **122:** 517-527

Poveda A, Pamblanco M, Tafrov S, Tordera V, Sternglanz R, Sendra R (2004) Hif1 is a component of yeast histone acetyltransferase B, a complex mainly localized in the nucleus. The Journal of Biological Chemistry **279:** 16033-16043

Povirk LF (1996) DNA damage and mutagenesis by radiomimetic DNA-cleaving agents: bleomycin, neocarzinostatin and other enediynes. Mutation Research **355:** 71-89

Prudden J, Evans JS, Hussey SP, Deans B, O'Neill P, Thacker J, Humphrey T (2003) Pathway utilization in response to a site-specific DNA double-strand break in fission yeast. The EMBO Journal **22:** 1419-1430

Pryde F, Jain D, Kerr A, Curley R, Mariotti FR, Vogelauer M (2009) H3 k36 methylation helps determine the timing of cdc45 association with replication origins. PloS One **4:** e5882

Pursell ZF, Isoz I, Lundstrom EB, Johansson E, Kunkel TA (2007) Yeast DNA polymerase epsilon participates in leading-strand DNA replication. Science **317:** 127-130

Qin S, Parthun MR (2002) Histone H3 and the histone acetyltransferase Hat1p contribute to DNA double-strand break repair. Molecular and Cellular Biology **22:** 8353-8365

Qin S, Parthun MR (2006) Recruitment of the type B histone acetyltransferase Hat1p to chromatin is linked to DNA double-strand breaks. Molecular and Cellular Biology **26:** 3649-3658

Rahal EA, Henricksen LA, Li Y, Williams RS, Tainer JA, Dixon K (2010) ATM regulates Mre11-dependent DNA end-degradation and microhomology-mediated end joining. Cell Cycle **9:** 2866-2877

Rahman S, Sowa ME, Ottinger M, Smith JA, Shi Y, Harper JW, Howley PM (2011) The Brd4 extraterminal domain confers transcription activation independent of pTEFb by recruiting multiple proteins, including NSD3. Molecular and Cellular Biology **31:** 2641-2652

Rajeshkumar NV, De Oliveira E, Ottenhof N, Watters J, Brooks D, Demuth T, Shumway SD, Mizuarai S, Hirai H, Maitra A, Hidalgo M (2011) MK-1775, a potent Wee1 inhibitor, synergizes with gemcitabine to achieve tumor regressions, selectively in p53-deficient pancreatic cancer xenografts. Clinical cancer research : an official journal of the American Association for Cancer Research **17:** 2799-2806

Rao B, Shibata Y, Strahl BD, Lieb JD (2005) Dimethylation of histone H3 at lysine 36 demarcates regulatory and nonregulatory chromatin genome-wide. Molecular and Cellular Biology **25:** 9447-9459

Rea S, Eisenhaber F, O'Carroll D, Strahl BD, Sun ZW, Schmid M, Opravil S, Mechtler K, Ponting CP, Allis CD, Jenuwein T (2000) Regulation of chromatin structure by site-specific histone H3 methyltransferases. Nature **406:** 593-599

Reddy BD, Wang Y, Niu L, Higuchi EC, Marguerat SB, Bahler J, Smith GR, Jia S (2011) Elimination of a specific histone H3K14 acetyltransferase complex bypasses the RNAi pathway to regulate pericentric heterochromatin functions. Genes & Development **25:** 214-219

Reddy YV, Ding Q, Lees-Miller SP, Meek K, Ramsden DA (2004) Non-homologous end joining requires that the DNA-PK complex undergo an autophosphorylation-dependent rearrangement at DNA ends. The Journal of Biological Chemistry **279:** 39408-39413

Remus D, Blanchette M, Rio DC, Botchan MR (2005) CDK phosphorylation inhibits the DNA-binding and ATP-hydrolysis activities of the Drosophila origin recognition complex. The Journal of Biological Chemistry **280:** 39740-39751

Rentas S, Saberianfar R, Grewal C, Kanippayoor R, Mishra M, McCollum D, Karagiannis J (2012) The SET domain protein, Set3p, promotes the reliable execution of cytokinesis in Schizosaccharomyces pombe. PloS One **7:** e31224

Rhind N, Furnari B, Russell P (1997) Cdc2 tyrosine phosphorylation is required for the DNA damage checkpoint in fission yeast. Genes & Development **11:** 504-511

Robyr D, Suka Y, Xenarios I, Kurdistani SK, Wang A, Suka N, Grunstein M (2002) Microarray deacetylation maps determine genome-wide functions for yeast histone deacetylases. Cell **109:** 437-446

Rogakou EP, Boon C, Redon C, Bonner WM (1999) Megabase chromatin domains involved in DNA double-strand breaks in vivo. The Journal of Cell Biology **146:** 905-916

Roguev A, Schaft D, Shevchenko A, Aasland R, Stewart AF (2003) High conservation of the Set1/Rad6 axis of histone 3 lysine 4 methylation in budding and fission yeasts. The Journal of Biological Chemistry **278:** 8487-8493

Roguev A, Schaft D, Shevchenko A, Pijnappel WW, Wilm M, Aasland R, Stewart AF (2001) The Saccharomyces cerevisiae Set1 complex includes an Ash2 homologue and methylates histone 3 lysine 4. The EMBO Journal **20:** 7137-7148

Rosaleny LE, Ruiz-Garcia AB, Garcia-Martinez J, Perez-Ortin JE, Tordera V (2007) The Sas3p and Gcn5p histone acetyltransferases are recruited to similar genes. Genome Biology **8:** R119

Rosati R, La Starza R, Veronese A, Aventin A, Schwienbacher C, Vallespi T, Negrini M, Martelli MF, Mecucci C (2002) NUP98 is fused to the NSD3 gene in acute myeloid leukemia associated with t(8;11)(p11.2;p15). Blood **99:** 3857-3860

Rosidi B, Wang M, Wu W, Sharma A, Wang H, Iliakis G (2008) Histone H1 functions as a stimulatory factor in backup pathways of NHEJ. Nucleic Acids Research **36:** 1610-1623

Roth DB, Wilson JH (1985) Relative rates of homologous and nonhomologous recombination in transfected DNA. Proceedings of the National Academy of Sciences of the United States of America **82:** 3355-3359

Roth DB, Wilson JH (1986) Nonhomologous recombination in mammalian cells: role for short sequence homologies in the joining reaction. Molecular and Cellular Biology **6:** 4295-4304

Rothkamm K, Kruger I, Thompson LH, Lobrich M (2003) Pathways of DNA double-strand break repair during the mammalian cell cycle. Molecular and Cellular Biology **23:** 5706-5715

Roukos V, Kinkhabwala A, Colombelli J, Kotsantis P, Taraviras S, Nishitani H, Stelzer E, Bastiaens P, Lygerou Z (2011) Dynamic recruitment of licensing factor Cdt1 to sites of DNA damage. Journal of Cell Science **124:** 422-434

Rubnitz J, Subramani S (1984) The minimum amount of homology required for homologous recombination in mammalian cells. Molecular and Cellular Biology **4:** 2253-2258

Rustici G, Mata J, Kivinen K, Lio P, Penkett CJ, Burns G, Hayles J, Brazma A, Nurse P, Bahler J (2004) Periodic gene expression program of the fission yeast cell cycle. Nature Genetics **36:** 809-817

Sadaie M, Shinmyozu K, Nakayama J (2008) A conserved SET domain methyltransferase, Set11, modifies ribosomal protein Rpl12 in fission yeast. The Journal of Biological Chemistry **283:** 7185-7195

Sallmyr A, Tomkinson AE, Rassool FV (2008) Up-regulation of WRN and DNA ligase IIIalpha in chronic myeloid leukemia: consequences for the repair of DNA double-strand breaks. Blood **112:** 1413-1423

Sanders SL, Portoso M, Mata J, Bahler J, Allshire RC, Kouzarides T (2004) Methylation of histone H4 lysine 20 controls recruitment of Crb2 to sites of DNA damage. Cell **119:** 603-614

Sanso M, Vargas-Perez I, Quintales L, Antequera F, Ayte J, Hidalgo E (2011) Gcn5 facilitates Pol II progression, rather than recruitment to nucleosome-depleted stress promoters, in Schizosaccharomyces pombe. Nucleic Acids Research **39:** 6369-6379

Santaguida S, Musacchio A (2009) The life and miracles of kinetochores. The EMBO Journal **28**: 2511-2531

Santenard A, Torres-Padilla ME (2009) Epigenetic reprogramming in mammalian reproduction: contribution from histone variants. Epigenetics : official journal of the DNA Methylation Society **4:** 80-84

Santocanale C, Diffley JF (1998) A Mec1- and Rad53-dependent checkpoint controls late-firing origins of DNA replication. Nature **395:** 615-618

Sartori AA, Lukas C, Coates J, Mistrik M, Fu S, Bartek J, Baer R, Lukas J, Jackson SP (2007) Human CtIP promotes DNA end resection. Nature **450:** 509-514

Schaft D, Roguev A, Kotovic KM, Shevchenko A, Sarov M, Neugebauer KM, Stewart AF (2003) The histone 3 lysine 36 methyltransferase, SET2, is involved in transcriptional elongation. Nucleic Acids Research **31:** 2475-2482

Schalch T, Duda S, Sargent DF, Richmond TJ (2005) X-ray structure of a tetranucleosome and its implications for the chromatin fibre. Nature **436:** 138-141

Schneider J, Bajwa P, Johnson FC, Bhaumik SR, Shilatifard A (2006) Rtt109 is required for proper H3K56 acetylation: a chromatin mark associated with the elongating RNA polymerase II. The Journal of Biological Chemistry **281**: 37270-37274

Schramke V, Neecke H, Brevet V, Corda Y, Lucchini G, Longhese MP, Gilson E, Geli V (2001) The set1Delta mutation unveils a novel signaling pathway relayed by the Rad53-dependent hyperphosphorylation of replication protein A that leads to transcriptional activation of repair genes. Genes & Development **15:** 1845-1858

Schwartz BE, Ahmad K (2005) Transcriptional activation triggers deposition and removal of the histone variant H3.3. Genes & Development **19**: 804-814

Seki M, Nakagawa T, Seki T, Kato G, Tada S, Takahashi Y, Yoshimura A, Kobayashi T, Aoki A, Otsuki M, Habermann FA, Tanabe H, Ishii Y, Enomoto T (2006) Bloom helicase and DNA topoisomerase IIIalpha are involved in the dissolution of sister chromatids. Molecular and Cellular Biology **26:** 6299-6307

Senga T, Sivaprasad U, Zhu W, Park JH, Arias EE, Walter JC, Dutta A (2006) PCNA is a cofactor for Cdt1 degradation by CUL4/DDB1-mediated N-terminal ubiquitination. The Journal of Biological Chemistry **281:** 6246-6252

Shankaranarayana GD, Motamedi MR, Moazed D, Grewal SI (2003) Sir2 regulates histone H3 lysine 9 methylation and heterochromatin assembly in fission yeast. Current Biology : CB **13:** 1240-1246

Shechter D, Ying CY, Gautier J (2004) DNA unwinding is an Mcm complex-dependent and ATP hydrolysis-dependent process. The Journal of Biological Chemistry **279:** 45586-45593

Shi X, Hong T, Walter KL, Ewalt M, Michishita E, Hung T, Carney D, Pena P, Lan F, Kaadige MR, Lacoste N, Cayrou C, Davrazou F, Saha A, Cairns BR, Ayer DE, Kutateladze TG, Shi Y, Cote J, Chua KF, Gozani O (2006) ING2 PHD domain links histone H3 lysine 4 methylation to active gene repression. Nature **442:** 96-99

Shi Y, Lan F, Matson C, Mulligan P, Whetstine JR, Cole PA, Casero RA (2004) Histone demethylation mediated by the nuclear amine oxidase homolog LSD1. Cell **119:** 941-953

Shim EY, Chung WH, Nicolette ML, Zhang Y, Davis M, Zhu Z, Paull TT, Ira G, Lee SE (2010) Saccharomyces cerevisiae Mre11/Rad50/Xrs2 and Ku proteins regulate association of Exo1 and Dna2 with DNA breaks. The EMBO Journal **29:** 3370-3380

Shim YS, Jang YK, Lim MS, Lee JS, Seong RH, Hong SH, Park SD (2000) Rdp1, a novel zinc finger protein, regulates the DNA damage response of rhp51(+) from Schizosaccharomyces pombe. Mol Cell Biol **20:** 8958-8968

Shiozaki K, Russell P (1995) Cell-cycle control linked to extracellular environment by MAP kinase pathway in fission yeast. Nature **378:** 739-743

Shirai A, Sadaie M, Shinmyozu K, Nakayama J (2010) Methylation of ribosomal protein L42 regulates ribosomal function and stress-adapted cell growth. The Journal of Biological Chemistry **285:** 22448-22460

Shogren-Knaak M, Ishii H, Sun JM, Pazin MJ, Davie JR, Peterson CL (2006) Histone H4-K16 acetylation controls chromatin structure and protein interactions. Science **311:** 844-847

Shogren-Knaak M, Peterson CL (2006) Switching on chromatin: mechanistic role of histone H4-K16 acetylation. Cell Cycle **5:** 1361-1365

Singleton BK, Torres-Arzayus MI, Rottinghaus ST, Taccioli GE, Jeggo PA (1999) The C terminus of Ku80 activates the DNA-dependent protein kinase catalytic subunit. Molecular and Cellular Biology **19:** 3267-3277

Sinha M, Peterson CL (2008) A Rad51 presynaptic filament is sufficient to capture nucleosomal homology during recombinational repair of a DNA double-strand break. Molecular Cell **30:** 803-810

Smeets MF, Francesconi S, Baldacci G (2003) High dosage Rhp51 suppression of the MMS sensitivity of DNA structure checkpoint mutants reveals a relationship between Crb2 and Rhp51. Genes Cells **8:** 573-586.

Sollier J, Lin W, Soustelle C, Suhre K, Nicolas A, Geli V, de La Roche Saint-Andre C (2004) Set1 is required for meiotic S-phase onset, double-strand break formation and middle gene expression. The EMBO Journal **23:** 1957-1967

Sterner DE, Berger SL (2000) Acetylation of histones and transcription-related factors. Microbiology and Molecular Biology Reviews : MMBR **64:** 435-459

Stiff T, O'Driscoll M, Rief N, Iwabuchi K, Lobrich M, Jeggo PA (2004) ATM and DNA-PK function redundantly to phosphorylate H2AX after exposure to ionizing radiation. Cancer Research **64:** 2390-2396

Strahl BD, Allis CD (2000) The language of covalent histone modifications. Nature **403:** 41-45

Strahl BD, Grant PA, Briggs SD, Sun ZW, Bone JR, Caldwell JA, Mollah S, Cook RG, Shabanowitz J, Hunt DF, Allis CD (2002) Set2 is a nucleosomal histone H3-selective methyltransferase that mediates transcriptional repression. Molecular and Cellular Biology **22:** 1298-1306

Su TT (2006) Cellular responses to DNA damage: one signal, multiple choices. Annual Review of Genetics **40:** 187-208

Sugawara N, Wang X, Haber JE (2003) In vivo roles of Rad52, Rad54, and Rad55 proteins in Rad51-mediated recombination. Molecular Cell **12:** 209-219

Sugiyama A, Tanaka K, Okazaki K, Nojima H, Okayama H (1994) A zinc finger protein controls the onset of premeiotic DNA synthesis of fission yeast in a Mei2-independent cascade. The EMBO Journal **13:** 1881-1887

Sun JM, Spencer VA, Chen HY, Li L, Davie JR (2003) Measurement of histone acetyltransferase and histone deacetylase activities and kinetics of histone acetylation. Methods **31:** 12-23

Sun Y, Jiang X, Chen S, Fernandes N, Price BD (2005) A role for the Tip60 histone acetyltransferase in the acetylation and activation of ATM. Proceedings of the National Academy of Sciences of the United States of America **102:** 13182-13187

Sun Y, Jiang X, Xu Y, Ayrapetov MK, Moreau LA, Whetstine JR, Price BD (2009) Histone H3 methylation links DNA damage detection to activation of the tumour suppressor Tip60. Nature Cell Biology **11:** 1376-1382

Sung P (1997) Yeast Rad55 and Rad57 proteins form a heterodimer that functions with replication protein A to promote DNA strand exchange by Rad51 recombinase. Genes & Development **11:** 1111-1121

Sutcliffe EL, Parish IA, He YQ, Juelich T, Tierney ML, Rangasamy D, Milburn PJ, Parish CR, Tremethick DJ, Rao S (2009) Dynamic histone variant exchange accompanies gene induction in T cells. Molecular and Cellular Biology **29**: 1972-1986

Svendsen JM, Harper JW (2010) GEN1/Yen1 and the SLX4 complex: Solutions to the problem of Holliday junction resolution. Genes & Development **24:** 521-536

Svendsen JM, Smogorzewska A, Sowa ME, O'Connell BC, Gygi SP, Elledge SJ, Harper JW (2009) Mammalian BTBD12/SLX4 assembles a Holliday junction resolvase and is required for DNA repair. Cell **138:** 63-77

Syljuasen RG, Sorensen CS, Hansen LT, Fugger K, Lundin C, Johansson F, Helleday T, Sehested M, Lukas J, Bartek J (2005) Inhibition of human Chk1 causes increased initiation of DNA replication, phosphorylation of ATR targets, and DNA breakage. Molecular and Cellular Biology **25:** 3553-3562

Syntichaki P, Topalidou I, Thireos G (2000) The Gcn5 bromodomain co-ordinates nucleosome remodelling. Nature **404:** 414-417

Szostak JW, Orr-Weaver TL, Rothstein RJ, Stahl FW (1983) The double-strand-break repair model for recombination. Cell **33:** 25-35

Szuts D, Kitching L, Christov C, Budd A, Peak-Chew S, Krude T (2003) RPA is an initiation factor for human chromosomal DNA replication. Nucleic Acids Research **31:** 1725-1734

Takeda T, Toda T, Kominami K, Kohnosu A, Yanagida M, Jones N (1995) Schizosaccharomyces pombe atf1+ encodes a transcription factor required for sexual development and entry into stationary phase. The EMBO Journal **14:** 6193-6208

Tamburini BA, Tyler JK (2005) Localized histone acetylation and deacetylation triggered by the homologous recombination pathway of double-strand DNA repair. Molecular and Cellular Biology **25:** 4903-4913

Tanaka K, Okazaki K, Okazaki N, Ueda T, Sugiyama A, Nojima H, Okayama H (1992) A new cdc gene required for S phase entry of Schizosaccharomyces pombe encodes a protein similar to the cdc 10+ and SWI4 gene products. The EMBO Journal **11:** 4923-4932

Tanaka T, Knapp D, Nasmyth K (1997) Loading of an Mcm protein onto DNA replication origins is regulated by Cdc6p and CDKs. Cell **90:** 649-660

Tardat M, Brustel J, Kirsh O, Lefevbre C, Callanan M, Sardet C, Julien E (2010) The histone H4 Lys 20 methyltransferase PR-Set7 regulates replication origins in mammalian cells. Nature Cell Biology **12:** 1086-1093

Tardat M, Murr R, Herceg Z, Sardet C, Julien E (2007) PR-Set7-dependent lysine methylation ensures genome replication and stability through S phase. The Journal ofCcell Biology **179:** 1413-1426

Tercero JA, Labib K, Diffley JF (2000) DNA synthesis at individual replication forks requires the essential initiation factor Cdc45p. The EMBO Journal **19:** 2082-2093

Tinline-Purvis H, Savory AP, Cullen JK, Dave A, Moss J, Bridge WL, Marguerat S, Bahler J, Ragoussis J, Mott R, Walker CA, Humphrey TC (2009) Failed gene conversion leads to extensive end processing and chromosomal rearrangements in fission yeast. The EMBO Journal **28:** 3400-3412

Tomita K, Matsuura A, Caspari T, Carr AM, Akamatsu Y, Iwasaki H, Mizuno K, Ohta K, Uritani M, Ushimaru T, Yoshinaga K, Ueno M (2003) Competition between the Rad50 complex and the Ku heterodimer reveals a role for Exo1 in processing double-strand breaks but not telomeres. Molecular and Cellular Biology **23:** 5186-5197

Tsai CJ, Kim SA, Chu G (2007) Cernunnos/XLF promotes the ligation of mismatched and noncohesive DNA ends. Proceedings of the National Academy of Sciences of the United States of America **104:** 7851-7856

Tsubouchi H, Ogawa H (2000) Exo1 roles for repair of DNA double-strand breaks and meiotic crossing over in Saccharomyces cerevisiae. Molecular Biology of the Cell **11:** 2221-2233

Tsukamoto Y, Kato J, Ikeda H (1997) Silencing factors participate in DNA repair and recombination in Saccharomyces cerevisiae. Nature **388:** 900-903

Tu S, Bulloch EM, Yang L, Ren C, Huang WC, Hsu PH, Chen CH, Liao CL, Yu HM, Lo WS, Freitas MA, Tsai MD (2007) Identification of histone demethylases in Saccharomyces cerevisiae. The Journal of Biological Chemistry 282: 14262-14271

van Holde KE (1988) Chromatin. Springer-Verlag; New York

van Attikum H, Fritsch O, Hohn B, Gasser SM (2004) Recruitment of the INO80 complex by H2A phosphorylation links ATP-dependent chromatin remodeling with DNA double-strand break repair. Cell **119:** 777-788

Vanoosthuyse V, Valsdottir R, Javerzat JP, Hardwick KG (2004) Kinetochore targeting of fission yeast Mad and Bub proteins is essential for spindle checkpoint function but not for all chromosome segregation roles of Bub1p. Molecular and Cellular Biology **24:** 9786-9801

Veaute X, Jeusset J, Soustelle C, Kowalczykowski SC, Le Cam E, Fabre F (2003) The Srs2 helicase prevents recombination by disrupting Rad51 nucleoprotein filaments. Nature **423:** 309-312

Vempati RK, Jayani RS, Notani D, Sengupta A, Galande S, Haldar D (2010) p300-mediated acetylation of histone H3 lysine 56 functions in DNA damage response in mammals. The Journal of Biological Chemistry **285**: 28553-28564

Viladevall L, St Amour CV, Rosebrock A, Schneider S, Zhang C, Allen JJ, Shokat KM, Schwer B, Leatherwood JK, Fisher RP (2009) TFIIH and P-TEFb coordinate transcription with capping enzyme recruitment at specific genes in fission yeast. Molecular Cell **33:** 738-751

Virsik-Kopp P, Rave-Frank M, Hofman-Huther H, Schmidberger H (2003) Role of DNA-PK in the process of aberration formation as studied in irradiated human glioblastoma cell lines M059K and M059J. International Journal of Radiation Biology **79:** 61-68

Vojnic E, Simon B, Strahl BD, Sattler M, Cramer P (2006) Structure and carboxyl-terminal domain (CTD) binding of the Set2 SRI domain that couples histone H3 Lys36 methylation to transcription. The Journal of Biological Chemistry **281:** 13-15

Wagner EJ, Carpenter PB (2012) Understanding the language of Lys36 methylation at histone H3. Nature Reviews Molecular Cell Biology **13:** 115-126

Wang GG, Cai L, Pasillas MP, Kamps MP (2007) NUP98-NSD1 links H3K36 methylation to Hox-A gene activation and leukaemogenesis. Nature Cell Biology **9:** 804-812

Wang H, Zeng ZC, Perrault AR, Cheng X, Qin W, Iliakis G (2001) Genetic evidence for the involvement of DNA ligase IV in the DNA-PK-dependent pathway of non-homologous end joining in mammalian cells. Nucleic Acids Research **29:** 1653-1660

Wang M, Wu W, Rosidi B, Zhang L, Wang H, Iliakis G (2006) PARP-1 and Ku compete for repair of DNA double strand breaks by distinct NHEJ pathways. Nucleic Acids Research **34:** 6170-6182

Wang X, Haber JE (2004) Role of Saccharomyces single-stranded DNA-binding protein RPA in the strand invasion step of double-strand break repair. PLoS biology **2:** E21

Wang Y, Kallgren SP, Reddy BD, Kuntz K, Lopez-Maury L, Thompson J, Watt S, Ma C, Hou H, Shi Y, Yates JR, 3rd, Bahler J, O'Connell MJ, Jia S (2012) Histone H3 lysine 14 acetylation is required for activation of a DNA damage checkpoint in fission yeast. The Journal of Biological Chemistry **287:** 4386-4393

Wang Z, Zang C, Rosenfeld JA, Schones DE, Barski A, Cuddapah S, Cui K, Roh TY, Peng W, Zhang MQ, Zhao K (2008) Combinatorial patterns of histone acetylations and methylations in the human genome. Nature Genetics **40:** 897-903

Ward IM, Chen J (2001) Histone H2AX is phosphorylated in an ATR-dependent manner in response to replicational stress. The Journal of Biological Chemistry **276:** 47759-47762

Waterborg JH (2001) Dynamics of histone acetylation in Saccharomyces cerevisiae. Biochemistry **40:** 2599-2605

Watson A, Mata J, Bahler J, Carr A, Humphrey T (2004) Global gene expression responses of fission yeast to ionizing radiation. Mol Biol Cell **15:** 851-860

Weterings E, Verkaik NS, Bruggenwirth HT, Hoeijmakers JH, van Gent DC (2003) The role of DNA dependent protein kinase in synapsis of DNA ends. Nucleic Acids Research **31:** 7238-7246

Whetstine JR, Nottke A, Lan F, Huarte M, Smolikov S, Chen Z, Spooner E, Li E, Zhang G, Colaiacovo M, Shi Y (2006) Reversal of histone lysine trimethylation by the JMJD2 family of histone demethylases. Cell 125: 467-481

White S, Khaliq F, Sotiriou S, McInerny CJ (2001) The role of DSC1 components cdc10+, rep1+ and rep2+ in MCB gene transcription at the mitotic G1-S boundary in fission yeast. Current Genetics **40:** 251-259

Whitehall S, Stacey P, Dawson K, Jones N (1999) Cell cycle-regulated transcription in fission yeast: Cdc10-Res protein interactions during the cell cycle and domains required for regulated transcription. Molecular Biology of the Cell **10:** 3705-3715

Winkler GS, Kristjuhan A, Erdjument-Bromage H, Tempst P, Svejstrup JQ (2002) Elongator is a histone H3 and H4 acetyltransferase important for normal histone acetylation levels in vivo. Proceedings of the National Academy of Sciences of the United States of America **99:** 3517-3522

Wippo CJ, Krstulovic BS, Ertel F, Musladin S, Blaschke D, Sturzl S, Yuan GC, Horz W, Korber P, Barbaric S (2009) Differential cofactor requirements for histone eviction from two nucleosomes at the yeast PHO84 promoter are determined by intrinsic nucleosome stability. Molecular and Cellular Biology **29:** 2960-2981

Wiren M, Silverstein RA, Sinha I, Walfridsson J, Lee HM, Laurenson P, Pillus L, Robyr D, Grunstein M, Ekwall K (2005) Genomewide analysis of nucleosome density histone acetylation and HDAC function in fission yeast. The EMBO Journal **24:** 2906-2918

Wittschieben BO, Fellows J, Du W, Stillman DJ, Svejstrup JQ (2000) Overlapping roles for the histone acetyltransferase activities of SAGA and elongator in vivo. The EMBO Journal **19:** 3060-3068

Wittschieben BO, Otero G, de Bizemont T, Fellows J, Erdjument-Bromage H, Ohba R, Li Y, Allis CD, Tempst P, Svejstrup JQ (1999) A novel histone acetyltransferase is an integral subunit of elongating RNA polymerase II holoenzyme. Molecular Cell **4:** 123-128

Wu L, Hickson ID (2003) The Bloom's syndrome helicase suppresses crossing over during homologous recombination. Nature **426:** 870-874

Wu X, Lieber MR (1996) Protein-protein and protein-DNA interaction regions within the DNA end-binding protein Ku70-Ku86. Molecular and Cellular Biology 16: 5186-5193

Wuarin J, Buck V, Nurse P, Millar JB (2002) Stable association of mitotic cyclin B/Cdc2 to replication origins prevents endoreduplication. Cell **111:** 419-431

Wysocka J, Myers MP, Laherty CD, Eisenman RN, Herr W (2003) Human Sin3 deacetylase and trithorax-related Set1/Ash2 histone H3-K4 methyltransferase are tethered together selectively by the cell-proliferation factor HCF-1. Genes & Development **17:** 896-911

Xhemalce B, Miller KM, Driscoll R, Masumoto H, Jackson SP, Kouzarides T, Verreault A, Arcangioli B (2007) Regulation of histone H3 lysine 56 acetylation in Schizosaccharomyces pombe. The Journal of Biological Chemistry **282**: 15040-15047

Xiao B, Jing C, Wilson JR, Walker PA, Vasisht N, Kelly G, Howell S, Taylor IA, Blackburn GM, Gamblin SJ (2003a) Structure and catalytic mechanism of the human histone methyltransferase SET7/9. Nature **421:** 652-656

Xiao T, Hall H, Kizer KO, Shibata Y, Hall MC, Borchers CH, Strahl BD (2003b) Phosphorylation of RNA polymerase II CTD regulates H3 methylation in yeast. Genes & Development **17:** 654-663

Xie A, Kwok A, Scully R (2009) Role of mammalian Mre11 in classical and alternative nonhomologous end joining. Nature Structural & Molecular Biology **16:** 814-818

Xue-Franzen Y, Johnsson A, Brodin D, Henriksson J, Burglin TR, Wright AP (2010) Genome-wide characterisation of the Gcn5 histone acetyltransferase in budding yeast during stress adaptation reveals evolutionarily conserved and diverged roles. BMC Genomics **11:** 200

Yanagi K, Mizuno T, You Z, Hanaoka F (2002) Mouse geminin inhibits not only Cdt1-MCM6 interactions but also a novel intrinsic Cdt1 DNA binding activity. The Journal of Biological Chemistry **277:** 40871-40880

Yanow SK, Lygerou Z, Nurse P (2001) Expression of Cdc18/Cdc6 and Cdt1 during G2 phase induces initiation of DNA replication. The EMBO Journal **20:** 4648-4656

Youdell ML, Kizer KO, Kisseleva-Romanova E, Fuchs SM, Duro E, Strahl BD, Mellor J (2008) Roles for Ctk1 and Spt6 in regulating the different methylation states of histone H3 lysine 36. Molecular and Cellular Biology **28:** 4915-4926

Yu S, Teng Y, Waters R, Reed SH (2011) How chromatin is remodelled during DNA repair of UV-induced DNA damage in Saccharomyces cerevisiae. PLoS Genetics **7:** e1002124

Yu Y, Song C, Zhang Q, DiMaggio PA, Garcia BA, York A, Carey MF, Grunstein M (2012) Histone H3 lysine 56 methylation regulates DNA replication through its interaction with PCNA. Molecular Cell **46:** 7-17

Yuan J, Chen J (2011) The role of the human SWI5-MEI5 complex in homologous recombination repair. The Journal of Biological Chemistry **286:** 9888-9893

Zeng L, Zhou MM (2002) Bromodomain: an acetyl-lysine binding domain. FEBS letters **513:** 124-128

Zhang L, Eugeni EE, Parthun MR, Freitas MA (2003) Identification of novel histone post-translational modifications by peptide mass fingerprinting. Chromosoma **112:** 77-86

Zhang W, Bone JR, Edmondson DG, Turner BM, Roth SY (1998) Essential and redundant functions of histone acetylation revealed by mutation of target lysines and loss of the Gcn5p acetyltransferase. The EMBO Journal **17:** 3155-3167

Zhao X, Chabes A, Domkin V, Thelander L, Rothstein R (2001) The ribonucleotide reductase inhibitor Sml1 is a new target of the Mec1/Rad53 kinase cascade during growth and in response to DNA damage. The EMBO Journal **20:** 3544-3553

Zhu Y, Takeda T, Nasmyth K, Jones N (1994) pct1+, which encodes a new DNA-binding partner of p85cdc10, is required for meiosis in the fission yeast Schizosaccharomyces pombe. Genes & Development **8:** 885-898

Zhu Z, Chung WH, Shim EY, Lee SE, Ira G (2008) Sgs1 helicase and two nucleases Dna2 and Exo1 resect DNA double-strand break ends. Cell **134:** 981-994

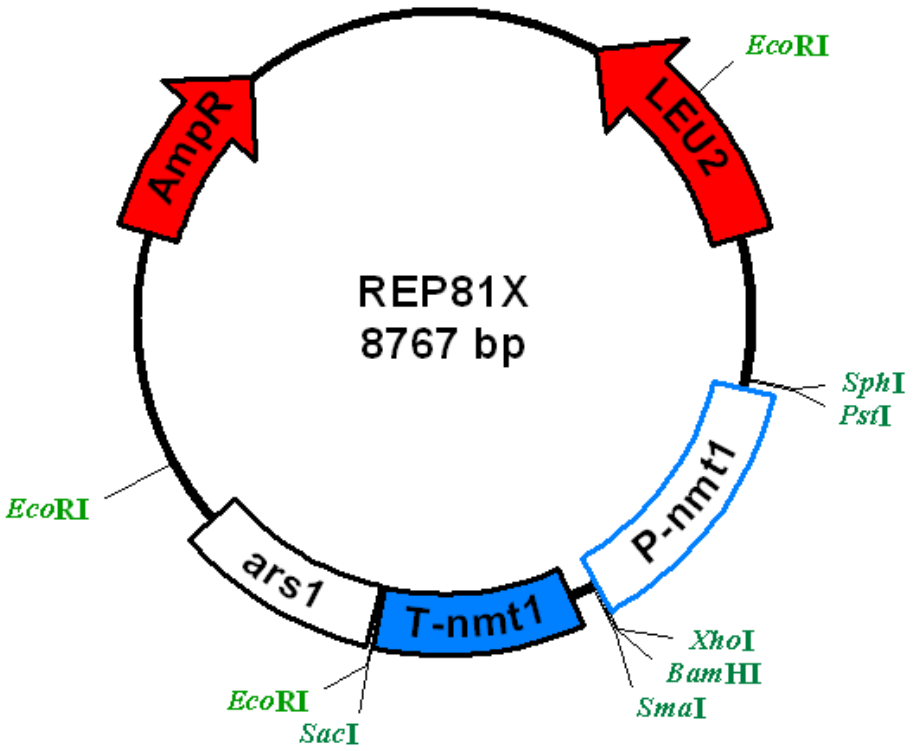
Zou L, Elledge SJ (2003) Sensing DNA damage through ATRIP recognition of RPA-ssDNA complexes. Science **300:** 1542-1548

Zlatanova J, Thakar A (2008) H2A.Z: view from the top. Structure **16**: 166-179

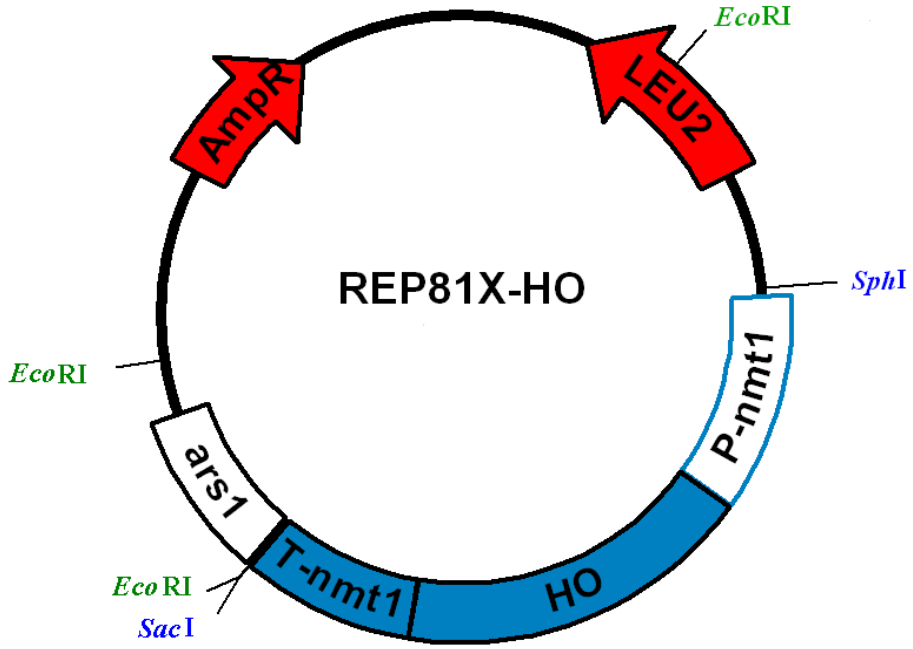
Appendices

Appendix I Plasmids used in this study

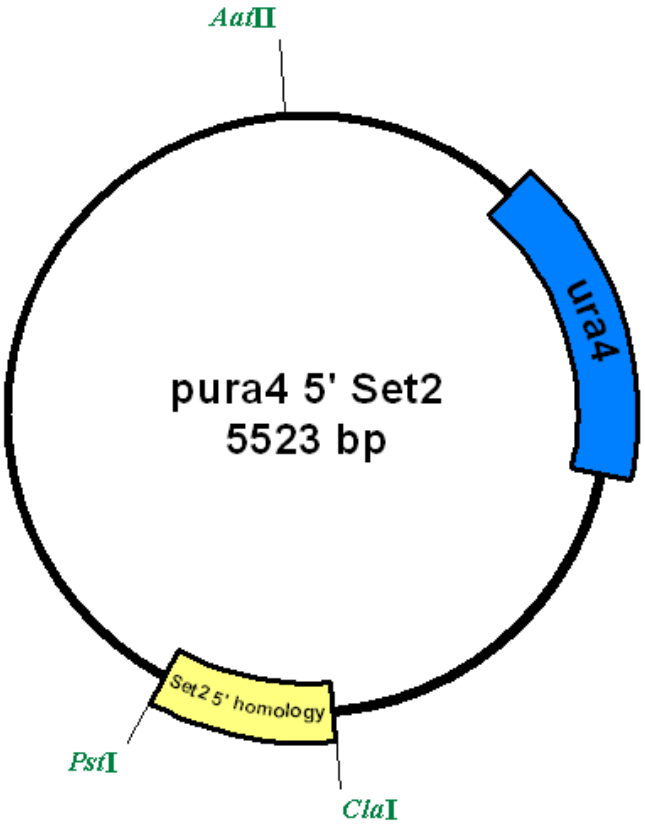
Number	Name	Insert	Backbone	Source	Notes
15	pJK210	*ura4*	pJK210		See Keeney *et al,* 2004
28	pREP81X-HO	*HO*	pREP81X	Lab stock	Shown below
38	pREP3X	*LEU2*	pREP3X	Lab stock	
40	pREP81X	-	pREP81X	Lab stock	Shown below
41	pREP82X	-	pREP82X	Lab stock	
100	PS	*LEU2* and *PstI* fragment	pAL19	Kind gift from A. Carr	See Manolis *et al,* 2001
101	PI	*LEU2* and *EcoRI* fragment	pAL19	Kind gift from A. Carr	See Manolis *et al,* 2001
102	pAL19	*LEU2*	pAL19	Kind gift from A. Carr	See Manolis *et al,* 2001
156	pREP82X-HO	*HO*	pREP82X	Lab stock	
207	pADH-GFP	*adh-GFP*	pFA6a	Lab stock	
248	p*ura4*-5' Set2	5' *set2*	pJK210	This study	Shown below
249	pSet2-R255G	*set2-R255G*	pJK210	This study	Shown below
255	pREP3X-Gcn5	*gcn5*	pREP3X	This study	Shown below
268	pREP81X-Cdt1-*LEU2*	*cdt1*	pREP81X	Kind gift from S. Kearsey	
269	pREP81X-Cdc18-*hph*	*cdc18*	pREP81X	Kind gift from S. Kearsey	



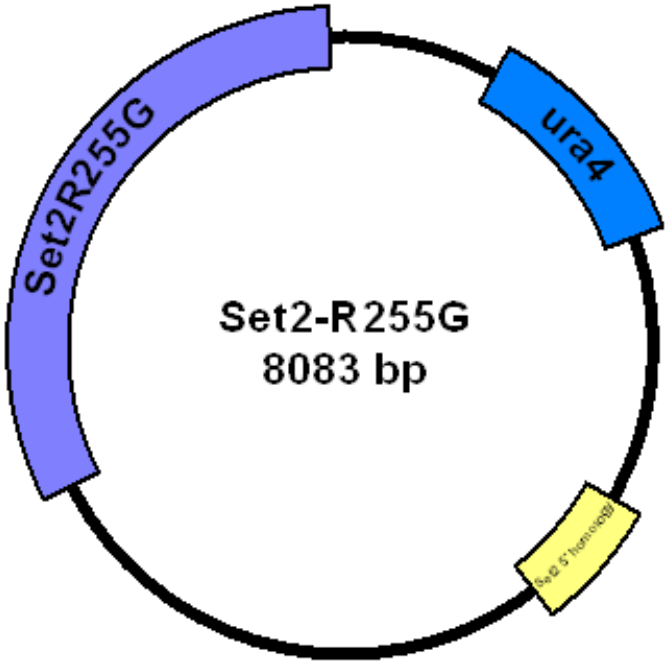
pREP81X (p40); this *LEU2* multi-copy plasmid contains the thiamine repressible *nmt* promoter. A kind gift from Fekret Osman (Osman et al., 1996).



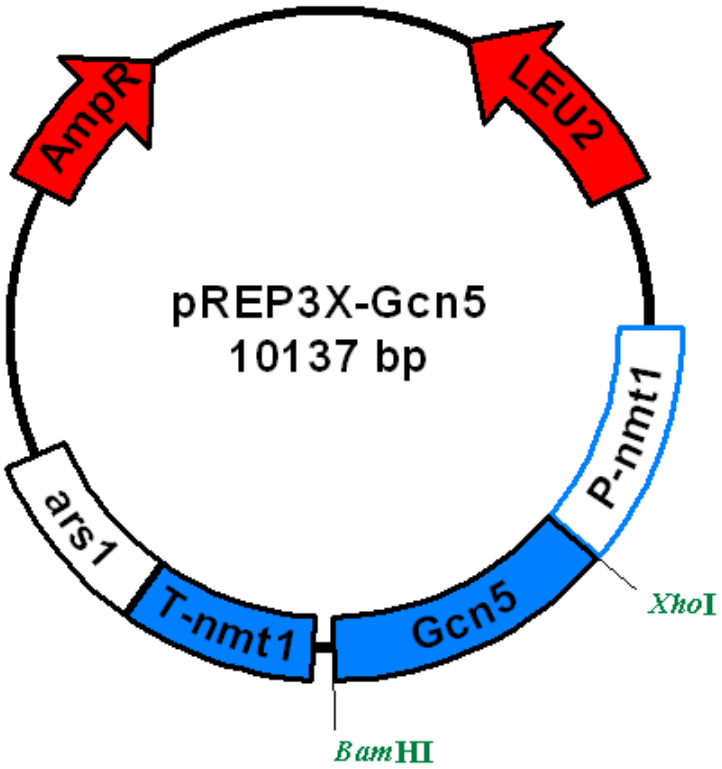
pREP81X-*HO* (p28) contains the *S. cerevisiae* HO-endonuclease ORF under control of the thiamine repressible *nmt* promoter. A kind gift from Fekret Osman (Osman et al., 1996).



p*ura4* 5' Set2 (p248) contains 5' homology to *set2*$^{+}$ downstream of a *ura4* marker. Construction shown in Appendix VIII.



pSet2-R255G (p249) contains *set2-R255G* adjacent to a *ura4* marker, with homology downstream from *set2*$^{+}$. Construction shown in Appendix VIII.



pREP3X-Gcn5 (p255) contains the Gcn5 ORF under control of the thiamine repressible *nmt* promoter.

Appendix II Oligonucleotides used in this study

Homology	Sequence	Orientation	RS	Notes	No.
set2	GTGATTGCAAAATCCTGCGAGCGA	R	-	For creation of Set2 R255G mutant	545
set2	TCGCTCGCAGGATTTTGCAATCAC	F	-	For creation of Set2 R255G mutant	546
set2	ATATGACGTCTTTTTGTCCATTATCATACA	F	*AatII*	For creation of Set2 R255G mutant	577
set2	ATATGACGTCTAGTATTAAAATATTACATC	R	*AatII*	For creation of Set2 R255G mutant	578
set2	ATATATCGATAACTGCGACAAGTAGCAACG	F	*ClaI*	For PCR of *set2* downstream homology	579
set2	ATATCTGCATTTATTACTCGTGGAACCATT	R	*PstI*	For PCR of *set2* downstream homology	580
ura4	GCTGATATGCCTTCCAACCAGC	R	-	For confirmation of *set2-R255G cells*	384
set2	ATATATCTCGAGATGCAGACGGCATCATCTCT	F	*XhoI*	Creation of *set2* OP vector	599
set2	ATATATCCCGGGACTATAGTATGGTAGACGTT	R	*SmaI*	Creation of *set2* OP vector	600
gcn5	ATATATCTCGAGATGTCGAATTCGTTAAATGA	F	*XhoI*	Creation of *gcn5* OP vector	597
gcn5	ATATATGGATCCTTAATCGGCTAAGTGTGAAT	R	*Bam HI*	Creation of *gcn5* OP vector	632
LEU2	CCGCTCGGCCAAACAACC	R	-	Confirmation of OP vector	73

Oligonucleotide sequences, orientation (forward (F) or reverse (R)), region homologous to (homology), any restriction site (RS) and use in this study (notes) are given. Number with no prefix refers to position in Humphrey lab collection. All oligonucleotide primers were purchased from Sigma Aldrich.

Appendix III Analysis of nineteen histone-modifying mutants

Mutant	Bleomycin response	IR response	GC	NHEJ
*set1*Δ	R	R (survival curve)	Increased	Decreased
*set2*Δ	R	R (survival curve)	Increased	Decreased
*mst2*Δ	R	R (survival curve)	Increased	Decreased
*sir2*Δ	R	WT	Increased	WT
*set5*Δ	R	WT	WT	-
*hst2*Δ	R	WT	-	-
*set6*Δ	R	WT	WT	-
*set8*Δ	R	WT	WT	-
*set9*Δ	R	WT	-	-
*set3*Δ	WT	WT	Increased	Decreased
*set13*Δ	R	WT	Decreased	WT
*clr3*Δ	R	WT	WT	-
*gcn5*Δ	WT	WT	Decreased	Increased
*set10*Δ	R	WT	WT	-
*SPBC16C6.01c*Δ	R	WT	WT	-
*set11*Δ	R	WT	Increased	WT
*hat1*Δ	R	WT	Decreased	WT
*elp3*Δ	S	S	WT	-
*clr4*Δ	WT	WT	Decreased	-

Table shows response to bleomycin and IR, either resistant compared to wildtype (R), sensitive compared to wildtype (S) or wildtype response (WT). In addition, GC levels as determined using the DSB assay are shown as increased, decreased or wildtype (WT). For those mutants analysed by the plasmid-rejoining assay, NHEJ levels are shown as increased, decreased or wildtype (WT).

Appendix IV Genetic determinants of site-specific DSB-induced marker loss

Genetic background	% NHEJ/ SCC	p value	% GC	p value	% Ch^{16} loss	p value	% LOH	p value	% spontaneous Ch^{16} loss
Wildtype Ch^{16}-RMGAH	20 ± 2.3	-	55 ± 2.3	-	17 ± 1.4	-	7 ± 1.0	-	0
Wildtype Ch^{16}-RMYAH	4 ± 0.8	-	67 ± 1.4	-	20 ± 0.8	-	8 ± 0.6	-	0
set1Δ (RMGAH)	17 ± 1.8	0.93	67 ± 2.0	<0.01	8 ± 1.0	0.03	6 ± 0.6	0.02	1
set2Δ (RMGAH)	16 ± 4.6	0.57	72 ± 3.4	0.02	5 ± 2.2	0.02	5 ± 1.5	0.09	0
set2Δ	2 ± 0.5	0.63	79 ± 0.9	<0.01	13 ± 0.1	0.09	5 ± 1.3	0.09	1
mst2Δ (RMGAH)	10 ± 0.4	0.02	80 ± 1.0	<0.01	7 ± 0.9	<0.01	1 ± 0.9	<0.01	0
sir2Δ (RMGAH)	11 ± 0.6	0.02	74 ± 1.4	<0.01	11 ± 0.9	0.08	4 ± 0.3	<0.01	1
set3Δ	3 ± 0.4	0.33	74 ± 1.5	<0.01	17 ± 1.2	0.02	4 ± 1.0	0.04	0
set11Δ	3 ± 0.3	0.29	80 ± 0.4	<0.01	12 ± 1.1	0.01	5 ± 0.3	<0.01	1
hat1Δ	4 ± 0.7	0.72	39 ± 3.6	<0.01	42 ± 1.4	<0.01	13 ± 1.8	0.05	1
set13Δ	5 ± 0.2	0.06	54 ± 2.8	0.02	28 ± 2.4	0.08	11 ± 0.4	<0.01	0
clr4Δ	5 ± 1.9	0.15	39 ± 6.5	0.08	9 ± 5.4	0.50	0 ± 0.2	0.03	42
gcn5Δ	33 ± 1.6	<0.01	45 ± 3.0	<0.01	14 ± 1.5	0.18	6 ± 0.1	0.04	1
set5Δ	7 ± 2.9	0.41	66 ± 1.6	0.86	17 ± 3.4	0.88	6 ± 0.8	0.60	1
set6Δ	3 ± 0.3	0.35	70 ± 2.4	0.21	18 ± 1.8	0.18	8 ± 0.7	0.43	0
set8Δ	5 ± 0.8	0.47	72 ± 0.8	0.19	15 ± 1.8	0.09	8 ± 1.2	0.69	0
clr3Δ	11 ± 2.0	0.06	72 ± 3.0	0.49	11 ± 2.1	0.11	4 ± 0.6	<0.01	1
SPBC16C6.01Δ	4 ± 0.6	0.67	69 ± 4.1	0.27	19 ± 1.8	0.83	8 ± 1.8	0.68	0
elp3Δ	18 ± 1.0	<0.01	72 ± 1.0	0.09	6 ± 0.5	<0.01	3 ± 0.4	0.03	0
set10Δ	5 ± 0.1	0.71	67 ± 4.6	0.94	17 ± 5.0	0.85	10 ± 0.1	0.19	0
lig4Δ (RMGAH)	18 ± 1.3	0.85	61 ± 2.0	0.03	14 ± 0.4	0.18	7 ± 1.0	0.13	0
ku70Δ (RMGAH)	14 ± 1.5	0.17	82 ± 1.7	0.02	2 ± 0.2	0.01	1 ± 0.2	0.04	0
set2Δlig4Δ (RMGAH)	25 ± 2.0	0.19	69 ± 1.8	<0.01	5 ± 0.8	<0.01	2 ± 0.3	0.01	0
set2Δku70Δ	8 ± 2.5	0.20	81 ± 5.0	0.07	8 ± 2.4	0.03	5 ± 1.6	0.14	0
exo1Δ (RMGAH)	8 ± 1.6	0.02	66 ± 2.3	0.02	17 ± 0.4	0.74	9 ± 0.8	0.50	0
set2Δexo1Δ (RMGAH)	20 ± 3.2	0.3	66 ± 4.7	0.28	9 ± 0.7	0.02	3 ± 0.8	0.18	1
set2-R255G (RMGAH)	12 ± 1.8	0.24	70 ± 1.8	<0.01	12 ± 1.7	0.10	5 ± 0.1	<0.01	0
set2Δgcn5Δ	21 ± 1.4	<0.01	71 ± 1.7	0.65	5 ± 0.2	0.01	2 ± 0.3	<0.01	1
gcn5Δlig4Δ	23 ± 1.5	<0.01	56 ± 1.5	0.02	14 ± 2.2	0.07	6 ± <0.01	0.03	0
gcn5Δ Gcn5 OP	4 ± 0.5	<0.01	92 ± 1.0	<0.01	2 ± 0.4	<0.01	0 ± 0	<0.01	0
cdk9-T212E	3 ± 1.0	0.47	20 ± 8.8	0.02	68 ± 11.7	0.04	4 ± 4.0	0.39	0

For each genetic background the assay was repeated three times (with independent isolates), such that >1000 colonies were scored. Mean ± the standard errors of the three experiments are shown. A single blank vector control was also analysed in each genetic background to give a spontaneous level of Ch^{16} loss, which was subtracted to calculate the break-induced values shown above. P values are calculated against wildtype Ch^{16}-RMYAH unless otherwise stated.

Appendix V 140 transcripts are up-regulated in untreated *set2*Δ cells compared to wildtype

	Systematic	*set2*Δ level	Description	Principle GO term
1	vtc4	194.14	vacuolar transporter chaperone complex subunit (predicted)	Vacuole processing
2	prl61	16.96	antisense RNA (predicted)	No annotation
3	SPBCPT2R1.06c	10.75	pseudogene	No annotation
4	SPAC212.08c	10.53	GPI anchored protein (predicted)	No annotation
5	SPAC186.01	10.03	cell surface glycoprotein (predicted)	Cell adhesion
6	SPAC212.02	7.33	sequence orphan	No annotation
7	SPBCPT2R1.02	7.24	sequence orphan	No annotation
8	SPAC186.09	6.59	pyruvate decarboxylase (predicted)	Amino acid metabolism
9	SPAC212.06c	6.12	DNA helicase in rearranged telomeric region, truncated	No annotation
10	SPBC1348.03	5.96	S. pombe specific 5TM protein family	No annotation
11	SPAC186.04c	5.87	N-terminal of transmembrane channel, trunucated	No annotation
12	SPNCRNA.448	5.38	non-coding RNA (predicted)	No annotation
13	SPAC977.02	5.36	S. pombe specific 5TM protein family	No annotation
14	SPBPB2B2.17c	5.20	S. pombe specific 5TM protein family	No annotation
15	tlh1	5.01	RecQ type DNA helicase	DNA recombination
16	SPNCRNA.871	4.78	antisense RNA (predicted)	No annotation
17	SPAC212.01c	4.77	S. pombe specific DUF999 family protein 2	No annotation
18	SPAC977.03	4.76	methyltransferase (predicted)	No annotation
19	SPBC1348.01	4.71	S. pombe specific DUF999 protein family 5	No annotation
20	SPBCPT2R1.04c	4.65	S. pombe specific DUF999 protein family 10	No annotation
21	SPAC750.06c	4.63	S. pombe specific DUF999 protein family 4	No annotation
22	SPAC186.06	4.62	ER unfolded protein response protein (predicted)	Signalling
23	SPAC750.05c	4.41	S. pombe specific 5TM protein family	No annotation
24	SPAC750.03c	4.40	methyltransferase (predicted)	No annotation
25	rec10	4.34	meiotic recombination protein Rec10	Meiosis
26	SPBPB2B2.16c	4.31	MFS family membrane transporter (predicted)	Transport
27	SPAC186.05c	4.31	human TMEM165 homolog	No annotation
28	SPAC977.01	4.26	S. pombe specific 5TM protein family	No annotation
29	SPBC1348.04	4.20	methyltransferase (predicted)	No annotation
30	SPBPB2B2.19c	4.12	S. pombe specific 5TM protein family	No annotation
31	SPBC1348.05	4.12	membrane transporter (predicted)	Transport
32	SPBPB2B2.18	4.04	sequence orphan	No annotation
33	SPBC1348.07	3.93	S. pombe specific DUF999 protein family 6	No annotation
34	SPAC977.04	3.90	truncated C terminal region of membrane transporter	No annotation
35	SPBPB2B2.14c	3.89	S. pombe specific DUF999 protein family 8	No annotation
36	SPBCPT2R1.05c	3.82	pseudogene	No annotation
37	meu6	3.82	meiotic chromosome segregation protein Meu6	Meiosis
38	SPNCRNA.70	3.82	non-coding RNA (predicted)	No annotation
39	meu27	3.79	S. pombe specific UPF0300 family protein 5	No annotation
40	SPCC777.04	3.76	amino acid transporter (predicted)	Transport
41	SPAC869.03c	3.75	urea transporter (predicted)	Transport
42	SPAC212.05c	3.71	pseudogene	No annotation
43	SPAC750.07c	3.59	S. pombe specific GPI anchored protein family 1	No annotation
44	SPNCRNA.1210	3.55	antisense RNA (predicted)	No annotation
45	SPBCPT2R1.03	3.41	hypothetical protein	No annotation

	Systematic	*set2*Δ level	Description	Principle GO term
46	SPAC977.07c	3.41	cell surface glycoprotein (predicted)	Cell adhesion
47	SPBC1348.08c	3.40	cell surface glycoprotein (predicted)	Cell adhesion
48	SPAC212.04c	3.34	S. pombe specific DUF999 family protein 1	Response to stress
49	SPBPB2B2.15	3.33	conserved fungal family	No annotation
50	SPNCRNA.700	3.29	antisense RNA (predicted)	No annotation
51	mug136	3.24	acetylglucosaminyltransferase (predicted)	Carbohydrate metabolism
52	SPNCRNA.560	3.19	antisense RNA (predicted)	No annotation
53	SPNCRNA.284	3.19	non-coding RNA (predicted)	No annotation
54	spn6	3.19	septin Spn6 (predicted)	No annotation
55	SPAC977.06	3.14	S. pombe specific DUF999 family protein 3	DNA repair
56	dmc1	3.14	RecA family ATPase Dmc1	Transport
57	pma2	3.12	P-type proton ATPase, P3-type Pma2	No annotation
58	SPBPB2B2.08	3.05	conserved fungal protein	No annotation
59	crp79	3.04	poly(A) binding protein Crp79	Transport
60	SPNCRNA.952	2.91	antisense RNA (predicted), possible alternative UTR	No annotation
61	SPNCRNA.610	2.91	antisense RNA (predicted)	No annotation
62	SPNCRNA.1079	2.89	antisense RNA (predicted), possible alternative UTR	No annotation
63	SPNCRNA.647	2.80	antisense RNA (predicted)	No annotation
64	SPNCRNA.1179	2.78	antisense RNA (predicted)	No annotation
65	SPNCRNA.371	2.78	non-coding RNA, centromeric (predicted)	No annotation
66	SPNCRNA.1697	2.74	antisense RNA (predicted)	No annotation
67	ppk31	2.67	serine/threonine protein kinase Ppk31 (predicted)	Signalling
68	SPAC5H10.04	2.65	NADPH dehydrogenase (predicted)	No annotation
69	isp4	2.62	OPT oligopeptide transporter family Isp4	Transport
70	ght5	2.62	hexose transporter Ght5	Transport
71	SPNCRNA.713	2.57	antisense RNA (predicted)	No annotation
72	SPNCRNA.1006	2.50	antisense RNA (predicted)	No annotation
73	SPNCRNA.1539	2.50	antisense RNA (predicted)	No annotation
74	SPNCRNA.691	2.49	antisense RNA (predicted)	No annotation
75	meu25	2.48	sequence orphan Meu25	Meiosis
76	pol4	2.48	DNA polymerase X family	DNA repair
77	SPNCRNA.1591	2.48	antisense RNA (predicted)	No annotation
78	rdh54	2.45	ATP-dependent DNA helicase Rdh54	DNA repair
79	SPNCRNA.1300	2.45	intergenic RNA (predicted)	No annotation
80	SPNCRNA.616	2.43	antisense RNA (predicted)	No annotation
81	SPNCRNA.1438	2.42	antisense RNA (predicted)	No annotation
82	SPNCRNA.838	2.41	antisense RNA (predicted)	No annotation
83	lsk1	2.41	P-TEFb-associated cyclin-dependent protein kinase Lsk1	Signalling
84	SPNCRNA.1271	2.40	antisense RNA (predicted), possible alternative UTR	No annotation
85	SPNCRNA.803	2.40	antisense RNA (predicted)	No annotation
86	SPNCRNA.601	2.38	intergenic RNA (predicted)	No annotation
87	SPNCRNA.1178	2.38	antisense RNA (predicted)	No annotation
88	SPNCRNA.678	2.37	antisense RNA (predicted)	No annotation
89	SPCC1742.01	2.37	sequence orphan	No annotation
90	SPNCRNA.1337	2.36	antisense RNA (predicted)	No annotation
91	SPNCRNA.1535	2.35	antisense RNA (predicted)	No annotation
92	SPNCRNA.1172	2.35	intergenic RNA (predicted)	No annotation
93	SPNCRNA.731	2.34	antisense RNA (predicted)	No annotation
94	SPNCRNA.1454	2.34	antisense RNA (predicted)	No annotation
95	SPNCRNA.1687	2.33	antisense RNA (predicted)	No annotation

	Systematic	*set2*Δ level	Description	Principle GO term
96	map4	2.33	cell surface agglutination protein Map4	Cell adhesion
97	SPBPB2B2.06c	2.31	phosphoprotein phosphatase (predicted)	No annotation
98	SPNCRNA.1450	2.31	antisense RNA (predicted)	No annotation
99	mcp3	2.29	sequence orphan	Meiosis
100	mel1	2.28	alpha-galactosidase, melibiase	Carbohydrate metabolism
101	SPNCRNA.551	2.27	antisense RNA (predicted)	No annotation
102	SPNCRNA.1421	2.26	antisense RNA (predicted)	No annotation
103	SPNCRNA.1183	2.26	antisense RNA (predicted)	No annotation
104	akr1	2.26	palmitoyltransferase Akr1 (predicted)	Transport
105	SPBC947.04	2.24	cell surface glycoprotein (predicted), DIPSY family	Cell adhesion
106	SPNCRNA.232	2.22	non-coding RNA, centromeric (predicted)	No annotation
107	SPBC17D1.07c	2.21	GTPase regulator (predicted)	Signalling
108	SPNCRNA.773	2.21	antisense RNA (predicted)	No annotation
109	SPNCRNA.1026	2.20	antisense RNA (predicted)	No annotation
110	SPNCRNA.569	2.20	antisense RNA (predicted)	No annotation
111	SPNCRNA.953	2.18	intergenic RNA (predicted)	No annotation
112	SPNCRNA.1062	2.16	intergenic RNA (predicted), possible alternative UTR	No annotation
113	SPCC1450.09c	2.16	phospholipase (predicted)	Lipid metabolism
114	SPNCRNA.230	2.15	non-coding RNA, centromeric (predicted)	No annotation
115	SPNCRNA.1525	2.15	antisense RNA (predicted)	No annotation
116	SPNCRNA.990	2.15	antisense RNA (predicted)	No annotation
117	SPAC3G9.11c	2.14	pyruvate decarboxylase (predicted)	Amino acid metabolism
118	SPNCRNA.1446	2.14	antisense RNA (predicted), possible alternative UTR	No annotation
119	SPNCRNA.1647	2.14	antisense RNA (predicted)	No annotation
120	SPBC1348.11	2.13	membrane transporter, pseudogene	No annotation
121	SPNCRNA.836	2.12	antisense RNA (predicted)	No annotation
122	SPCC777.03c	2.12	nifs homolog, possible cysteine desulfurase	No annotation
123	SPNCRNA.361	2.11	non-coding RNA, centromeric (predicted)	No annotation
124	prl11	2.10	non-coding RNA, poly(A)-bearing (predicted)	No annotation
125	SPNCRNA.359	2.09	non-coding RNA, centromeric (predicted)	No annotation
126	mug132	2.09	S. pombe specific UPF0300 family protein 3	No annotation
127	alp1	2.09	tubulin specific chaperone cofactor D, Alp1	Cytoskeleton organisation
128	SPAC186.03	2.09	L-asparaginase (predicted)	Amino acid metabolism
129	SPNCRNA.1456	2.08	antisense RNA (predicted)	No annotation
130	SPNCRNA.1027	2.06	antisense RNA (predicted)	No annotation
131	SPAC1F8.04c	2.04	hydrolase (predicted)	Response to stress
132	SPNCRNA.613	2.04	antisense RNA (predicted)	No annotation
133	SPNCRNA.1195	2.03	antisense RNA (predicted)	No annotation
134	spn5	2.03	septin Spn5	Meiosis
135	mok11	2.01	alpha-1,3-glucan synthase Mok11	Carbohydrate metabolism
136	SPNCRNA.1339	2.01	intergenic RNA (predicted)	No annotation
137	SPNCRNA.1028	2.01	antisense RNA (predicted)	No annotation
138	fta5	2.00	cell surface glycoprotein	Cell adhesion
139	nsk1	2.00	Clp1-interacting protein Nsk1	No annotation
140	SPNCRNA.653	2.00	antisense RNA (predicted)	No annotation

The *set2*Δ level is compared to wildtype, where the normal level of transcript for untreated wildtype cells is 1.0.

Appendix VI Forty-six transcripts are down-regulated in untreated *set2*Δ cells compared to wildtype

	Systematic	set2Δ level	Description	Principle GO term
1	SPNCRNA.879	0.50	intergenic RNA (predicted)	No annotation
2	SPCC737.04	0.50	S. pombe specific UPF0300 family protein 6	No annotation
3	SPNCRNA.1474	0.49	intergenic RNA (predicted)	No annotation
4	SPNCRNA.583	0.49	antisense RNA (predicted)	No annotation
5	SPNCRNA.1352	0.48	intergenic RNA (predicted)	No annotation
6	mug146	0.48	meiotically upregulated gene Mug46	Ascospore formation
7	SPNCRNA.1527	0.48	intergenic RNA (predicted), possible alternative UTR	No annotation
8	SPNCRNA.1541	0.47	intergenic RNA (predicted)	No annotation
9	hsp9	0.47	heat shock protein Hsp9	Cytoskeleton organisation
10	SPAC23H3.15c	0.47	sequence orphan	Response to stress
11	SPCPB16A4.07	0.47	sequence orphan	No annotation
12	SPNCRNA.1000	0.46	intergenic RNA (predicted), possible alternative UTR	No annotation
13	SPCC330.03c	0.46	NADPH-hemoprotein reductase (predicted)	Response to stress
14	SPNCRNA.571	0.46	antisense RNA (predicted)	No annotation
15	caf5	0.45	spermine family transmembrane transporter Caf5	Transport
16	SPAC637.03	0.45	conserved fungal protein	Response to stress
17	ecl2	0.44	extender of the chronological lifespan protein Ecl2	No annotation
18	SPNCRNA.1435	0.44	antisense RNA (predicted)	No annotation
19	urg1	0.43	GTP cyclohydrolase II (predicted)	Vitamin metabolism
20	SPBC11C11.06c	0.43	sequence orphan	Response to stress
21	SPBC947.05c	0.41	ferric-chelate reductase (predicted)	Transport
22	SPNCRNA.1691	0.41	intergenic RNA (predicted), possible alternative UTR	No annotation
23	SPNCRNA.1055	0.40	intergenic RNA (predicted), possible alternative UTR	No annotation
24	gst2	0.40	glutathione S-transferase Gst2	Response to stress
25	SPBC725.03	0.39	conserved fungal protein	Response to stress
26	SPNCRNA.609	0.39	antisense RNA (predicted), possible alternative UTR	No annotation
27	SPAPJ691.02	0.39	yippee-like protein	Response to stress
28	SPBC215.11c	0.38	aldo/keto reductase, unknown biological role	Response to stress
29	SPCC338.18	0.37	sequence orphan	Response to stress
30	SPBC16D10.08c	0.37	heat shock protein Hsp104 (predicted)	Response to stress
31	SPNCRNA.276	0.37	non-coding RNA (predicted)	No annotation
32	SPNCRNA.1287	0.36	intergenic RNA (predicted), possible alternative UTR	No annotation
33	SPBC21C3.19	0.36	SBDS family protein Rtc3 (predicted)	Response to stress
34	car1	0.34	arginase Car1	Amino acid metabolism
35	SPNCRNA.935	0.34	intergenic RNA (predicted), possible alternative UTR	No annotation
36	cta3	0.34	P-type ATPase, calcium transporting Cta3	Transport
37	SPBC19C7.04c	0.25	conserved fungal protein	No annotation
38	SPCC70.04c	0.25	sequence orphan	No annotation
39	alr2	0.24	alanine racemase Alr2 (predicted)	Amino acid metabolism
40	ssa1	0.22	heat shock protein Ssa1 (predicted)	Response to stress
41	zym1	0.22	metallothionein Zym1	Response to stress
42	SPNCRNA.781	0.21	intergenic RNA (predicted)	No annotation
43	bub1	0.14	serine/threonine protein kinase Bub1	Chromatin modification
44	ecl1	0.12	extender of the chronological lifespan protein Ecl1	No annotation
45	hsp16	0.12	heat shock protein Hsp16	Response to stress
46	SPNCRNA.319	0.10	non-coding RNA (predicted)	No annotation

The *set2*Δ level is compared to wildtype, where the normal level of transcript for untreated wildtype cells is 1.0.

Appendix VII Transcripts with altered expression following bleomycin treatment in *set2*Δ cells compared to wildtype.

Category 1: Thirty transcripts that are increased in wildtype cells following bleomycin treatment and increased less in *set2*Δ cells

Systematic	Difference *set2*Δ	Difference WT	Description
cdt2	1.03	1.44	WD repeat protein Cdt2
SPNCRNA.1696	0.52	0.93	antisense RNA (predicted)
ams2	0.31	0.77	cell cycle regulated GATA-type transcription factor Ams2
SPNCRNA.958	0.19	0.40	intergenic RNA (predicted), possible alternative UTR
SPNCRNA.863	0.19	0.58	intergenic RNA (predicted)
SPNCRNA.532	0.16	0.39	non-coding RNA (predicted)
SPNCRNA.1457	0.15	0.39	antisense RNA (predicted)
SPNCRNA.1324	0.15	0.38	antisense RNA (predicted)
SPNCRNA.1654	0.13	0.66	antisense RNA (predicted)
atf31	0.09	0.34	transcription factor Atf31
SPNCRNA.1469	0.09	0.33	antisense RNA (predicted)
SPNCRNA.586	0.07	0.36	non-coding RNA (predicted)
SPNCRNA.605	0.07	0.35	antisense RNA (predicted)
SPNCRNA.827	0.06	0.30	antisense RNA (predicted), possible alternative UTR
SPAC11D3.01c	0.06	0.30	conserved fungal protein
SPNCRNA.858	0.05	0.28	antisense RNA (predicted), possible alternative UTR
SPNCRNA.1259	0.05	0.27	antisense RNA (predicted), possible alternative UTR
SPNCRNA.1345	0.05	0.35	antisense RNA (predicted)
SPAC1002.16c	0.05	0.43	nicotinic acid plasma membrane transporter (predicted)
SPBC8E4.02c	0.04	0.29	sequence orphan
SPNCRNA.698	0.04	0.28	intergenic RNA (predicted), possible alternative UTR
SPNCRNA.1129	0.03	0.26	intergenic RNA (predicted)
SPNCRNA.551	0.02	0.24	antisense RNA (predicted)
mug95	0.02	0.35	sequence orphan
SPAPB18E9.04c	0.02	0.34	sequence orphan
SPNCRNA.1018	0.02	0.27	antisense RNA (predicted), possible alternative UTR
SPAC212.08c	0.01	0.30	GPI anchored protein (predicted)
SPNCRNA.797	0.01	0.22	antisense RNA (predicted)
SPNCRNA.1494	0.01	0.38	intergenic RNA (predicted), possible alternative UTR
SPNCRNA.1306	0.00	0.23	intergenic RNA (predicted)

Category 2: Fifty-six transcripts that are increased following bleomycin treatment in wildtype cells, and decreased following bleomycin treatment in *set2*Δ cells

Systematic	Difference *set2*Δ	Difference WT	Description
cdc18	-0.30	0.13	MCM loader
SPNCRNA.1647	-0.25	0.09	antisense RNA (predicted)
fip1	-0.23	0.03	iron permease Fip1
SPNCRNA.678	-0.22	0.08	antisense RNA (predicted)
SPNCRNA.1198	-0.21	0.01	antisense RNA (predicted), possible alternative UTR
SPNCRNA.1392	-0.21	0.01	intergenic RNA (predicted), possible alternative UTR
SPNCRNA.746	-0.21	0.02	intergenic RNA (predicted)
SPNCRNA.1186	-0.18	0.24	intergenic RNA (predicted), possible alternative UTR
SPNCRNA.770	-0.18	0.04	antisense RNA (predicted)
SPNCRNA.1310	-0.17	0.15	intergenic RNA (predicted)
SPAPB18E9.05c	-0.17	0.17	dubious
SPNCRNA.1633	-0.17	0.20	antisense RNA (predicted), possible alternative UTR
SPNCRNA.898	-0.16	0.07	antisense RNA (predicted)
SPNCRNA.909	-0.15	0.12	intergenic RNA (predicted)
SPCC569.04	-0.15	0.09	sequence orphan
SPNCRNA.1642	-0.15	0.14	antisense RNA (predicted)
SPNCRNA.243	-0.13	0.11	non-coding RNA (predicted)
SPNCRNA.709	-0.13	0.11	intergenic RNA (predicted)
SPNCRNA.1591	-0.12	0.19	antisense RNA (predicted)
SPNCRNA.1370	-0.12	0.13	intergenic RNA (predicted)
SPNCRNA.1408	-0.11	0.24	antisense RNA (predicted)
SPNCRNA.358	-0.11	0.18	non-coding RNA (predicted)
SPNCRNA.1525	-0.11	0.12	antisense RNA (predicted)
SPNCRNA.833	-0.10	0.17	antisense RNA (predicted)
SPNCRNA.937	-0.10	0.23	antisense RNA (predicted)
SPNCRNA.953	-0.10	0.38	intergenic RNA (predicted)
SPNCRNA.1159	-0.10	0.13	intergenic RNA (predicted)
SPNCRNA.1363	-0.10	0.12	antisense RNA (predicted)
SPNCRNA.325	-0.10	0.40	non-coding RNA (predicted)
SPNCRNA.905	-0.09	0.11	antisense RNA (predicted)
SPNCRNA.1096	-0.09	0.17	antisense RNA (predicted)
SPNCRNA.621	-0.08	0.14	intergenic RNA (predicted)
pma2	-0.08	0.26	P-type proton ATPase, P3-type Pma2
SPNCRNA.1183	-0.07	0.18	antisense RNA (predicted)
SPAC5H10.04	-0.06	0.15	NADPH dehydrogenase (predicted)
SPNCRNA.1047	-0.06	0.16	antisense RNA (predicted), possible alternative UTR
SPNCRNA.1361	-0.06	0.18	intergenic RNA (predicted)
SPNCRNA.691	-0.06	0.15	antisense RNA (predicted)
SPNCRNA.1079	-0.06	0.19	antisense RNA (predicted), possible alternative UTR
SPNCRNA.1450	-0.06	0.18	antisense RNA (predicted)
SPNCRNA.1045	-0.06	0.18	antisense RNA (predicted)
rps3002	-0.05	0.20	40S ribosomal protein S30 (predicted)

Systematic	Difference *set2*Δ	Difference WT	Description
SPNCRNA.928	-0.05	0.29	antisense RNA (predicted)
SPNCRNA.838	-0.05	0.19	antisense RNA (predicted)
SPNCRNA.807	-0.05	0.21	antisense RNA (predicted), possible alternative UTR
SPNCRNA.75	-0.04	0.17	non-coding RNA (predicted)
SPNCRNA.1687	-0.04	0.20	antisense RNA (predicted)
SPNCRNA.1305	-0.03	0.18	antisense RNA (predicted)
SPNCRNA.705	-0.03	0.23	antisense RNA (predicted)
SPNCRNA.695	-0.03	0.19	antisense RNA (predicted)
SPNCRNA.1602	-0.03	0.18	antisense RNA (predicted)
prl43	-0.02	0.36	non-coding RNA, poly(A)-bearing (predicted)
seb1	-0.02	0.28	RNA-binding protein Seb1
SPNCRNA.1588	-0.01	0.27	antisense RNA (predicted)
SPBC557.05	-0.01	0.22	arrestin
SPNCRNA.604	0.00	0.22	intergenic RNA (predicted)

Category 3: Six transcripts that are reduced following bleomycin treatment in wildtype cells, and further decreased in *set2*Δ cells

Systematic	Difference *set2*Δ	Difference WT	Description
SPAP14E8.02	-0.41	-0.15	FHA domain protein Tos4 (predicted)
cdt1	-0.38	-0.14	replication licensing factor Cdt1
cdc22	-0.37	-0.08	ribonucleoside reductase large subunit Cdc22
fio1	-0.27	-0.02	iron transport multicopper oxidase Fio1
sod1	-0.24	0.00	superoxide dismutase Sod1
rpl22	-0.21	-0.01	60S ribosomal protein L22 (predicted)

Category 4: Ninety-one transcripts that are increased in *set2*Δ cells following bleomycin treatment, and less increased in wildtype.

Systematic	Difference *set2*Δ	Difference WT	Description
hsp16	3.75	0.25	heat shock protein Hsp16
ssa1	3.14	0.44	heat shock protein Ssa1 (predicted)
SPBC16D10.08c	2.37	0.48	heat shock protein Hsp104 (predicted)
ctr4	1.71	0.45	copper transporter complex subunit Ctr4
SPCC338.18	1.56	0.34	sequence orphan
slt1	1.70	0.57	sequence orphan Slt1
SPBC21C3.19	1.26	0.24	SBDS family protein Rtc3 (predicted)
SPBC4F6.17c	1.52	0.65	mitochondrial heatshock protein Hsp78 (predicted)
SPNCRNA.781	1.15	0.32	intergenic RNA (predicted)
SPNCRNA.1271	0.92	0.13	antisense RNA (predicted), possible alternative UTR
hsp9	1.05	0.28	heat shock protein Hsp9
psi1	1.26	0.54	DNAJ domain protein, involved in translation initiation Psi1
SPBC3B9.01	1.21	0.52	Hsp70 nucleotide exchange factor (predicted)
ctr5	0.82	0.16	copper transporter complex subunit Ctr5
SPNCRNA.850	0.66	0.14	antisense RNA (predicted)
SPNCRNA.276	0.77	0.25	non-coding RNA (predicted)
SPNCRNA.1094	0.52	0.01	intergenic RNA (predicted)
ecl2	0.56	0.05	extender of the chronological lifespan protein Ecl2
urg2	0.63	0.12	uracil phosphoribosyltransferase (predicted)
SPNCRNA.1109	0.62	0.12	antisense RNA (predicted)
urg1	0.56	0.08	GTP cyclohydrolase II (predicted)
mug35	0.68	0.20	sequence orphan
SPBC725.03	0.68	0.23	conserved fungal protein
SPBC1711.12	0.69	0.27	oxidised protein hydrolase (predicted)
SPNCRNA.719	0.66	0.25	antisense RNA (predicted), possible alternative UTR
SPAPB1A10.05	0.83	0.42	sequence orphan
SPACUNK4.16c	0.76	0.35	alpha,alpha-trehalose-phosphate synthase (predicted)
SPNCRNA.1273	0.42	0.02	antisense RNA (predicted)
tps1	0.56	0.17	alpha,alpha-trehalose-phosphate synthase [UDP-forming]
SPNCRNA.1541	0.47	0.09	intergenic RNA (predicted)
SPNCRNA.801	0.61	0.24	antisense RNA (predicted), possible alternative UTR
SPNCRNA.1115	0.47	0.09	intergenic RNA (predicted), possible alternative UTR
SPNCRNA.477	0.52	0.15	non-coding RNA (predicted)
sti1	0.65	0.28	chaperone activator Sti1 (predicted)
mug9	0.51	0.16	conserved fungal protein
SPNCRNA.1409	0.43	0.09	intergenic RNA (predicted)
SPBC1271.08c	0.53	0.19	sequence orphan
SPNCRNA.1211	0.42	0.08	antisense RNA (predicted)
SPBC11C11.06c	0.37	0.03	sequence orphan
SPNCRNA.1272	0.35	0.01	antisense RNA (predicted)
SPNCRNA.687	0.51	0.18	antisense RNA (predicted)
SPNCRNA.1206	0.34	0.02	antisense RNA (predicted)
SPBC1683.04	0.33	0.02	glycosyl hydrolase family 3 (predicted)
SPNCRNA.750	0.44	0.13	antisense RNA (predicted), possible alternative UTR

Systematic	Difference *set2*Δ	Difference WT	Description
SPNCRNA.1637	0.35	0.04	antisense RNA (predicted)
SPBC1685.12c	0.39	0.08	dubious
SPNCRNA.1676	0.47	0.17	intergenic RNA (predicted)
SPNCRNA.1608	0.39	0.09	antisense RNA (predicted)
gal10	0.34	0.04	UDP-glucose 4-epimerase/aldose 1-epimerase Gal10
SPCTRNAGLU.09	0.31	0.01	tRNA Glutamic acid
SPBC1105.13c	0.67	0.38	sequence orphan
SPBC30D10.14	0.54	0.26	dienelactone hydrolase family (predicted)
SPNCRNA.529	0.67	0.38	non-coding RNA (predicted)
ntp1	0.48	0.19	alpha,alpha-trehalase Ntp1
SPNCRNA.1353	0.36	0.08	antisense RNA (predicted)
SPBC1711.08	0.45	0.17	chaperone activator Aha1 (predicted)
SPAPB24D3.07c	0.30	0.02	sequence orphan
tsn1	0.31	0.03	translin
SPBPB2B2.05	0.59	0.32	peptidase family C26 protein
SPNCRNA.1327	0.51	0.24	intergenic RNA (predicted)
SPNCRNA.665	0.34	0.07	antisense RNA (predicted)
etr1	0.47	0.20	enoyl-[acyl-carrier protein] reductase (predicted)
SPNCRNA.1300	0.28	0.01	intergenic RNA (predicted)
SPCC191.01	0.40	0.14	sequence orphan
SPCPB16A4.07	0.36	0.10	sequence orphan
SPNCRNA.1322	0.33	0.07	antisense RNA (predicted)
SPNCRNA.583	0.28	0.03	antisense RNA (predicted)
SPNCRNA.1382	0.29	0.04	antisense RNA (predicted)
rhp54	0.89	0.64	Rad54 homolog Rhp54
SPAC458.06	0.25	0.00	WD repeat protein involved in autophagy Atg18c
SPCC338.06c	0.35	0.11	heat shock protein Hsp20 family (predicted)
rds1	0.39	0.15	conserved fungal protein
SPNCRNA.1373	0.42	0.18	antisense RNA (predicted)
SPAC521.03	0.31	0.07	short chain dehydrogenase (predicted)
SPBC725.10	0.36	0.13	tspO homolog, involved in the transport of haem (predicted)
SPBC12C2.04	0.34	0.10	NAD binding dehydrogenase family protein
SPBPB7E8.02	0.34	0.11	PSP1 family protein
ctr6	0.26	0.03	vacuolar copper transporter Ctr6
SPNCRNA.1384	0.23	0.01	intergenic RNA (predicted), possible alternative UTR
SPNCRNA.1550	0.31	0.09	intergenic RNA (predicted), possible alternative UTR
SPNCRNA.855	0.35	0.13	intergenic RNA (predicted)
ctt1	0.47	0.25	catalase
gpx1	0.33	0.12	glutathione peroxidase Gpx1
SPNCRNA.983	0.40	0.18	antisense RNA (predicted)
SPNCRNA.531	0.35	0.14	non-coding RNA (predicted)
SPAC3G6.05	0.27	0.06	Mvp17/PMP22 family protein 1 (predicted)
cbp1	0.22	0.02	CENP-B homolog
SPBTRNALEU.06	0.35	0.15	tRNA Leucine
SPAC13C5.04	0.34	0.14	amidotransferase (predicted)
SPAC11D3.13	0.37	0.17	ThiJ domain protein
ubx3	0.40	0.20	UBX domain protein Ubx3, Cdc48 cofactor

Category 5: Sixty-two transcripts are decreased in wildtype following bleomycin treatment but increased following bleomycin treatment in *set2*Δ cells

Systematic	Difference *set2*Δ	Difference WT	Description
mug135	0.68	-0.02	cell surface glycoprotein (predicted), DUF1773 family protein 3
SPNCRNA.1095	0.46	-0.15	intergenic RNA (predicted)
SPCTRNAILE.09	0.37	-0.02	tRNA Isoleucine
snR88	0.37	-0.04	small nucleolar RNA snR88
SPNCRNA.1475	0.36	-0.03	antisense RNA (predicted), possible alternative UTR
SPNCRNA.574	0.36	-0.05	antisense RNA (predicted)
SPNCRNA.1098	0.35	-0.21	intergenic RNA (predicted)
SPNCRNA.1287	0.34	-0.05	intergenic RNA (predicted), possible alternative UTR
cut3	0.31	-0.04	condensin complex subunit Cut3
SPBTRNATYR.03	0.30	0.00	tRNA Tyrosine
SPBTRNAGLN.03	0.29	-0.01	tRNA Glutamine
ppk34	0.27	-0.09	serine/threonine protein kinase Ppk34
ecl1	0.27	-0.03	extender of the chronological lifespan protein Ecl1
SPNCRNA.601	0.25	-0.06	intergenic RNA (predicted)
SPBTRNAMET.05	0.25	-0.03	tRNA Methionine
SPNCRNA.1529	0.24	-0.02	antisense RNA (predicted)
SPNCRNA.360	0.24	-0.18	non-coding RNA, centromeric (predicted)
SPNCRNA.818	0.24	-0.03	antisense RNA (predicted)
SPBC582.10c	0.23	-0.05	ATP-dependent DNA helicase Rhp16b (predicted)
SPAC664.13	0.22	-0.02	sequence orphan
SPAC6C3.03c	0.21	-0.01	sequence orphan
cut12	0.21	-0.05	spindle pole body protein Cut12
SPBTRNATYR.04	0.21	-0.06	tRNA Tyrosine
SPATRNAVAL.03	0.21	-0.01	tRNA Valine
SPCC320.06	0.20	-0.01	conserved fungal protein
SPNCRNA.1005	0.20	-0.02	antisense RNA (predicted)
SPNCRNA.1242	0.18	-0.04	intergenic RNA (predicted), possible alternative UTR
SPNCRNA.76	0.18	-0.12	non-coding RNA (predicted)
SPATRNALEU.02	0.18	-0.02	tRNA Leucine
mug153	0.18	-0.08	sequence orphan
vps24	0.18	-0.02	ESCRT III complex subunit Vps24
SPBPB2B2.15	0.18	-0.05	conserved fungal family
atg18	0.17	-0.06	WD repeat protein involved in autophagy Atg18a
SPCC584.16c	0.17	-0.06	sequence orphan
isp4	0.17	-0.05	OPT oligopeptide transporter family Isp4
meu2	0.17	-0.11	sequence orphan
pck1	0.17	-0.07	protein kinase C (PKC)-like Pck1
tim11	0.16	-0.12	F0-ATPase subunit E (predicted)
SPNCRNA.361	0.16	-0.15	non-coding RNA, centromeric (predicted)
SPNCRNA.394	0.15	-0.06	non-coding RNA (predicted)
SPNCRNA.1509	0.13	-0.07	intergenic RNA (predicted), possible alternative UTR
SPBC6B1.03c	0.13	-0.10	Pal1 family protein
SPCPB1C11.02	0.13	-0.12	amino acid permease (predicted)
SPBTRNAASP.04	0.13	-0.11	tRNA Aspartic acid
SPNCRNA.792	0.12	-0.14	intergenic RNA (predicted), possible alternative UTR
SPNCRNA.741	0.12	-0.12	antisense RNA (predicted)
snoZ7	0.11	-0.11	small nucleolar RNA Z7

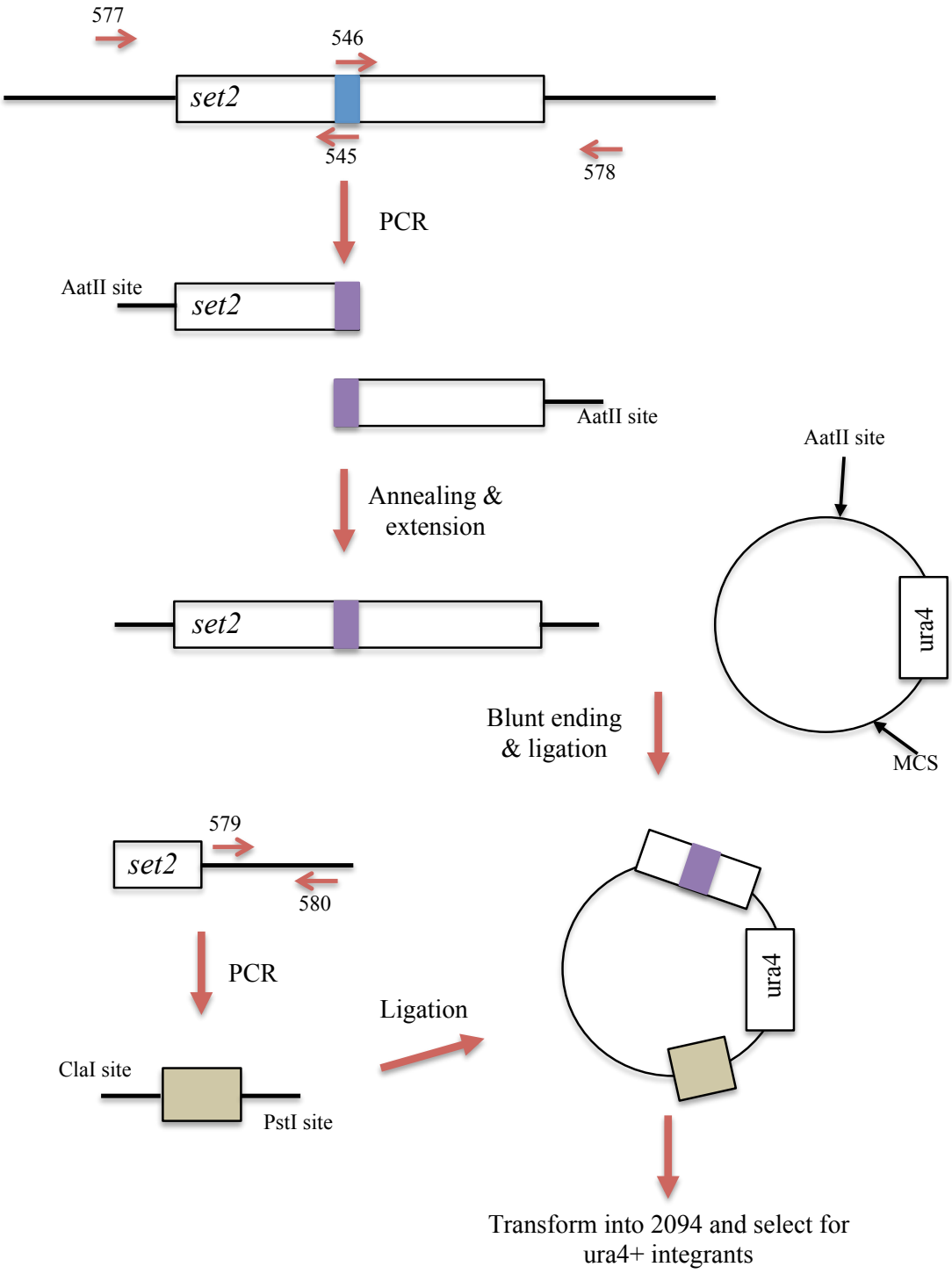
Systematic	Difference *set2*Δ	Difference WT	Description
SPBTRNAARG.04	0.11	-0.15	tRNA Arginine
mug28	0.10	-0.14	RNA-binding protein Mug28
SPBPB2B2.11	0.10	-0.20	nucleotide-sugar 4,6-dehydratase (predicted)
ymr31	0.09	-0.12	mitochondrial ribosomal protein Ymr1 (predicted)
SPNCRNA.950	0.09	-0.18	intergenic RNA (predicted)
SPNCRNA.234	0.08	-0.20	non-coding RNA, centromeric (predicted)
rps29	0.07	-0.26	40S ribosomal protein S29 (predicted)
SPNCRNA.507	0.07	-0.15	non-coding RNA (predicted)
SPNCRNA.1181	0.04	-0.23	antisense RNA (predicted)
SPNCRNA.1325	0.04	-0.22	intergenic RNA (predicted), possible alternative UTR
SPNCRNA.1507	0.02	-0.18	antisense RNA (predicted)
SPAC212.12	0.02	-0.45	S. pombe specific GPI anchored protein family
cta3	0.02	-0.18	P-type ATPase, calcium transporting Cta3
SPNCRNA.1657	0.02	-0.21	intergenic RNA (predicted), possible alternative UTR
ade6	0.01	-0.19	phosphoribosylaminoimidazole carboxylase Ade6

Category 6: Five transcripts are decreased in wildtype cells following bleomycin treatment but decreased less in *set2*Δ cells

Systematic	Difference *set2*Δ	Difference WT	Description
SPAC869.01	-0.02	-0.61	amidase (predicted)
SPNCRNA.1459	-0.03	-0.27	intergenic RNA (predicted), possible alternative UTR
SPNCRNA.1554	-0.04	-0.25	intergenic RNA (predicted), possible alternative UTR
hri1	-0.05	-0.25	eIF2 alpha kinase Hri1
SPNCRNA.1210	-0.10	-0.40	antisense RNA (predicted)

In all cases, the difference (in *set2*Δ cells or wildtype; WT) relates to the change in expression level relative to before treatment with bleomycin, where the level before treatment is standardised to 1.0. Therefore, a negative value represents a decrease in transcript level following DNA damage, whereas a positive value represents an increase in transcript level following DNA damage. Transcripts were classed to be significantly different if the difference between *set2*Δ and wildtype differences was greater than 0.2.

Appendix VIII Cloning plan for *set2-R255G* strain construction



Creation of *set2-R255G* mutant An A to G point mutation at residue 763 was introduced into *set2* using PCR. Wildtype DNA was used as the template, and two partially complementary, overlapping fragments were amplified using primers containing the mutation (545 and 546) and primers containing an AatII restriction site (577 and 578). Equal quantities of the two PCR fragments were mixed and the complementary ends annealed at 100°C for 2 minutes, followed by cooling to room temperature; the full length, mutation containing fragment was PCR amplified. *set2* downstream homology was amplified from wildtype DNA using primers 579 and 580, containing ClaI and PstI restriction sites respectively. The PCR fragment was digested with ClaI and PstI and ligated to ClaI and PstI digested p15 to create p248. The mutation-containing fragment was blunt ended and ligated into AatII digested and blunt ended p248, to create p249. p249 was linearised with SacI and transformed into wildtype cells (TH2094). Candidates were selected on U- plates, and PCR confirmed using primers 546 and 384. Sequencing was used to confirm the presence of the mutation.